

Assessing the temporal patterns of mid-Cretaceous floral change in Portugal – a palynological and chemostratigraphic approach

Von der Naturwissenschaftlichen Fakultät der
Gottfried Wilhelm Leibniz Universität Hannover
zur Erlangung des Grades

Doktor der Naturwissenschaften (Dr. rer. nat.)

genehmigte Dissertation

von

Maurits Horikx M.Sc.

geboren am 18.03.1986 in Amsterdam, (Niederlande).

2015

Referent: Prof. Dr. Ulrich Heimhofer

Korreferent: Prof. Dr. Peter Hochuli

Korreferent: Prof. Dr. Francois Holtz

Korreferentin: Prof. Dr. Andrea Hampel

Tag der Promotion: 15.07.2015

Table of Contents

ABSTRACT	3
KURZFASSUNG	5
CHAPTER 1 <i>Introduction and synopsis.....</i>	9
CHAPTER 2 <i>Integrated stratigraphy of shallow marine Albian strata from the southern Lusitanian Basin of Portugal</i>	25
CHAPTER 3 <i>Albian angiosperm pollen from shallow marine strata in the Lusitanian Basin, Portugal</i>	51
CHAPTER 4 <i>Terrestrial climate and vegetation records from shallow marine deposits: Implications for angiosperm pollen distribution during the Albian</i>	93
CHAPTER 5 <i>Conclusions</i>	115
APPENDICES <i>Appendix 1-23</i>	117
ACKNOWLEDGEMENTS	141
CURRICULUM VITAE.....	145
LIST OF PUBLICATIONS.....	147

Abstract

The mid-Cretaceous (Aptian-Turonian 120-90 Ma) was characterized by globally significantly warmer conditions than at present times and experienced several episodes of enhanced volcanic activity and major changes in atmospheric CO₂. Perturbations in the ocean-atmospheric and carbon system significantly impacted the biota in both the marine and terrestrial realm. Unlike in the marine realm, the role and impact of these major disturbances on the terrestrial realm has received only minor attention. Major changes in the terrestrial realm include the significant transformation in the existing plant community, associated with the early radiation and diversification of flowering plants (angiosperms), especially during the Albian interval (113-100.5 Ma). Furthermore, the role of climate as an external trigger for the angiosperm radiation remains mostly unclear, mostly due to a lack of detailed and continuous, well-constrained terrestrial records with a sound temporal framework. Continental sequences in the northern part of the Lusitanian Basin of western Portugal represent the most important fossil archives with angiosperm floras at mid-latitudes of presumed Aptian-Albian age. In contrast to the wealth of information available on the biology and systematic relationships of early angiosperms obtained from these fossil-rich deposits, the temporal patterns of their evolution are poorly constrained. Unlike macrofossils, terrestrial palynomorphs from marine strata in the southern part of the Lusitanian Basin provide an excellent tool to track vegetation changes with continuous stratigraphic coverage. These deposits allow the establishment of well-constrained stratigraphic ages essential to investigate the potential link between climate evolution and its impact on the angiosperm pollen diversification as well as changes in the accompanying continental vegetation composition.

Dating of the different sections in the southern part of the Lusitanian Basin was performed by a combined approach of dinoflagellate cyst biostratigraphy, carbon isotope stratigraphy and strontium isotope stratigraphy from pristine oyster and rudist shells. The São Julião section, located near the town of Ericeira serves hereby as reference curve and covers the early Albian to early Cenomanian interval, with an extended late Albian succession.

An in-depth analysis of the angiosperm pollen assemblage from São Julião provides the most diverse angiosperm pollen record from the Albian to date with a significantly higher stratigraphic resolution compared to previous studies. The angiosperm pollen record shows a striking sequence of appearances of important angiosperm pollen morphologies; monocolpates, polyporates and tricolpates appear from the early Albian and tricolporates from the late Albian onwards. A significant rise in poly-aperturate pollen diversity is recorded from Middle and Upper Albian strata. Previously, the classical Potomac Group succession from the Atlantic Coastal Plain, eastern USA was used to show the continuous radiation of angiosperm pollen during the Albian. By incorporating the new data from São Julião, the age of the angiosperm pollen Subzones II-B and II-C of the continental Potomac Group succession is discussed and revised.

Palynological (spore-pollen composition) and clay mineral analyses are used to reconstruct paleo-environmental changes from the terrestrial realm in the Lusitanian Basin. The reconstructed vegetation thriving in the continental hinterland shows a dominance of Cheirolepidacean and Taxodiacean gymnosperms, with an understory of ferns and angiosperms. The ratio between xerophytic and hygrophytic palynomorphs and changes in the clay mineral composition are used to reconstruct moisture availability. Our results show a congruent aridification trend from the early Albian to early Cenomanian interval, punctuated by an interval associated with enhanced humidity during the late Albian. The angiosperm pollen composition shows an increasing dominance of poly-aperturate pollen of eudicot affinity over monocolpate pollen of magnoliid-monocot affinity, as expressed by the E/(M-M) ratio. The rise in the E/(M-M) ratio is concurrent with rising global sea surface temperatures and interpreted to represent the northward migration of poly-aperturate pollen producing parent-plants from lower latitudes into the Lusitanian Basin during the Albian. Despite the possibility of undersampling and the absence of rare angiosperm taxa during particular time intervals, total angiosperm pollen diversities are higher during periods of more arid conditions. This observation contrasts to the established view of humidity as trigger for angiosperm dominance during the mid-Cretaceous.

Keywords: early angiosperm radiation, palynology, paleoclimate, Lusitanian Basin, Albian

Kurzfassung

In der mittleren Kreidezeit (Aptium bis Turonium vor etwa 120–90 Ma) war es im Vergleich zur heutigen Zeit weltweit erheblich wärmer, die vulkanische Aktivität war erhöht und der CO₂-Gehalt der Atmosphäre war starken Schwankungen unterworfen. Umwälzungen im Ozean-Atmosphäre-System und im Kohlenstoffkreislauf hatten großen Einfluss auf die marine und die terrestrische Lebenswelt. Im Gegensatz zum marinen Lebensraum wurden die Folgen dieser Veränderungen auf den terrestrischen Lebensraum bisher kaum untersucht. Zu den weitreichenden Veränderungen im terrestrischen Raum gehören der Wandel der bestehenden Pflanzenvergesellschaftungen und die damit einhergehende frühe Radiation und Ausbreitung von Blütenpflanzen (Angiospermen) besonders während des Albiums (113–110.5 Ma). Die Rolle des Klimas als Auslöser der Angiospermen-Radiation ist auf Grund des Mangels an vollständigen und gut datierten terrestrischen Abfolgen bisher noch unklar. Die kontinentalen Ablagerungen im nördlichen Lusitanischen Becken von Westportugal sind die wichtigsten Archive fossiler Angiospermenfloren aus den mittleren Breiten des Aptiums und Albiums. Im Gegensatz zur Fülle an Informationen über die Biologie und Systematik der frühen Angiospermen aus diesen Ablagerungen, ist deren zeitliche Entwicklung nur unzureichend definiert. Terrestrische Palynomorphe aus den marinen Ablagerungen des Lusitanischen Beckens stellen im Gegensatz zu Makrofossilien ein exzellentes Werkzeug dar, um Veränderungen der Vegetation im zeitlichen Zusammenhang nachzuvollziehen. Diese sedimentären Ablagerungen ermöglichen eine genaue Datierung, welche essentiell ist zur Erforschung des Zusammenhangs zwischen der Klimaveränderung und deren Einfluss auf die Ausbreitung der Angiospermen Pollen sowie der Veränderung kontinentaler Vegetation.

Die Datierung verschiedener Aufschlüsse im südlichen Lusitanischen Becken erfolgte durch eine Kombination von Biostratigrafie basierend auf Dinoflagellatenzysten und Isotopenstratigrafie mit Hilfe von Kohlenstoff und Strontium. Das dafür untersuchte Probenmaterial stammte von diagenetisch unveränderten Austern- und Rudistenschalen. Die Daten des São Julião Aufschluss in der Nähe der Stadt Ericeira dienen hierbei als Referenzkurve und umfassen das frühe Albiums bis frühe Cenomanium mit einer stark ausgedehnten Abfolge des späten Albiums.

Eine detaillierte Analyse der Angiospermpollen-Vergesellschaftung in São Julião ergab die bisher höchste Diversität von Angiospermen einer Alb-zeitlichen Abfolge mit weit besserer stratigrafischer Auflösung als die meisten früheren Studien. Wichtige Angiospermpollen mit signifikanter Morphologie treten in auffälliger Reihenfolge auf: Monokolpate, polykolpate und tricolpate Pollen erschienen zum ersten Mal im frühen Albium während trikolorpate Pollen erst im späten Albium auftreten. Ein signifikanter Diversitätsanstieg der poly-aperturaten Pollen ist in den Sedimenten des mittleren bis oberen Albiums zu beobachten. Die klassische Potomac Group Abfolge der Atlantischen Küstenebene in den östlichen USA diente bisher zur Anschauung der kontinuierlichen Alb-zeitlichen Radiation der Angiospermen. Unter Berücksichtigung der neuen Daten aus São Julião wurde die Datierung der Angiospermpollen Subzonen II-B und II-C der kontinentalen Potomac Group Abfolge diskutiert und korrigiert.

Palynologische (Vergesellschaftung von Sporen und Pollen) und Tonmineral-Analysen wurden zur Rekonstruktion von paläoklimatischen Veränderungen des terrestrischen Hinterlandes des Lusitanischen Beckens genutzt. Die rekonstruierte Vegetation des Hinterlandes wird von Cheirolepidaceen und Taxodiaceen dominiert; im Unterholz finden sich Farne und Blütenpflanzen. Die Wasserverfügbarkeit für Pflanzen kann über das Verhältnis von Xerophyten-Palynomorphen zu Hygrophyten-Palynomorphen und die Tonmineralzusammensetzung rekonstruiert werden. Unsere Daten zeigen einen Trend zunehmender Aridifizierung vom frühen Albium bis ins frühe Cenomanium, welcher durch mehrere kurze Intervalle erhöhter Humidität während des späten Albiums unterbrochen wird. Die Angiospermpollen-Zusammensetzung zeigt eine ansteigende Dominanz von poly-aperturaten Pollen mit eudikotyledonischer Affinität gegenüber monokolpaten Pollen mit magnoliid-monokotyledonischer Affinität, bekannt als E/(M-M) Verhältnis. Ein Anstieg dieses Verhältnisses wird begleitet von zunehmenden globalen Oberflächenwassertemperaturen. Gleichzeitig wird der Anstieg

auch als Anzeichen für die Alb-zeitliche Migration jener Pflanzen, die poly-aperturate Pollen bilden, aus niederen Breiten nach Norden in das Hinterland des Lusitanischen Beckens betrachtet. Trotz möglicher Unterabtastung und der Abwesenheit von seltenen Angiospermen Taxa während bestimmter Zeitintervalle ist die gesamte Vielfalt der Angiospermen Pollen in trockeneren Perioden größer. Diese Beobachtung steht in starkem Kontrast zur wissenschaftlichen Ansicht, dass Feuchtigkeit für die starke Dominanz der Angiospermen in der mittleren Kreide verantwortlich ist.

Schlüsselwörter: Radiation der frühen Angiospermen, Palynologie, Paläoklima, Lusitanisches Becken, Albium

1. Introduction

1.1 Mid-Cretaceous climate

The mid-Cretaceous period (Aptian to Turonian, 120-90 Ma; Gradstein et al. 2012) represents one of the best examples of 'greenhouse' climatic conditions from the Phanerozoic. This geological interval is characterized by high rates of sea floor spreading, Large Igneous Provinces (LIPS), high sea-surface temperatures, high atmospheric $p\text{CO}_2$, an enhanced global hydrological cycle, high sea levels and a low equator-to-pole thermal gradient (e.g. Huber et al. 1995, Weissert et al. 1998, Wilson & Norris 2001, Ufnar et al. 2002, 2004, Jenkyns et al. 2004, Wortmann et al. 2004, Steuber et al. 2005, Bice et al. 2006, Hay & Floegel 2012; Fig. 1). Mid-Cretaceous sea surface temperatures were presumably 10°C warmer than at present (Bice et al. 2003) and marked by a gradual rise in temperature from the Aptian to the Turonian, culminating in a thermal maximum at the Cenomanian-Turonian boundary (Clarke & Jenkyns 1999, Friedrich et al. 2012). Long-term records based on $\delta^{18}\text{O}$ paleothermometry and organic biomarkers (TEX_{86}) of Aptian and Albian age indicate sea-surface temperatures of 31-36°C at low-latitudes and 24-28°C at the southern high latitudes (Schouten et al. 2003, Dumitrescu et al. 2006, Forster et al. 2007, Jenkyns et al. 2012). The rise in global mean temperatures was accompanied by a continuous sea-level increase during the Aptian to Turonian (Haq et al. 1987, Sahagian et al. 1996, Kominz et al. 2008).

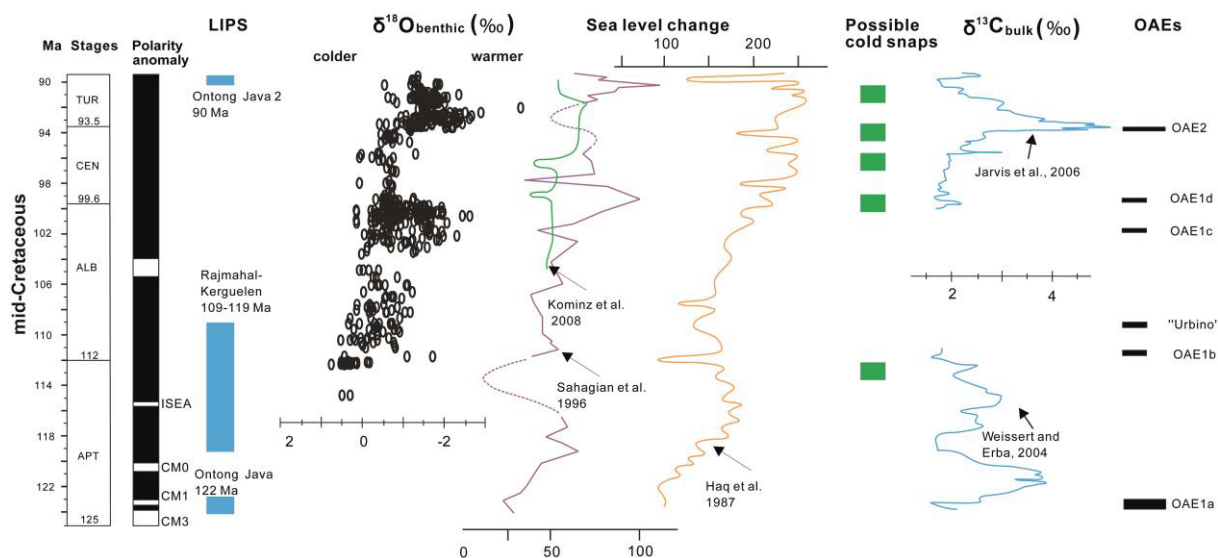


Fig. 1. Summary of mid-Cretaceous environmental changes, showing LIPS (Larson, 1991), $\delta^{18}\text{O}$ of benthic foraminifers (Friedrich et al., 2012), global sea-level curve (Haq et al., 1987, Sahagian et al., 1996, Kominz et al., 2008), possible cold snaps, $\delta^{13}\text{C}$ of bulk rocks (Weissert & Erba, 2004, Jarvis et al., 2006), and OAEs (Schlanger & Jenkyns, 1976, Jenkyns, 1980, Bralower et al., 1994). Figure modified from Hu et al. (2012).

On shorter time scales, the notion of equitable, ice-free and hot conditions during the 'mid-Cretaceous Greenhouse' is challenged. For instance, a significant decline in calcareous nannofossil species-richness and expansion towards lower latitudes as well as the occurrence of dropstones and glendonites at higher latitudes in the marine realm was linked to continental ice-sheets build-up during the Aptian-Albian interval (Frakes & Francis 1988, De Lurio & Frakes 1999, Price 1999, Mutterlose et al. 2009). Likewise, a highly sensitive climate system is inferred from significant changes in the carbon pool as expressed from carbon ($\delta^{13}\text{C}$) isotope records (e.g. Scholle & Arthur, 1980, Giorgioni et al. 2012) and from intervals marked by the formation of dark, organic-rich, laminated and finely grained sediments in marine records, linked to periods of enhanced anoxic bottom water conditions.

These deposits, known as Oceanic Anoxic Events (OAEs) coincided with dramatic perturbations in the carbon cycle (Schlanger & Jenkyns 1976, Arthur et al. 1990, Weissert & Erba, 2004, Trabuchio-Alexandre et al. 2011). Mid-Cretaceous OAEs are expressed as the lower Aptian OAE 1a (Selli Event ~120 Ma), the Albian OAE 1b (Paquier Event), OAE 1c, and OAE 1d (Breistroffer Event) and the

Cenomanian-Turonian OAE 2 (Bonarelli Event ~94 Ma). The exact mechanisms triggering OAEs remain under debate but have been linked to abrupt temperature increases, induced by a rapid atmospheric CO₂ influx by volcanic degassing, the dissociation of methane hydrates or a combination of both, as well as differences in ocean circulation, primary production and temperature-induced changes in solubility (Arthur & Sageman 1994, Erbacher et al. 2001, Strauss 2006, Jenkyns 2010).

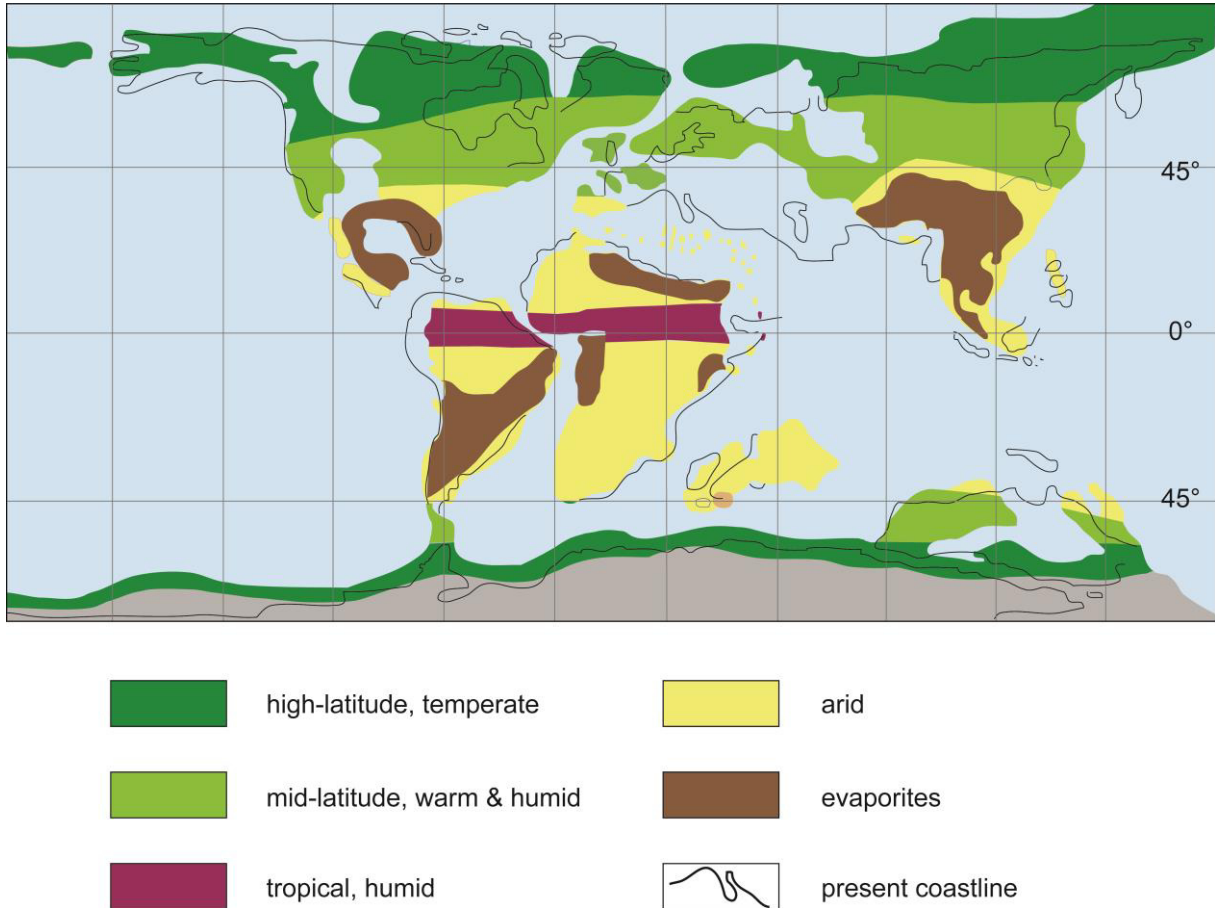


Fig. 2. Albian climate zones from the terrestrial realm, after Chumakov et al. (1995). Figure modified from Hay & Floegel (2012).

These perturbations in the ocean-atmospheric and carbon system had a profound effect on the continental and marine biota during the mid-Cretaceous. Unlike the marine realm, the terrestrial realm has received far less attention. Based on compilations from fossil findings and sedimentary features, Chumakov et al. (1995) reconstructed broadly defined terrestrial climate zones for the Cretaceous (Fig. 2). The climate zones in the northern latitudes are characterized by temperate humid belts and the mid-latitudes by warm and humid belts. The lower latitudes are composed of an arid belt and the equatorial regions of a humid belt, corresponding to the modern Intertropical Convergence Zone (ITCZ). Extremely high temperatures have been inferred (>42°C) for the terrestrial realm at low latitudes during the Turonian, suggesting that the equatorial regions might have been devoid of vegetation (Bice et al. 2006, Hay & Floegel 2012). Fossil plant material show more hospitable temperatures with mean annual temperature estimates of 10°C for high latitudes and between 19–26°C at mid-latitudes (Spicer & Parrish 1986, Wolfe & Upchurch 1987, Parrish et al. 1998, Arens & Harris 2015).

1.2 The rise of angiosperms

The most dramatic change during the mid-Cretaceous in the terrestrial realm is the transformation of the vegetation composition associated with the radiation and diversification of early angiosperms (flowering plants). The typical vegetation consisting of ginkgoales, conifers, pteridophytes and cycadales (Fig. 3) was displaced and eventually dominated by angiosperms during the late Cretaceous (Crane & Lidgard 1989, Crane et al. 1995, Wing & Boucher 1998). It has been suggested that the angiosperm evolution provided the opportunity for other biological lineages (e.g. pollinating insects) to co-evolve (Grimaldi 1999, Cardinal & Danforth 2013). Today, angiosperms are the most abundant and diverse group of terrestrial plants with 200,000 species classified in more than 300 families (Endress 2010). Modern angiosperms represent over 90% of the total land plant species and include a rich diversity in reproductive morphology (flower shape, size and function) and form (Crepet & Niklas 2009). Furthermore, extant flowering plants display a wide range of lifestyles, ranging from small-sized aquatics to giant forest trees and dominate in almost all environments and every continent across the globe, except in the northernmost latitudes and at high altitudes (Wing & Boucher 1998, Soltis & Soltis 2004). In contrast to the wealth of information on modern and fossil angiosperm phylogeny and biology (e.g. Doyle & Endress 2010, 2014), the temporal and spatial patterns of the early angiosperms radiation remain relatively unknown.

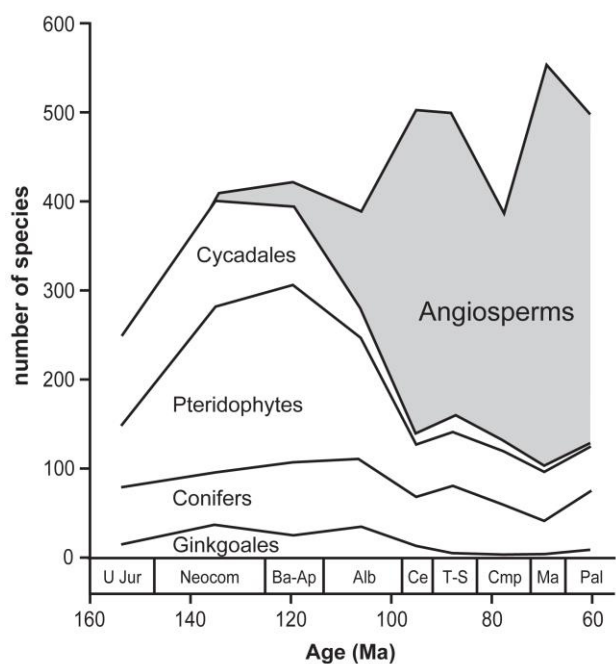


Fig. 3. Absolute species diversity of Cretaceous plant assemblages (adopted and modified from Lidgard & Crane 1988). Angiosperms first appear during the early Cretaceous and show a dramatic rise in the number of species during the Albian.

The origin and radiation of early angiosperms has been investigated from two research areas; the fossil record and molecular data. The first appearance of angiosperms from molecular clock estimates varies significantly and so far no consensus has been reached. Using several data sets, the origination date of angiosperms took place between 275-163 Ma during the Triassic to Jurassic period (Magallón & Sanderson, 2005, Smith et al. 2010, Magallón 2010, Clarke et al. 2011). Evidence for a pre-Cretaceous origin of angiosperms has been recorded from the fossil record, albeit these findings were later questioned. For instance, *Archaeofructus* was first reported as the oldest known angiosperm of late Jurassic age (Sun et al. 1998, 2002), but the age of the deposits was later revised to a Barremian-Aptian age by radiometric dating (Zhou et al. 2003). Indirect evidence for a Triassic-Jurassic origin of angiosperms is derived from the presence of the biological marker oleanane in Jurassic sediments, which has been suggested as a biomarker for angiosperms (Moldowan et al. 1994) as well as the presence of conspicuous angiosperm-like pollen from middle Triassic strata (Cornet 1989, Hochuli & Feist-Burkhardt 2004, 2013). According to Axelrod (1952, 1970) angiosperms originated in tropical uplands in the Permian or Triassic and invaded into lowland basins during the Cretaceous, triggered

by more equable climates. However, despite the wealth and nearly worldwide sampling, the lack of unambiguous Triassic to Jurassic aged angiosperm fossil findings does not favor a pre-Cretaceous origin for flowering plants (Doyle 2012).

So far, the earliest unequivocal fossils of flowering plants appear relatively late in the fossil record compared to other major plant groups (Fig. 3) and consist of pollen from the Valanginian-Hauterivian interval (c. 136 Ma). These small and monocolpate pollen are related to the genus *Clavatipollenites* (Gübeli et al. 1984, Hughes & McDougall 1987). Angiosperm pollen are identified by a columellar exine structure, connecting the inner (nexine) and outer (sexine) wall layers, which separates them from gymnosperm pollen. The earliest angiosperm pollen are found in the paleo-equatorial regions of Northern Gondwana and later spread towards the higher latitudes, whereby monocolpate pollen of monocot or magnoliid affinity appeared before poly-aperturate pollen, which are characterized by three or more apertures and of eudicot affinity (Brenner 1976, Hickey & Doyle 1977). The first angiosperms from eastern Asia are reported from the Barremian in China and Japan (Li & Liu 1994, Legrand et al. 2014, Zhang et al. 2014), from South America from the Aptian (Romero & Archangelsky 1986), in Antarctica from the early Albian (Truswell 1990) and in Canada from the middle Albian (Norris 1967). According to compilations of fossil angiosperm taxa, the Albian interval is marked by a significant rise in angiosperm diversity (Lidgard & Crane 1988).

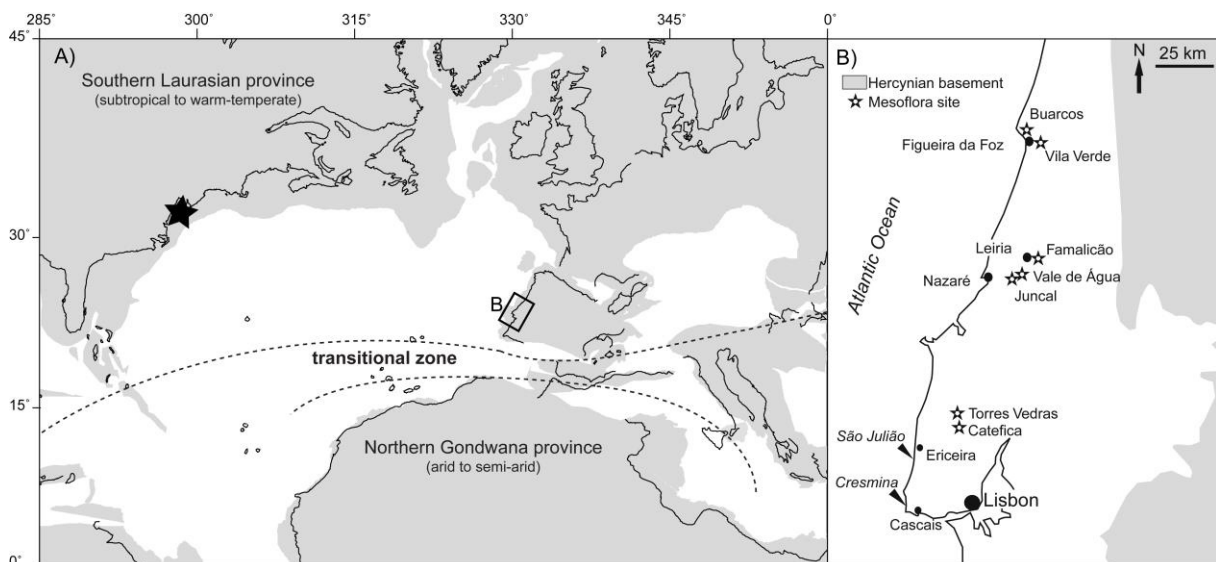


Fig. 4. (A) Palaeogeographic map of the North Atlantic and Tethyan realm during the early Albian (~105 Ma, modified after Geomar map generator; www.ods.de). The black star marks the position of the Potomac Group succession of eastern North America. Major floral belts and corresponding climates are derived from Brenner (1976) and Chumakov et al. (1995). (B) Location of the Lusitanian Basin in Portugal, the white stars represent the location of important meso- and macrofossil sites. The shallow marine Cresmina and São Julião sections of Albian age are located in the southern part of the Lusitanian Basin (Figure adopted and modified from Dinis et al. 2010).

1.3 The Potomac Group succession and the Lusitanian Basin: classical archives of mid-Cretaceous angiosperm fossil findings

The continental sequences of western Portugal and eastern USA (Potomac Group) represent the most important fossil archives with angiosperm floras from the mid-Cretaceous at mid-latitudes (Fig. 4). The Lusitanian Basin in Portugal provides a diverse and exceptionally preserved assemblage of macro- and mesofossil angiosperm remains (stamens, fruits, carpels, anthers, seeds, flowers and leaves) from several localities and stratigraphic levels (Saporta 1894, Teixeira, 1945, 1946, 1947, 1948, 1950, 1952, Friis et al. 1999, 2010, Mendes et al. 2011, 2014). Some of the reproductive structures even contained *in-situ* pollen in the stamens or on the stigma. In total, over 150 different types of angiosperms have been found of mostly monocot and/or magnoliid affinity, with rare occurrences of eudicots. According to Diéguez et al. (2010), the mid-Cretaceous vegetation in Iberia was composed of Charophytes, spore producing plants and angiosperms near fresh-water environments, whereas Taxodiaceae and Cupressaceae conifers occupied riverbanks and mangroves and Cheirolepidiaceae conifers dominated upland areas. For the last decades, the Potomac Group is used as the ‘classical’ succession to demonstrate the continuous diversification of angiosperms in the Cretaceous. The record is characterized by a distinct morphological diversification and increased abundance of angiosperm pollen and leaves (Brenner 1963, Dilcher 1974, Hickey & Wolfe 1975, Doyle & Hickey

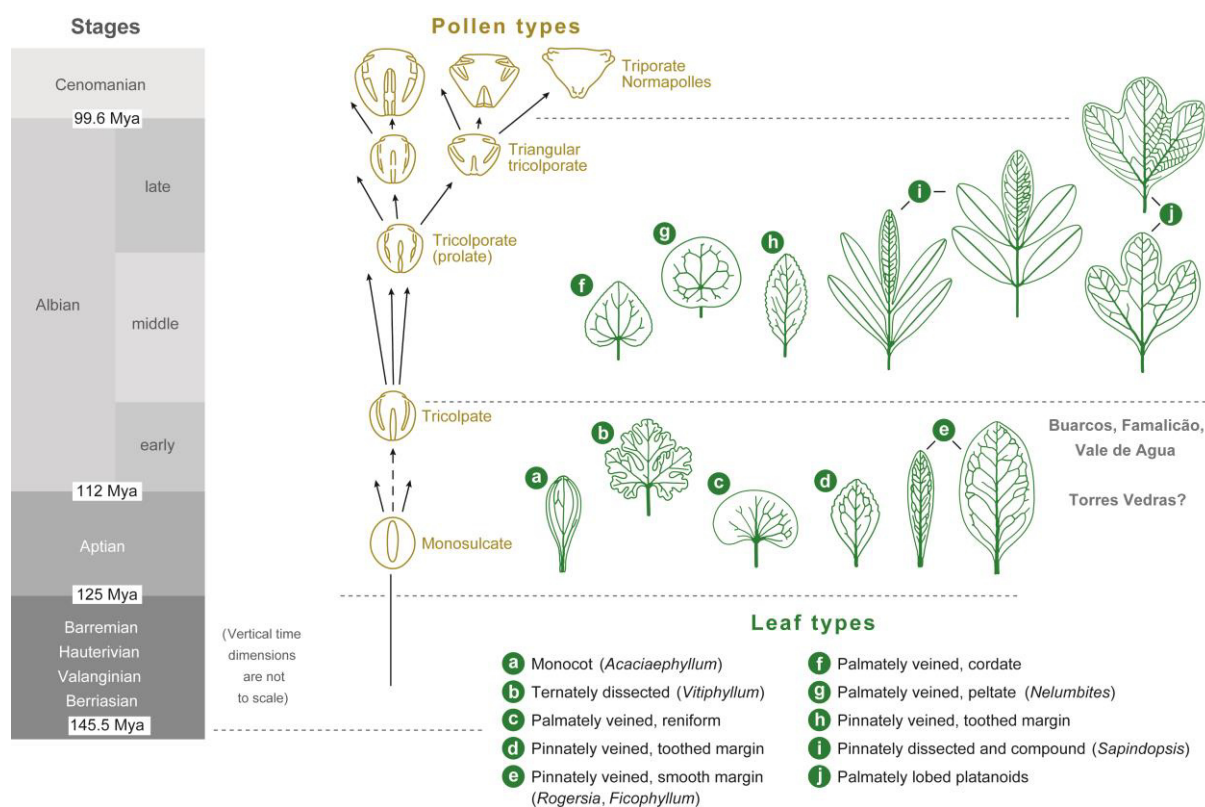


Fig. 5. Stratigraphic diversification sequence of major angiosperm pollen and leaf types in the Potomac Group of eastern North America, with correlations to angiosperm macrofossil localities in the Lusitanian Basin, Portugal (modified from Doyle 2012). Abbreviation: Mya, million years ago.

1976, Doyle & Robbins 1977, Upchurch 1984). The oldest fossil angiosperm leaves are rare, simple and are usually pinnately veined (*Vitiphyllum*) with irregular venation, followed by peltate leaves, palmately lobed and also pinnately dissected and compound leaves (*Sapindopsis*) (Fig. 5). These early angiosperms most likely had an herbaceous (Hickey & Doyle 1977, Taylor & Hickey 1992) or woody understory lifestyle (Feild et al. 2004). The discovery of fragmentary records of fossil angiosperm wood during the Albian provides the first evidence of a shift towards an arborescent lifestyle (Wing & Boucher 1998, Phillippe et al. 2008). According to Peralta-Medina & Falcon-Lang

(2012), the establishment of megathermal forests dominated by angiosperms only took place during the late Cretaceous.

Despite the wealth of information from the angiosperm macro- and mesofossil records, the fluvio-deltaic deposits of the Potomac Group and Portuguese records are derived from siliciclastic-rich strata with poor stratigraphic age control. Compared to the relatively fragmentary record of these macro- and mesofossil assemblages, palynological studies from the marine realm provide an excellent tool to track vegetation changes with continuous stratigraphic coverage. Palynological studies investigate both terrestrial (pollen and spores) fossils and marine fossils including single-celled algae (e.g. dinoflagellate cysts). Spores and pollen are derived from land plants thriving on the continents and are sensitive indicators to reconstruct short- and long-term variations in climate (Kujau et al. 2013). Marine dinoflagellate cysts significantly diversified during the Mesozoic and reached a diversity climax in the Cretaceous. These microfossils have been used as important biostratigraphic marker fossils to accurately date marine deposits with a temporal resolution far better than terrestrial-based palynomorphs, especially during the Albian (MacRae et al. 1996, Traverse 2007). On the other hand, terrestrial-derived palynomorphs have the advantage that in contrast to virtually all other fossils, they are transported over large distances by wind and water and are found in continental and marine sedimentary archives (Kürschner & Hengreen 2010). Based on these land-sea correlations, a continuous stratigraphic coverage can be expected for continental-derived palynomorphs from shallow marine strata compared to conventional, terrestrial records (Abbink 1998). Shallow marine records are especially good sedimentary archives as the close proximity to adjacent land masses reduces the effect of several processes (ocean circulation, transportation path, dilution of the terrestrial signal) that could affect the composition of the palynological record.

Recently, biostratigraphic evidence from the marine realm was used to recalibrate the age of the important angiosperm records from the continental-derived Potomac Group and Portuguese macrofossil successions (Hochuli et al. 2006, Heimhofer et al. 2007). These authors were able to show that the Potomac record contains a number of hiatuses and that some stratigraphic intervals (early Aptian to early Albian) were severely underrepresented. Whereas the early angiosperm radiation phase during the Barremian to middle Albian is now well documented from the Cresmina section in the Lusitanian Basin, continuous and high-resolution records into the late Albian to Cenomanian are still missing (Heimhofer et al. 2005).

2. Aims and objectives of the study

Until now, detailed, high-resolution and continuous studies into the temporal patterns of angiosperm evolution during the mid-Cretaceous are mostly lacking. In order to constrain the temporal resolution and pace of the early angiosperm radiation, well-dated shallow marine records with nicely preserved angiosperm pollen need to be investigated. In this study, sections in the southern Lusitanian Basin were used as sedimentary archives, with a particular focus on the São Julião section. The well-dated proximal marine section provides an ideal opportunity to investigate changes in the early angiosperm pollen evolution coupled with changes in the accompanying palynoflora and other climatic indices during the Albian-Cenomanian interval.

(1) Provide a well-dated reference record from shallow marine strata in the Lusitanian Basin.

Shallow marine strata of several sections in the southern Lusitanian Basin, Portugal have been logged and sampled in detail and a particular focus is placed on the establishment of a solid stratigraphic framework in order to reconstruct detailed (angiosperm) pollen records. In contrast to previously published records of these strata, the temporal resolution of these sections in this study will be significantly improved by a combined approach of several independent dating tools (e.g. dinoflagellate cyst biostratigraphy and chemostratigraphy).

(2) Describe the angiosperm pollen assemblage and provide detailed information on the temporal and diversification patterns.

Currently, most of the angiosperm pollen records from the Albian have been carried out in low resolution or are based on compilations of several records. The shallow marine deposits from the São Julião section provide a more or less continuous record to investigate angiosperm pollen patterns in high-resolution during the early Albian to early Cenomanian interval. The coastal location of the outcrop is prone to high erosion rates and easily accessible, allowing for the investigation of fresh and well-preserved angiosperm pollen. The high-resolution sampling, good preservation potential of the palynomorphs and solid temporal framework will significantly enhance our understanding of the temporal patterns during an important phase in the early angiosperm pollen diversification and allows a comparison to other palynological studies covering age-equivalent deposits to be made.

(3) Investigate the link between the angiosperm diversification and concurrent changes continental climate from the Lusitanian Basin during the Albian.

It has been suggested that paleo-environmental changes played a pivotal role in the rise of angiosperms during the mid-Cretaceous (Raven & Axelrod 1974, Coiffard et al. 2012, Chaboureau et al. 2014). However, continuous and long-ranging records with a particular focus on the early angiosperm diversification and terrestrial climate changes during the Albian are mostly lacking. The results from the total spore-pollen association and the clay mineral composition from the São Julião section allows a reconstruction of the angiosperm pollen distribution during an important interval in the early angiosperm radiation to be made and is linked to coeval changes in the accompanying terrestrial vegetation composition and changes in humidity.

3. Synopsis

An important aspect in describing changes in the terrestrial palynomorphs record is a detailed age-assignment of the investigated strata. **Chapter 2** deals with the lithological description and correlation of several coastal sections of in the southern part of the Lusitanian Basin, Portugal. These sections (Magoito, Praia das Maças and São Julião) were described, logged on a bed-by-bed basis and sampled in detail. The thick (192 m) São Julião section thereby serves as the reference record. Using a combined approach of chemo- and biostratigraphy, a detailed stratigraphic age-assignment of the different sections provides an early Albian to early Cenomanian age. Comparison of São Julião with the Guincho section, located in the southern Lusitanian Basin of early Albian to late Albian age shows a significantly expanded late Albian succession at São Julião. Correlation of the Portuguese carbon isotope curves with other hemipelagic and well-dated Albian records in Italy and France further constrain the age of the different sections. The new stratigraphic age-model significantly improves the correlation and age assignments from previous authors and serves as an excellent temporal framework for future studies.

A high-resolution angiosperm pollen record covering early Albian to early Cenomanian strata from the São Julião section is presented in **Chapter 3**. The palynological record is characterized by increased diversity among monocolpate and poly-aperture pollen and includes both already described as well as previously undescribed (informal) species. In total, 79 different angiosperm pollen species are recorded and described. The majority (49) of the species are poly-aperture pollen of eudicot affinity. The early Albian is characterized by a dominance of monocolpate angiosperm pollen with few poly-aperturate pollen grains; strata of middle and late Albian age record a significant increase of poly-aperturate pollen. Furthermore, biostratigraphic descriptions of several of the recorded angiosperm pollen are given, as well as a comparison and correlation of the Portuguese angiosperm pollen assemblage with the Potomac Group succession (USA). Based on our new data, a revised age of the palynological Subzones II-B and II-C in the Potomac Group succession is provided. Despite a major rise in diversity, angiosperm pollen abundances remain mostly subordinate in the total palynoflora (<10%), reflecting the subordinate role of angiosperms within the continental biomass.

Currently, only few continuous and high-resolution studies exist with a particular focus on changes in continental climate and vegetation response during the Albian. In **Chapter 4**, changes in the spore-pollen composition and in the clay mineral record are used to reconstruct the terrestrial climate from the São Julião section. The reconstructed vegetation from the spore-pollen composition shows a dominance of Cheirolepidaceae and Taxodiacean conifers, with minor abundances of ferns and angiosperms. The terrestrial climate in the Lusitanian Basin is marked by a clear aridification trend from the early Albian to early Cenomanian, punctuated by an interval of increased moisture availability during the late Albian. The angiosperm pollen record shows a distinct rise in eudicot over magnoliid-monocot dominance concurrent with rising sea surface temperatures as derived from the marine realm. This observation is interpreted to represent the northward migration of mostly eudicots from the lower latitudes towards the Lusitanian Basin. Despite an apparent observed offset between the raw (counted) angiosperm pollen diversity and expected species richness indices, the data is interpreted to represent higher angiosperm pollen diversities during periods of enhanced aridity.

In **Chapter 5**, the most important conclusions of the thesis as well as a final synthesis of the current study are presented and subsequently discussed.

4. References

- Abbink, O., 1998. Palynological Investigations in the Jurassic of the North Sea region. Ph.D. thesis, Universiteit Utrecht, The Netherlands, 192 pp. Published thesis.
- Arens, N.C., Harris, E.B., 2015. Paleoclimatic reconstruction for the Albian–Cenomanian transition based on a dominantly angiosperm flora from the Cedar Mountain Formation, Utah, USA. *Cretaceous Research* 53, 140-152.
- Arthur, M.A., Jenkyns, H.C., Brumsack, H.-J., Schlanger, S.O., 1990. Stratigraphy, geochemistry, and paleoceanography of organic-carbon-rich Cretaceous sequences, in *Cretaceous Resources, Events and Rhythms*, NATO ASI Ser., vol. 304, edited by R. N. Ginsburg and B. Beaudoin, pp. 75–119.
- Arthur, M.A., Sageman, B.B., 1994. Marine shales: depositional mechanisms and environments of ancient deposits. *Annual Review of Earth and Planetary Sciences* 22, 499-551.
- Axelrod, D., 1952. A theory of angiosperm evolution. *Evolution* 6, 29–60.
- Axelrod, D., 1970. Mesozoic paleogeography and early angiosperm history. *Botanical Review* 36, 277–319.
- Bice, K.I., Bralower, T.J., Duncan, R.A., Huber, B.T., Leckie, R.M. and Sageman, B.B., 2003. http://www.whoi.edu/ccod/CCOD_report.html.
- Bice, K.L., Birgel, D., Meyers, P.A., Dahl, K.A., Hinrichs, K.-U., and Norris, R.D., 2006, A multiple proxy and model study of the Cretaceous upper ocean temperatures and atmospheric CO₂ concentrations: *Paleoceanography* 21, 17pp.
- Bralower, T.J., Arthur, M.A., Leckie, R.M., Sliter, W.V., Allard, D., Schlanger, S.O., 1994. Timing and paleoceanography of oceanic dysoxia/anoxia in the late Barremian to early Aptian, *Palaios* 9, 335–369.
- Brenner, G.J., 1963. The spores and pollen of the Potomac Group of Maryland. *Maryland Department of Geology, Mines and Water Resources* 27, 1–215.
- Brenner, G.J., 1976. Middle Cretaceous floral provinces and early migration of angiosperms. In: Beck, C.B. (Ed.), *Origin and Early Evolution of Angiosperms*. Columbia University Press, New York, 23–44.
- Cardinal, S., Danforth, B. N., 2013. Bees diversified in the age of eudicots. *Proceedings of the Royal Society B, Biological Sciences* 280, 10 pp.
- Chaboureaud, A.C., Sepulchre, P., Donnadiou, Y., Franc, A., 2014. Tectonic-driven climate change and the diversification of angiosperms. *Proceedings of the National Academy of Sciences* 111, 14066-14070.
- Chumakov, N.M., Zharkov, M.A., Herman, A.B., Doludenko, M.P., Kalandadze, N.M., Lebedev, E.L., Ponomarenko, A.G. and Rautian, A.S., 1995. Climatic belts of the mid-Cretaceous time. *Stratigraphy and Geological Correlation* 3, 241-260.
- Coiffard, C., Gomez, B., Daviero-Gomez, V., Dilcher, D.L., 2012. Rise to dominance of angiosperm pioneers in European Cretaceous environments. *Proceedings of the National Academy of Sciences*, 109, 20955-20959.
- Clarke, J.T., Warnock, R.C.M., Donoghue, P.C.J., 2011. Establishing a time-scale for plant evolution. *New Phytologist* 192, 266–301.
- Clarke, L.J., Jenkyns, H.C., 1999. New oxygen isotope evidence for long-term Cretaceous climatic change in the Southern Hemisphere. *Geology* 27, 699-702.
- Cornet, B., 1989. Late Triassic angiosperm-like pollen from the Richmond rift basin of Virginia, U.S.A. *Palaeontographica Abteilung B* 213, 37–87

- Crane, P.R., Lidgard, S., 1989. Angiosperm diversification and paleolatitudinal gradients in Cretaceous floristic diversity. *Science* 246, 675-678.
- Crane, P.R., Friis, E.M., Pedersen, K.R., 1995. The origin and early diversification of angiosperms. *Nature* 374, 27-33.
- Crepet, W.L., Niklas, K.J., 2009. Darwin's second "abominable mystery": Why are there so many angiosperm species? *American Journal of Botany* 96, 366-381.
- De Lurio, J.L., Frakes, L.A., 1999. Glendonites as a paleoenvironmental tool: implications for early Cretaceous high latitude climates in Australia. *Geochimica Et Cosmochimica Acta* 63, 1039-1048.
- Diéguez, C., Peyrot, D., Barrón, E. 2010. Flora and vegetation patterns of the Iberian Peninsula from the Rhaetian–Hettangian boundary to the Cretaceous–Tertiary boundary. *Review of Palaeobotany and Palynology* 162, 325-340.
- Dilcher D.L., 1974. Approaches to the identification of angiosperm leaf remains. *Botanical Review* 40, 1–157
- Dinis, J.L., Oliveira, F.P., Rey, J., Duarte, I.L., 2010. Finding geological heritage: legal issues on private property and fieldwork. The case of outstanding early angiosperms (Barremian to Albian, Portugal). *Geoheritage* 2, 77-90.
- Doyle, J.A., 2012. Molecular and Fossil Evidence on the Origin of Angiosperms. *Annual Review of Earth and Planetary Sciences* 40, 301-326.
- Doyle, J.A., Hickey, L.J., 1976. Pollen and leaves from the mid-Cretaceous Potomac Group and their bearing on early angiosperm evolution. In: Beck, C.B. (Ed.), *Origin and Early Evolution of Angiosperms*. Columbia University Press, New York, 139–206.
- Doyle, J.A., Robbins, E.I., 1977. Angiosperm pollen zonation of the continental Cretaceous of the Atlantic coastal plain and its application to deep wells in the Salisbury Embayment. *Palynology* 1, 43–78.
- Doyle, J.A., Endress, P.K., 2010. Integrating Early Cretaceous fossils into the phylogeny of living angiosperms: Magnoliidae and eudicots. *Journal of Systematics and Evolution* 48, 1–35.
- Doyle, J.A., Endress, P.K., 2014. Integrating Early Cretaceous fossils into the phylogeny of living angiosperms: ANITA lines and relatives of Chloranthaceae. *International Journal of Plant Sciences*, 175, 555-600.
- Dumitrescu, M., Brassell, S.C., Schouten, S., Hopmans, E.C., Sinninghe Damsté, J.S., 2006. Instability in tropical Pacific sea-surface temperatures during the early Aptian. *Geology* 34, 833–836,
- Endress, P.K., 2010. Flower Structure and Trends of Evolution in Eudicots and Their Major Subclades 1. *Annals of the Missouri Botanical Garden* 97, 541-583.
- Erbacher, J., Huber, B.T., Norris, R.D., Markey, M., 2001. Increased thermohaline stratification as a possible cause for an ocean anoxic event in the Cretaceous period. *Nature* 409, 325–327.
- Feild, T.S., Arens, N.C., Doyle, J.A., Dawson, T.E., Donoghue, M.J., 2004. Dark and disturbed: A new image of early angiosperm ecology. *Paleobiology* 30, 82–107.
- Forster, A., Schouten, S., Baas, M., Sinninghe Damsté, J.S., 2007. Mid-Cretaceous (Albian–Santonian) sea surface temperature record of the tropical Atlantic Ocean. *Geology* 35, 919-922.
- Frakes, L.A. Francis, J.E., 1988. A guide to Phanerozoic cold polar climates from high-latitude ice-rafting in the Cretaceous. *Nature* 333, 547–549.
- Friedrich, O., Norris, R.D., Erbacher, J., 2012. Evolution of middle to Late Cretaceous oceans -A 55 m.y. record of Earth's temperature and carbon cycle. *Geology* 40, 107-110.

-
- Friis, E.M., Pedersen, K.R., Crane, P.R., 1999. Early angiosperm diversification: the diversity of pollen associated with angiosperm reproductive structures in Early Cretaceous floras from Portugal. *Annals of the Missouri Botanical Garden* 86, 259–296.
- Friis, E.M., Pedersen, K.R., Crane, P.R., 2010. Diversity in obscurity: fossil flowers and the early history of angiosperms. *Philosophical Transactions of the Royal Society B: Biological Sciences* 365, 369–382.
- Giorgioni, M., Weissert, H., Bernasconi, S.M., Hochuli, P.A., Coccioni, R., Keller, C.E., 2012. Orbital control on carbon cycle and oceanography in the mid-Cretaceous greenhouse. *Paleoceanography* 27, PA1204.
- Gradstein, F.M., Ogg, J., Schmitz, M.A., Ogg, G., 2012. *A Geologic Time Scale 2012*. Elsevier Publishing Company.
- Grimaldi, D., 1999. The co-radiations of pollinating insects and angiosperms in the Cretaceous. *Annals of the Missouri Botanical Garden*, 373–406.
- Gübeli, A., Hochuli, P.A., Wildi, W., 1984. Lower Cretaceous turbiditic sediments from the Central Rif chain (northern Morocco). *Palynology, stratigraphy and palaeogeographic setting*. *Geol. Rundschau* 73, 1081–1114.
- Haq, B.U., Hardenbol, J., Vail, P.R., 1987. Chronology of fluctuating sea levels since the Triassic. *Science* 235, 1156–1167.
- Hay, W.W., Floegel, S., 2012. New thoughts about the Cretaceous climate and oceans. *Earth-Science Reviews* 115, 262–272.
- Heimhofer, U., Hochuli, P.A., Burla, S., Dinis, J.L., Weissert, H., 2005. Timing of Early Cretaceous angiosperm diversification and possible links to major paleoenvironmental change. *Geology* 33, 141–144.
- Heimhofer, U., Hochuli, P.A., Burla, S., Weissert, H., 2007. New records of Early Cretaceous angiosperm pollen from Portuguese coastal deposits: Implications for the timing of the early angiosperm radiation. *Review of Palaeobotany and Palynology* 144, 39–76.
- Hickey, L.J., Wolfe, J.A., 1975. The bases of angiosperm phylogeny: vegetative morphology. *Annals of the Missouri Botanical Garden*, 538–589.
- Hickey, L.J., Doyle, J.A., 1977. Early Cretaceous fossil evidence for angiosperm evolution. *Botanical Review* 43, 3–104.
- Hochuli, P.A., Heimhofer, U., Weissert, H., 2006. Timing of early angiosperm radiation: recalibrating the classical succession. *Journal of the Geological Society* 163, 587–594.
- Hochuli, P.A., Feist-Burkhardt, S., 2004. A boreal early cradle of Angiosperms? Angiosperm-like pollen from the Middle Triassic of the Barents Sea (Norway). *Journal of Micropalaeontology* 23, 97–104.
- Hochuli, P.A., Feist-Burkhardt, S., 2013. Angiosperm-like pollen and Afropollis from the Middle Triassic (Anisian) of the Germanic Basin (northern Switzerland). *Frontiers in plant science* 4, 344.
- Hu, X., Wagreich, M., Yilmaz, I.O., 2012. Marine rapid environmental/climatic change in the Cretaceous greenhouse world. *Cretaceous Research* 38, 1–6.
- Huber, B.T., Hodell, D.A., Hamilton, C.P., 1995. Middle-Late Cretaceous climate of the southern 1268 high latitudes: stable isotopic evidence for minimal 1269 equator-to-pole thermal gradients. *Geological Society of America Bulletin* 107, 1164–1191.
- Hughes, N.F., McDougall, A.B., 1987. Records of angiospermid pollen entry into the English Early Cretaceous succession. *Review of Palaeobotany and Palynology* 50, 255–272.

-
- Jarvis, I., Gale, A.S., Jenkyns, H.C., Pearce, M. A., 2006. Secular variation in Late Cretaceous carbon isotopes: A new $\delta^{13}\text{C}$ carbonate reference curve for the Cenomanian- Campanian (99.6–70.6 Ma), *Geological Magazine* 141, 561–608.
- Jenkyns, H.C., 1980. Cretaceous anoxic events: From continents to oceans, *Journal of the Geological Society* 137, 171–188.
- Jenkyns, H.C., Forster, A., Schouten, S., Sinninghe Damsté, J.S., 2004. High temperatures in the Late Cretaceous Arctic Ocean, *Nature* 432, 888–892.
- Jenkyns, H.C., 2010. Geochemistry of oceanic anoxic events. *Geochemistry Geophysics Geosystems* 11, 30 pp.
- Jenkyns, H., Schouten-Huibers, L., Schouten, S., Sinninghe Damsté, J.S., 2012. Warm Middle Jurassic-Early Cretaceous high-latitude sea-surface temperatures from the Southern Ocean. *Climate of the Past* 8, 215-226.
- Kominz, M., Browning, J., Miller, K., Sugarman, P., Mizintseva, S., Scotese, C., 2008. Late Cretaceous to Miocene sea-level estimates from the New Jersey and Delaware coastal plain coreholes: An error analysis. *Basin Research* 20, 211-226.
- Kujau, A., Heimhofer, U., Hochuli, P. A., Pauly, S., Morales, C., Adatte, T., Föllmi, K., Ploch, I., Mutterlose, J., 2013. Reconstructing Valanginian (Early Cretaceous) mid-latitude vegetation and climate dynamics based on spore–pollen assemblages. *Review of Palaeobotany and Palynology* 197, 50-69.
- Kürschner, W.M., Herengreen W.G.F., 2010. Triassic palynology of central and northwestern Europe: a review of palynofloral diversity patterns and biostratigraphic subdivisions. In: Lucas SG (ed) *The Triassic Timescale*. Geological Society of London, Special Publications 334, 263–283.
- Larson, R.L., 1991. Geological consequences of superplumes. *Geology* 19, 963-966.
- Legrand, J., Yamada, T., Nishida, H., 2014. Palynofloras from the upper Barremian-Aptian Nishihiro Formation (Outer Zone of southwest Japan) and the appearance of angiosperms in Japan. *Journal of plant research* 127, 221-232.
- Li, W., Liu, Z., 1994. The Cretaceous palynofloras and their bearing on stratigraphic correlation in China. *Cretaceous Research* 15, 333–365.
- Lidgard, S., Crane, P.R., 1988. Quantitative analyses of the early angiosperm radiation. *Nature* 331, 344-346.
- Magallón S., Sanderson M. 2005. Angiosperm divergence times: the effect of genes, codon positions, and time constraints. *Evolution* 59, 1653–1670.
- Magallón, S., 2010. Using fossils to break long branches in molecular dating: a comparison of relaxed clocks applied to the origin of angiosperms. *Systematic Biology* 59, 384–399.
- MacRae, R.A., Fensome, R.A., Williams, G.L., 1996). Fossil dinoflagellate diversity, originations, and extinctions and their significance. *Canadian Journal of Botany* 74, 1687-1694.
- Mendes, M.M., Dinis, J., Pais, J., Friis, E.M., 2011. Early Cretaceous flora from Vale Painho (Lusitanian Basin, western Portugal): an integrated palynological and mesofossil study. *Review of Palaeobotany and Palynology* 166, 152-162
- Mendes, M.M., Dinis, J., Pais, J., Friis, E.M., 2014. Vegetational composition of the Early Cretaceous Chicalhão flora (Lusitanian Basin, western Portugal) based on palynological and mesofossil assemblages. *Review of Palaeobotany and Palynology* 200, 65-81.
- Moldowan, J.M., Dahl, J., Huizinga, B.J., Fago, F.J., Hickey, L.J., Peakman, T.M., D.W., Taylor., 1994. The molecular fossil record of oleanane and its relation to angiosperms. *Science* 265, 768-771.

-
- Mutterlose, J., Bornemann, A., Herrle, J., 2009. The Aptian–Albian cold snap: evidence for “mid” Cretaceous icehouse interludes. *Neues Jahrbuch für Geologie und Paläontologie Abhandlungen* 252, 217–225.
- Norris, G., 1967. Spores and pollen from the Lower Colorado Group (Albian–?Cenomanian) of Central Alberta. *Palaeontographica Abteilung B* 120, 72–115.
- Parrish, J.T., Daniel, I.L., Kennedy, E.M., Spicer, R.A., 1998. Paleoclimatic significance of mid-Cretaceous floras from the middle Clarence Valley, New Zealand. *Palaios* 13, 149-159.
- Peralta-Medina, E., Falcon-Lang, H. J. 2012. Cretaceous forest composition and productivity inferred from a global fossil wood database. *Geology* 40, 219-222.
- Philippe, M., Gomeza, B., Girard, V., Coiffard, C., Daviero-Gomez, V., Thevenard, F., Billon-Bruyat, J-P., Myette, G., Latil, J-L., Leloeuff, J., Néraudeau, D., Olivero, D., Schögl, J., 2008. Woody or not woody? Evidence for early angiosperm habit from the Early Cretaceous fossil wood record of Europe. *Palaeoworld* 17, 142–152.
- Price, G.D., 1999. The evidence and implications of polar ice during the Mesozoic. *Earth-Science Reviews* 48, 183-210.
- Raven, P.H., Axelrod, D.I., 1974. Angiosperm biogeography and past continental movements. *Annals of the Missouri Botanical Garden*, 539-673.
- Romero, E.J., Archangelsky, S., 1986. Early Cretaceous angiosperm leaves from southern South America. *Science* 234, 1580-1582.
- Sahagian, D., Pinous, O., Olfieriev, A., Zakharov, V., 1996. Eustatic curve for the Middle Jurassic-Cretaceous based on Russian platform and Siberian stratigraphy: zonal resolution. *AAPG Bulletin-American Association of Petroleum Geologists* 80, 1433-1458.
- Saporta, G.D., 1894. Flore fossile du Portugal. Nouvelles contributions à la flore Mésozoïque. Accompagnées d'une notice stratigraphique par Paul Choffat. Imprimerie de l'Académie Royale des Sciences, Lisbon.
- Schouten, S., Hopmans, E.C., Forster, A., van Breugel, Y., Kuypers, M.M.M., Sinninghe Damsté, J.S., 2003. Extremely high sea-surface temperatures at low latitudes during the middle Cretaceous as revealed by archaeal membrane lipids: *Geology* 31, 1069–1072.
- Schlanger, S., Jenkyns, H., 1976. Cretaceous oceanic anoxic events: causes and consequences. *Geologie en mijnbouw* 55, 179-184
- Scholle, P. A., Arthur, M.A., 1980. Carbon isotope fluctuations in Cretaceous pelagic limestones: Potential stratigraphic and petroleum exploration tool, *AAPG Bulletin-American Association of Petroleum Geologists*. 64, 67–87.
- Smith S., Beaulieu J., Donoghue M., 2010. An uncorrelated relaxed-clock analysis suggests an earlier origin for flowering plants. *Proceedings of the National Academy of Sciences, USA* 107, 5897–5902.
- Soltis, P.S., Soltis, D.E., 2004. The origin and diversification of the angiosperms. *American Journal of Botany* 91, 1614–1626.
- Spicer, R.A., Parrish, J.T., 1986. Paleobotanical evidence for cool north polar climates in middle Cretaceous (Albian-Cenomanian) time. *Geology* 14, 703-706.
- Steuber, T., Rauch, M., Mase, J.-P., Graaf, J., Malkoč, M., 2005. Low-latitude seasonality of Cretaceous temperatures in warm and cold episodes. *Nature* 437, 1341–1344.
- Strauss, H., 2006. Anoxia through time. In *Past and Present Water Column Anoxia*, pp. 3-19.

-
- Sun G., Dilcher D.L., Zheng S., Zhou Z., 1998. In search of the first flower: a Jurassic angiosperm, *Archaeofructus*, from northeast China. *Science* 282, 1692–95
- Sun G., Ji Q., Dilcher D.L., Zheng S., Nixon K.C., Wang X., 2002. *Archaeofructaceae*, a new basal angiosperm family. *Science* 296, 899–904
- Taylor, D.W., Hickey, L.J., 1992. Phylogenetic evidence for the herbaceous origin of angiosperms. *Plant Systematics and Evolution*, 180(3-4), 137-156.
- Teixeira, C., 1945. *Nymphéacées Fossiles du Portugal*. Serviços Geológicos de Portugal, Lisbon.
- Teixeira, C., 1946. Flora cretácica de Esgueira (Aveiro). *Portugaliae Acta Biologica* 1, 235–242.
- Teixeira, C., 1947. Nouvelles recherches et revision de la flore de Cercal. *Brontéia - Sér. de Ciênc. Naturais* I, 5–15.
- Teixeira, C., 1948. Flora mesozóica portuguesa Part I. Serviços Geológicos de Portugal, Lisbon.
- Teixeira, C., 1950. Flora Mesozoica Portuguesa II. Serv. Geol, Portugal, Lisboa. 35 pp.
- Teixeira, C., 1952. Notes sur quelques gisements des végétaux fossiles du Crétacé des environnements de Leiria. *Revista da Faculdade de Ciências – Universidade de Lisboa* 2, ser. C2, pp. 133–154.
- Trabucho-Alexandre, J., van Gilst, R.I., Rodriguez-Lopez, J.P., de Boer, P.L., 2011. The sedimentary expression of oceanic anoxic event 1b in the North Atlantic, *Sedimentology* 58, 1217–1246.
- Traverse, A., 2007. *Paleopalynology* Dordrecht: Springer, 813pp.
- Truswell, E.M., 1990. Cretaceous and Tertiary vegetation of Antarctica: a palynological perspective. In: *Antarctic Palaeobiology*, eds. Taylor, T.N., Taylor, E.L., 71-88.
- Ufnar, D.F., González, L.A., Ludvigson, G.A., Brenner, R.L., Witzke, B.J., 2002. The mid-Cretaceous water bearer: isotope mass balance quantification of the Albian hydrologic cycle. *Palaeogeography, Palaeoclimatology, Palaeoecology* 188, 51-71.
- Ufnar, D.F., González, L.A., Ludvigson, G.A., Brenner, R.L., Witzke, B.J., 2004. Evidence for increased latent heat transport during the Cretaceous (Albian) greenhouse warming. *Geology* 32, 1049-1052.
- Upchurch, G. Jr. 1984. Cuticular anatomy of angiosperm leaves from the Lower Cretaceous Potomac Group. I. Zone I leaves. *American Journal of Botany* 71, 192–202.
- Weissert, H., Lini, A., Föllmi, K.B., Kuhn, O., 1998. Correlation of Early Cretaceous carbon isotope stratigraphy and platform drowning events: a possible link? *Palaeogeography, Palaeoclimatology, Palaeoecology* 137, 189-203.
- Weissert, H., Erba, E., 2004. Volcanism, CO₂ and palaeoclimate: a Late Jurassic–Early Cretaceous carbon and oxygen isotope record. *Journal of the Geological Society* 161, 695-702.
- Wing, S.L., Boucher, L.D., 1998. Ecological aspects of the Cretaceous flowering plant radiation. *Annual Review of Earth and Planetary Sciences* 26, 379-421.
- Wolfe, J.A., Upchurch, G.R., 1987. North American nonmarine climates and vegetation during the Late Cretaceous. *Palaeogeography, Palaeoclimatology, Palaeoecology* 61, 33-77.
- Wortmann, U.G., Herrle, J.O., Weissert, H. 2004. Altered carbon cycling and coupled changes in Early Cretaceous weathering patterns: evidence from integrated carbon isotope and sandstone records of the western Tethys. *Earth and Planetary Science Letters* 220, 62-82.
- Wilson, P.A., Norris, R.D., 2001. Warm tropical ocean surface and global anoxia during the mid-Cretaceous period. *Nature* 412, 425– 429.

Zhang, M., Dai, S., Pan, B., Wang, L., Peng, D., Wang, H., Zhang, X., 2014. The palynoflora of the Lower Cretaceous strata of the Yingen-Ejinaqi Basin in North China and their implications for the evolution of early angiosperms. *Cretaceous Research* 48, 23-38.

Zhou Z., Barrett P.M., Hilton J., 2003. An exceptionally preserved Lower Cretaceous ecosystem. *Nature* 421, 807–814.

Integrated stratigraphy of shallow marine Albian strata from the southern Lusitanian Basin of Portugal

Maurits Horikx¹, Ulrich Heimhofer¹, Jorge Dinis², Stefan Huck¹

¹Institute of Geology, Leibniz University Hannover, Callinstrasse. 30, 30167 Hannover, Germany.

²IMAR – Institute of Marine Research, Earth Sciences Department, University of Coimbra, 3000-272 Coimbra, Portugal.

1. Abstract

Stratigraphic age assignment of Cretaceous shoal water deposits is notoriously difficult and often hampered by the lack of typical index fossils and the prevalence of sedimentary gaps. Here we present new bio- and chemostratigraphic data for three sections located in the Lusitanian Basin, Portugal, composed of Albian strata. Sections are correlated and dated using dinoflagellate cyst biostratigraphy, strontium-isotope stratigraphy based on oyster and rudist shells and carbon isotope stratigraphy. The measured Sr-isotope values from pristine shells are in line with global open marine $^{87}\text{Sr}/^{86}\text{Sr}$ values from the Albian. Correlation of the Portuguese C-isotope curve with hemipelagic Albian reference records and the presence of typical Albian dinoflagellate cysts further constrain the age of the different sections. The proximal-marine and thick (~190 m) São Julião section serves hereby as reference curve. Correlation with the independently well-dated and more distal Guincho section in the Lusitanian Basin slightly revise the age of the São Julião and Magoito sections compared to previously published results. Furthermore, our new findings demonstrate the time-transgressive nature of marine deposition in the southern Lusitanian Basin. The onset of marine conditions in the Água Doce Member and the deposition of rudist bearing carbonates of the Ponta da Galé Member are diachronous and started significantly earlier in the southernmost part of the basin compared to the north.

In summary, the combined geochemical and biostratigraphic results provide an enhanced time control and slightly revise the age of the sections in comparison to previously published studies while providing lithological descriptions, Sr-isotope derived ages and carbon isotope records. Furthermore, the carbon-isotope record of São Julião can be correlated with Italian (Umbria-Marche Basin) and French (Vocontian Trough) sections and highlights the applicability of shallow marine deposits as chemostratigraphic archives.

Keywords: Lusitanian Basin, Albian, carbon isotopes, strontium-isotope stratigraphy, intrabasinal correlation, dinoflagellate cyst biostratigraphy

2. Introduction

The Albian stage (113.0–100.5 Ma, Gradstein et al. 2012) was first described by d’Orbigny (1842) and is the youngest chronostratigraphic unit of the Lower Cretaceous. In the past, the Aptian-Albian boundary was based on different ammonite zones. However, due to the endemic and sparse occurrence of most of the ammonite marker species, an exact definition of the boundary has not been established (Kennedy et al. 2000; Hancock 2001; Owen 2002, Mutterlose et al. 2003). The Albian is further subdivided into the early (113–110.7 Ma), middle (110.7–107.7 Ma) and the long-lasting late (107.7–100.5 Ma) Albian (Gradstein et al. 2012). The first occurrence (FO) of the ammonite *Lyellicerias lyelli* was proposed to mark the early-middle Albian boundary, while the middle to late Albian boundary is marked by the FO of the ammonite *Diploceras cristatum* (Gale et al. 2011). The Albian-Cenomanian boundary is well-defined and is based on the lowest occurrence of the planktonic foraminifera, *Rotalipora globotruncanoides*. The GSSP section is located at Mont Risou, SE France (Gale et al. 1996, 2011, Kennedy et al. 2000).

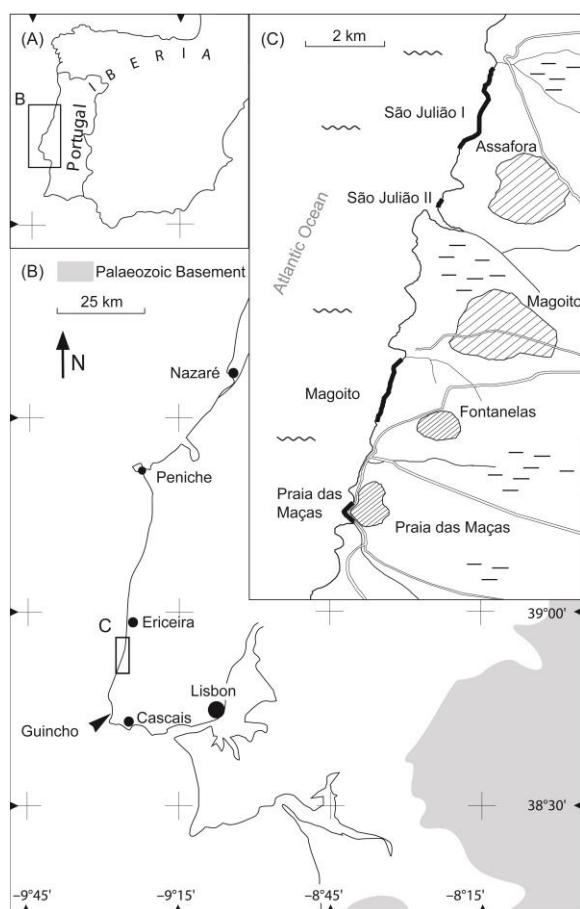


Fig. 1. (A) Map of the study area located in western Iberia. (B) Map of the study area showing the location of the Guincho and the sections described in this study between the towns of Ericeira and Cascais. (C) Detailed map showing exact position of the São Julião (I + II), Magoito and Praia das Maças sections along the coastal strip south of Ericeira (figure adopted and modified from Heimhofer et al. 2005).

In open marine settings, the Albian sedimentary record is punctuated by the episodic formation of organic carbon-rich deposits, some of which are regarded as oceanic anoxic events (OAEs). This includes the Paquier horizon (OAE1b) located at the base of the Albian as well as the terminal Albian Niveau Breistroffer (OAE1d), which are both associated with negative and positive carbon isotope anomalies, respectively (Petrizzo et al. 2008, Gale et al. 2011, Giorgioni et al. 2012).

Most stratigraphic studies from the Albian focused on open marine deposits and only few coastal marine records have been investigated. An exception is represented by the well exposed and shallow marine records from the Lusitanian Basin.

The Lusitanian Basin of central Portugal represents a classical area for the study of early Cretaceous strata. The sedimentary deposits have been first described during the 19th century (Choffat 1885, 1886, 1900, Sharpe 1850) and additional studies have been carried out later on (e.g., Rey 1979, 1992,

Rey 1993). Well exposed sections from the Albian along the coastal cliffs between the towns of Ericeira and Cascais and more inland in the southern part of the Lusitanian Basin have been intensively studied. Topics include terrestrial and marine microfossils (Rey et al. 1977, Berthou et al. 1980, Medus & Berthou 1980, Hasenboehler 1981, Chapman 1982, Berthou & Hasenboehler, 1982, Medus 1982, Berthou 1984, Berthou & Leereveld 1990, Heimhofer et al. 2005, 2007, 2012), lithostratigraphy (Rey 1972, 1979, 1982, 1992, 1993) and sedimentology (Dinis & Trincão, 1995, Dinis 2001, Dinis et al. 2002). However, the lack of well-described high-resolution lithological and sedimentological logs inhibits the relocation of important fossil findings and lithostratigraphic boundaries in the Albian strata of the Lusitanian Basin. In this study, several sections from well exposed and easily accessible coastal sections (São Julião, Magoito and Praia das Maças) of Albian and early Cenomanian age are presented along a north-south transect. These sections are located between the towns of Ericeira and Praia das Maças in the southern part of the Lusitanian Basin (Fig. 1). The sections are in close proximity (~20 km) and contain proximal-marine to lagoonal deposits. Age assignment is difficult using conventional biostratigraphic techniques, as many important marker fossils are absent e.g., calcareous nannofossils and planktonic foraminifera) or very rare (ammonites). Alternatively, an integrated approach using different independent dating methods (dinoflagellate cyst biostratigraphy, carbon isotopes and strontium-isotopes from low-Mg calcite oyster and rudist shells) is used. In addition, the sections are compared to the already well-studied Guincho section located 25 km more to the south, which has been studied using strontium-isotope, lithological, sedimentological (Dinis et al. 2002, Heimhofer et al. 2007, 2012) and carbon isotope data (Burla 2007).

The aims of the study are:

- (1) Provide detailed lithological logs and sedimentological information for the Albian strata in the southern sector of the Lusitanian Basin.
- (2) Establish an intrabasinal correlation scheme for the studied sections.
- (3) Provide an integrated bio- and chemostratigraphic framework for the Albian and early Cenomanian aged Galé Formation.

3. Geological Setting

3.1 Geological evolution of the southern Lusitanian Basin

The Lusitanian Basin is located in the westernmost part of the Iberian Peninsula and is situated between the Hercynian highlands to the east and a number of horst structures (incl. the Berlengas Islands) to the west (Dinis et al. 2008). The northernmost boundary is located near the town of Aveiro, while the Arrabida Chain marks the southernmost boundary (Rasmussen et al. 1998). During the Triassic and Jurassic the Lusitanian Basin experienced subsidence due to regional and local rifting phases. Lower Cretaceous strata in the Lusitanian Basin was deposited on a passive margin related to the opening of the Atlantic and Tethys oceans during this time (Rey 1982). Palaeogeographically, the study area was located at ~30°N (Stampfli & Borel, 2002) during early Cretaceous times.

During the early Cretaceous, sedimentation of marine and terrestrial deposits was confined to the central and southern part of the Lusitanian Basin (Rey 1979, Cunha & Pena dos Reis, 1995, Dinis et al. 2008). The Berriasian was marked by the progradation of fluvial deposits and restricted marine conditions. This phase ends with a major unconformity in the late Berriasian (Dinis et al. 2008). A long term sea level rise lasted from the Valanginian to the Barremian. The Aptian-Albian transition is marked by a major unconformity covering huge parts of the Lusitanian Basin (Dinis & Trincão, 1995, Heimhofer et al. 2007). This unconformity was most probably caused by the opening of the Atlantic gateway and subsequent basin uplift (Dinis et al. 2002) and is overlain by coarse grained siliciclastics (Rodízio Formation) deposited diachronous throughout the basin in fluvial-deltaic settings. These deposits were covered by near-shore marine deposits and shoal-water carbonate platforms of the Galé Formation of Albian age. The absence of carbonate platforms and the formation of lagoonal and

terrestrial deposits mark the transition to the Caneças Formation. This regression phase is probably related to the compression of Africa, caused by the anti-clockwise rotation of the Iberian plate (Dinis et al. 2008).

3.2 Stratigraphy of Albian deposits in the southern Lusitanian Basin

The Rodízio Formation corresponds to the 'Couches d'Almargem partie supérieure' of Choffat (1885) and the 'Grès d'Almargem supérieurs' of Rey (1992) and consists of three members (Berthou & Lauerjat 1979, Dinis et al. 2002). The Rodízio Formation is overlain by marine deposits of the Galé Formation. The Galé Formation can be identified in large areas of the southern Lusitanian Basin and has been further subdivided into the Água Doce Member and the Ponta da Galé Member (Fig. 2) by Rey (1992). The Água Doce Member corresponds to the 'couches à *Knemiceras uhligi*' and the Ponta da Galé Member to the 'couches à *Polyconites subverneuil*' of Choffat (1885).

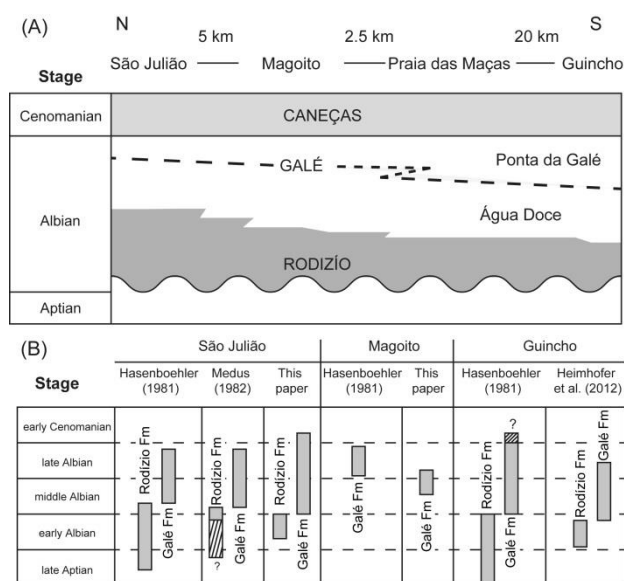


Fig. 2. (A) Synthetic lithostratigraphic chart covering the Aptian, Albian and early Cenomanian in the southern part of the Lusitanian Basin (see text for detailed description; figure modified from Dinis et al. 2008). Lines indicate distance between the different outcrops. (B) Compilation of the existing stratigraphic assignments of the Rodízio and Galé Formations in sections located in the southern Lusitanian Basin. Data from Hasenboehler (1981) and Medus (1982) based on palynostratigraphy; Heimhofer et al. (2012) based on chemo- and palynostratigraphy.

The lowermost Água Doce Member is mainly composed of alternating marly, carbonate- and sandstone-rich coastal-marine deposits. More marine conditions are evidenced by increasingly thicker limestone beds towards the top of this member and mark the transition to the overlying carbonate-rich Ponta da Galé Member (Rey 1992). This member is defined by the occurrence of the first rudist beds and shows an overall deepening trend (Rey 1992). Up to now, dating these deposits was essentially based on palynostratigraphy. More recently the Guincho section has been dated using dinoflagellate biostratigraphy combined with strontium-isotope stratigraphy (Heimhofer et al. 2012). An overview of these earlier studies (Hasenboehler 1981, Medus 1982, Heimhofer et al. 2012) from the São Julião, Magoito and Guincho sections is given in Fig. 2.

4. Material and Methods

Fieldwork for this study was carried out during two campaigns to Portugal in spring 2012 and 2013. During fieldwork, the coastal sections at São Julião (I & II), Magoito and Praia das Maças have been logged in detail (Fig. 3). Individual beds (> 10 cm) were logged using measurement tape and subsequently described. Samples were taken using a geological hammer and weathered-surfaces were avoided to reduce the possibility of contamination. Sampling close to magmatic sills and dykes was bypassed due to the risk of chemical alteration and thermally altered palynological samples. The

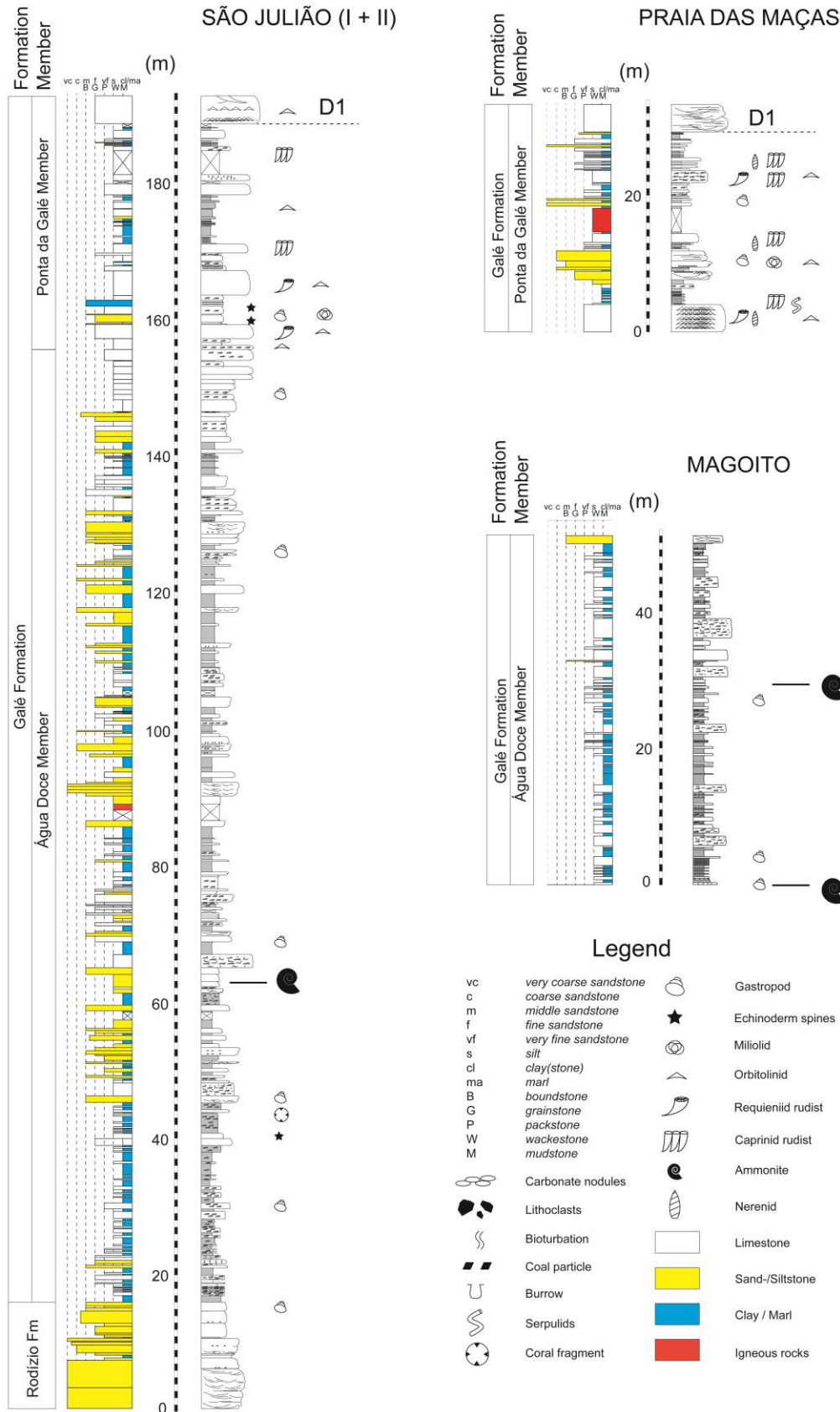


Fig. 3. High-resolution sedimentological lithological log of the São Julião, Magoito and Praia das Maças sections. The left-hand column indicates texture of carbonates (Durham classification) or grain size of siliciclastics, right-hand column shows weathering profile, macrofossil content and sedimentary structures. D1 shows marker horizon of Berthou & Lauverjat (1979) and Hasenboehler (1981). Lithological units follow Rey (1992) and Dinis et al. (2008). Ammonite occurrences at Magoito based on Hasenboehler (1981).

sections were sampled for carbon isotope stratigraphy and dinoflagellate cyst biostratigraphy. Oyster and rudist shells were collected for strontium-isotope stratigraphy. Dinoflagellate cyst sampling resolution is roughly every ~3 meter and for carbon isotope analysis ~1 meter. Lithological units and nomenclature follow Rey (1992) and Dinis et al. (2008).

4.1 Dinoflagellate biostratigraphy

A total of 97 samples (37 barren) were used for dinoflagellate cyst biostratigraphy selected from various lithologies, incl. siltstone, claystone, fine-grained sandstone and limestone. Samples have been cleaned before being prepared at the Geological Survey NRW, Krefeld, Germany using standard palynological treatment as described in Traverse (2007). After treatment the remaining organic matter was mounted on two slides per sample. The samples were studied with an OLYMPUS BX 53 transmitted light microscope, equipped with a XC50 digital camera. Preservation of the palynomorphs is generally good to very good.

4.2 Carbon and oxygen isotopes

Measurement of stable carbon and oxygen isotopes of sedimentary carbonates has been carried out on powdered bulk sample material on 271 samples. Sample powders were obtained using a micro-drill, dried for 24 h at 40°C, and subsequently analyzed for carbon and oxygen isotope composition. Where possible, the drilling of bioclasts and bioerosion structures has been avoided to reduce the risk of heterogeneity in bulk rock samples (Garrecht Metzger & Fike 2013). A Thermo Fisher Scientific Gasbench II carbonate device connected to a Thermo Fisher Scientific Delta V Advantage isotope ratio mass spectrometer, available at the Leibniz University Hannover, Germany, has been used for stable isotope analyses. Repeated analyses of certified carbonate standards (CO-1, NBS-18, NBS-19) show an external reproducibility $\pm 0.1\text{‰}$ for $\delta^{18}\text{O}$ and $\pm 0.08\text{‰}$ for $\delta^{13}\text{C}_{\text{carb}}$. Values are expressed in conventional delta notation relative to the V-PDB international standard, in per mil (‰).

4.3 Strontium-isotopes

Oyster and rudist shells were collected from the São Julião section. Before further processing, visual inspection of the shells was performed to avoid sampling of bioeroded parts, cements and other impurities within the shell structure. Oyster and rudist shells were then cut using a diamond saw, placed on a slide and polished. To further assess the preservation state of the shell, a HC5-LM cathodoluminescence (CL) microscope with hot cathode located at the Ruhr University Bochum, Germany was used. Following CL microscopy, only the most pristine parts of the shell were eventually selected, and powders were generated using a micro-drill. Sample powders were measured for the trace element content of Sr, Mg, Fe, and Mn at the stable isotope laboratory at Ruhr-University Bochum. Samples exceeding the threshold value for trace element concentrations were discarded. Finally, the Sr-isotope ratios were measured in the most pristine samples with a thermal ionization mass-spectrometer (Finnigan MAT 262) located at the Ruhr-University Bochum, Germany. Reference materials (USGS EN-1, NIST SRM 987) were measured in 2012–2013. The long-term standard mean ratios for reference materials (USGS EN-1, NIST NBS 987) are 0.709170 ($n=17$; 2σ mean= $2.0\cdot 10^{-6}$) and 0.710246 ($n=29$; 2σ mean= $2.0\cdot 10^{-6}$), respectively. Strontium-isotope ratios were adjusted to a USGS EN-1 value of 0.709175 and were subsequently compared to the strontium-isotope stratigraphy look-up table to derive numerical ages (version 4: 08/2003, Howarth & McArthur 1997, McArthur et al. 2001).

5. Results

5.1 Sedimentological description

5.1.1 São Julião

The São Julião section I is located ~5 km south of the town of Ericeira and starts at São Julião beach from where it can be continuously followed south (Table 1). The stratigraphic section stretches for 3 km with a dip of 2-3° to the south. The exposed succession ends with 2 distinct limestone beds on top of a clay-rich interval. Due to more favorable sampling conditions, the uppermost 12 m of the succession (São Julião II) was sampled at a different locality ~2 km further south. In total, the São Julião section has a thickness of 192 m (Fig. 3).

Table 1. GPS coordinates of start and end points of the logged sections in the southern Lusitanian Basin.

Section name	Base		Top	
	Latitude	Longitude	Latitude	Longitude
São Julião I	38°55'847"	9°25'241"	38°54'714"	9°25'854"
São Julião II	38°54'026"	9°26'116"	38°54'053"	9°26'090"
Magoito	38°51'763"	9°26'959"	38°50'934"	9°27'425"
Praia das Maças	38°49'733"	9°28'181"	38°49'577"	9°28'199"

At São Julião I, the lowermost 16 m are composed of coarse to medium-grained sandstones of the Rodízio Formation (Fig. 4A). The multicolored sandstones show meter-scale cross-bedding structures and are sometimes intercalated by small clay- and siltstone layers, especially near the top. Charcoal fragments occur frequently embedded in the sandstones. The sedimentary inventory and the lack of marine palynomorphs in the lower and middle part of the Rodízio Formation indicate a terrestrial, most probably fluvial to deltaic depositional environment. The Rodízio Formation is overlain by the Galé Formation which has a total thickness of 176 m. The lower Água Doce Member is marked by the transition from coarse grained sand-rich fluvial deposits to an alternation of marls and white-brown colored limestone beds. The interval from 16-51 m consists of nodular limestone beds (mostly wackestones) interbedded with bioturbated marls. Macrofossils include indeterminate oysters, gastropods (often as endocasts) and other bivalves indicating shallow-marine conditions. The interval 51-65 m is more siliciclastic-rich and consists mostly of well-bedded, fine to middle grained, white-brown sand- and siltstones alternating with claystone deposits. Oyster fragments are common and oyster-rich beds can be found in the lower part of this interval. At 62 m, several well-preserved specimens of the ammonite *Knemiceras uhligi* have been found (Fig. 3). The next interval (65 to 85 m) is again more carbonate-rich and characterized by an alternation of marls and wacke- to packstones. A massive limestone bed at 65 m can be easily spotted in the field and marks the base of this interval (Fig. 4B). Here, the degree of bioturbation is higher compared to the lowermost part. Common macrofossils include oysters (often showing intense bioerosion) and gastropods. The interval from 85-

Fig. 4 (next page). Field images from São Julião, Magoito and Praia das Maças. (A) Lower part of the São Julião section with the transition of coarse-grained siliciclastic Rodízio Formation to the marls and carbonates of the Galé Formation. Height of the cliff is ca. 30 m. (B) Middle part of the São Julião section with a thick, well-visible carbonate bed at ~65 m, which can be easily traced along the outcrop. Height of the cliff is ca. 30 m. (C) Top part of the São Julião section showing the transition from the Água Doce Member to the carbonate beds with the first macroscopic rudist remains of the Ponta da Galé Member. Rudist-bearing beds are indicated by (R). Height of the cliff is ca. 35 m. (D) Topmost thick (~3.5 m) orbitolinids-rich bed of the São Julião section, which serves as marker horizon and corresponds to the D1 bed of Berthou & Lauverjat (1979) and Hasenboehler (1981). (E) Lower part of the Magoito section showing a monotonous succession of marls and carbonates. Height of the cliff is ca. 40 m (F) Close-up of mass accumulations of large nereneid-type gastropods, from the Praia das Maças section. (G) Overview of Praia das Maças section, with viewing direction to the north.



130 m is dominated by siliciclastics, ranging from silt- to coarse yellow-white sandstones, with few dispersed carbonate beds. Fossil content is mainly represented by oyster shells. Thin (1 to 5 cm) coal-draperes also occur within the sandstones. The carbonates and sandstones often display strong bioturbation and bivalves and oysters are more common in the topmost part of this interval. These findings indicate deposition under very shallow marine to coastal conditions. The interval from 130-159 m is marked by an increase in limestone beds intercalated by clay and fine-grained sand- to siltstones. These limestones can be classified as wacke- and packstones. Oysters are common and often better preserved than in the underlying beds.

The FO of macroscopic rudist remains is located at 159 m and marks the transition from the Água Doce to the Ponta da Galé Member (Rey 1992). The Ponta da Galé Member (159–192 m) is composed of massive carbonate beds with a maximum thickness of 3 m intercalated by marls and claystones. Macrofossils are abundant and include echinoderms, nereneid gastropods, rudist bivalves, orbitolinids and miliolinids indicating a shoal-water platform setting.

The massive limestone beds are intercalated with clays and marls, which often contain numerous oysters. A total of four different rudist-bearing horizons can be found. The lowermost two horizons at 159 m and 163 m contain the requieniid-type rudist *Apricardia carentonensis*. The upper two horizons contain *Mathesia darderi* and are located at 169 m and 184 m, respectively (Fig. 4C). At 170 m, an interval of several meters thick is composed of thin-bedded black-green colored clays, marls and subordinate wackestones. The presence of abundant orbitolinids and small oyster remains indicate an open shelf environment. The top of São Julião I is marked by a distinct ochre-colored sand-rich limestone bed overlain by a strongly bioturbated micritic wackestone. Sampling continued further south at São Julião II with an exposure gap of 3.5 m, followed by thin-layered marls and carbonates containing *Mathesia darderi*. The section ends with an up to 4 m thick, pale sandy limestone bed rich in orbitolinids, which can be easily spotted in the field (Fig. 4D). This distinct bed serves as a basin-wide marker horizon and has been termed D1 'discontinuité' by Berthou & Lauerjat (1979) and Hasenboehler (1981). According to these authors, this horizon marks the boundary between the Galé Formation and the Canéças Formation.

5.1.2 Magoito

The Magoito section is located between the São Julião and Praia das Maças sections, some 5 km south of São Julião (Fig. 1). Here, the strata gently dip to the south (1–2°) and can be continuously followed for several kilometers. The succession crops out along the coastal cliffs and has an estimated total thickness of up to 150 m. However, large parts of this cliff section are inaccessible due to its steepness and only the lowermost part of the Magoito section was sampled, resulting in a total thickness of 51 m. The succession is characterized by the small-scale alternation of well-bedded grey-colored clays, marls and nodular wacke- to packstone layers (Fig. 4E). Sand- and siltstones occur only subordinate throughout the studied interval. The deposits contain numerous bivalves and gastropod remains. Gastropod abundances decrease section-up. Oysters and oyster shell debris are also present. The thicknesses of the individual clay and marl layers range between 10–100 cm. In most of the limestone beds bioturbation is common. Hasenboehler (1981) found the ammonite *Knemiceras uhligi* in two levels at Magoito, approximately at ~1 m and ~30 m (Fig. 3). Sedimentological and fossil data indicate a marine, well oxygenated depositional setting with varied siliciclastic input. Despite the proximity to the São Julião section, a lithostratigraphic bed-to-bed correlation between the two outcrops is difficult due to the monotonous alternation of marls and carbonates and the absence of distinct marker beds.

5.1.3 Praia das Maças

The Praia das Maças section starts at the large parking space just north of the town of Praia das Maças and corresponds to the "Parking de la Source" section of Berthou & Lauerjat (1979). The base of the section sampled at Praia das Maças can be correlated to the second rudist-bearing bed at São Julião (165 m). At Praia das Maças, this 4 m thick bed contains a rich biofacies, including several types of rudists, large orbitolinids, nereneids and pectinids. Large indeterminable requieniid-type rudists occur at 2 m in the middle of the bed. A distinct serpulid-rich layer with remains of the rudist *Mathesia darderi* can be found on top of this bed. This massive limestone is followed by a few meters of thin-bedded oyster-rich marls overlain by an interval made up of several thick-bedded, carbonate-rich sandstones with well-developed cross bedding (7–11 m). The sandstones contain a rich and diverse fossil assemblage including orbitolinids, miliolinids, gastropods, bivalves and oysters. The above-lying interval is made up of marls and limestones with a distinct horizon (at 13 m) containing

mass accumulations of large nereneid-type gastropods (Fig. 4F). Between 14 m and 18 m, a magmatic sill intercalates the sedimentary succession. The sill is overlain by an alternation of thin-bedded marls and limestone beds, some of which contain gastropod and oyster remains. At 22 m, a thick (1.8 m) and strongly bioturbated limestone bed containing the rudist *Mathesia darderi* as well as gastropods, orbitolinids and miliolinids is observed, which is overlain by a second mass accumulation of nereneid-type gastropods at 24 m. The above lying interval (24–29) m is characterized by thin-bedded marls and limestones, with numerous oyster remains. The top is represented by a conspicuous ~3.5 m thick and massive limestone bed, which is characterized by high quartz content and by the occurrence of echinoids and orbitolinids and corresponds to the D1 marker horizon (Berthou & Lauverjat 1979). In total, the Praia das Maças section covers a thickness of 30 m (Fig. 4G).

5.2 Dinoflagellate biostratigraphy

To refine the biostratigraphic resolution of the studied sections a total of 60 productive palynological samples (out of 97 samples) have been investigated for age-diagnostic dinoflagellates. Studied slides cover the São Julião section (43 samples), Magoito section (9 samples) as well as the Praia das Maças section (8 samples). No evidence of reworking from older deposits has been found. As already indicated by Berthou & Leereveld (1990) and Heimhofer et al. (2007), the dinoflagellate cyst association in the Lusitanian Basin reflects rather a Boreal than a Tethyan character and the biostratigraphic assignment of the observed age-diagnostic forms follows the zonation scheme published by Monteil & Foucher (1998). Important age-diagnostic dinoflagellates at São Julião include *Dinopterygium cladoides*, *Xiphophoridium alatum*, *Chichaouadinium vestitum* and *Palaeohystrichophora* cf. *infusorioides*. Within the Rodízio Formation, age-diagnostic dinoflagellate cysts are absent. The FO of *D. cladoides* at 16.9 m is located just above the transition from the siliciclastics of the Rodízio Formation to the marl-limestone alternation of the Galé Formation (Fig. 5). The FO of *X. alatum* and *C. vestitum* is found at 19.7 m. All three species have consistent occurrences throughout the section. *P.* cf. *infusorioides* is observed for the first time at 172.4 m. The last occurrence (LO) of *C. vestitum* is at 175.9 m. The base of the Magoito section already contains *D. cladoides*, *X. alatum* and *C. vestitum* and consistent occurrences are found throughout the section. *P.* cf. *infusorioides* is absent at Magoito.

At Praia das Maças, *D. cladoides* and *X. alatum* can be found throughout the section. *C. vestitum* is only found in the lower part of the section and the LO of *C. vestitum* is recorded at 11.9 m. *P.* cf. *infusorioides* is found consistently only in the upper part of the section (FO at 21.8 m).

5.3 Carbon isotope stratigraphy

The carbon isotope ($\delta^{13}\text{C}_{\text{carb}}$) values derived from analysis of inorganic carbonate vary between -1.7‰ and 3.8‰ and show some clear variations with stratigraphic height for the studied sections at São Julião, Magoito, and Praia das Maças (Fig. 5).

Due to the lack of carbonate-bearing strata, no $\delta^{13}\text{C}$ record could be obtained for the Rodízio Formation (0–16 m) at São Julião. The interval 16.6–24 m is characterized by a trend from slightly negative to positive values ranging from -0.4‰ to 1.8‰. This is followed by relative stable values in the range of ~2.0‰ (24–51 m). Only few suitable carbonate-bearing horizons mark the interval 51–66 m with an overall shift of 1‰ towards more positive values (up to 2.8‰). This is followed by a decreasing trend from relatively positive (2.2‰) towards less positive (1‰) values, which characterizes the interval 66–100 m. A rapid return towards more positive values (mean 1.3‰) in the lowermost part characterizes the next interval (100–111.3 m) followed by decreasing values. The interval 111–142.5 m is characterized by fluctuating $\delta^{13}\text{C}$ values (0.4–2.8‰). The lower part displays some unusually low values (as low as -1.7‰), likely a result of diagenesis. The top half shows more

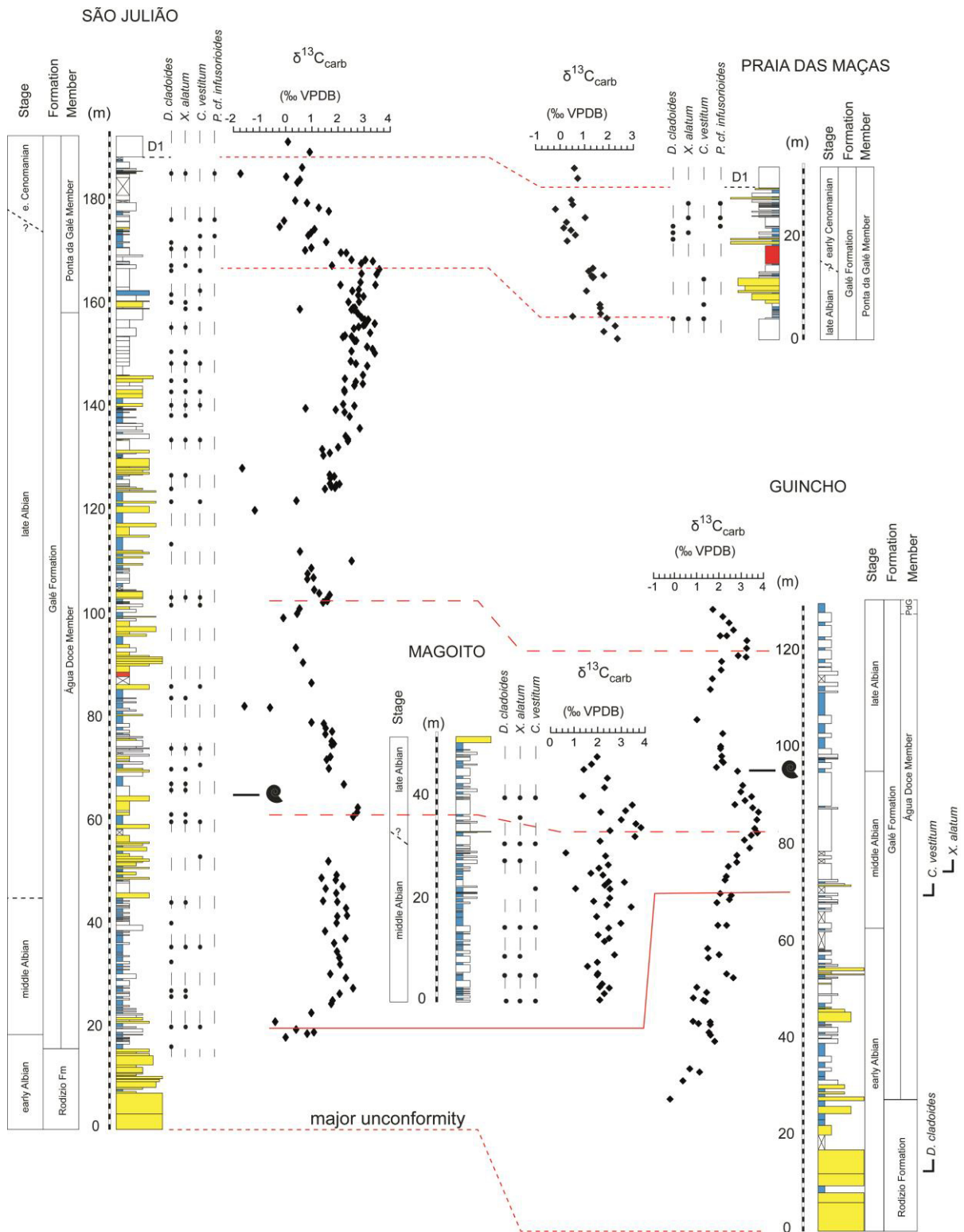


Fig. 5. Lithological log, dinoflagellate cyst distribution, $\delta^{13}\text{C}$ curve and stratigraphic age of the São Julião, Magoito, Praia das Maças and Guincho sections. Outstanding negative $\delta^{13}\text{C}$ values may reflect diagenetic alteration. Stippled lines indicate lithostratigraphic correlation, striped lines chemostratigraphic correlation and solid lines biostratigraphic correlation. Black circles represent occurrences of important age-diagnostic dinoflagellate cysts. Age assessment at Guincho from Heimhofer et al. (2007, 2012). Ammonite symbol indicates the presence of *K. uhligi* (Hasenboehler 1981, Dinis et al. 2002, this study (see text)). PdG, Ponta da Galé Member; major unconformity based on Aptian-Albian unconformity of Dinis & Trincão (1995) and Dinis et al. (2002).

positive values (mean 2.2‰). This is followed by an interval (142.5-168 m) characterized by stable values of around 2.8‰. The most positive values (up to 3.6‰) measured at São Julião are also recorded in this interval. The top part of the São Julião record (168–192 m) shows a distinct negative shift in $\delta^{13}\text{C}$ from $\sim 2.7\text{‰}$ to $\sim 0.5\text{‰}$.

The Magoito section is differentiated into three chemostratigraphic intervals. The lowermost interval (0–31 m) is characterized by stable values (mean of 2.2‰) despite significant scatter. A distinct shift towards more positive values reaching up to 3.8‰ (mean 3.2‰) characterizes the overlying interval (31–38 m). In the uppermost part of the section a trend to less positive $\delta^{13}\text{C}$ values (mean 1.9‰) is observed.

The Praia das Maças section is characterized by decreasing $\delta^{13}\text{C}$ values from bottom to top with values range from -0.1 to 2.4‰ (mean 1.2‰).

5.4 Trace element concentrations and Sr isotope geochemistry

Following initial visual and CL-microscopy screening, a total of 19 oysters and 4 rudist samples were selected for trace element analysis (Table 2). The preservation of rudist shells is good and pristine, indicated by non-luminescent (blue to dark color) shell material (Figs. 6A, B). In contrast, the quality of preservation in oyster shells varies and sometimes displays bright orange-colored luminescent parts, related to growth lines (Figs. 6C, D) which are associated with the incorporation of microcrystalline

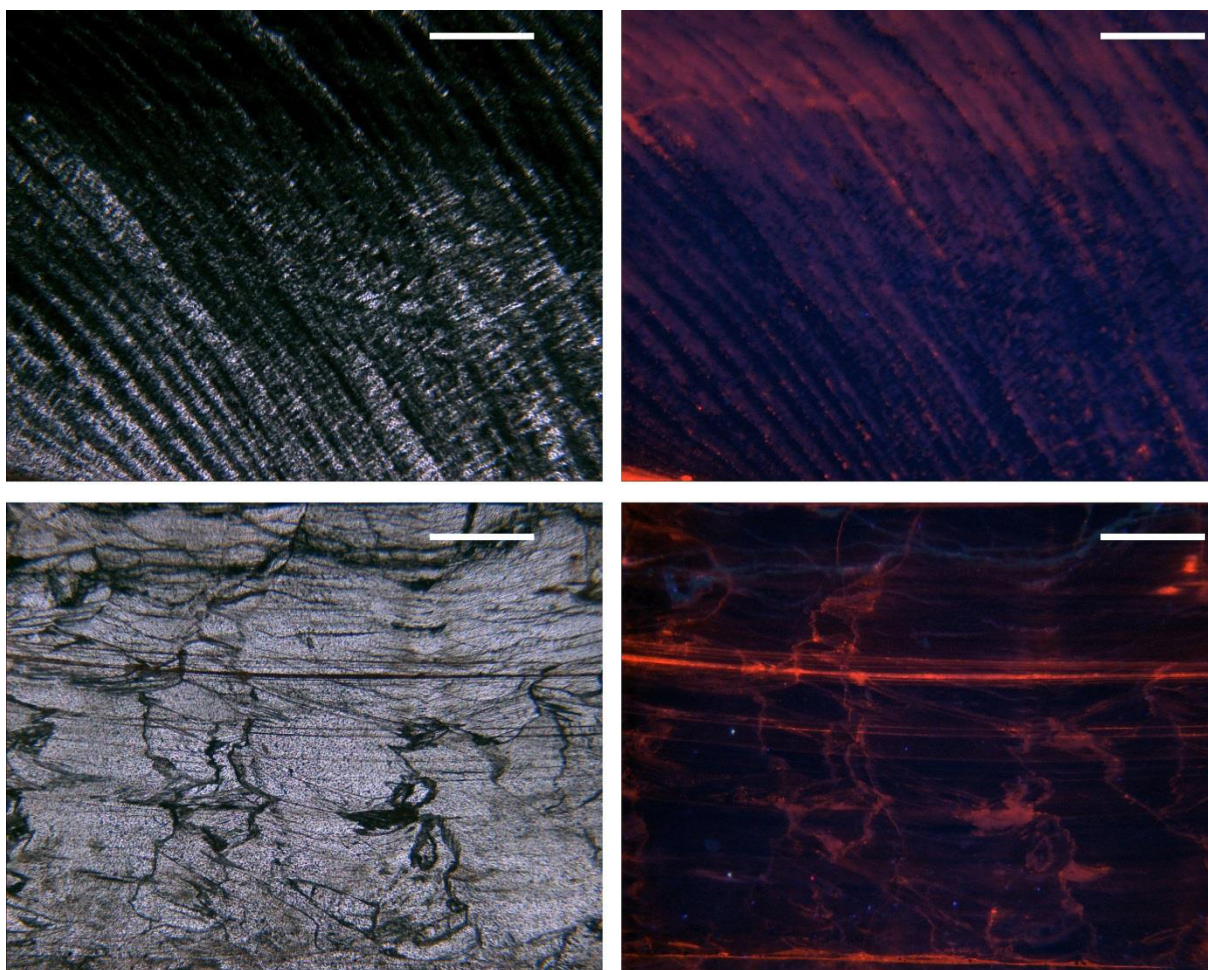


Fig. 6. Photomicrographs of sections through analyzed shell material. A) Well-preserved rudist shell under transmitted light (sample SJMH-185-1). B) Same rudist shell under CL; non-luminescent dark blue color indicates pristine preservation. C) Oyster shell under transmitted light (sample SJMH-66-3). D) Same oyster shell under CL, note the patchy luminescence pattern with dull orange luminescence along boundaries of individual calcite crystals. Scale bar 0.5 mm.

cement in the shell. These areas have been avoided when drilling. Measured concentrations of Mn in oyster shell calcite vary between 5 and 491 ppm, Fe between 72 to 5286 ppm and Sr between 699 and 964 ppm. For low-Mg calcite rudist shells the Mn concentrations range between 10 to 74 ppm, Fe between 96 to 649 ppm and Sr between 1193 and 1384 ppm (Table 2).

The degree of diagenetic alteration of primary shell calcite of carbonate-secreting organisms is verified by the use of trace element concentrations (Brand & Veizer, 1980, Al-Aasm & Veizer 1986, Veizer et al. 1999). For low-Mg calcite rudist shells precipitated under normal marine conditions, Mn and Fe values of <100 ppm and Sr values >1000 ppm have been proposed as cut-off values, reflecting insignificant diagenetic overprint (Steuber 1999, Steuber et al. 2005). Schneider et al. (2009) proposed values of <250 ppm for Mn and <700 ppm for Fe from late Jurassic oysters in the Lusitanian Basin based on comparison with modern oyster material. Slightly different threshold values have been proposed by other authors (e.g., McArthur et al. 2000, Wierzbowski & Joachimski, 2007). In this study, we follow the cut-off values of Steuber et al. (2005) for rudist calcite. Sample SJMH-185-3 contains 138 ppm Fe and has been included in this paper, as this sample is considered pristine based on the overall non-luminescence under CL. For oysters we follow the cut-off values of Schneider et al. (2009). Based on the concentrations of the trace elements Mn, Fe and Sr, 6 oyster samples and 2 rudist samples have been discarded (Table 2).

Table 2. Sample number, sample height, trace element concentrations, strontium-isotope ratios with standard deviations and calculated numerical ages. Asterisks indicate rudist samples.

Sample	Height (m)	Trace elements (ppm)				$^{87}\text{Sr}/^{86}\text{Sr}$	Mean ($\times 10^{-6}$)	Calculated Age (Ma)		
		Sr	Mg	Fe	Mn			Min	Mean	Max
SJMH-13	17.6	699	733	349	55	0.707404	7	105.85	108.03	108.72
SJ-27.1	45.0	784	816	345	67	0.707414	7	104.4	106.53	108.09
SJMH-46	54.2	819	1330	702	233	0.707439	6	99.10		103.1
SJMH-50	58.2	841	989	145	19	0.707422	7	96.16		107.44
SJMH-62	71.3	868	596	134	29	0.707436	7	98.15		103.85
SJMH-66 (3)	73.9	729	969	72	22	0.707432	6	97.35	104.68	104.93
SJMH-66 (4)	73.9	808	1073	81	22	0.707431	6	97.20		105.33
SJMH-73	78.0	786	987	668	104	0.707456	6	NA	NA	NA
SJ-76.1	127.2	716	875	74	26	0.707453	6	NA	NA	NA
SJ-78.2	130.6	962	1602	244	85	0.707458	6	NA	NA	NA
SJMH-137	131.5	820	1009	504	46	0.707447	7	NA	NA	NA
SJMH-149	141.8	855	816	259	39	0.707440	6	99.62		102.4
SJMH-179(1)	160.1	943	409	262	32	0.707430	7	97.04	100.35	105.8
*SJMH-185(1)	163.4	1384	1410	96	10	0.707429	7	96.91	100.2	106.07
*SJMH-185(3)	163.4	1182	1102	138	13	0.707425	6	96.45	98.55	106.85
Samples with trace-elemental values exceeding the defined threshold values (see text)										
SJMH-35	46.0	702	3533	3560	426					
SJMH-82(1)	89.7	906	1432	2602	184					
SJMH-82(2)	89.7	964	1489	1759	207					
SJMH-139	132.9	783	2929	5286	491					
SJMH-150	142.2	810	1961	723	93					
*SJMH-175(1)	158.6	1193	1510	158	22					
*SJMH-175(2)	158.6	1312	1981	649	74					
SJMH-179(2)	160.1	867	1662	741	118					

The measured $^{87}\text{Sr}/^{86}\text{Sr}$ values from pristine oysters and low-Mg calcite rudist shells vary from 0.707404 ± 0.000007 to 0.707458 ± 0.000007 (Table 2). Overall, the measured Sr-isotope ratios show a gradually increasing trend from the base to the middle part of the São Julião section followed by a decreasing trend in the uppermost part. Sr-isotope ratios in the lower to middle interval (0–78 m) range from 0.707404 to 0.707456. A large gap in the Sr-isotope record (78–127 m) is caused by the absence of well-preserved shell material in this siliciclastic-rich part of the Água Doce Member. The highest

$^{87}\text{Sr}/^{86}\text{Sr}$ values are observed just above this barren interval (127–142 m) with values reaching up to 0.707458 (sample SJ-78.2). The topmost samples (160–165 m) show lower $^{87}\text{Sr}/^{86}\text{Sr}$ values ranging between 0.707430 and 0.707425.

6. Discussion

6.1 Dinoflagellate cyst biostratigraphy

The FO of *D. cladoides* slightly above the Rodízio Formation at São Julião (Fig. 5) corresponds to an early Albian according to Monteil & Foucher (1998). Berthou (1984) placed the FO of *D. cladoides* in the middle Albian. The FO of *C. vestitum* and *X. alatum* (19.7 m) mark the transition to the middle Albian (Monteil and Foucher 1998). An upper middle Albian age has been proposed in the Boreal realm for the FO of *C. vestitum* by Nøhr-Hansen & McIntyre (1998) and middle to late Albian age by Stover et al. (1996). *P. cf. infusorioides* is consistently found in the upper part at São Julião and Praia das Maças. A latest Albian age has been inferred for the FO of *P. infusorioides* by Foucher (1981) and Oboh-Ikuenobe et al. (2007). *P. cf. infusorioides* was not recorded at Magoito and Guincho. *C. vestitum* was not found above 172.4 m at São Julião and above 11.9 m at Praia das Maças. According to some authors (Verdier, 1975, Williams et al., 2004, Oboh-Ikuenobe et al. 2007), the absence of *C. vestitum* marks the Albian-Cenomanian boundary. The base at Magoito is marked by the presence of *D. cladoides*, *C. vestitum* and *X. alatum* indicating an age not older than middle Albian. The dinoflagellate cyst ages corroborate the age-range of the requieniid-type rudist *Apricardia carentonensis*. *A. carentonensis* was found at 158 and 164 m at São Julião and has previously been reported from Cenomanian (Berthou et al. 1980, Scott 2010) and late Albian deposits (Berthou et al. 1979). *Mathesia darderi* was found at 169 m and 184 m at São Julião and in 4 beds at Praia das Maças. According to Fenerci-Masse et al (2011), this rudist species has an age range from the late Barremian to middle Albian. *M. darderi* was reported in late Albian deposits from eastern Spain (Masse et al. 1998).

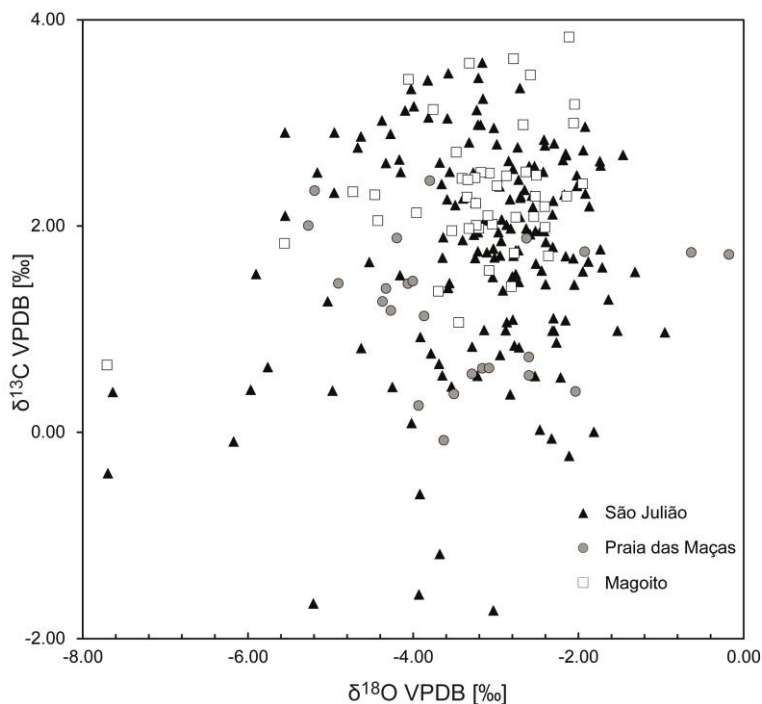


Fig. 7. Crossplot of $\delta^{18}\text{O}$ and $\delta^{13}\text{C}$ values from Magoito (squares), Praia das Maças (circles) and São Julião (diamonds) sections. The overall low covariance ($R^2 = 0.0461$; $n = 271$) indicates limited diagenetic alteration.

6.2 Reliability and application of the $\delta^{13}\text{C}$ record

Carbon isotope records have been used by several authors as a stratigraphic correlation tool in pelagic and hemipelagic Cretaceous deposits (e.g., Weissert 1989, Menegatti et al. 1998). Furthermore, the applicability of carbon isotope stratigraphy in shallow marine deposits is demonstrated in other studies (e.g., Jenkyns 1995, Burla et al. 2008, Huck et al. 2011). However, diagenesis influencing the $\delta^{13}\text{C}$ record is likely and trends in the $\delta^{13}\text{C}$ record should be treated with caution. The carbon-isotope record from the shallow-marine sections at Magoito and São Julião show a higher scatter and shifts in amplitude than the more distal Guincho section (Fig. 3) within the same stratigraphic interval and demonstrate the increased sensitivity of shallow-marine deposits to local (respiration, freshwater input, primary productivity) factors compared to more open marine deposits (Jenkyns & Clayton 1986, Jenkyns 1995, Immenhauser et al. 2003, Huck et al. 2011). Notwithstanding, cross plots of $\delta^{18}\text{O}$ and $\delta^{13}\text{C}$ values (Fig. 7) are interpreted to reflect only limited diagenetic alteration for the different sections (São Julião; $R^2 = 0.02$; Praia das Maças; $R^2 = 0.01$; Magoito; $R^2 = 0.16$).

6.3 Preservation of rudist and oyster shells

The strontium-isotope record has been extensively used to date marine sediments (Jones et al. 1994, Bralower et al. 1997, Howarth & McArthur 1997, McArthur et al. 2000, 2001, Korte et al. 2003, Steuber et al. 2005, Schneider et al. 2009, Huck et al. 2011) from the Mesozoic era. Most of the work focused on carbonate fine-fraction, brachiopods, belemnites and rudist shells found in open marine deposits. The use of oyster shells in strontium-isotope studies is less straightforward, due to the shallow-marine paleoenvironmental habitat of these organisms. Caution is needed to assess the quality of oyster shell material as the direct influence of river-derived freshwater may alter the trace element concentration in the shell (Schneider et al. 2009). Notwithstanding, Sr-isotope chemostratigraphy can be applied using oyster shells from Mesozoic shallow-marine deposits (Jones et al. 1994, Burla et al. 2009, Schneider et al. 2009, Heimhofer et al. 2012).

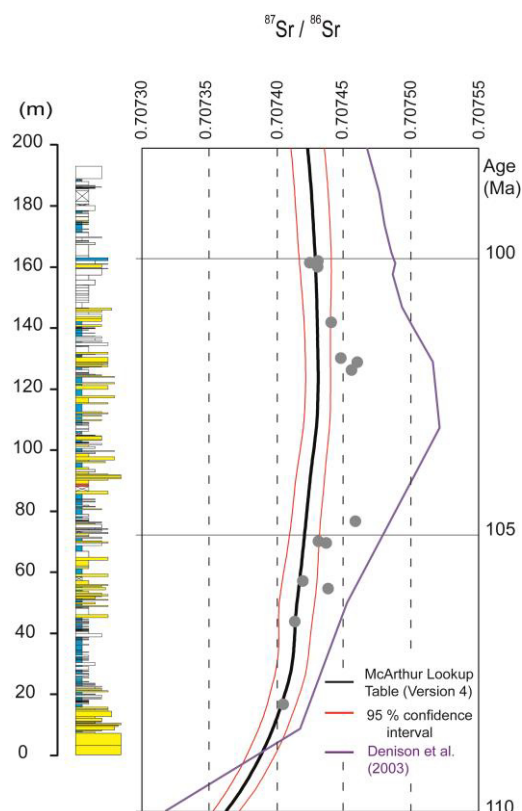


Fig. 8. Early Albian to early Cenomanian $^{87}\text{Sr}/^{86}\text{Sr}$ values from São Julião, Portugal (grey dots) and Texas & Oklahoma USA (purple line; Denison et al. 2003), compared to the LOWESS best-fit curve look-up table of McArthur et al. 2001 (black line). The red lines represent the 95% confidence interval. Data points from USA are based on average $^{87}\text{Sr}/^{86}\text{Sr}$ values per lithostratigraphic interval.

A comparison between the Sr-isotope pattern obtained at São Julião and the corresponding shape of the global strontium-isotope curve (Howarth & McArthur 1997, McArthur et al. 2001) shows a good overall correlation, in particular in the basal and upper part of the curve (Fig. 8). Nonetheless, four samples in the middle part of São Julião (interval 78-132 m) clearly deviate from the global Sr-isotope trend. Since a diagenetic control of these values can be ruled out given the good preservation state of the shell material, the higher $^{87}\text{Sr}/^{86}\text{Sr}$ values may reflect the effect of decreasing sea surface salinity associated with enhanced continental run-off. In fact, the presence of oyster shells and the absence of other marine fossils in these horizons at São Julião (at 78, 127, 130, 132 m) may point to reduced salinity. However, to shift the Sr isotope composition of marine surface waters, a large amount of freshwater input is needed (Ingram & Sloan, 1992, Bryant et al. 1995, Holmden & Hudson, 2003, Reinhardt et al. 2003, Sessa et al. 2012).

6.4 Conversion into absolute ages

$^{87}\text{Sr}/^{86}\text{Sr}$ values from pristine oyster and rudist samples are converted into absolute ages (Table 2) according to the LOWESS best fit curve (Howarth & McArthur 1997, McArthur et al. 2001). In general, the numerical ages from São Julião are in good agreement with the global trend. Only 4 samples from the middle part (78-132 m) clearly deviate from the global Sr-isotope curve and failed to provide a definitive age (see 5.3). A middle Albian age (108.0 Ma) is inferred from the lowermost sample at São Julião (17.6 m) and increasingly younger ages are found higher up the section. The transition from the middle to late Albian is tentatively placed at ~44 m at São Julião, just below sample SJ-27.1 (45m, 106.5 Ma). Subsequent samples indicate a very long and expanded late Albian age for the remaining part of the section (Fig. 5; Table 2). The youngest Sr-isotope obtained ages come from samples at 165 m and have been dated at 100.2-98.6 Ma. This corresponds to an early Cenomanian age (Gradstein et al. 2012).

The paucity of existing strontium-isotope studies from the late Albian hampers detailed correlation. One exception is a study for the middle and late Albian from Texas and Oklahoma, USA (Fig. 8) from Denison et al. (2003). However, the reported $^{87}\text{Sr}/^{86}\text{Sr}$ values in that study are in clear contrast to the shape of the LOWESS best-fit curve from the middle and late Albian with much higher reported values and highlight the lack of $^{87}\text{Sr}/^{86}\text{Sr}$ data from this time period. Furthermore, the use of strontium-isotope derived numerical ages for the Albian is not straightforward as the strontium-isotope curve forms a long-invariant plateau and subtle changes in the strontium-isotope record will have large offsets in the age-determination (Howarth & McArthur 1997, McArthur et al. 2001). Notwithstanding, the similarity between our data and the global Sr-isotope record further demonstrate the applicability of low-Mg calcite in oyster and rudist shells in shallow marine depositional records of Albian to Cenomanian age to obtain numerical ages.

6.5 Carbon-isotope based correlation with open marine Albian records

Carbon-isotope records covering the Albian are scarce and mainly derived from hemipelagic succession, often studied with focus on black shale deposition, including OAE 1b in the early Albian and OAE 1d in the late Albian (Herrle et al. 2004, Giorgioni et al. 2012). High-resolution and stratigraphically well-constrained sections are known from the Umbria-Marche Basin of Italy and from the Vocontian Trough of SE France (Reichert 2005, Gale et al. 2011, Giorgioni et al. 2012). A thick (~500 m) hemipelagic section from the Vocontian Trough covers Aptian to Cenomanian strata and was dated via planktonic foraminifera, calcareous nannofossils, and ammonites (Gale et al 1996, Herrle & Mutterlose 2003). The Umbria-Marche Basin record has a thickness of ~65 m and has been dated using planktonic foraminifera (Fiet et al. 2001). Correlation of the two records shows a good overall consilience, differences relate to the small-scale structure and the differing amplitude of the $\delta^{13}\text{C}$ trends (Giorgioni et al. 2012).

Chemostratigraphic correlation between basinal and shoal-water successions is notoriously difficult and hampered by the general vulnerability of the near-shore record to erosion, hiatus formation and associated diagenetic overprinting (e.g., Patterson & Walter 1994, Immenhauser et al. 2003, Burla et al. 2009). Despite these problems, major trends of the $\delta^{13}\text{C}$ record can often be identified in shoal water sections and serve as important stratigraphic tie points (e.g., Grötsch et al. 1998, Parente et al. 2008, Robinson 2011, Huck et al. 2013).

Based on the existing stratigraphic framework derived essentially from biostratigraphy and Sr-isotope data, the carbon-isotope record of São Julião can be correlated with both the Italian and French sections (Fig. 9). The middle Albian carbon isotope stages Al 2-7 (covering large parts of the *H. planispira* and *T. primula* biozones) of Gale et al. (2011) are correlated with the interval between ~17 and 51 m at São Julião, which shows a comparable trend. The above lying part of the succession is dominated by siliciclastic deposition resulting in a limited sampling resolution for $\delta^{13}\text{C}_{\text{carb}}$ samples between 51 and 120 m. In contrast, the distinct carbon isotope trend characterizing the upper part of São Julião (120-192 m) can be correlated well with the late Albian-early Cenomanian trend observed in the basinal reference curves. Of particular significance is a pronounced negative shift in the order of 0.5 to 1.0‰ marking the Albian-Cenomanian boundary in the Vocontian Trough (Gale et al. 2011),

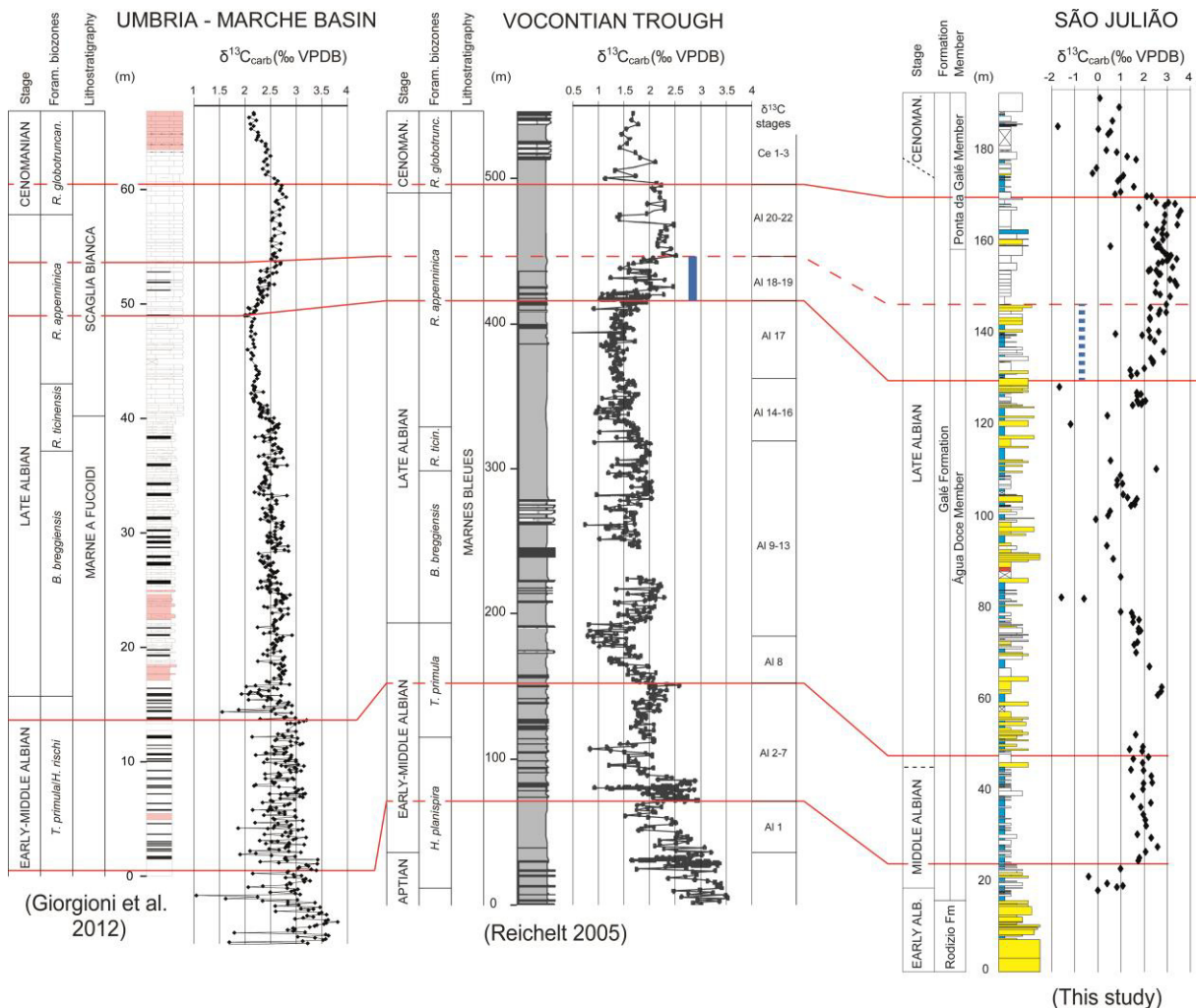


Fig 9. Chemostratigraphic correlation of the São Julião section with stratigraphically well-constrained Albian $\delta^{13}\text{C}$ records from the Umbria-Marche Basin, Italy (Giorgioni et al. 2012) and the Vocontian Trough, SE France (Reichelt 2005). Correlation of Italian and French sections based on Giorgioni (2012). Solid blue bar represent OAE 1d interval as defined by Petrizzo et al. (2008), striped blue bar shows tentative position of OAE 1d at São Julião.

which corresponds well to a similar negative trend located at ~170 m within the Ponta da Galé Member.

During the late Albian, the presence of black shale events (OAE 1d Breistoffer event) and associated positive $\delta^{13}\text{C}$ excursions have been reported (e.g., Wilson & Norris 2001, Bornemann et al. 2005, Petrizzo et al. 2008 and references therein). Organic-rich strata deposited during this interval have been found in several basinal localities (e.g., Gale et al. 1996, Nederbragt et al. 2001, Wilson & Norris 2001, Giraud et al. 2003, Bornemann et al. 2005). Based on the existing correlation, the São Julião section should cover the OAE 1d event and its tentative position within the coastal sedimentary record can be presumed (Fig. 9). At first glance, the corresponding interval does neither show enrichment in organic carbon nor other anomalies regarding its lithology and biofacies. However, further investigations have to be carried out in order to constrain the stratigraphic position and sedimentary expression of the late Albian OAE 1d within the studied section.

6.6 Refining the stratigraphy of the Albian in the southern Lusitanian Basin

Until now, a clear correlation of the different Albian sections in the southern part of the Lusitanian basin was not published. Biostratigraphic stages and substages, often described from regional areas instead of local sections-, have been obtained using dinoflagellate cysts, pollen and spores and few ammonites (e.g., Berthou et al. 1980, Berthou & Leereveld 1990, Berthou & Hasenboehler 1982, Hasenboehler 1981, Medus 1982), ostracods and rudists (Berthou & Lauverjat 1979), and large benthic foraminifera and echinoids (Berthou 1984). Unfortunately, detailed lithological descriptions of the different sections were not provided in these studies.

In order to improve the intrabasinal correlation of the different sections in the southern Lusitanian Basin, the records from São Julião and Magoito presented in this study are compared with those already published from Guincho (Burla 2007, Heimhofer et al. 2007, 2012). The fluvial-deltaic deposits of the Rodízio Formation are interpreted to be deposited diachronous across the Lusitanian Basin, starting in the southern part of the Lusitanian Basin (Dinis & Trincão 1995). A late Aptian to middle Albian age has been inferred based on palynomorphs (Hasenboehler 1981, Dinis & Trincão 1995). However, a combined litho- and biostratigraphic study by Heimhofer et al. (2007) indicates an early Albian age for the entire Rodízio Formation at Guincho. A middle Albian age is inferred for the lower beds of the Galé Formation at São Julião from the Sr-isotope derived ages and the FO of *X. alatum* and *C. vestitum* (Fig. 5). Our results for the lower part of the Galé Formation at São Julião corroborate with previous palynostratigraphic studies (Fig. 2). A late Aptian to middle Albian age is inferred by Hasenboehler (1981) for the Rodízio Formation and the transition to the Galé Formation at São Julião based on the presence of *X. alatum* and *D. cladoides* in the topmost part. Medus (1982) used the spores and pollen content to place the Rodízio Formation at São Julião into the early and middle Albian and the Galé Formation in the middle and late Albian, but failed to mention the exact age-diagnostic palynomorphs.

A middle Albian age is inferred for the lowermost beds at Magoito and São Julião based on the presence of *X. alatum* and *C. vestitum*. Moreover, our results suggest a significantly earlier start of marine conditions in the Galé Formation at Guincho compared to São Julião and Magoito (Fig. 5). At São Julião, this is corroborated by Sr-isotope derived ages from the lowermost sample (17.6 m). The base of Magoito has been dated as late Albian by Hasenboehler (1981) based on the FO of *Cribroperidinium intricatum*. However, the stratigraphic significance of this find is questioned by Oboh-Ikuenobe et al (2007), who placed the FO of *C. intricatum* already in the early Albian. The middle-late Albian transition at São Julião could not be constrained from the biostratigraphic data. However, the middle-late Albian transition is tentatively placed at 44 m based on strontium-isotope derived ages. The middle-late Albian transition at Guincho is placed just above the positive (~1‰) carbon isotope excursion and the presence of the ammonite *Knemiceras uhligi* (Fig. 5). *K. uhligi* is also found at Magoito by Hasenboehler (1981) and in deposits from the late Albian in Portugal, Spain, Iran and Venezuela as well as from the middle Albian in France and from the middle-late Albian in Lebanon (Geyer et al. 1997).

Although the C- and Sr-isotope records from São Julião and Guincho are in good agreement, certain minor stratigraphic discrepancies occur between the two sections. This could be related to different methodologies applied in this work and the study of Heimhofer et al. (2007), including the lack of trace element concentrations data and the use of a laser-ablation multi-collector ICPMS which results in less precise results ($2\sigma = 2 \times 10^{-5}$). The carbon isotopic trend in the interval 100–111.3 m at São Julião allows a tentative correlation with the top of Guincho (120–128 m). The first rudist beds at Guincho occur within this interval. In contrast, at São Julião, the first rudist beds occur in the Ponta da Galé Member (Rey 1992) at 159 m (Fig. 5). This indicates significantly earlier deposition of rudist-rich shallow-water limestones in the south-western part of the Lusitanian Basin compared to its northern part. This observation is in accordance to Rey (1979, 1992) and Chapman (1982), who both suggested that the rudist beds are deposited diachronous across the basin, starting in the south-western part of the Lusitanian Basin. This contrasts with Berthou and Hasenboehler (1982) who propose a time-equivalent FO of rudists. Sr-isotope derived ages at 165 m indicate an early Cenomanian age (Gradstein et al. 2012). This is corroborated by the LO of the dinoflagellate *C. vestitum* at 175.9 m (São Julião) and at 11.9 m (Praia das Maças). The absence of this biostratigraphic marker species indicates an early Cenomanian age (Verdier, 1975, Williams et al., 2004, Oboh-Ikuenobe et al. 2007). An early Cenomanian age for the topmost part of the Galé Formation is in contrast with previous authors (e.g., Berthou & Lauverjat 1979, Hasenboehler 1981, Berthou 1984) who placed this boundary above the D1 marker horizon.

In summary, the combined geochemical and biostratigraphic data corroborate and slightly revise the existing stratigraphic framework of the São Julião and Magoito sections from previously published papers (e.g., Berthou et al. 1980, Berthou & Hasenboehler 1982, Medus 1982) while providing high resolution lithological descriptions, Sr-isotope derived ages and carbon isotope records.

7. Conclusions

(1) For the first time a high-resolution study has been performed using carbon isotopes, dinoflagellate biostratigraphy and strontium isotope stratigraphy from low Mg-calcite shell material to correlate the different Albian coastal sections in the southern Lusitanian Basin. Furthermore, detailed lithological logs for the different outcrops are provided.

(2) The shallow marine deposits have been dated and resulted in an early Albian age for the Rodízio Formation and a middle Albian to early Cenomanian age for the Galé Formation (Água Doce and Ponta da Galé Member) at São Julião. A late Albian to early Cenomanian age for the Ponta da Galé Member at Praia das Maças and a middle to late Albian age for the Água Doce Member at Magoito. An early Cenomanian age for the topmost Galé Formation slightly deviates from previous studies.

(3) The strontium-isotope derived ages are in good agreement with the global $^{87}\text{Sr}/^{86}\text{Sr}$ record and demonstrate the applicability of strontium isotope stratigraphy based on low Mg-calcite from oyster and rudist shells in shallow marine depositional settings.

(4) The onset of marine conditions in the lowermost Galé Formation overlying the fluvial-deltaic Rodízio Formation at São Julião and Magoito occurs in the middle Albian and is significantly delayed compared to Guincho. Furthermore, the establishment of a rudist-rich, shallow-water carbonate platform starts significantly earlier at the Guincho locality, which is located further south.

(5) Comparison with Albian carbon-isotope records from SE France and Italy further constrain the age assignment of the São Julião section and shows the applicability of Sr- and C-isotope stratigraphy in shallow marine deposits.

Acknowledgements

We thank Dieter Buhl and Christiane Wenske for laboratory assistance, Rolf Neuser for CL-microscopy assistance and Hans-Ulrich Metzger for providing the oyster and rudist thin-sections. Peter Skelton is thanked for rudist identification, Peter Hochuli for help with the dinoflagellate identification and Jean Cors for field assistance. The insightful comments by two anonymous reviewers are gratefully appreciated. This work was funded by the Deutsche Forschungsgemeinschaft (DFG project HE4467/6-1).

8. References

- Al-Aasm, I. S., Veizer, J., 1986. Diagenetic stabilization of aragonite and low-Mg calcite, I. Trace elements in rudists. *Journal of Sedimentary Petrology* 56, 138–152.
- Berthou, P-Y., Lauerjat, J., 1979. Essai de Synthèse paléogéographique et paléobiostratigraphique du Bassin occidental portugais au cours du Crétacé supérieur. *Ciencias Terra Lisboa* 5, 121-144
- Berthou, P-Y., Fouchier, J. C., Lecocq, B., Moron, J. M., 1980. Aperçu sur les kystes de Dinoflagellés de l'Albien et du Cénomaniens du Bassin Occidental Portugais. *Cretaceous Research* 1, 125–141.
- Berthou, P-Y., Hasenboehler, B., 1982. Les kystes de dinoflagelles de l'Albien et du Cenomanien de la region de Lisbonne (Portugal). *Cuadernos Geologia Ibérica* 8, 761-779.
- Berthou, P-Y., Leereveld, H., 1990. Stratigraphic implications of palynological studies on Berriasian to Albian deposits from western and southern Portugal. *Review of Palaeobotany and Palynology* 66, 313–344.
- Berthou, P-Y., Ferreira Soares, A., Lauerjat, J., 1979. Mid Cretaceous Events Iberian field Conference 77. Guide 1, Partie Portugal. *Cuadernos de Geologia Ibérica* 5, 31–124
- Berthou, P-Y., 1984. Albian-Turonian stage boundaries and subdivisions in the western Portuguese Basin, with special emphasis on the Cenomanian-Turonian boundary in the ammonite facies and rudist fades. *Bulletin of the Geological Society of Denmark* 33, 41-45.
- Bornemann, A., Pross, J., Reichelt, K., Herrle, J. O., Hemleben, C., Mutterlose, J., 2005. Reconstruction of short-term palaeoceanographic changes during the formation of the Late Albian 'Niveau Breistroffer' black shales (Oceanic Anoxic Event 1d, SE France). *Journal of the Geological Society* 162, 623-639.
- Bralower, T. J., Fullagar, P. D., Paull, C. K., Dwyer, G. S., Leckie, R. M., 1997. Mid-Cretaceous strontium isotope stratigraphy of deep-sea sections. *Geological Society of America Bulletin* 109, 1421–1442.
- Brand, U., Veizer, J., 1980. Chemical diagenesis of a multicomponent carbonate system—1: trace elements. *J. Sediment. Petrol.* 50, 1219–1236.
- Bryant, J. D., Jones, D. S., Mueller, P. A., 1995. Influence of freshwater flux on $^{87}\text{Sr}/^{86}\text{Sr}$ chronostratigraphy in marginal marine environments and dating of vertebrate and invertebrate faunas. *Journal of Paleontology* 69, 1-6.
- Burla, S., 2007. Response of Atlantic coastal environments (Portugal) to mid-Cretaceous climate change: Insights from sedimentology and isotope geochemistry. Unpublished PhD Thesis, ETH Zürich, 147pp.
- Burla, S., Heimhofer, U., Hochuli, P., Weissert, H., Skelton, P.W., 2008. Changes in sedimentary patterns of coastal and deep-sea successions from the North Atlantic (Portugal) linked to Early Cretaceous environmental change. *Palaeogeography, Palaeoclimatology, Palaeoecology* 257, 38–57.

Burla, S., Oberli, F., Heimhofer, U., Wiechert, U., Weissert, H., 2009. Improved time control on Cretaceous coastal deposits: New results from Sr isotope measurements using laser ablation. *Terra Nova* 21, 401–409.

Chapman, J. L., 1982. Morphology, classification and interpretation of Aptian and Albian angiosperm pollen from Portugal. Unpublished PhD Thesis, University of Cambridge, 355pp

Choffat, P., 1885. Recueil de monographies stratigraphiques sur le système Crétacique du Portugal. 1^{ère} étude: contrées de Cintra, de Bellas et de Lisbonne. *Memórias da Secção dos Trabalhos Geológicos de Portugal* Lisbon, 68.

Choffat, P., 1886. Recueil d'études paleontologiques sur la faune crétacique du Portugal. I – Espèces nouvelles ou peu connues. *Memórias da Secção dos Trabalhos Geológicos de Portugal*, Lisbon, 43.

Choffat, P., 1900. Recueil de monographies stratigraphiques sur le Système Crétacique du Portugal - Deuxième étude - Le Crétacé supérieur au Nord du Tage. Direction des Services Géologiques du Portugal, Lisbon, 1-287.

Cunha, P. P., Pena dos Reis, R., 1995. Cretaceous sedimentary and tectonic evolution of the northern sector of the Lusitanian Basin. *Cretaceous Research* 16, 155-170.

Denison, R. E., Miller, N. R., Scott, R. W., Reaser, D. F., 2003. Strontium isotope stratigraphy of the Comanchean Series in north Texas and southern Oklahoma. *Geological Society of America Bulletin* 115, 669–682.

Dinis, J. L., Trincão, P., 1995. Recognition and stratigraphical significance of the Aptian unconformity in the Lusitanian Basin, Portugal. *Cretaceous Research* 16, 171–186.

Dinis, J. L., 2001. Definição da Formação da Figueira da Foz–Aptiano a Cenomaniano do sector central da margem oeste ibérica. *Comunicações do Instituto Geológico e Mineiro* 88, 127-160.

Dinis, J. L., Rey, J., De Graciansky, P. C., 2002. The Lusitanian Basin (Portugal) during the late Aptian- Albian: Sequential arrangement, proposal of correlations, evolution. *Comptes Rendus Geoscience* 334, 757-764.

Dinis, J. L., Rey, J., Cunha, P. P., Callapez, P., Pena dos Reis, R., 2008. Stratigraphy and allogenic controls of the western Portugal Cretaceous: an updated synthesis. *Cretaceous Research* 29, 772–780.

d'Orbigny, A., 1842. *Paléontologie française. Terrains crétacés. 2. Gastropodes.* Masson, Paris, p. 456.

Fenerci-Masse, M., Masse, J-P., Kolodziej, B., Ivanov, M., Idakieva, V., 2011. *Mathesia darderi* (Astre)(Bivalvia, Hippuritoidea, Monopleuridae): Morphological, biogeographical and ecological changes in the Mediterranean domain during the late Barremian–Albian. *Cretaceous Research* 32, 407-421.

Fiet N., Beaudoin B., Parize O., 2001. Lithostratigraphic analysis of Milankovich cyclicity in pelagic Albian deposits of central Italy: implications for the duration of the stage and substages. *Cretaceous Research* 22, 265-275

Foucher, J. C., 1981. Kystes de dinoflagelles du Crétacé Moyen Européen: proposition d'une échelle biostratigraphique pour le domaine Nord-occidental. *Cretaceous Research* 2, 331-338.

Gale, A. S., Kennedy, W. J., Burnett, J. A., Caron, M., 1996. The Late Albian to Early Cenomanian succession at Mont Risou near Rosans (Drome, SE France): an integrated study (ammonites, inoceramids, nannofossils, planktonic foraminifera and carbon isotopes). *Cretaceous Research* 17, 515-606.

Gale, A. S., Bown, P., Caron, M., Crampton, J., Crowhurst, S. J., Kennedy, W. J., Petrizzo, M. R., Wray, D. S., 2011. The uppermost Middle and Upper Albian succession at the Col de Palluel, Hautes-Alpes, France: An integrated study (ammonites, inoceramid bivalves, planktonic foraminifera,

nannofossils, geochemistry, stable oxygen and carbon isotopes, cyclostratigraphy). *Cretaceous Research* 32, 59-130.

Garrecht Metzger, J., Fike, D. A., 2013. Techniques for assessing spatial heterogeneity of carbonate $\delta^{13}\text{C}$ values: Implications for craton-wide isotope gradients. *Sedimentology* 60, 1405-1431.

Geyer, O. F., Kuss, J., Bachmann, M., 1997. On some Albian ammonites from northeastern Sinai (Egypt). *Paläontologische Zeitschrift* 71, 221-229.

Giorgioni, M., 2012. Long- and short-term changes in Tethyan oceanography and in global carbon cycling during Albian-Cenomanian time. Unpublished PhD Thesis, ETH Zürich, 147pp.

Giorgioni, M., Weissert, H., Bernasconi, S. M., Hochuli, P. A., Coccioni, R., Keller, C. E., 2012. Orbital control on carbon cycle and oceanography in the mid-Cretaceous greenhouse. *Paleoceanography* 27, PA1204.

Giraud, F., Olivero, D., Baudin, F., Reboulet, S., Pittet, B., Proux, O., 2003. Minor changes in surface-water fertility across the oceanic anoxic event 1d (latest Albian, SE France) evidenced by calcareous nannofossils. *International Journal of Earth Sciences* 92, 267-284.

Gradstein, F. M., Ogg, J., Schmitz, M. A., Ogg, G., 2012: A Geologic Time Scale 2012. Elsevier Publishing Company.

Grötsch, J., Billing, I. A. N., Vahrenkamp, V., 1998. Carbon-isotope stratigraphy in shallow-water carbonates: implications for Cretaceous black-shale deposition. *Sedimentology* 45, 623-634.

Hancock, J. M., 2001. A proposal for a new position for the Aptian/Albian boundary. *Cretaceous Research* 22, 677-683.

Hasenboehler, B., 1981. Étude paleobotanique et palynologie de l'Albien et du Cénomaniens du "Bassin Occidental Portugais" au sud de l'accident de Nazaré (Portugal). Université Pierre et Marie Curie, Paris, Thèse 3ème Cycle. Unpublished PhD thesis, 348pp.

Heimhofer, U., Hochuli, P. A., Burla, S., Dinis, J. L., Weissert, H., 2005. Timing of Early Cretaceous angiosperm diversification and possible links to major paleoenvironmental change. *Geology* 33, 141-144.

Heimhofer, U., Hochuli, P. A., Burla, S., Weissert, H., 2007. New records of Early Cretaceous angiosperm pollen from Portuguese coastal deposits: Implications for the timing of the early angiosperm radiation. *Review of Palaeobotany and Palynology* 144, 39-76.

Heimhofer, U., Hochuli, P. A., Burla, S., Oberli, F., Adatte, T., Dinis, J. L. Weissert, H., 2012. Climate and vegetation history of western Portugal inferred from Albian near-shore deposits (Galé Formation, Lusitanian Basin). *Geological Magazine* 149, 1046-1064.

Herrle, J. O., Mutterlose, J., 2003. Calcareous nannofossils from the Aptian-Lower Albian of southeast France: palaeoecological and biostratigraphic implications. *Cretaceous Research* 24, 1-22.

Herrle, J. O., Köbber, P., Friedrich, O., Erlenkeuser, H., Hemleben, C., 2004. High-resolution carbon isotope records of the Aptian to Lower Albian from SE France and the Mazagan Plateau (DSDP Site 545): a stratigraphic tool for paleoceanographic and paleobiologic reconstruction. *Earth and Planetary Science Letters* 218, 149-161.

Holmden, C., Hudson, J. D., 2003. $^{87}\text{Sr}/^{86}\text{Sr}$ and Sr/Ca Investigation of Jurassic mollusks from Scotland: Implications for paleosalinities and the Sr/Ca ratio of seawater. *Geological Society of America Bulletin* 115, 1249-1264.

Howarth, R. J., McArthur, J. M., 1997. Statistics for strontium isotope stratigraphy: a robust LOWESS fit to the marine Sr-isotope curve for 0 to 206 Ma, with look-up table for derivation of numeric age. *The Journal of Geology* 105, 441-456.

Huck, S., Heimhofer, U., Rameil, N., Bodin, S., Immenhauser, A., 2011. Strontium and carbon-isotope chronostratigraphy of Barremian-Aptian shoal-water carbonates: Northern Tethyan platform drowning predates OAE 1a. *Earth and Planetary Science Letters* 304, 547–558.

Huck, S., Heimhofer, U., Immenhauser, A., Weissert, H., 2013. Carbon-isotope stratigraphy of Early Cretaceous (Urgonian) shoal-water deposits: diachronous changes in carbonate-platform production in the north-western Tethys. *Sedimentary Geology* 290, 157–174.

Immenhauser, A., Della Porta, G., Kenter, J. A., Bahamonde, J. R., 2003. An alternative model for positive shifts in shallow-marine carbonate $\delta^{13}\text{C}$ and $\delta^{18}\text{O}$. *Sedimentology* 50(5), 953-959.

Ingram, B. L., Sloan, D., 1992. Strontium isotopic composition of estuarine sediments as paleosalinity – paleoclimate indicator. *Science* 255, 68–72.

Jenkyns, H. C., Clayton, C. J., 1986. Black shales and carbon isotopes in pelagic sediments from the Tethyan Lower Jurassic. *Sedimentology* 33, 87-106.

Jenkyns, H. C., 1995. Carbon-isotope stratigraphy and paleoceanographic significance of the Lower Cretaceous shallow-water carbonates of Resolution Guyot, Mid-Pacific Mountains. In *Proceedings of the Ocean Drilling Program, Scientific Results* 143, 99-104.

Jones, C. E., Jenkyns, H. C., Coe, A. L., Hesselbo, S. P., 1994. Strontium isotopic variations in Jurassic and Cretaceous seawater. *Geochimica et Cosmochimica Acta* 58, 3061-3074.

Kennedy, W. J., Gale, A. S., Bown, P. R., Caron, M., Davey, R. J., Gröcke, J., Wray, D. S., 2000. Integrated stratigraphy across the Aptian-Albian boundary in the Marnes Bleues, at the Col de Pre.-Guittard, Arnanon Drome, and at Tartonne Alpes-de-Haute-Provence, France: A candidate global boundary stratotype section and boundary point for the base of the Albian Stage. *Cretaceous Research* 21, 591-720.

Korte, C., Kozur, H. W., Bruckschen, P., Veizer, J., 2003. Strontium-isotope evolution of Late Permian and Triassic seawater. *Geochimica et Cosmochimica Acta* 67, 47–62.

Masse, J-P., Arias, C., Vilas, L., 1998. Lower Cretaceous rudist faunas of Southeast Spain: An overview. *Geobios* 31, 193-210.

McArthur, J. M., Crame, A. J., Thirlwall, M. F., 2000. Major revision of Late Cretaceous stratigraphy of Antarctica using strontium isotope stratigraphy. *Journal of Geology* 108, 623–640.

McArthur, J. M., Howarth, R. J., Bailey, T. R., 2001. Strontium isotope stratigraphy: LOWESS Version 3. Best-fit line to the marine Sr-isotope curve for 0 to 509 Ma and accompanying look-up table for deriving numerical age. *Journal of Geology* 109, 155–169.

Medus, J., Berthou, P-Y., 1980. Palynoflores dans la coupe de l'Albien de Foz do Folcao (Portugal). *Geobios* 13, 263–269.

Medus, J., 1982. Palynofloristic correlations of two Albian sections of Portugal. *Cuadernos Geología Ibérica* 8, 781–809.

Menegatti, A. P., Weissert, H., Brown, R. S., Tyson, R. V., Farrimond, P., Strasser, A., Caron, M., 1998. High-resolution $\delta^{13}\text{C}$ stratigraphy through the Early Aptian “Livello selli” of the Alpine tethys. *Paleoceanography* 13, 530-545.

Monteil, E., Foucher, J. C., 1998. Cretaceous biochronostratigraphy. In: De Graciansky, P.-C., Hardenbol, J., Jacquin, T., Vail, P. (Eds.), *Mesozoic and Cenozoic Sequence Stratigraphy of European Basins*. SEPM Special Publication, vol. 60. chart.

Mutterlose, J., Bornemann, A., Luppold, F. W., Owen, H. G., Ruffell, A., Weiss, W., Wray, D., 2003. The Vöhrum section (northwest Germany) and the Aptian/Albian boundary. *Cretaceous Research* 24, 203-252.

-
- Nederbragt, A. J., Fiorentino, A., Klosowska, B., 2001. Quantitative analysis of calcareous microfossils across the Albian–Cenomanian boundary oceanic anoxic event at DSDP Site 547 (North Atlantic). *Palaeogeography, Palaeoclimatology, Palaeoecology* 166, 401-421.
- Nøhr-Hansen, H., McIntyre, D. J., 1998. Upper Barremian to upper Albian (Lower Cretaceous) dinoflagellate cyst assemblages, Canadian arctic archipelago. *Palynology* 22, 143-166.
- Oboh-Ikuenobe, F. E., Benson, D. G., Scott, R. W., Holbrook, J. M., Evetts, M. J., Erbacher, J., 2007. Re-evaluation of the Albian–Cenomanian boundary in the US Western Interior based on dinoflagellate cysts. *Review of Palaeobotany and Palynology* 144, 77-97.
- Owen, H. G., 2002. The base of the Albian Stage; comments on recent proposals. *Cretaceous Research* 23, 1-13.
- Parente, M., Frija, G., Di Lucia, M., Jenkyns, H. C., Woodfine, R. G., Baroncini, F., 2008. Stepwise extinction of larger foraminifers at the Cenomanian–Turonian boundary: A shallow-water perspective on nutrient fluctuations during Oceanic Anoxic Event 2 (Bonarelli Event). *Geology* 36, 715-718.
- Patterson, W. P., Walter, L. M., 1994. Depletion of ^{13}C in seawater ΣCO_2 on modern carbonate platforms: Significance for the carbon isotopic record of carbonates. *Geology* 22, 885-888.
- Petrizzo, M. R., Huber, B. T., Wilson, P. A., Macleod, K.G. 2008. Late Albian paleoceanography of the western subtropical North Atlantic. *Paleoceanography* 23, PA001517.
- Rasmussen, E. S., Lombolt, S., Andersen, C., Vejbæk, O. V., 1998. Aspects of the structural evolution of the Lusitanian Basin in Portugal and the shelf and slope area offshore Portugal. *Tectonophysics* 300, 199–225.
- Reichelt, K., 2005. Late Aptian-Albian of the Vocontian Basin (SE-France) and Albian of NE-Texas: Biostratigraphic and paleoceanographic implications by planktic foraminifera faunas. Unpublished PhD Thesis, pp. 125.
- Reinhardt, E. G., Fitton, R. J., Schwarcz, H. P., 2003. Isotopic (Sr, O, C) indicators of salinity and taphonomy in marginal marine systems. *The Journal of Foraminiferal Research* 33, 262-272.
- Rey, J., 1972. Recherches géologiques sur le Crétacé inférieur de l'Estremadura (Portugal). *Memórias dos Serviços Geológicos de Portugal, Nova Série* 21.
- Rey, J., Bilotte, M., Peybernes, B., 1977. Analyse biostratigraphique et paléontologique de l'Albien marin d'Estremadura (Portugal). *Géobios* 10, 369–393.
- Rey, J., 1979. Le Crétacé inférieur de la marge atlantique portugaise: biostratigraphie, organisation séquentielle, evolution paléogéographique. *Ciencias Terra* 5, 97-120.
- Rey, J., 1982. Dynamique et paléoenvironnements du bassin mésozoïque d'Estremadura (Portugal), au Crétacé inférieur. *Cretaceous Research* 3, 103–111.
- Rey, J., 1992. Les unités lithostratigraphiques du Crétacé inférieur de la région de Lisbonne. *Comunicações dos Serviços Geológicos de Portugal* 78, 103–124.
- Rey, J., 1993. Stratigraphie séquentielle sur une plate-forme à sédimentation mixte: exemple du Crétacé inférieur du Bassin Lusitanien). *Comunicações do Instituto Geológico e Mineiro* 79, 87–97.
- Robinson, S. A., 2011. Shallow-water carbonate record of the Paleocene-Eocene Thermal Maximum from a Pacific Ocean guyot. *Geology* 39, 51-54.
- Sessa, J. A., Ivany, L. C., Schlossnagle, T. H., Samson, S. D., Schellenberg, S. A., 2012. The fidelity of oxygen and strontium isotope values from shallow shelf settings: Implications for temperature and age reconstructions. *Palaeogeography, Palaeoclimatology, Palaeoecology* 342-343, 27-39.

Schneider, S., Fürisch, F. T., Werner, W., 2009. Sr-isotope stratigraphy, of the Upper Jurassic of central Portugal (Lusitanian Basin) based on oyster shells. *International Journal of Earth Science* 98, 1949–1970.

Scott, R. W., 2010. Numerical Ages of Selected Rudist Bivalvia: Preliminary Results. *Turkish Journal of Earth Sciences* 19, 769-790.

Sharpe, D. 1850. On the secondary district of Portugal which lies on the North of the Tagus. *Quarterly Journal of the Geological Society of London* 6, 135-201.

Stampfli, G. M., Borel, G. D., 2002. A plate tectonic model for the Paleozoic and Mesozoic constrained by dynamic plate boundaries and restored synthetic oceanic isochrons. *Earth and Planetary Science Letters* 196, 17–33.

Steuber, T., 1999. Isotopic and chemical intra-shell variations in low-Mg calcite of rudist bivalves Mollusca-Hippuritacea): disequilibrium fractionation and late Cretaceous seasonality. *International Journal of Earth Science* 88, 551-570.

Steuber, T., Rauch, M., Masse, J.-P., Graaf, J., Malkoč, M., 2005. Low-latitude seasonality of Cretaceous temperatures in warm and cold episodes. *Nature* 437, 1341–1344.

Stover, L. E., Brinkhuis, H., Damassa, S. P., De Verteuil, L., Helby, R. J., Monteil, E., Partridge, A. D., Powell, A. J., Riding, J. B., Smelror, M., Williams, G. L., 1996. Mesozoic–Tertiary dinoflagellates, acritarchs and prasinophytes. In: Jansonius, J., McGregor, D.C. (Eds.), *Palynology: Principles and Applications, Volume II*. Am. Assoc. Stratigr. Palynol. Found., 1, 641–750.

Traverse, A., 2007. *Paleopalynology* Dordrecht: Springer, 813pp.

Veizer, J., Ala, D., Azmy, K., Bruckschen, P., Buhl, D., Bruhn, F., Carden, G. A. F., Diener, A., Ebner, S., Godderis, Y., Jasper, T., Korte, C., Pawellek, S., Podlaha, O. G., Strauss, H., 1999. ^{87}Sr , $\delta^{13}\text{C}$ and $\delta^{18}\text{O}$ evolution of Phanerozoic seawater. *Chemical Geology* 161, 59–88.

Verdier, J.-P., 1975. Les kystes de dinoflagellés de la section de Wissant et leur distribution stratigraphique au Crétacé Moyen. *Revue de Micropaléontologie* 17, 191-197.

Weissert, H., 1989. C-isotope stratigraphy, a monitor of paleoenvironmental change: a case study from the Early Cretaceous. *Surveys in Geophysics* 10, 1–61.

Wierzbowski, H., Joachimski, M., 2007. Reconstruction of late Bajocian–Bathonian marine palaeoenvironments using carbon and oxygen isotope ratios of calcareous fossils from the Polish Jura Chain (central Poland). *Palaeogeography, Palaeoclimatology, Palaeoecology* 254, 523-540.

Williams, G. L., Brinkhuis, H., Pearce, M. A., Fensome, R.A., Weegink, J. W., 2004. Southern ocean and global dinoflagellate cyst events compared: index events for the Late Cretaceous– Neogene. In: Exon, N.F., Kenneth, J.P., Malone, M.J. (Eds.), *Proceedings of the Ocean Drilling Program, Scientific Results* 189, 1–98:

Wilson, P. A., Norris, R. D., 2001. Warm tropical ocean surface and global anoxia during the mid-Cretaceous period. *Nature* 412, 425-429.

Albian angiosperm pollen from shallow marine strata in the Lusitanian Basin, Portugal

Maurits Horikx¹, Peter A. Hochuli², Susanne Feist-Burkhardt³, Ulrich Heimhofer¹

¹Institute of Geology, Leibniz University Hannover, Callinstrasse 30, 30167 Hannover, Germany.

²Palaeontological Institute, University of Zürich, Karl Schmid-Strasse 4, 8006 Zürich, Switzerland.

³SFB Geological Consulting & Services, Odenwaldstrasse 18, 64372 Ober-Ramstadt, Germany.

1. Abstract

The evolution of angiosperms significantly changed the composition of the terrestrial vegetation during the mid-Cretaceous. In contrast to the wealth of information available on the biology and systematic relationships of early angiosperms, the temporal patterns of their evolution and radiation are poorly constrained. Here we present a continuous angiosperm pollen record from well-dated shallow marine deposits in the Lusitanian Basin, Portugal. The São Julião section provides a solid stratigraphic framework to track angiosperm pollen distribution patterns from the early Albian to early Cenomanian at mid-latitudes. In comparison to previous angiosperm pollen records from the Lusitanian basin, the section shows an extended late Albian succession and provides new insights into the diversification of early angiosperms during this important interval. Productive palynological samples were analysed and 79 different angiosperm pollen types have been recorded. Throughout the Albian angiosperm pollen represent only a minor component of the total palynoflora. The early Albian pollen record is characterized by highly diverse assemblages of monoaperturate pollen of monocot or "magnoliid" affinity and by the first appearance of polyporate and tricolpate pollen of eudicot affinity. A distinct diversification phase among tri- and poly-aperturate pollen (e.g., *Cretacaeiporites*, *Retitrescolpites*, *Rousea*, *Striatopollis* and *Tricolpites*) and the presence of conspicuous pollen grains assigned to *Dichastopollenites* characterize the middle and late Albian palynological assemblages. Thus, the section records a striking sequence of appearances of important angiosperm pollen morphologies. Monocolpates, polyporates and tricolpates appear in the early Albian whereas tricolporates appear from the lower part of the late Albian onwards. Furthermore, well-constrained biostratigraphic ranges of selected angiosperm pollen from mid-latitudes are presented. In view of these new data, the temporal framework of the palynological Subzones II-B and II-C in the Potomac Group succession from the Atlantic Coastal Plain, eastern USA is revised to a middle to late Albian age.

Keywords: Albian, early angiosperm radiation, palynology, biostratigraphy

2. Introduction

Mid-Cretaceous floras are characterized by the diversification and radiation of early angiosperms coinciding with a dramatic drop in the diversity of many gymnosperm and pteridophyte lineages (Lidgard & Crane 1988, Crane & Lidgard 1989, Lidgard & Crane 1990, Crane et al. 1995). The oldest widely accepted angiosperm remains consist of rare monocolpate pollen (*Clavatipollenites*) of Valanginian age (Gübeli et al. 1984, Hughes & McDougall 1987, Hughes 1994). Angiosperms appeared in the lower latitudes and spread diachronously to higher latitudes. In most ecosystems angiosperms dominated the vegetation by the end of the Late Cretaceous (Lidgard & Crane 1988, Crane & Lidgard 1989). The oldest tri-aperturate pollen of eudicot affinity are recorded from the Barremian-Aptian of lower latitudes (Doyle et al. 1977, Penny 1986, 1988, Regali & Viana 1989, Schrank & Mahmoud 2002, Ibrahim 2002, Heimhofer & Hochuli 2010) and from the Albian onwards in middle latitudes (Doyle & Robbins 1977, Heimhofer et al. 2007).

The Lusitanian Basin represents an excellent study area to track early angiosperm radiation patterns during the mid-Cretaceous. Here, important angiosperm meso- and macrofossil remains, including reproductive organs, leaves, fruits and seeds have been found and described (Saporta, 1894, Teixeira, 1948, Groot & Groot 1962, Friis & Pedersen 2011, Friis et al. 1994, 1997, 1999, 2000a, 2000b, 2001, 2009, 2010, 2011, Mendes et al. 2011, 2014a, 2014b). The Potomac Group succession (Atlantic Coastal Plain, eastern USA) represents another classical important angiosperm pollen archive from the mid-Cretaceous (Brenner 1963, Doyle 1992). The compilation of Doyle & Robbins (1977) from the continental succession was used to demonstrate the continuous changes in angiosperm pollen morphology and evolution from the Aptian to Cenomanian. Due to the absence of adequate biostratigraphic marker species or radiometric dating these deposits lack independent time control.

In contrast, shallow marine strata provide an excellent archive for studying angiosperm pollen distribution patterns. The stratigraphic assignment of shallow marine deposits has been improved significantly by the use of strontium-isotope stratigraphy in low-Mg calcite fossils (e.g., oysters, rudists), dinoflagellate cyst biostratigraphy and of age-diagnostic ammonite and rudist findings. A continuous pollen record with well-constrained stratigraphic age control can be established, given that preservation is good and does not change throughout the studied succession. So far, two shallow marine sections from Portugal (Luz and Cresmina) provided a composite record to track the angiosperm pollen evolution between the late Barremian and the early late Albian (Heimhofer et al. 2007, Heimhofer et al. 2012). The late Albian (107.7–100.5 Ma) represents a long interval of the Albian period (113–100.5 Ma) (Gradstein et al. 2012). However, until now this interval is not adequately covered by palynological studies from the Lusitanian Basin (Heimhofer et al. 2005, 2007).

Here we present a high-resolution angiosperm pollen record from the independently dated shallow marine São Julião section in the Lusitanian Basin. This section covers strata of early Albian to early Cenomanian age with a significantly expanded late Albian succession and documents the distribution pattern of angiosperm pollen during an important but poorly documented phase in the early radiation of angiosperms.

The aim of this study is four-fold:

- (1) Provide a continuous and high-resolution angiosperm pollen record from a stratigraphically calibrated succession in the Lusitanian Basin.
- (2) Extend the existing angiosperm pollen record into the late Albian and early Cenomanian.
- (3) Provide biostratigraphic age-ranges for selected angiosperm pollen species and morphological groups.
- (4) Compare the stratigraphic angiosperm pollen succession from São Julião with the existing zonation based on the Potomac Group succession.

3. Geological Setting

The São Julião section (section part I) is located in the Lusitanian Basin, 5 km south of the town of Ericeira (base location: N38°55'847", W9°25'241"). The stratigraphic section with a total thickness of 192 m stretches for 3 km with a dip of 2-3° to the south and is easily accessible along the beach (Fig. 1). A detailed description of the São Julião outcrop is provided by Horikx et al. (2014). Due to unfavourable sampling conditions at the São Julião locality, the topmost 12 m of the composite section were sampled at a different locality 2 km further south (São Julião section part II).

3.1 Lithostratigraphy and sedimentological evolution

The Lusitanian Basin is located in the westernmost part of the Iberian Peninsula and filled with Mesozoic strata deposited on a passive continental margin. During the mid-Cretaceous the Lusitanian Basin was positioned at a paleolatitude of about 25°N (Stampfli & Borel 2002; Fig. 1). During the Early Cretaceous deposition of fluvial and shallow marine sediments was confined to the central and southern part of the Lusitanian Basin. A sea level rise during the Valanginian-Barremian led to the deposition of more open marine strata (Rey 1979, Cunha & Pena dos Reis 1995, Dinis et al. 2008). A break in sedimentation, related to the anti-clockwise rotation of Iberia during the Aptian-Albian transition, is expressed by a major unconformity (MU), well-known from large parts of the Lusitanian Basin (Dinis & Trincão 1995, Dinis et al. 2002). After this phase of non-deposition and/or erosion, coarse-grained siliciclastics, with cross-bedded sands and conglomerates (Rodízio Formation) were deposited diachronously across the southern Lusitanian Basin (Dinis & Trincão 1995, Rey et al. 2006, Dinis et al. 2008). At São Julião, the lowermost outcropping beds (0–16 m) correspond to the topmost part of the Rodízio Formation (Fig. 2). These fluvio-deltaic sediments are overlain by near-shore marine strata of the Galé Formation.

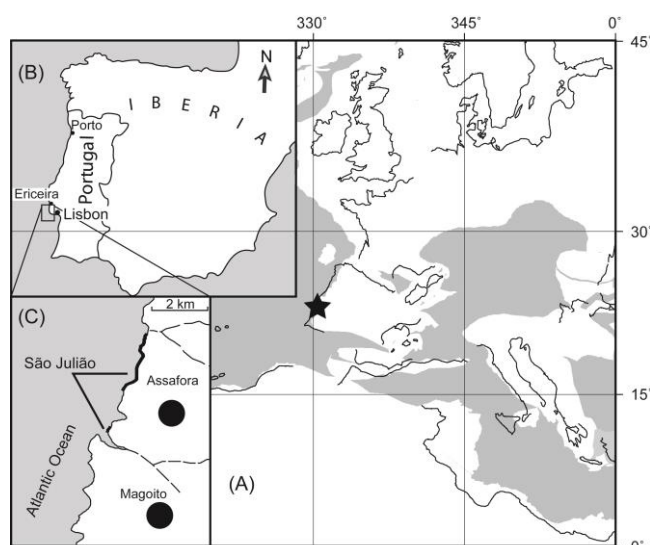


Fig. 1. (A) Paleogeographic map for the Albian (105 Ma) and location of the São Julião section. (Map generated at <http://www.ods.de>). (B) Location of the studied section on the Iberian Peninsula near the town of Ericeira. (C) Map of the study area showing the location of the coastal São Julião section (section part I and II, thick black lines) close to the villages of Assafora and Magoito, ca. 5 km south of Ericeira.

According to Rey (1992) the Galé Formation can be subdivided into two lithological units, the Água Doce Member and Ponta da Galé Member, respectively. The Água Doce Member (16–158 m) is composed of alternating thin (often sub-meter scale), shallow marine sandstone and sand-rich limestone beds with interbedded marls and clays, indicating variations in detrital input (Horikx et al. 2014). A shallow marine depositional setting for the Água Doce Member is corroborated by the common occurrences of bivalve and gastropod remains and the high content of opaque phytoclasts, plant-derived membranes, cuticles and terrestrial palynomorphs in palynological samples. The first occurrence (FO) of macroscopic rudist remains marks the boundary to the overlying Ponta da Galé Member (158–192 m; Rey 1992). This member consists of thick rudist-rich limestone beds with intercalated orbitolinid-rich marls and variegated claystones. The top of the section is marked by the

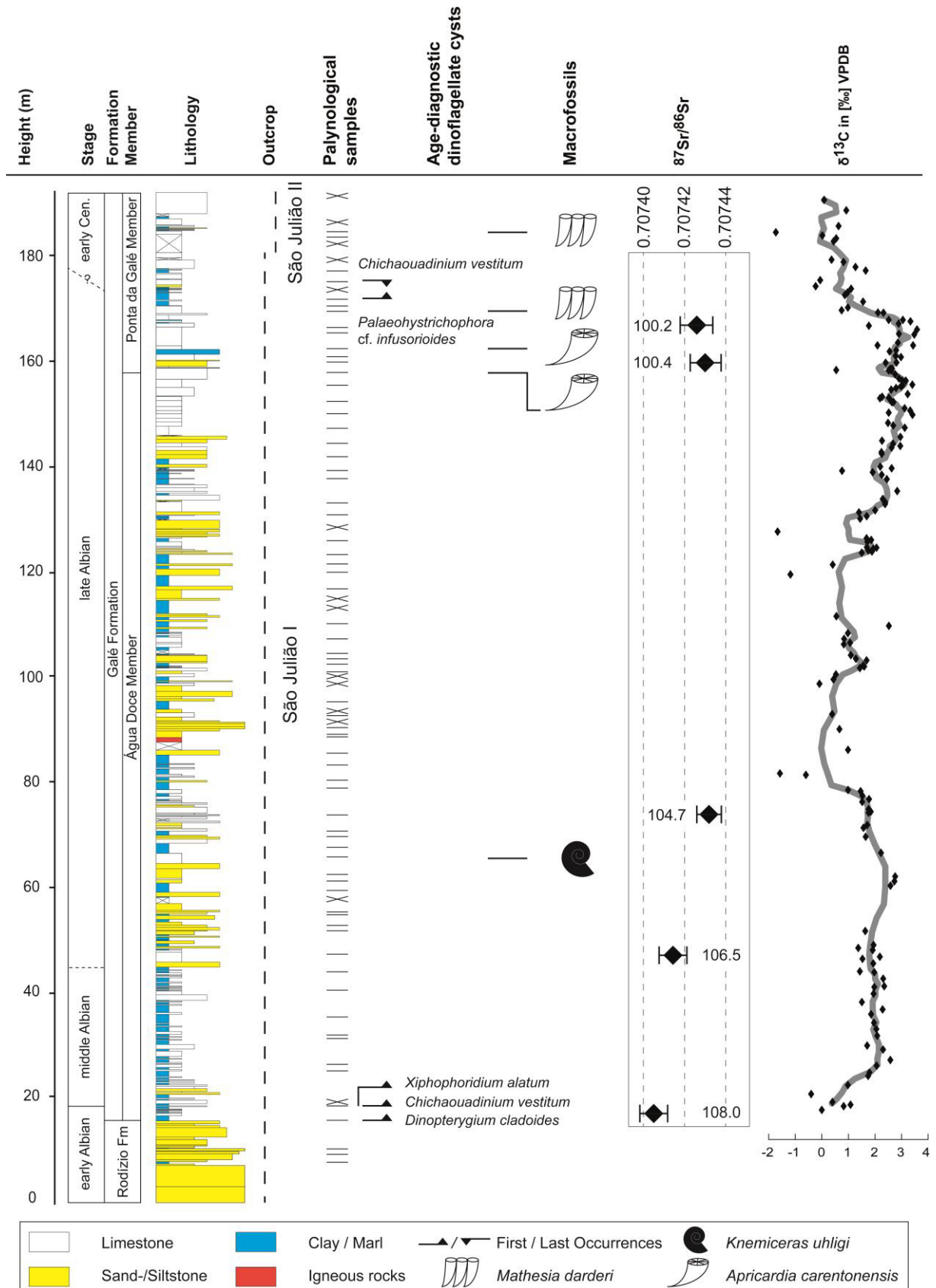


Fig. 2. Lithological log and age assignment of the São Julião section with the first and last occurrences of age-diagnostic dinoflagellate cysts and the position of biostratigraphically important macrofossils. Lines indicate the position of palynological samples, crosses indicate barren samples. Carbon-isotope record and strontium-isotope derived numerical ages with 2σ error bars measured on pristine oyster and rudist shells after Horikx et al. (2014). Lithological units follow Rey (1992).

presence of a conspicuous, about 4 m thick pale-coloured sandy limestone bed rich in orbitolinids, which serves as a regional marker bed (D1 of Berthou & Lauverjat 1979).

3.2 Integrated stratigraphy of the São Julião section

Throughout the São Julião section, typical Early Cretaceous marker fossils (e.g., ammonites, calcareous nannoplankton, planktonic foraminifera) are almost absent and stratigraphic age-assignments of these strata were based on bio- and lithostratigraphic correlations with more open marine strata (e.g., Berthou et al. 1980, Hasenboehler 1981, Médus 1982, Berthou 1984). Recently the section was dated by dinoflagellate cyst biostratigraphy, strontium-isotope ratios from pristine low-Mg calcite oyster or rudist shells as well as carbon-isotope chemostratigraphy (Horikx et al. 2014; Fig. 2). At São Julião, the lowermost 16 m are devoid of age-diagnostic dinoflagellate cysts, oysters and rudist shells. According to Heimhofer et al. (2007) the Rodízio Formation deposited above the MU throughout the Lusitanian Basin is of post-Aptian age. Evidence for an early Albian age is derived from the FO of the dinoflagellate cyst *Dinoptygium cladoides* (Monteil & Foucher 1998; Fig. 2) at 17 m in the lowermost Água Doce Formation. The FO of the typical middle Albian dinoflagellates *Xiphophoridium alatum* and *Chichaouadinium vestitum* (Monteil & Foucher 1998), as well as strontium-isotope derived numerical ages place the early-middle Albian boundary at ~18 m (Horikx et al. 2014). Age diagnostic dinoflagellate cysts characteristic for the middle to late Albian boundary are absent. Based on Sr-isotope data and the presence of the ammonite *Knemiceras uhligi* of late Albian age, this boundary is placed at ~44 m (Horikx et al. 2014). The presence of the rudists *Apricardia carentonensis* and *Mathesia darderi* between 158-184 m corroborates a late Albian age (Horikx et al. 2014). *A. carentonensis* has been reported from the late Albian to early Cenomanian (Berthou et al. 1979) and *M. darderi* was reported from the late Albian in Spain (Masse et al. 1998). The Albian-Cenomanian boundary is tentatively placed between 165 and 175 m in the uppermost part of the section based on the FO of *Palaeohystrichophora* cf. *infusorioides* and the disappearance of *Chichaouadinium vestitum* (Foucher 1981, Williams et al. 2004), combined with strontium-isotope derived numerical ages (Horikx et al. 2014). The overall age-assignment of the São Julião record is further corroborated by the correlation of the carbon-isotope trend with other stratigraphically well-constrained marine sections in the Lusitanian Basin (Portugal), the Umbria-Marche Basin (Italy) and the Vocontian Trough (France) (Horikx et al. 2014 and references therein).

4. Material and Methods

The section was logged bed-by-bed during two field campaigns in 2012 and 2013. Palynological samples were taken from various lithologies (claystones, marl, sandstones and limestones). In order to minimize the risk of contamination, samples from soft lithologies were taken after removal of the surficial scree. In total, 82 sediment samples were selected for palynological analyses. All samples were cleaned and dried for 24h at 40°C. Between 10-30 gram of sample material was sent to the Geological Survey of Nordrhein-Westfalen in Krefeld, Germany for palynological preparation. In order to remove carbonates and silicates, samples were treated with HCl and HF following standard procedures (Traverse, 2007). Polyvinyl alcohol was used as the mounting medium and embedded by Elvacite 2044TM epoxy resin. From each of the 68 productive samples, two palynological strew mounts were prepared and analysed for their palynological content, with a particular focus on angiosperm pollen. The quality of preservation of the palynomorphs is good to excellent as indicated by the preservation of delicate, fine sculptured and thin-walled (angiosperm) pollen and the generally low frequency of damaged palynomorphs. Samples were studied with an OLYMPUS BX 53 transmitted light microscope using a 100x oil immersion objective and differential interference contrast. The presence/absence diagram of the angiosperm pollen in the productive samples was plotted using the Tilia software of Grimm (1991). Light photomicrographs were taken with an OLYMPUS XC 50 digital camera. All slides and remaining palynomorph residues are stored at the Institute for Geology in Hanover, Germany. In order to identify and exclude contamination by modern pollen, suspicious pollen

grains were analysed under fluorescence light using an X-Cite 120Q light source. Cretaceous angiosperm pollen grains emit distinctly less fluorescence than modern pollen, or no fluorescence at all, and can be readily distinguished from potential modern contamination. A selection of the described angiosperm pollen grains were analysed using confocal laser scanning microscopy (CLSM) at the Biology Department of the Technische Universität Darmstadt, Germany. CLSM provides high resolution, fluorescence images of optical sections through an embedded specimen and is applicable to standard palynological slides without any further sample preparation. Optical sections were captured with an image resolution of 1024×1024 pixels and a distance between sections of less than 400 nm. Stacking the optical sections provided a three-dimensional view, with a much higher resolution and depth of field than in normal light microscopy (LM). Confocal images were taken on a Leica TCS_SP under oil immersion at an excitation wavelength of 488 nm and detection of emitted fluorescence light at 500nm and longer.

5. Results

The São Julião section contains rich assemblages of well-preserved angiosperm pollen. In total, 79 different angiosperm pollen species have been distinguished. The majority of these pollen grains (49 taxa) are of eudicot affinity (Fig. 3), whereas 30 different monocolpate pollen taxa of monocot or "magnoliid" affinity (which includes members of the magnoliid clade, the basal ANITA lines, and Chloranthaceae) are observed. Angiosperm pollen grains are illustrated on Plates I-VIII and morphological descriptions are provided in Appendix 1. The pollen grains were differentiated based on important morphological characteristics including size, shape and aperture configuration, exine structure and surface patterns such as ornamentation type, e.g., size and shape of the lumen and muri.

5.1 Systematic palynology

The recovered angiosperm pollen grains are compared with previously published records and - if possible - assigned to established taxa. However, numerous pollen grains from the São Julião record have not been described or differ significantly from previously published records and are catalogued as informal species.

Genus *Ajatipollis* Krutzsch 1970

Description and botanical affinity:

Tetrahedral tetrads of triporate pollen. Pores are arranged along the equator of the individual grains and grouped in clusters of three pores. Circular to subcircular shape of the individual grains but often folded, columellate, semitectate exine. Sometimes the columellae are very densely spaced and fused at their heads forming a perforate tectum. Size of tetrads 21-23 µm, individual grains 10-13 µm. *Ajatipollis* sp. 1 differs from the type species by its large pores (5-6 µm) and thick (2µm) exine.

Recorded species:

Ajatipollis sp. 1, Plate I, 1-2.

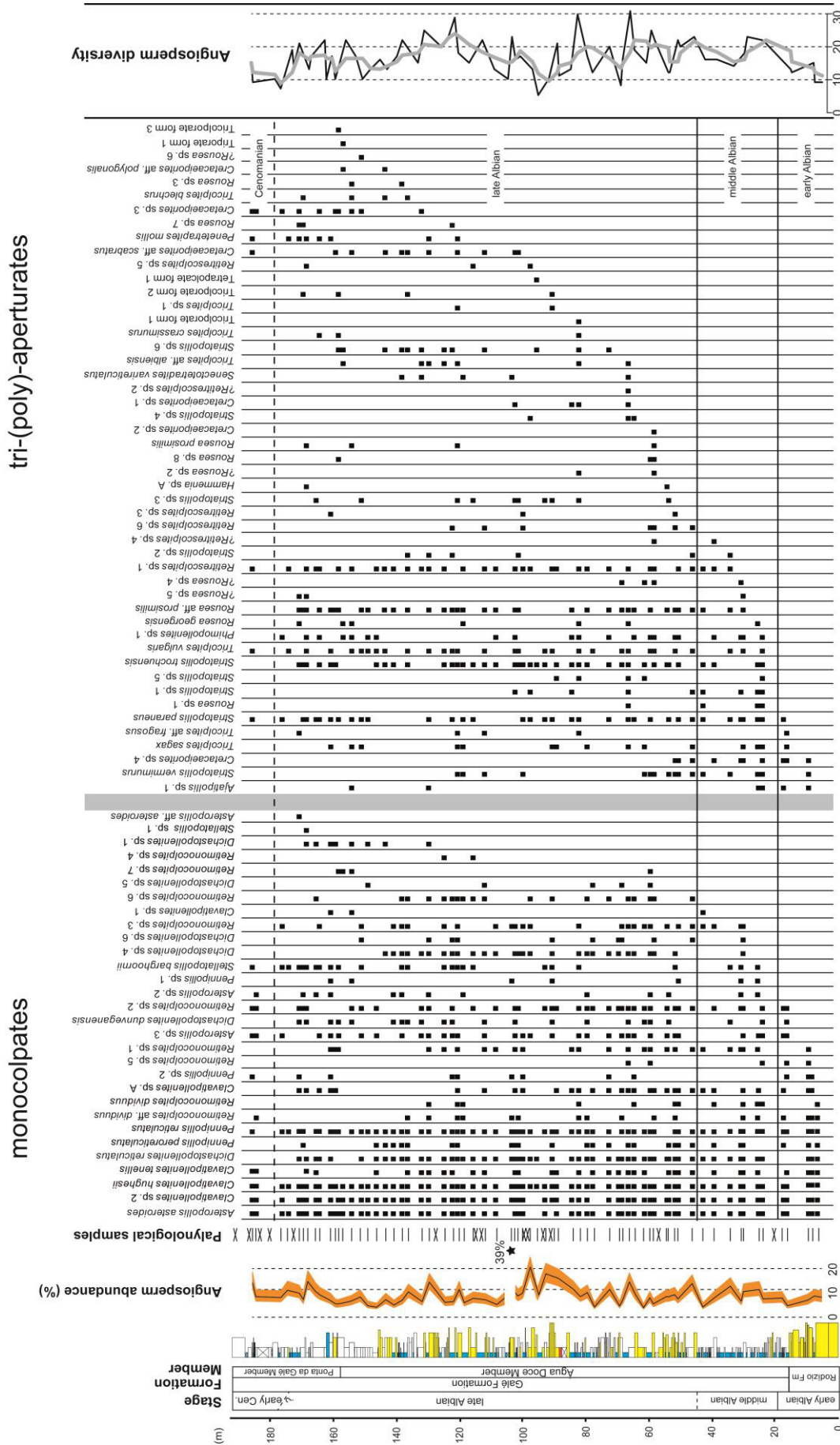


Fig. 3. Relative angiosperm pollen abundances of the total spore-pollen assemblage and stratigraphic distribution of angiosperm pollen in the São Julião section plotted against lithology and age. Orange shading indicates the 95% confidence interval. Horizontal lines indicate position of the productive samples, crosses indicate barren palynological samples. Angiosperm diversity represents the number of taxa per sample, grey line represents three-point moving average

Genus *Asteropollis* Hedlund & Norris 1968*Description and botanical affinity:*

Monocolpate with short 3- to 6-branched colpus (tri-to hexa-trichotomocolpate) confined to the equatorial region of the grain. Circular to sub-circular shape, columellate, semitectate exine. Sometimes the columellae are very densely spaced forming a perforate surface. Size of the pollen grain 14-28 μm . The exine structure and branched colpus of *Asteropollis* pollen is similar to extant *Hedyosmum* pollen of the Chloranthaceae family (Doyle 1969, Walker & Walker 1984).

Recorded species:

Asteropollis asteroides, Plate I, 3-4.

Asteropollis cf. *asteroides*, Plate I, 5-6.

Asteropollis sp. 2 sensu Heimhofer et al. (2007), Plate I, 8-9.

Asteropollis sp. 3 sensu Heimhofer et al. (2007), Plate I, 7.

Genus *Clavatipollenites* Couper 1958

Monocolpate, colpus broad and long, sometimes indistinct. Elliptical to circular shape, columellate, semitectate exine. Sometimes the columellae are very densely spaced and fused at their heads forming a perforate tectum. Size of the pollen grain 14-35 μm . Detailed analysis on exine structure and the presence of in-situ pollen in fossil reproductive structures place *Clavatipollenites* within the extant Chloranthaceae family (Couper 1953, Walker & Walker 1984, Archangelsky & Archangelsky 2013). However, the exact position of *Clavatipollenites* within Chloranthaceae is questioned. A close comparison of fossil fruits (Couperites) containing in-situ *Clavatipollenites* pollen to modern Chloranthaceae fruits places *Clavatipollenites* outside the modern family of Chloranthaceae (Pedersen et al. 1991). Likewise Doyle & Endress (2014) obtained ambiguous results about the exact position of Couperites in their phylogenetic analysis and argued that not all pollen assigned to *Clavatipollenites* are related to Chloranthaceae. According to other sources, *Clavatipollenites* show strong similarities to the pollen of *Austrobaileya* (Endress & Honegger, 1980) and *Trimenia* (Sampson & Endress, 1984).

Recorded species:

Clavatipollenites sp. A sensu Doyle and Robbins (1977), Plate I, 10-11.

Clavatipollenites hughesii, Plate I, 14-15.

Clavatipollenites sp. 1, Plate I, 12-13.

Clavatipollenites sp. 2 sensu Heimhofer et al. (2007), Plate I, 16.

Clavatipollenites tenellis, Plate II, 1-2.

Plate I. Scale bar in all photographs is 10 μm under LM, except otherwise indicated.

- 1-2. *Ajatipollis* sp. 1, SJMH-18, 135.8/3.7, 26.2 m
- 3-4. *Asteropollis asteroides*, SJMH-2, 143.8/11.9, 7.5 m
- 5-6. *Asteropollis* aff. *asteroides*, SSJ-1, 131.4/19.1, 172.4 m
7. *Asteropollis* sp. 3 sensu Heimhofer et al. 2007, SJMH-78, 125.9/15.3, 83.6 m
- 8-9. *Asteropollis* sp. 2 sensu Heimhofer et al. 2007, SJMH-18, 125.8/10.8, 26.2 m
- 10-11. *Clavatipollenites* sp. A sensu Doyle and Robbins 1977, SJMH-4, 130.9/13.7, 10.2 m
- 12-13. *Clavatipollenites* sp. 1, SJMH-32, 133.0/8.2, 44 m
- 14-15. *Clavatipollenites hughesii*. SJMH-56, 145.0/17.1, 66 m
16. *Clavatipollenites* sp. 2 sensu Heimhofer et al. 2007, SJMH-11, 128.0/12.4, 17 m

Plate II. Scale bar in all photographs is 10 μm under LM, except otherwise indicated.

- 1-2. *Clavatipollenites tenellis*, SJMH-4, 138.8/3.4, 10.2 m
3. *Cretacaeiporites* aff. *polygonalis*, SJMH-178, 126.8/10.4, 160 m
4. *Cretacaeiporites* aff. *scabratus*, SJMH-143, 138.6/7.0, 138.1 m
- 5-6. *Cretacaeiporites* sp. 1, SJMH-57, 134.4/15.4, 67.3 m
- 7-9. *Cretacaeiporites* sp. 2, SJMH-52, 133.4/9.9, 59.7 m
- 10-11. *Cretacaeiporites* sp. 3, SJS-9, 139.0/5.2, 166.4 m
- 12-13. *Cretacaeiporites* sp. 4, MAG-1, 148.8/7.8
14. *Dichastopollenites dunveganensis*, SJMH-100, 142.1/6.5, 104 m
15. *Dichastopollenites reticulatus*, SJMH-4, 149.6/4.1, 10.2 m
16. *Dichastopollenites reticulatus*, SJMH-4, 149.6/4.1, 10.2 m CLSM image, total stack projection.
- 17-18. *Dichastopollenites* sp. 1, SJMH-183, 142.3/15.2, 162.2 m

Plate III. Scale bar in all photographs is 10 μm under LM, except otherwise indicated.

1. *Dichastopollenites* sp. 4 sensu Heimhofer et al. 2007, SJMH-54, 134.8/2.1, 60.7 m
2. *Dichastopollenites* sp. 4 sensu Heimhofer et al. 2007, SJMH-54, 134.8/2.1, 60.7 m, CLSM image, total stack projection.
- 3-4. *Dichastopollenites* sp. 5 sensu Heimhofer et al. 2007, SJMH-60, 130.7/18.1, 69.6 m
- 5-6. *Dichastopollenites* sp. 6 sensu Heimhofer et al. 2007, SJMH-119, 131.4/13.7, 170.1 m

-
7. *Dichastopollenites* sp. 6 sensu Heimhofer et al. 2007, SJMH-119, 131.4/13.7, 170.1 m, CLSM image, total stack projection.
- 8-9. *Hammenia* sp. A sensu Burger 1993, MAG-20, 132.5/6.0
10. *Penetetrapites mollis*, SSJ-1, 132.5/20.6, 172.4 m
11. *Penetetrapites mollis*, SSJ-1, 132.5/20.6, 172.4 m, CLSM image, total stack projection.
- 12-13. *Pennipollis peroreticulatus*, SJMH-101, 148.0/14.7, 105.3 m
- 14-15. *Pennipollis reticulatus*, SJMH-101, 136.6/21.9, 105.3 m
- 16-17. *Pennipollis* sp. 1, SJMH-12.5, 135.8/7.4, 17.3 m
18. *Pennipollis* sp. 2, SJMH-4, 126.8/7.5, 10.2 m
19. *Pennipollis* sp. 2, SJMH-4, 126.8/7.5, 10.2 m, CLSM image, total stack projection.

Plate IV. Scale bar in all photographs is 10 μ m under LM, except otherwise indicated.

- 1-2. *Phimopollenites* sp. 1, SJMH-156, 143.3/7.1, 148 m
- 3-4. *Retimonocolpites dividuus*, SJMH-18, 34.4/17.3, 26.2 m
- 5-6. *Retimonocolpites* aff. *dividuus*, SJMH-4, 151.0/11.7, 10.2 m
- 7-8. *Retimonocolpites* sp. 1, SJMH-18, 127.2/18.2, 26.2 m
- 9-10. *Retimonocolpites* sp. 2, SJMH-54, 128.6/17.1, 60.7 m
- 11-12. *Retimonocolpites* sp. 3, SJMH-21.7, 124.9/11.5, 31.7 m
- 13-14. *Retimonocolpites* sp. 4, SJMH-114, 142.1/21.5, 117.4 m
15. *Retimonocolpites* sp. 5 sensu Heimhofer et al. 2007, SJMH-4, 134.9/8.7, 10.2 m
- 16-17. *Retimonocolpites* sp. 7, SJMH-178, 140.3/9.7, 160 m
- 18-20. *Retimonocolpites* sp. 6, SJMH-90, 129.5/14.8, 97.7 m

Plate V. Scale bar in all photographs is 10 μ m under LM, except otherwise indicated.

- 1-2. *Retitrescolpites* sp. 1, PM-19, 144.0/5.1
- 3-4. ?*Retitrescolpites* sp. 2, SJMH-57, 147.1/17.9, 67.3 m
- 5-6. *Retitrescolpites* sp. 3, SJMH-183, 134.1/8.1, 162.2 m
- 7-8. ?*Retitrescolpites* sp. 4, SJMH-52, 130.4/2.6, 59.7 m
- 9-10. *Retitrescolpites* sp. 5, SJS-16, 137.2/10.1, 170.1 m
11. *Retitrescolpites* sp. 6, SJMH-36, 149.9/18.2, 47.3 m
- 12-13. *Rousea georgensis*, SJMH-18, 133.8/5.6, 26.2 m

-
- 14-15. *Rousea* aff. *prosimilis*, SJMH-24, 149.2/9.5, 35 m
 16-17. *Rousea* sp. 1, SJMH-18, 127.6/4.4, 26.2 m
 18-19. ?*Rousea* sp. 2, SJMH-52, 132.0/11.4, 59.7 m
 20. *Rousea* sp. 3, SJMH-147, 129.8/12.2, 139.8 m

Plate VI. Scale bar in all photographs is 10 μ m under LM, except otherwise indicated.

1. *Rousea* sp. 3, SJMH-147, 129.8/12.2, 139.8 m
 2-3. ?*Rousea* sp. 4; SJMH-21.7, 127.1/14.1, 31.7 m
 4. ?*Rousea* sp. 4; SJMH-21.7, 127.1/14.1, 31.7 m, CLSM image, total stack projection.
 5-6. ?*Rousea* sp. 5, SSJ-1, 141.7/6.0, 172.4 m
 7-8. ?*Rousea* sp. 6, MAG-33, 137.7/21.4
 9-10. *Rousea* *prosimilis*, SJS-16, 132.3/3.0, 170.1 m
 11-12. *Rousea*, sp. 7, SSJ-1, 133.7/3.8, 172.4 m
 13-14. *Rousea* sp. 8, SJMH-178, 129.8/9.5, 160 m
 15-16. *Senectotetradites varireticulatus*, SJMH-57, 139.1/18.8, 67.3 m
 17. *Stellatopollis barghoornii*, SJMH-114, 135.1/16.9, 117.4 m
 18-19. *Stellatopollis* sp. 1, SJS-16, 146.5/14.1, 170.1 m
 20-21. *Striatopollis paraneus*, SJMH-119, 147.0/8.0, 121.8 m
 22. *Striatopollis trochuensis*, SSJ-1, 130.0/11.3, 172.4 m, CLSM image, total stack projection.

Plate VII. Scale bar in all photographs is 10 μ m under LM, except otherwise indicated.

- 1-2. *Striatopollis trochuensis*, SSJ-1, 130.0/11.3, 172.4 m
 3-5. *Striatopollis vermimurus*, SJMH-54, 145.4/4.9, 60.7 m
 6-7. *Striatopollis* sp. 1, SJMH-21.7, 148.6/20.4, 31.7 m
 8. *Striatopollis* sp. 2, MAG-10, 149.6/21.4, CLSM image, total stack projection.
 9-10. *Striatopollis* sp. 2, MAG-10, 149.6/21.4
 11-12., *Striatopollis* sp. 3, SJMH-85, 141.8/7.3, 92.6 m
 13. *Striatopollis* sp. 4, SJMH-90, 137.0/7.0, 97.7 m
 14-15. *Striatopollis* sp. 5, SJMH-57, 145.3/12.2, 67.3 m
 16-18. *Striatopollis* sp. 6, SJMH-78, 128.8/7.2, 83.6 m

19-20. Tetracolpate form sp. 1, SJMH-88, 137.3/16.5, 95.85 m

Plate VIII. Scale bar in all photographs is 10 μ m under LM, except otherwise indicated.

1-2. *Tricolpites* aff. *albiensis*, SJMH-78, 136.5/19.5, 83.6 m

3-4. *Tricolpites blechrus*, SJMH-143, 127.9/20.5, 138.1 m

5-7. *Tricolpites crassimurus*, SJMH-78, 148.0/15.4, 83.6 m

8-10. *Tricolpites* aff. *fragosus*, SJMH-11, 135.5/5.9, 17 m

11. *Tricolpites sagax*, SJMH-18, 139.6/21.4, 26.2 m

12-14. *Tricolpites vulgaris*, SJMH-128, 137.3/17.5, 126 m

15-16. *Tricolpites* sp. 1, SJMH-119, 129.1/11.0, 121.8 m

17-18. Tricolporate form 1, SJMH-78, 150.2/9.0 83.6 m

19-20. Tricolporate form 2, SJMH-143, 140.5/8.0, 138.1 m

21-22. Tricolporate form 3, SJMH-178, 139.3/16.0, 160 m

23-24. Triporate form 1, SJMH-177, 143.2/10.1, 158.9 m

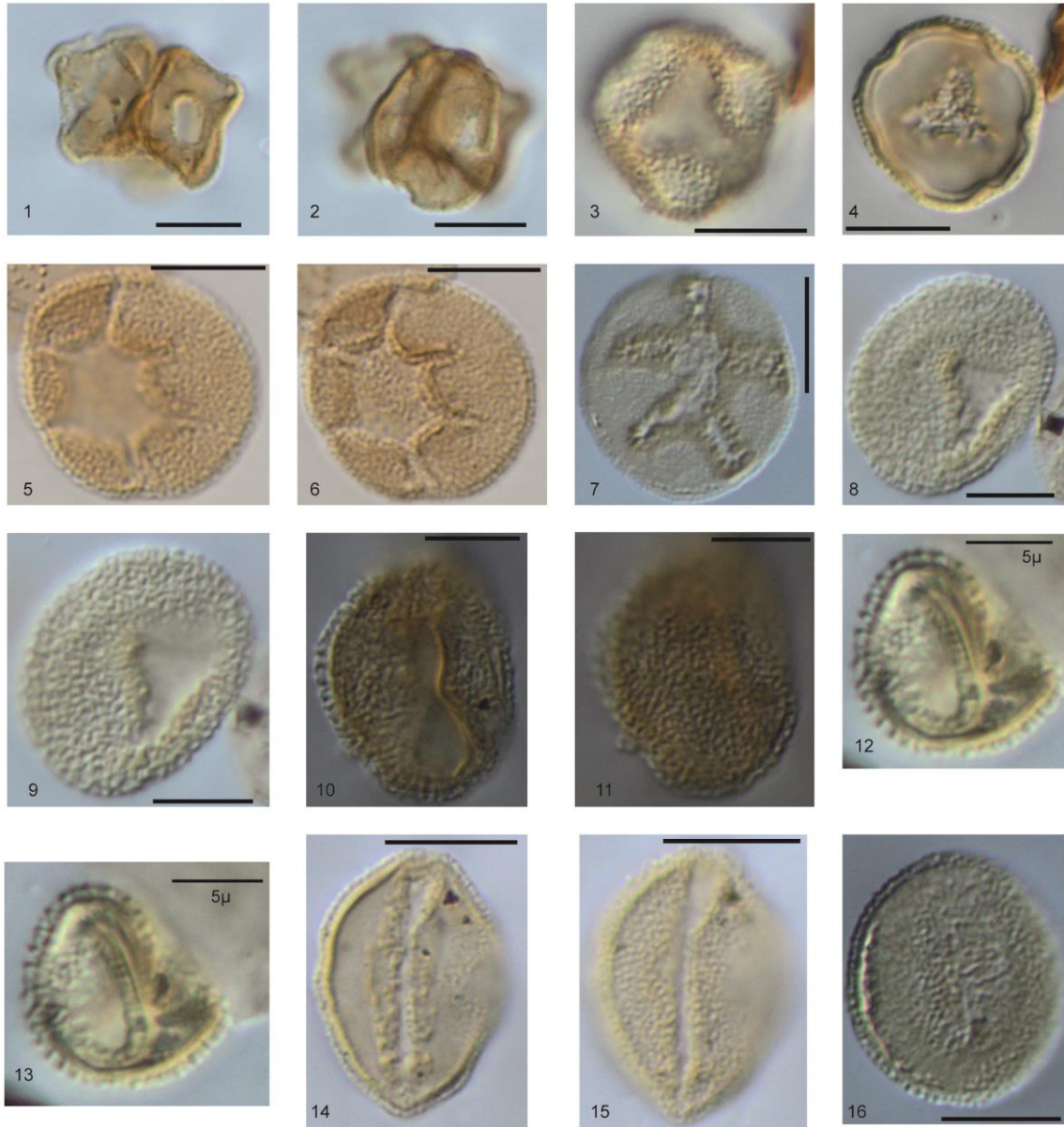


Plate I

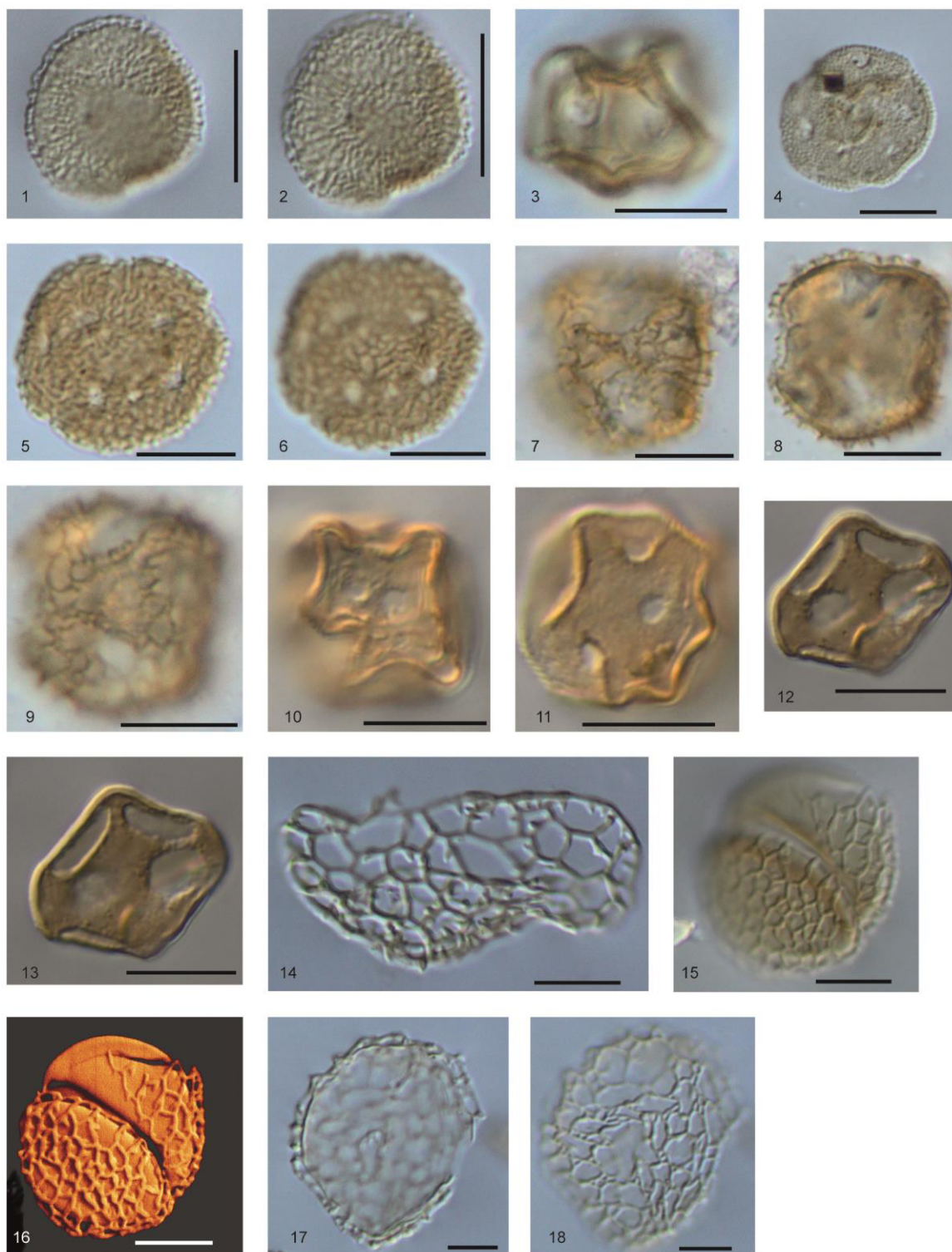


Plate II

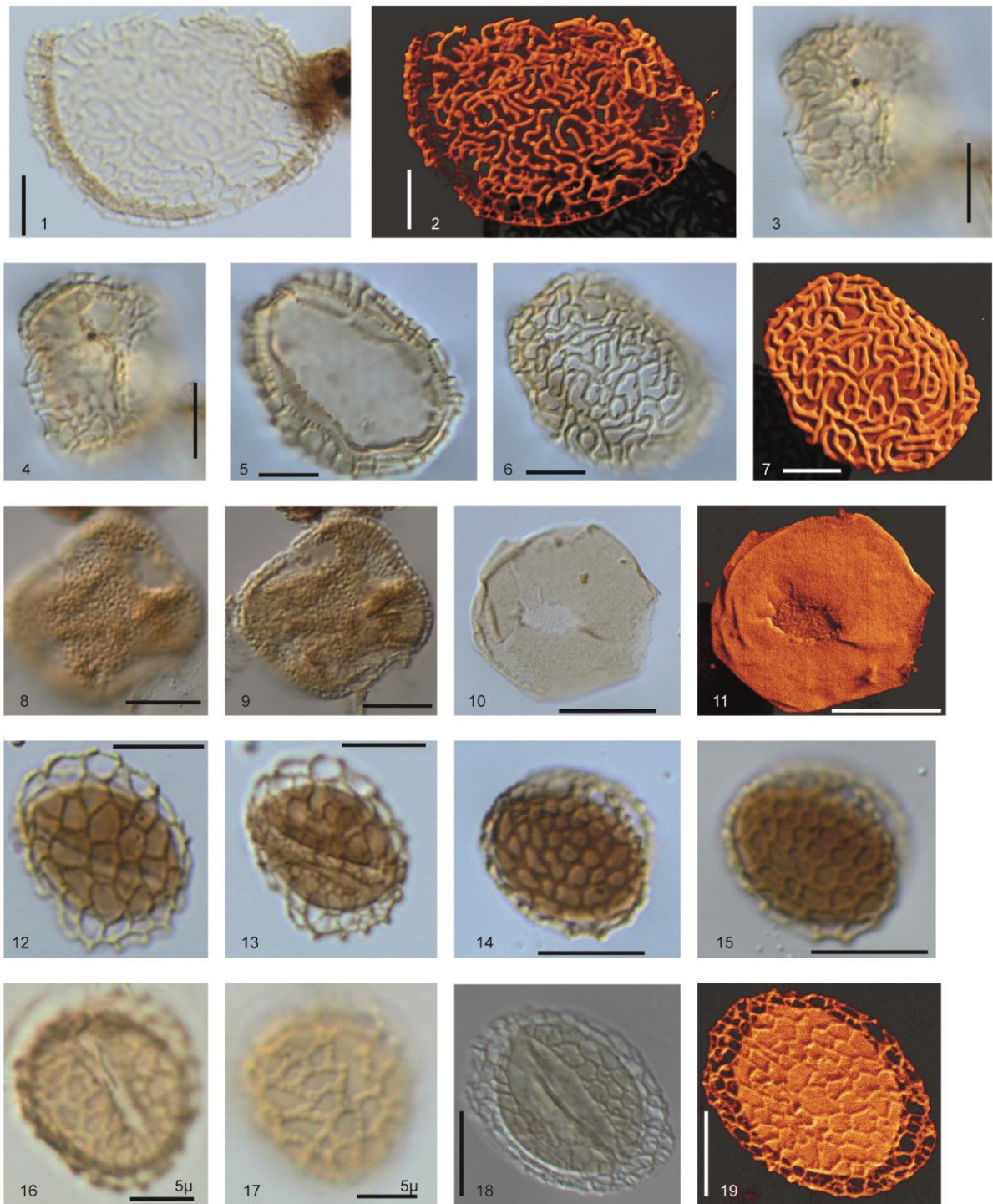


Plate III

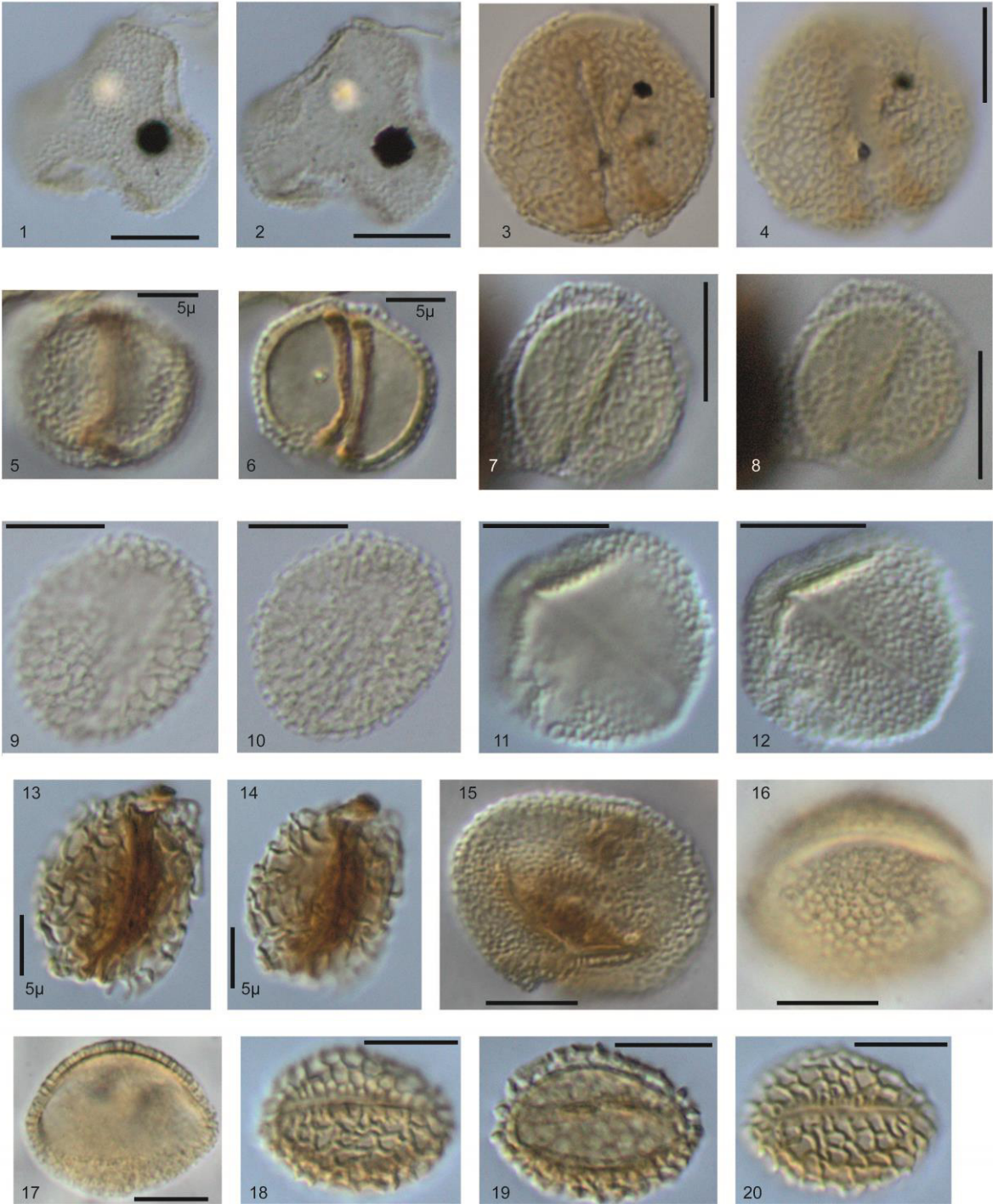


Plate IV

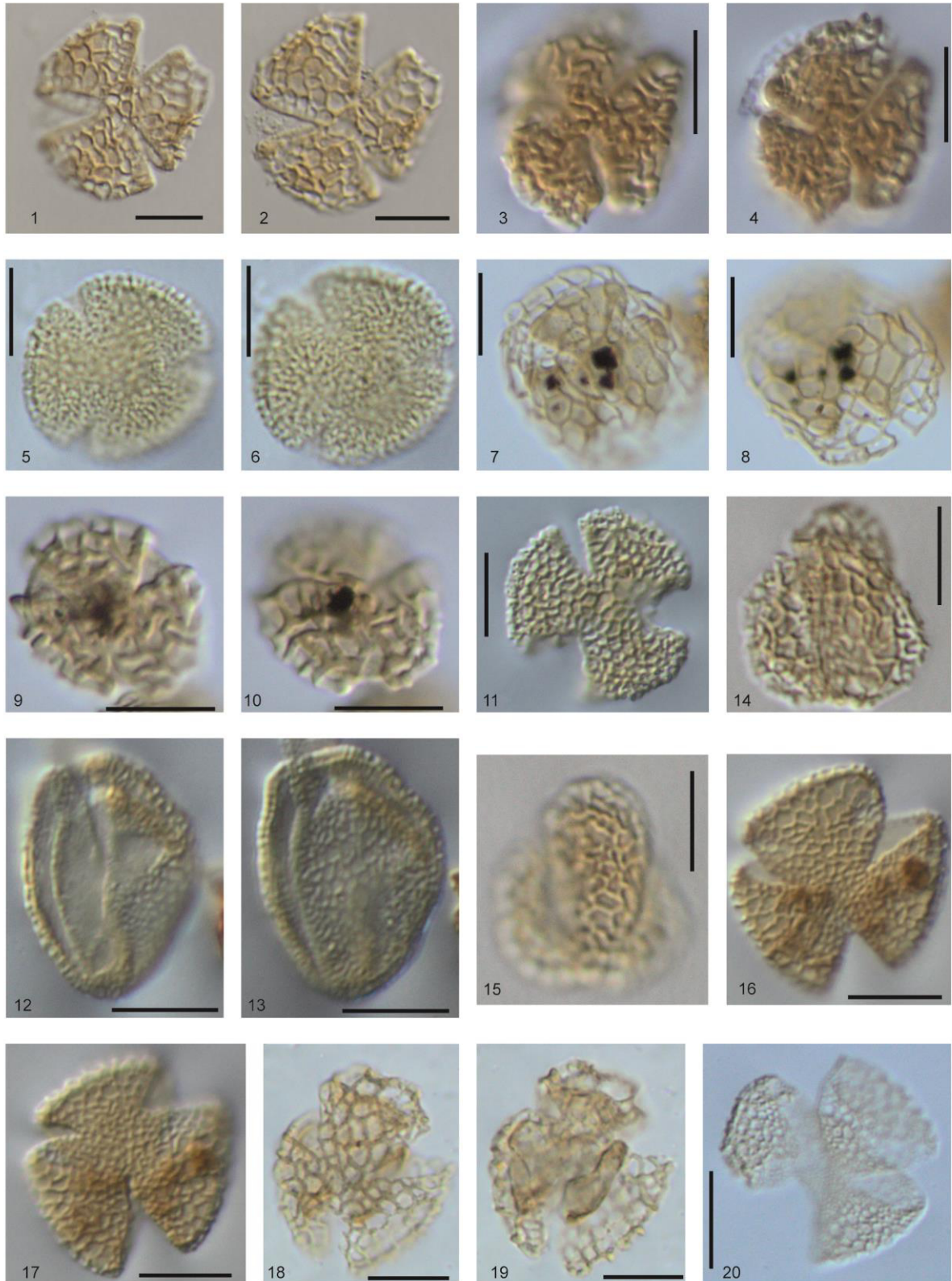


Plate V

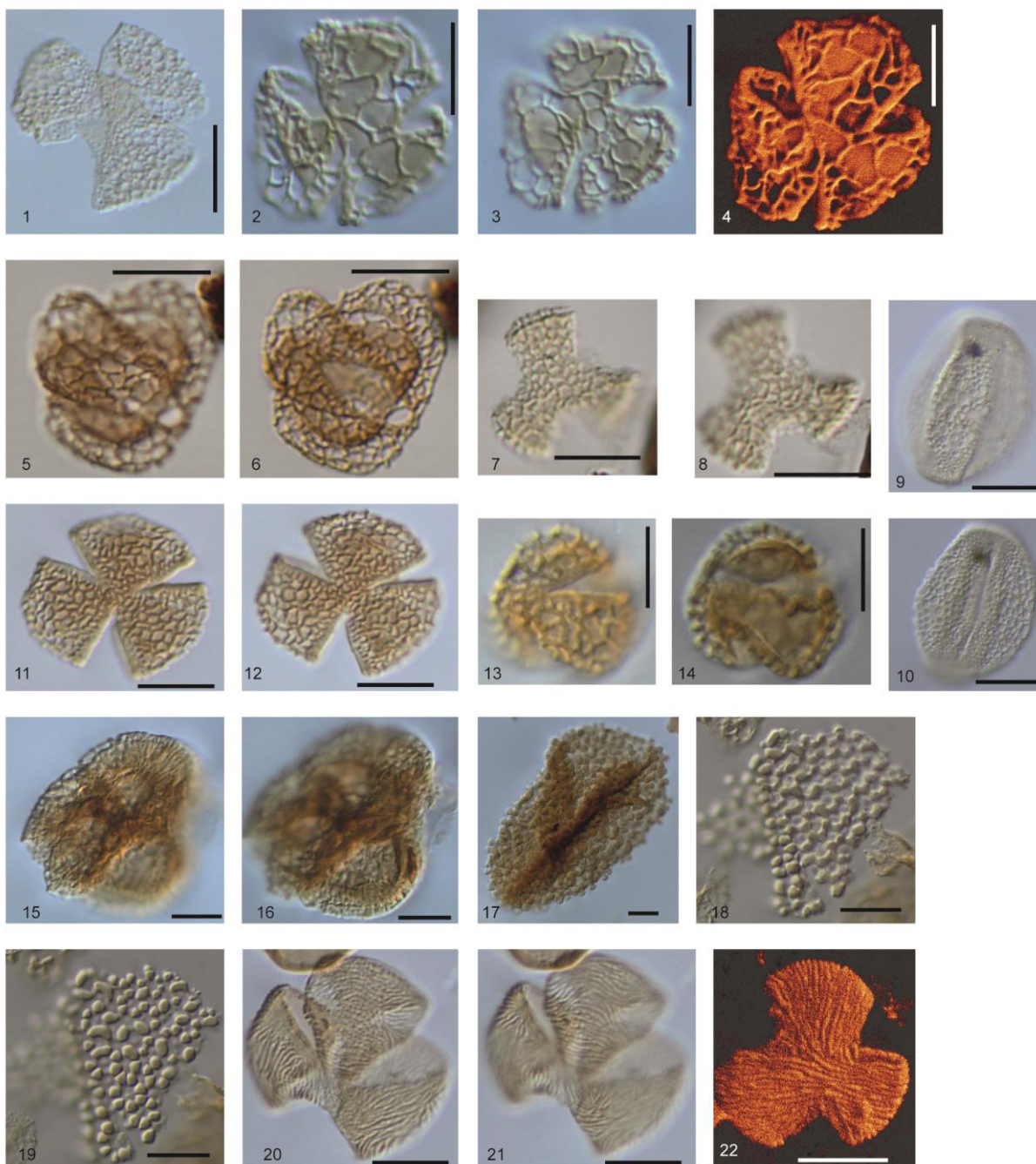


Plate VI

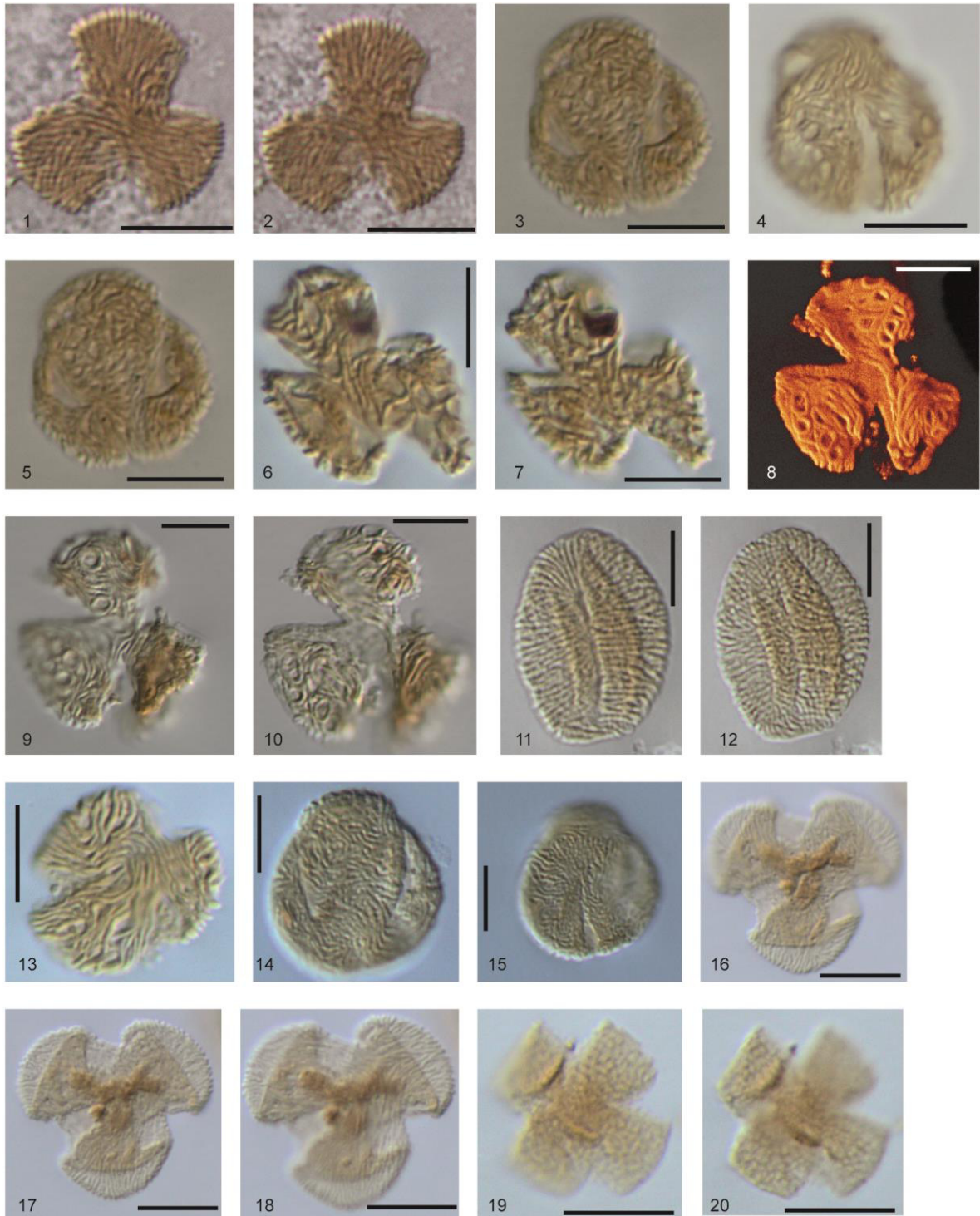


Plate VII

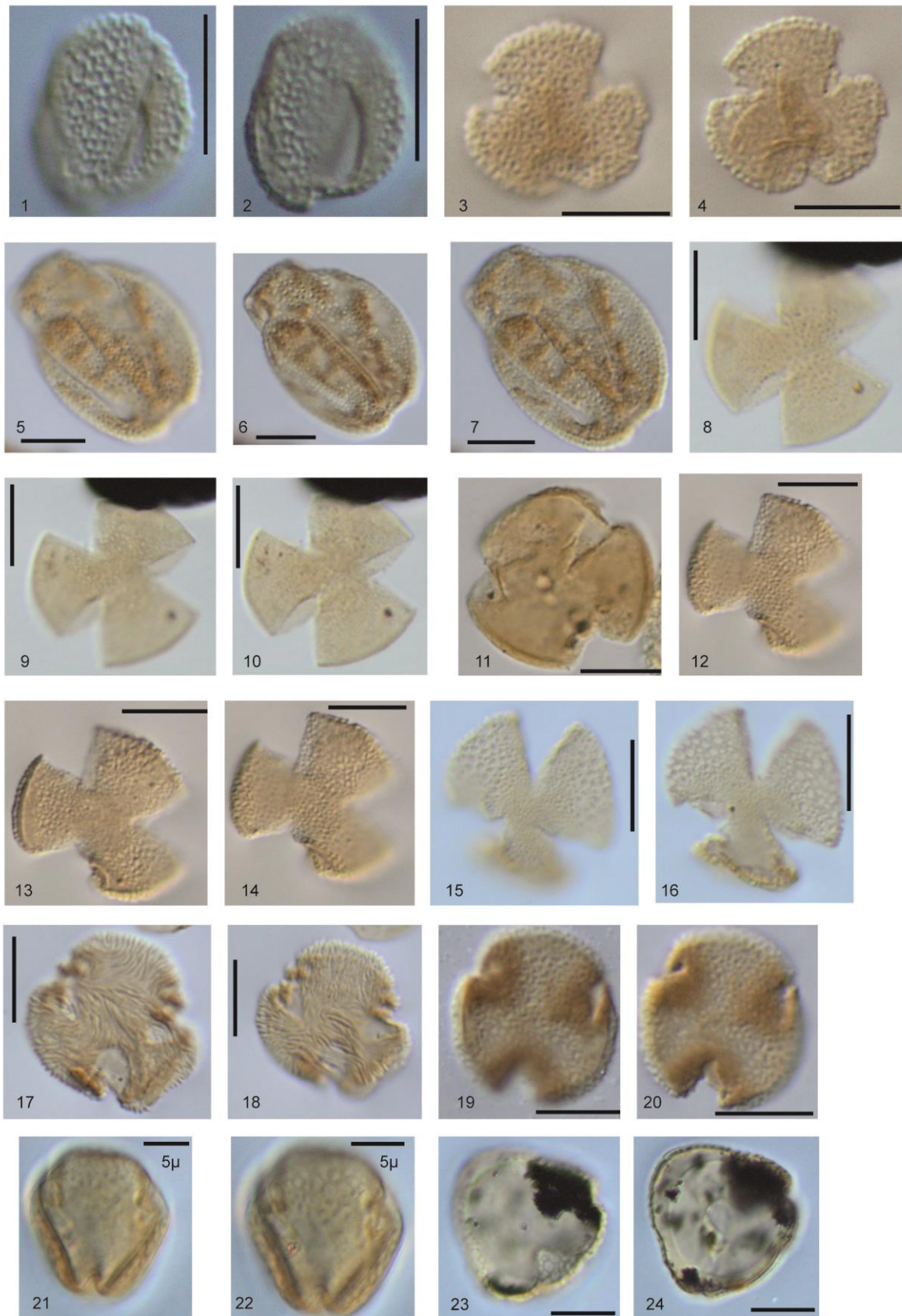


Plate VIII

Genus *Cretacaeiporites* Herngreen 1973*Description and botanical affinity:*

Pollen grains with multiple (mostly more than three) scattered pores. Subcircular to circular shape. Exine columellate, semitectate, striato-reticulate or reticulate-semitectate. Reticulum either homobrochate or heterobrochate, lumen size varies between 0.5-2.5 μm , sometimes irregular reticulum pattern. Size and number of pores vary, with size varying between 1.0-4.0 μm and both characters are species-dependent. Sometimes the muri surface looks verrucate through the overtopping columellae. Size of the grain 17-25 μm . Due to the wide range of pollen morphologies among *Cretacaeiporites*, the exact botanical affinity remains unclear. The exine structure of one species of *Cretacaeiporites* was studied with SEM and TEM by Ward & Doyle (1994) with inconclusive results.

Recorded species:

Cretacaeiporites aff. *polygonalis*, Plate II, 3.

Cretacaeiporites aff. *scabratus*, Plate II, 4.

Cretacaeiporites sp. 1, Plate II, 5-6.

Cretacaeiporites sp. 2, Plate II, 7-9.

Cretacaeiporites sp. 3, Plate II, 10-11.

Cretacaeiporites sp. 4, Plate II, 12-13.

Genus *Dichastopollenites* May 1975*Description and botanical affinity:*

Zonosulcate, colpus separates the pollen grains equatorially into two hemispheres. Circular to elliptical shape, reticulate-semitectate exine. Reticulum either homobrochate or heterobrochate. In some forms the meandering muri and lumina form an irregular reticulum 'maze' structure or the reticulum is composed of small lumina adjacent to larger lumen. Size of lumina varies between 1.0-12.0 μm . Muri width 0.3-1.4 μm . Sometimes the muri surface looks verrucate because of overtopping columellae. Size of the grain 20-50 μm . *Dichastopollenites* pollen have been compared to extant Nymphaeaceae (May 1975). However, in-situ pollen found on the surface of fossil Nymphaeales flowers show a remarkably different morphology than *Dichastopollenites* and question a direct affinity of *Dichastopollenites* pollen to Nymphaeaceae (Friis et al. 2001).

Recorded species:

Dichastopollenites dunveganensis, Plate II, 14.

Dichastopollenites reticulatus, Plate II, 15-16.

Dichastopollenites sp. 1, Plate II, 17-18.

Dichastopollenites sp. 4 sensu Heimhofer et al. (2007), Plate III, 1-2.

Dichastopollenites sp. 5 sensu Heimhofer et al. (2007), Plate III, 3-4.

Dichastopollenites sp. 6 sensu Heimhofer et al. (2007), Plate III, 5-7.

Genus *Hammenia* (Hedlund & Norris 1968) Ward 1986*Description and botanical affinity:*

Stephanocolpate with 6 brevicolpi. (Sub)circular shape, columellate, semitectate exine. Sometimes the columellae are very densely spaced and fused at their heads forming a perforate tectum. Size of the pollen grain ~23 µm. The recorded species from São Julião looks similar to *Hammenia* sp. A sensu Burger (1993) and differs from the type species *Hammenia fredericksburgensis* by developing nonequatorial apertures (Burger 1993).

Recorded species:

Hammenia sp. A sensu Burger (1993), Plate III, 8-9.

Genus *Penetetrapites* Hedlund & Norris 1968*Description and botanical affinity:*

Tri- or tetra-aperturate, three lenticular equatorial apertures, a fourth aperture developed at one pole. Polar aperture about half the diameter of the three equatorial apertures, sometimes almost circular, but variably developed. Oblate shape, scabrate to faintly perforate exine. Size of the pollen grain ~22 µm. Despite the unsettled taxonomic nature (e.g., Ward 1986), we treat *Penetetrapites* as angiospermous.

Recorded species:

Penetetrapites mollis, Plate III, 10-11.

Genus *Pennipollis* Friis et al. 2000b*Description and botanical affinity:*

Monocolpate, colpus almost reaching the apices. Subcircular to circular shape, reticulate-semitectate exine, sexine detached, acolumellate. Muri width 0.5-0.7 µm. Degree of suprategal ornamentation on the muri varies; verrucae in one row, in two rows or absent. Reticulum either homobrochate or heterobrochate. Lumen size 0.5-3.7 µm. Size of the pollen grain 15-27 µm. *Pennipollis* sp. 1 looks similar to "Retimono-knobble" (Penny 1992). A monocot affinity (Alismatales) of *Pennipollis* has been inferred (Friis et al. 2000b), albeit questioned by Doyle & Endress (2014).

Recorded species:

Pennipollis peroreticulatus, Plate III, 12-13.

Pennipollis reticulatus, Plate III, 14-15.

Pennipollis sp. 1, Plate III, 16-17.

Pennipollis sp. 2, Plate III, 18-19

Genus *Phimopollenites* Dettman 1973*Description and botanical affinity:*

Tricolpoidate, in the colpal areas the columellae are discrete and interlocked over the colpoids to form operculoid membranes. The colpoids are elliptical with ragged margins. Oblate to sub(circular) shape, reticulate-semitectate exine. Muri width 0.4 μm . Reticulum homobrochate, lumen size 0.8-1.2 μm . Size of the pollen grain $\sim 20 \mu\text{m}$. *Phimopollenites* sp. 1 differs from the type species by its wide aperture.

Recorded species:

Phimopollenites sp. 1, Plate IV, 1-2.

Genus *Retimonocolpites* Pierce 1961*Description and botanical affinity:*

Monocolpate, colpus long. Elliptical to circular shape, reticulate-semitectate exine. Following Archangelsky & Archangelsky (2013), both homobrochate and heterobrochate lumina are included in *Retimonocolpites*, in some forms the muri and lumina form an irregular reticulum structure. Muri width 0.2-0.6 μm , lumen size 0.5-3.6 μm . Sometimes the muri surface looks verrucate through the overtopping columellae. Size of the pollen grain 15-30 μm . *Retimonocolpites* displays a wide range of morphologies in exine structure, muri width, lumen size and shape, hampering a direct comparison to extant pollen groups.

Recorded species:

Retimonocolpites dividuus, Plate IV, 3-4.

Retimonocolpites aff. *dividuus*, Plate IV, 5-6.

Retimonocolpites sp. 1, Plate IV, 7-8.

Retimonocolpites sp. 2, Plate IV, 9-10.

Retimonocolpites sp. 3, Plate IV, 11-12.

Retimonocolpites sp. 4 Plate IV, 13-14.

Retimonocolpites sp. 5, Plate IV, 15.

Retimonocolpites sp. 6 Plate IV, 18-20.

Retimonocolpites sp. 7, Plate IV, 16-17.

Genus *Retitrescolpites* Sah 1967*Description and botanical affinity:*

Tricolpate, shape subcircular to circular, with reticulate-semitectate exine. Reticulum homobrochate, lumen size 1.5-3.0 μm . *Retitrescolpites* is distinguished from *Rousea* by homobrochate reticulation pattern with large lumina generally $>1 \mu\text{m}$, sometimes irregular reticulum pattern. Muri width 0.3-1.1 μm . Size of the pollen grain 19-23 μm . The recorded species from São Julião could not be assigned to previously described taxa and are listed as informal species.

Recorded species:

Retitrescolpites sp. 1, Plate V, 1-2.

?*Retitrescolpites* sp. 2, Plate V, 3-4.

Retitrescolpites sp. 3, Plate V, 5-6.

?*Retitrescolpites* sp. 4, Plate V, 7-8.

Retitrescolpites sp. 5, Plate V, 9-10.

Retitrescolpites sp. 6, Plate V, 11.

Genus *Rousea* Srivastava 1969

Description and botanical affinity:

Tricolpate, shape subcircular to circular, with reticulate-semitectate exine. Reticulum heterobrochate, lumen size 0.3-4.0 μm and on average $>1 \mu\text{m}$. *Rousea* is distinguished from *Retitricolpites* by its heterobrochate reticulation pattern and from *Tricolpites* by the lumen size exceeding $>1 \mu\text{m}$. In this paper, the term 'heterobrochate' lumen applies to the definition of a 'graded reticulum' (large lumina in the equator and small lumina at the poles) by Srivastava (1969) and of 'interspersed large and small lumina' by Erdtman (1966). Muri width 0.3-0.8 μm . Sometimes the muri surface looks verrucate through the overtopping columellae. Size of the pollen grain 16-26 μm . Several *Rousea* species display variations in exine structure, muri width, lumen size and shape not described in previous records and are listed here as informal species. According to Ward (1986), *Rousea* shows similarities to pollen of the Salicaceae.

Recorded species:

Rousea georgensis, Plate V, 12-13.

Rousea aff. *prosimilis*, Plate V, 14-15.

Rousea sp. 1, Plate V, 16-17.

?*Rousea* sp. 2, Plate V, 18-19.

Rousea sp. 3, Plate V, 20, Plate VI, 1.

?*Rousea* sp. 4, Plate VI, 2-4.

?*Rousea* sp. 5, Plate VI, 5-6.

?*Rousea* sp. 6, Plate VI, 7-8.

Rousea prosimilis, Plate VI, 9-10.

Rousea sp. 7, Plate VI, 11-12.

Rousea sp. 8, Plate VI, 13-14.

Genus *Senectotetradites* Dettman 1973*Description and botanical affinity:*

Tetrahedral tetrads of tricolpate pollen united in permanent tetrahedral tetrads, colpi narrow. Prolate to oblate shape, with reticulate-semitectate exine. The columellae are fused at their distal extremities to form a heterobrochate reticulum. Muri width 0.6 μm . Reticulum heterobrochate, size 1.7-3.0 μm . Tetrad size 44-40 μm , size of the individual pollen grains 22-32 μm .

Recorded species:

Senectotetradites varireticulatus, Plate VI, 15-16.

Genus *Stellatopollis* Doyle et al. 1976*Description and botanical affinity:*

Monocolpate, colpus long. Elliptical shape, reticulate-semitectate exine, with muri-bearing supratectal projections with triangular to elliptical heads. Supratectal elements are arranged in clusters of 4-8 (usually 6) projections. Projections irregularly shaped, mostly oval, round or triangular, apices of triangles directed at centre of lumina. Maximum size of the grain 50 μm , often only fragmentary material found. The crotonoid sculpture and single colpus suggests a possible affinity to pollen of Liliaceae (Doyle et al. 1975).

Recorded species:

Stellatopollis barghoornii, Plate VI, 17.

Stellatopollis sp. 1, Plate VI, 18-19.

Genus *Striatopollis* Krutzsch 1959*Description and botanical affinity:*

Tricolpate, shape subcircular to circular, with striate or striato-reticulate exine. Lumina in striato-reticulate pollen forms are circular to irregular. Sometimes the muri surface looks verrucate through the overtopping columellae. Size of the pollen grain 17-28 μm . Striate tricolpate pollen grains have been found in Albian fossil flowers related to Buxaceae (Pedersen et al. 2007).

Recorded species:

Striatopollis paraneus, Plate VI, 20-21.

Striatopollis trochuensis, Plate VI, 22. Plate VII, 1-2.

Striatopollis vermimurus, Plate VII, 3-5.

Striatopollis sp. 1, Plate VII, 6-7.

Striatopollis sp. 2, Plate VII, 8-10.

Striatopollis sp. 3, Plate VII, 11-12.

Striatopollis sp. 4, Plate VII, 13.

Striatopollis sp. 5, Plate VII, 14-15.

Striatopollis sp. 6, Plate VII, 16-18.

Tetracolpate forms

Tetracolpate, colpi long and broad. Shape subcircular to circular, reticulate-semitectate exine. Reticulum homobrochate, size 0.5-0.8 μm . Muri width 0.6 μm . Size of the pollen grain 17 μm . Columellae heads typically thickened (club-shaped).

Recorded species:

Tetracolpate form 1, Plate VII, 19-20.

Genus *Tricolpites* Cookson ex. Couper 1953

Description and botanical affinity:

Tricolpate, shape subcircular to circular, with reticulate-semitectate exine. Muri width 0.2-0.6 μm . Reticulum either homobrochate or heterobrochate. Size of the lumen 0.2-0.9 μm . Sometimes the columellae are very densely spaced and fused at their heads forming a perforate tectum. Size of the pollen grain 12-32 μm . *Tricolpites* is distinguished from *Retitrescolpites* and *Rousea* by the lumen size <1 μm .

Recorded species:

Tricolpites aff. *albiensis*, Plate VIII, 1-2.

Tricolpites blechrus, Plate VIII, 3-4.

Tricolpites crassimurus, Plate VIII, 5-7.

Tricolpites aff. *fragosus*, Plate VIII, 8-10.

Tricolpites sagax, Plate VIII, 11.

Tricolpites vulgaris, Plate VIII, 12-14.

Tricolpites sp. 1, Plate VIII, 15-16.

Tricolporate forms

Description and botanical affinity:

Tricolporate, circular to oblate shape. Exine structure striate, columellate, semitectate or reticulate-semitectate. Muri width 0.3-0.4 μm . Sometimes the columellae are very densely spaced and fused at their heads forming a perforate tectum. Size of the grains ~20 μm .

Recorded species:

Tricolporate form 1, Plate VIII, 17-18.

Tricolporate form 2, Plate VIII, 19-20.

Tricolporate form 3, Plate VIII, 21-22.

5.2 Stratigraphic distribution of angiosperm pollen

Relative abundances of the angiosperm pollen vary between 1-20%, but are mostly below 10% of the total spore-pollen count (Fig. 3). The accompanying palynoflora is dominated by the non-saccate gymnosperm pollen such as *Classopollis* and *Inaperturopollenites*, whereas *Araucariacites*, *Callialasporites*, *Exesipollenites*, *Cycadopites* and several spore types (e.g., *Cicatricosisporites*, *Leptolepidites*, *Deltoidospora*) occur only in subordinate numbers. Bisaccate pollen (average 1.4%) are consistently present but in low numbers.

5.2.1 Early Albian (0 to 18 m)

In the early Albian (represented by 5 samples) angiosperm pollen abundances fluctuate between 2 and 7% (average 5.3%) of the total palynoflora. The assemblages are characterized by the presence of monocolpate grains (17 species) belonging to *Asteropollis asteroides*, *Clavatipollenites hughesii*, *Clavatipollenites tenellis*, *Dichastopollenites reticulatus*, *Dichastopollenites dunveganensis*, *Pennipollis peroreticulatus*, *Pennipollis reticulatus*, and *Retimonocolpites dividuus*, as well as several informal species (Fig. 3). Rare occurrences of tricolpate and polyporate pollen grains are also found and include *Striatopollis vermimurus*, *Ajatipollis* sp. 1 and *Cretacaeiporites* sp. 4 at 10 m. *Tricolpites* aff. *fragosus*, *Tricolpites sagax* and *Striatopollis paraneus* first appear at 17 m.

5.2.2 Middle Albian (18 to 44 m)

During the middle Albian (represented by 7 samples) the relative abundance of angiosperm pollen is slightly higher and varies between 2 and 12% (average 6.9%). Newly appearing monocolpate pollen include members of the genera *Stellatopollis*, *Asteropollis* and *Clavatipollenites*. *Dichastopollenites* sp. 4 sensu Heimhofer et al. (2007) and *D.* sp. 6 sensu Heimhofer et al. (2007) first appear at 31 m. New tricolpate genera include *Rousea*, *Phimopollenites* and *Striatopollis trochuensis* at 25 m, *Tricolpites vulgaris* at 25 m, *Rousea georgensis* at 26 m, *Rousea* aff. *prosimilis* at 31 m and *Retitrescolpites* sp. 1 at 35 m (Fig. 3).

5.2.3 Late Albian to early Cenomanian (44 to 175 m)

During the late Albian to early Cenomanian (represented by 56 productive samples) the angiosperm pollen abundance fluctuates between 1 and 20% (average 8%). A single sample records a relative angiosperm abundance of 39% strongly dominated by *Pennipollis*. These high values are most probably an artefact, related to the presence of a pollen-sac in the processed sample. A distinct rise in angiosperm pollen abundance is observed between 85-110 m, followed by a subsequent decline towards background values of less than 10%. The late Albian shows a striking increase in tri- and poly-aperturate pollen first appearing within this interval.

Among monocolpate pollen forms, several (total of 7) informal species of the *Retimonocolpites*, *Asteropollis* and *Dichastopollenites* groups appear for the first time during the late Albian, *Dichastopollenites* sp. 5 sensu Heimhofer et al. (2007) first appears at 61 m. Newly appearing tricolpate pollen taxa are represented by *Striatopollis* (three new informal species), *Rousea* (7 new informal species) and *Retitrescolpites* (four new informal species). The diversification among *Tricolpites* pollen is indicated by the FO of *Tricolpites* aff. *albiensis* (67 m), *Tricolpites crassimurus* (84 m) and *Tricolpites blechrus* (138 m). Polyporates with a FO in the late Albian include rare occurrences of *Cretacaeiporites* sp. 2 (60 m), *Cretacaeiporites* sp. 1 (67 m) and *Cretacaeiporites* aff. *polygonalis* (145 m). *Cretacaeiporites* sp. 3 and *Cretacaeiporites* aff. *scabratus* first appear during the latest Albian. Rare occurrences of tricolporate pollen in the late Albian are evidenced by the FO of Tricolporate form 1 (84 m), Tricolporate form 2 (90 m) and Tricolporate form 3 (160 m). The obligate tetrad of *Senectotetradites varireticulatus* appears for the first time at 67 m, and *Penetetrapites mollis* at 122 m. Important last occurrences (LO) include *Striatopollis vermimurus* (122 m), *Retimonocolpites dividuus* (131 m), *Dichastopollenites* sp. 4 sensu Heimhofer et al. (2007) (145 m), *D.* sp. 5 sensu Heimhofer et al. (2007) (151 m) and *D.* sp. 6 sensu Heimhofer et al. (2007) (153 m).

6. Discussion

6.1 Timing of angiosperm pollen evolution and biostratigraphic significance

The Cresmina section represents another important archive to track the angiosperm pollen distribution during the Albian in the Lusitanian Basin. Located about 20 km to the south of São Julião, the section covers 129 m of early to late Albian deposits with diverse angiosperm pollen assemblages. The angiosperm pollen distribution in these near-shore deposits has been extensively studied (Hasenboehler 1981, Chapman 1982, Heimhofer et al. 2007, 2012) and recently the two sections have been correlated (Horikx et al. 2014). The Cresmina section covers an extended early Albian succession, whereas the late Albian strata are more carbonate rich and reduced in thickness (~30 m). The São Julião section with an extended late Albian is covered by 56 samples (compared to three samples from the Cresmina record) and therefore significantly expands the angiosperm pollen record towards the early Cenomanian in the Lusitanian Basin. Despite the absence of some angiosperm pollen types in the São Julião section as compared to the Cresmina section (e.g., *Artipollis praecox* and *Racemonocolpites exoticus*), both sections show very similar assemblages in the stratigraphically overlapping part (sensu Heimhofer et al. 2007, Appendix 1). Whereas the monocolpate pollen record in both sections is similar, a significantly higher diversity of tricolpate pollen is recorded from São Julião. This clear discrepancy and underrepresentation of tricolpate pollen in the Cresmina record may be related to differences in the composition of the vegetation thriving in the corresponding catchment area in the hinterland of the two sections.

The angiosperm pollen assemblage at São Julião section was previously studied by Médus & Berthou (1980). According to these authors, the lower part of the São Julião section, named 'Foz do Folcao', was characterized by a high diversity of tricolpate, tricolporoidate and tricolporate pollen, and a middle to late Albian age was attributed to it. Unfortunately, a more detailed comparison with this record is hampered by the low stratigraphic resolution of the data-set (11 productive samples), the unclear stratigraphic position of the palynological samples and the scant documentation.

The São Julião section provides valuable biostratigraphic information on the first appearance of the various morphological groups and important taxa of angiosperm pollen (Fig. 4). The early Albian angiosperm pollen assemblages are dominated by monocolpate pollen groups (*Asteropollis*, *Clavatipollenites*, and *Pennipollis*). Most of these groups have been recorded in pre-Albian strata of the Lusitanian Basin and are long-ranging (Heimhofer et al. 2007). *Asteropollis asteroides* is known to appear first during the Barremian-Aptian and to range up to the Cenomanian (Zhang et al. 2014), whereas *Clavatipollenites* is known from the Valanginian (Gübeli et al. 1984, Hughes & McDougall 1987, Hughes 1994). *Pennipollis* (as *Peromonolites*, Brenner 1963) is known from the Aptian up to the Cenomanian (Doyle & Robbins 1977, Doyle 1992, Heimhofer et al. 2007, Archangelsky et al. 2009). *Retimonocolpites dividuus* was first reported in North America from the Albian (e.g., Singh 1971, Doyle & Robbins 1977, Ward 1986) and from strata of early Albian age in England (as *Clavatipollenites rotundus*, Kemp 1968). *Retimonocolpites dividuus* ranges from the early Albian to the late Albian in São Julião and Cresmina (Heimhofer et al. 2007; Fig. 4) and to the Cenomanian in North America (Hedlund & Norris 1968, Doyle & Robbins 1977).

The FO of *Cretacaeiporites* sp. 4 in the early Albian represents one of the earliest records of polyporate pollen at mid-latitudes (Fig. 4). Polyporate pollen grains have been recorded by Hasenboehler (1981), Chapman (1982) and Barrón et al. (2015) from the late Albian of the Lusitanian Basin and from Spain. Jardiné & Magloire (1965), Hengreen (1973), Ibrahim (2002) and El-Beialy et al. (2011) reported *Cretacaeiporites* in Albian strata from low paleolatitudes in Africa and South America. The presence of *Cretacaeiporites* at São Julião represents a tropical floral element from lower latitudes and supports the concept that Iberia was located in a transitional area between the Northern Gondwana and Southern Laurasia floral zones.

Tricolpites and *Striatopollis* represent the first tricolpate pollen in the São Julião record (Fig. 3). The presence of *T. sagax*, *S. paraneus*, and *S. vermimurus* in early Albian strata predates earlier findings of these species at mid-latitudes. *T. sagax* was previously described from the middle Albian to early Cenomanian in North America and Spain (Norris 1967, Ward 1986, Barrón et al. 2015). At lower latitudes, *Striatopollis* is reported from the Barremian-Aptian in Egypt, Gabon and Congo and

represents one of the oldest tricolpate pollen groups (Doyle et al. 1977, Penny 1988). At mid-latitudes *S. paraneus* and *S. vermimurus* were found in middle Albian to early Cenomanian strata from Canada, USA and Iberia (Norris 1967, Hasenboehler 1981, Ward 1986, Villanueva-Amadoz et al. 2011). At São Julião *S. paraneus* continues from the early Albian onwards into the Cenomanian, whereas *S. vermimurus* disappears in the latest Albian (Fig. 4). The presence of *Striatopollis trochuensis* at São Julião (middle to late Albian) slightly postdates the finding of Heimhofer et al. (2007) from early Albian strata in Portugal. Other findings of *S. trochuensis* include the late Albian in Spain (Barrón et al. 2015) and North America (Norris 1967, Ward 1986) and the Cenomanian in Egypt (Ibrahim 1996, 2002).

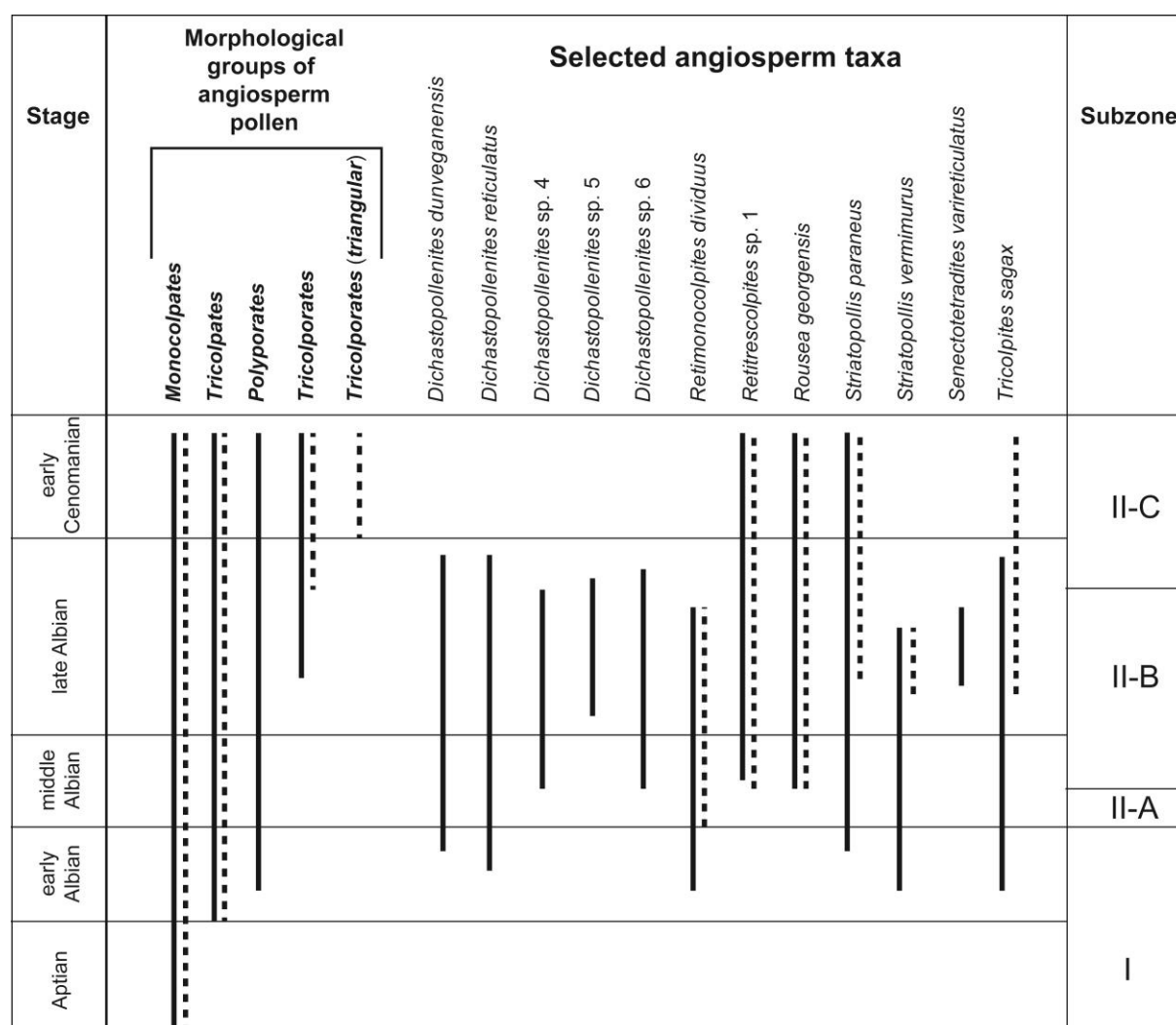


Fig. 4. Biostratigraphic age-range of selected angiosperm pollen taxa and morphological groups from the São Julião section and stratigraphic correlation to the palynological Subzones of the Potomac Group succession, eastern USA. Solid lines represent angiosperm pollen range chart from the São Julião section; dashed lines show the angiosperm pollen data from the Potomac Group succession.

Noteworthy are the FOs of several species of *Dichastopollenites* (*D.* sp. 4 sensu Heimhofer et al. 2007, *D.* sp. 5 sensu Heimhofer et al. 2007 and *D.* sp. 6 sensu Heimhofer et al. 2007) during the middle and late Albian (Fig. 3, Fig. 4). In the Lusitanian Basin these conspicuous pollen are relatively common in the palynological assemblages of middle to late Albian age (see also Heimhofer et al. 2007). *Dichastopollenites* sp. 5 first appears in the lower part of the late Albian (Heimhofer et al. 2007), whereas *D.* sp. 4 and *D.* sp. 6 first appear during the middle Albian (Fig. 4). The presence of *Dichastopollenites dunveganensis* in the early Albian coincides with the Cresmina record (Heimhofer et al. 2007), whereas the early Albian FO of *D. reticulatus* significantly extends the stratigraphic age

range of this species (Fig. 4). Previously, *D. reticulatus* was known only from the Cenomanian in Canada (May 1975).

At São Julião two species (*Penetetrapites mollis* and the obligate tetrads *Senectotetradites varireticulatus*) occur from the late Albian onwards (Fig. 4). *Penetetrapites mollis* has a global distribution and is a common element in palynological assemblages from the middle Albian to the Cenomanian (Hedlund & Norris 1968, Ward 1986, Villanueva-Amadoz et al. 2011), whereas *Senectotetradites varireticulatus* is documented from the latest Albian onwards from Spain and Australia (Burger 1993, Villanueva-Amadoz et al. 2011, Sender et al. 2012, Barrón et al. 2015).

The FO of tricolporate pollen grains in the lower part of the late Albian highlights a new step in angiosperm pollen evolution (Fig. 4) and corroborates the timing of the first tricolporates in previous studies. Tricolporate pollen have been reported from the late Albian in the Lusitanian Basin (Hasenboehler 1981, Chapman 1982), as well as from Canada, Egypt and Spain (Singh 1983, El-Beialy et al. 2010, Sender et al. 2012, Barrón et al. 2015).

6.2 Comments on the timing of the Potomac succession

The Potomac Group succession is characterized by the relatively low diversity of monocolpate angiosperm pollen and the absence of *Dichastopollenites* and polyporate pollen grains, but conversely it has a continuous and consistent presence of several tricolpates and monocolpates with a graded reticulum of the *Liliacidites* type compared to the Albian pollen records from shallow marine records in Portugal (Doyle & Robbins 1977, Heimhofer et al. 2007). However, these continental deposits lack independent age control and contain a number of major discontinuities. Previously, the dating of the palynological zones (Zone I and Subzone II-A) in the Potomac Group succession was revised based on comparison with stratigraphically well-constrained angiosperm pollen records from Cresmina and Luz in the Lusitanian Basin by Hochuli et al. (2006). The São Julião record expands the Portuguese pollen record into the early Cenomanian and allows a direct comparison with Subzones II-B and II-C of the Potomac succession to be made. According to Doyle & Hickey (1976) and Doyle & Robbins (1977), the angiosperm pollen composition in the middle part of Subzone II-B is very similar to the palynological assemblages of middle Albian marine strata in Oklahoma, whereas the upper part of Subzone II-B is of late Albian age (Hedlund & Norris 1968, Hedlund & Norris 1986). In contrast, Hochuli et al. (2006, p. 591) suggested a late Albian age for the entire Subzone II-B based on the presence of the late Albian index species *Cupuliferoidaepollenites parvulus*.

The lower part of Subzone II-B in the Potomac Group is marked by the FO of tricolpate pollen types and several of these (e.g., *Tricolpites* aff. *albiensis*, *T. crassimurus*) also occur at São Julião. However, the FOs and stratigraphic ranges of these species vary compared to São Julião and hamper a clear age assignment of the lower part of Subzone II-B. A typical element of Subzone II-B is *Tricolpites* sp. B sensu Doyle & Robbins (1977) that looks very similar to *Retitrescolpites* sp. 1 (Plate V, 1-2, Appendix 1). *Retitrescolpites* sp. 1 first appears in the middle Albian (Fig. 4) and *Rousea georgensis*, another Subzone II-B marker, during the middle Albian at São Julião (Fig. 4). Based on the appearance of *Retitrescolpites* sp. 1 and *Rousea georgensis* in the lower part of Subzone II-B, this level could be tentatively placed in the uppermost middle to earliest late Albian.

As shown in the range chart compiled by Hochuli et al. (2006) from the data of Doyle & Robbins (1977), the transition from the lower to the upper part of Subzone II-B is characterized by a 'sudden' diversity increase, suggesting another possible hiatus. This interval shows the further diversification of several tricolpates with long stratigraphic ranges. Of special interest however, is the striking LO of *Striatopollis vermimurus* in this interval and its disappearance from the palynological record during the latest Albian at São Julião (Doyle & Robbins 1977, Hochuli et al. 2006; Fig. 4). Therefore, the LO of *Striatopollis vermimurus* in the upper part of Subzone II-B is interpreted to represent a stratigraphic marker for a latest Albian age.

According to Doyle & Robbins (1977), Subzone II-B can be separated from the lower Subzone II-C by the presence of small, psilate tricolporates. Tricolporates are rare and hard to recognize and as these authors already indicate, "it is easy to confuse Subzone II-C floras with depauperate Subzone II-B floras" (Doyle & Robbins 1977 p. 58). A late Albian age for the lower part of Subzone II-C is

corroborated by the FO of several tricolporates in the late Albian at São Julião (Fig. 3, 4). The FO of tricolporate pollen grains with a conspicuous triangular shape (*Tricolporoidites triangulus*) in Subzone II-C marks an important event in angiosperm pollen morphology evolution. Furthermore, tricolporates become increasingly more abundant and diverse in younger (Zone III) sediments of the Potomac Group succession. Despite the presence of several tricolporate pollen in the late Albian in the Portuguese sections (Fig. 3, Fig. 4) triangular-shaped tricolporate pollen grains have not been recorded. The absence of triangular shaped tricolporates in the São Julião record may therefore point to an early Cenomanian age for the upper part of Subzone II-C.

7. Conclusions

(1) The São Julião section shows the distribution of new and already documented angiosperm pollen types considered typical for the mid-latitudes. The angiosperm pollen record documents rich assemblages of monocolpate pollen (30 taxa) of monocot or "magnoliid" affinity and tri- and poly-aperturate pollen (49 taxa) of eudicot affinity.

(2) The early Albian angiosperm pollen record is characterized by the common occurrence of monocolpate pollen grains and rare but diverse tricolpate grains. A striking diversification phase of tricolpates is observed during the middle and late Albian, whereas the FOs of several polyporate pollen species in the early Albian and tricolporate pollen in the late Albian highlight important events in angiosperm pollen evolution.

(3) Despite the conspicuous increase in diversity, relative angiosperm pollen abundances remain low throughout most of the Albian with an average of <10% of the total palynoflora.

(4) A direct correlation of the São Julião record with the Potomac Group succession in the eastern USA suggests a middle-late Albian age for the lower part of Subzone II-B and a late Albian age for the upper part of Subzone II-B and lower Subzone II-C. An early Cenomanian is suggested for the upper part of Subzone II-C marked by the FO of triangular-shaped tricolporate pollen.

Acknowledgements

We thank J. Dinis (University of Coimbra; Portugal) for field guidance and T. Meckel (TU Darmstadt, Germany) for assistance with the Confocal Laser Scanning Microscope. Financial support by the Deutsche Forschungsgemeinschaft (DFG project HE4467/6-1) and the Leibniz Universität Hannover, Germany to MH is gratefully acknowledged. This manuscript was significantly improved, thanks to the helpful comments of James A. Doyle and an anonymous reviewer.

8. References

- Archangelsky, S., Archangelsky, A., 2013. Aptian angiosperm pollen from the Ticó flora Patagonia, Argentina. *International Journal of Plant Sciences* 174, 559-571.
- Archangelsky, S., Barreda, V., Passalia, M.G., Gandolfo, M., Pramparo, M., Romero, E., Cúneo, R., Zamuner, A., Iglesias, A., Llorens, M., Puebla, G.G., Quattrocchio, M., Volkheimer, W., 2009. Early angiosperm diversification: evidence from southern South America. *Cretaceous Research* 30, 1073-1082.
- Barrón, E., Peyrot, D., Rodríguez-López, J.P., Meléndez, N., del Valle, R.L., Najarro, M., Rosales, I., Comas-Rengifo, M.J., 2015. Palynology of Aptian and upper Albian (Lower Cretaceous) amber-bearing outcrops of the southern margin of the Basque-Cantabrian basin (northern Spain). *Cretaceous Research* 52, 292-312.
- Berthou, P.-Y., 1984. Albian-Turonian stage boundaries and subdivisions in the western Portuguese Basin, with special emphasis on the Cenomanian–Turonian boundary in the ammonite facies and rudist facies. *Bulletin of the Geological Society of Denmark* 33, 41–45.
- Berthou, P.-Y., Lauerjat, J., 1979. Essai de synthèse paléogéographique et paléobiostratigraphique du Bassin occidental portugais au cours du crétacé supérieur. *Ciencias Terra Lisboa* 5, 121-144.
- Berthou, P.-Y., Ferreira Soares, A., Lauerjat, J., 1979. Mid Cretaceous Events Iberian field Conference 77. Guide 1, Partie Portugal. *Cuadernos de Geologia Iberica* 5, 31–124.
- Berthou, P.-Y., Fouchier, J.C., Lecocq, B., Moron, J.M., 1980. Aperçu sur les kystes de Dinoflagellés de l'Albien et du Cénomaniens du Bassin Occidental Portugais. *Cretaceous Research* 1, 125–141.
- Brenner, G.J., 1963. The spores and pollen of the Potomac Group of Maryland. *Maryland Department of Geology, Mines and Water Resources* 27, 1–215.
- Burger, D., 1993. Early and middle Cretaceous angiosperm pollen grains from Australia. *Review of Palaeobotany and Palynology* 78, 183-234.
- Chapman, J.L., 1982. Morphology, classification and interpretation of Aptian and Albian angiosperm pollen from Portugal. Unpublished PhD Thesis, University of Cambridge, 355 pp.
- Couper, R.A., 1953. Upper Mesozoic and Cainozoic spores and pollen grains from New Zealand. *New Zealand Geological Survey, Palaeontological Bulletin* 22, 1-77.
- Couper, R.A., 1958. British Mesozoic microspores and pollen grains. A systematic and stratigraphic study. *Palaeontographica Abteilung B* 103, 75–179.
- Crane, P.R., Lidgard, S., 1989. Angiosperm diversification and paleolatitudinal gradients in Cretaceous floristic diversity. *Science* 246, 675-678.
- Crane, P.R., Friis, E.M., Pedersen, K.R., 1995. The origin and early diversification of angiosperms. *Nature* 374, 27-33.
- Cunha, P.P., Pena dos Reis, R., 1995. Cretaceous sedimentary and tectonic evolution of the northern sector of the Lusitanian Basin. *Cretaceous Research* 16, 155–170.
- Dettmann, M.E., 1973. Angiospermous pollen from Albian to Turonian sediments of eastern Australia. *Special Publication, Geological Society of Australia* 4, 3–34.
- Dinis, J.L., Trincão, P., 1995. Recognition and stratigraphical significance of the Aptian unconformity in the Lusitanian Basin, Portugal. *Cretaceous Research* 16, 171–186.
- Dinis, J.L., Rey, J., De Graciansky, P.C., 2002. The Lusitanian Basin (Portugal) during the late Aptian-Albian: Sequential arrangement, proposal of correlations, evolution. *Comptes Rendus Geoscience* 334, 757–764.

-
- Dinis, J.L., Rey, J., Cunha, P.P., Callapez, P., Pena dos Reis, R., 2008. Stratigraphy and allogenic controls of the western Portugal Cretaceous: an updated synthesis. *Cretaceous Research* 29, 772–780.
- Doyle, J.A., 1969. Cretaceous angiosperm pollen of the Atlantic Coastal Plain and its evolutionary significance. *Journal of the Arnold Arboretum*, 1–35.
- Doyle, J.A., 1992. Revised palynological correlations of the lower Potomac Group (USA) and the Cocobeach sequence of Gabon (Barremian-Aptian). *Cretaceous Research* 13, 337–349.
- Doyle, J.A., Hickey, L.J., 1976. Pollen and leaves from the mid-Cretaceous Potomac Group and their bearing on early angiosperm evolution. In: Beck, C.B. (Ed.), *Origin and Early Evolution of Angiosperms*. Columbia University Press, New York, 139–206.
- Doyle, J.A., Robbins, E.I., 1977. Angiosperm pollen zonation of the continental Cretaceous of the Atlantic Coastal Plain and its application to deep wells in the Salisbury Embayment. *Palynology* 1, 43–78.
- Doyle, J.A., Endress, P.K., 2014. Integrating Early Cretaceous fossils into the phylogeny of living angiosperms: ANITA lines and relatives of Chloranthaceae. *International Journal of Plant Sciences* 175, 555–600.
- Doyle, J.A., Van Campo, M., Lugardon, B., 1975. Observations on exine structure of Eucommiidites and Lower Cretaceous angiosperm pollen. *Pollen et Spores* 17, 429–486.
- Doyle, J.A., Biens, P., Doerekamp, A., Jardiné, S., 1977. Angiosperm pollen from the pre-Albian Lower Cretaceous of equatorial Africa. *Bulletin des Centres de Recherche Exploration–Production Elf Aquitaine* 1, 451–473.
- El Beialy, S., El-Soughier, M., Mohsen, S.A., El Atfy, H., 2011. Palynostratigraphy and paleoenvironmental significance of the Cretaceous succession in the Gebel Rissu-1 well, north Western Desert, Egypt. *Journal of African Earth Sciences* 59, 215–226.
- El-Beialy, S.Y., El Atfy, H.S., Zavada, M.S., El Khoriby, E.M., Abu-Zie, R.H., 2010. Palynological, palynofacies, paleoenvironmental and organic geochemical studies on the Upper Cretaceous succession of the GPTSW-7 well, North Western Desert, Egypt. *Marine and Petroleum Geology* 27, 370–385.
- Eklund H, Doyle, J.A., Herendeen, P.S., 2004. Morphological phylogenetic analysis of living and fossil Chloranthaceae. *International Journal of Plant Sciences* 165, 107–151.
- Endress, P.K., Honegger, R., 1980. The pollen of the Austrobaileyaceae and its phylogenetic significance. *Grana* 19, 177–182.
- Erdtman, G., 1966. Pollen morphology and plant taxonomy Angiosperms. Hafner, New York. pp. 553
- Foucher, J.C., 1981. Kystes de Dinoflagellés du Cretacé Moyen Européen: Proposition d'une Echelle biostratigraphique pour le domaine Nord-occidental. *Cretaceous Research* 2, 331–338.
- Friis, E.M., Pedersen, K.R., 2011. *Canrightia resinifera* gen. et sp. nov., a new extinct angiosperm with *Retimonocolpites*-type pollen from the Early Cretaceous of Portugal: missing link in the eumagnoliid tree? *Grana* 50, 3–29.
- Friis, E.M., Pedersen, K.R., Crane, P.R., 1994. Angiosperm floral structures from the Early Cretaceous of Portugal. *Plant Systematics and Evolution* 8, 31–49.
- Friis, E.M., Crane, P.R., Pedersen, K.R., 1997. *Anacostia*, a new basal angiosperm from the Early Cretaceous of North America and Portugal with monocolpate/trichotomocolpate pollen. *Grana* 36, 225–244.

Friis, E.M., Pedersen, K.R., Crane, P.R., 1999. Early angiosperm diversification: the diversity of pollen associated with angiosperm reproductive structures in Early Cretaceous floras from Portugal. *Annals of the Missouri Botanical Garden* 86, 259–296.

Friis, E.M., Pedersen, K.R., Crane, P.R., 2000a. Reproductive structure and organization of basal angiosperms from the Early Cretaceous (Barremian or Aptian) of Western Portugal. *International Journal of Plant Sciences* 161, S169–S182.

Friis, E.M., Pedersen, K.R., Crane, P.R., 2000b. Fossil floral structures of a basal angiosperm with monocolpate, reticulate-acolumellate pollen from the Early Cretaceous of Portugal. *Grana* 39, 226–245.

Friis, E.M., Pedersen, K.R., Crane, P.R., 2001. Fossil evidence of water lilies (Nymphaeales) in the Early Cretaceous. *Nature* 410, 357–360.

Friis, E.M., Pedersen, K.R., Crane, P.R., 2010. Diversity in obscurity: fossil flowers and the early history of angiosperms. *Philosophical Transactions of the Royal Society B: Biological Sciences* 365, 369–382.

Friis, E.M., Pedersen, K.R., Crane, P.R., 2011. *Early flowers and angiosperm evolution*. Cambridge University Press.

Friis, E.M., Pedersen, K.R., Von Balthazar, M., Grimm, G.W., Crane, P.R., 2009. *Monetianthus mirus* gen. et sp. nov., a nymphaealean flower from the Early Cretaceous of Portugal. *International Journal of Plant Science* 170, 1086–1101.

Gradstein, F.M., Ogg, J., Schmitz, M.A., Ogg, G., 2012. *A Geologic Time Scale 2012*. Elsevier Publishing Company.

Grimm, E.C., 1991. *Tilia, Tiliagraph and TGView Software*, Illinois State Museum, Springfield, Illinois, USA.

Groot, J.J., Groot, C.R., 1962. Plant microfossils from Aptian, Albian and Cenomanian deposits of Portugal. *Comunicações dos Serviços Geológicos de Portugal* 46, 133–171.

Gübeli, A., Hochuli, P.A., Wildi, W., 1984. Lower Cretaceous turbiditic sediments from the Central Rif chain (Northern Morocco). *Palynology, stratigraphy and palaeogeographic setting*. *Geologische Rundschau* 73, 1081–1114.

Hasenboehler, B., 1981. *Étude paléobotanique et palynologique de l'Albien et du Cénomanién du "Bassin Occidental Portugais" au sud de l'accident de Nazaré (Portugal)*. Unpublished PhD thesis, Université Pierre et Marie Curie, Paris, Thèse 3ème Cycle, 348pp.

Hedlund, R.W., Norris, G., 1968. Spores and pollen grains from Fredericksburgian (Albian) strata, Marshall County, Oklahoma. *Pollen et Spores* 10, 129–159.

Hedlund, R.W., Norris, G., 1986. Dinoflagellate cyst assemblage from middle Albian strata of Marshall County, Oklahoma, USA. *Review of Palaeobotany and Palynology* 46, 293–309.

Heimhofer, U., Hochuli, P.A., 2010. Early Cretaceous angiosperm pollen from a low-latitude succession (Araipe Basin, NE Brazil). *Review of Palaeobotany and Palynology* 161, 105–126.

Heimhofer, U., Hochuli, P.A., Burla, S., Weissert, H., 2007. New records of Early Cretaceous angiosperm pollen from Portuguese coastal deposits: Implications for the timing of the early angiosperm radiation. *Review of Palaeobotany and Palynology* 144, 39–76.

Heimhofer, U., Hochuli, P.A., Burla, S., Dinis, J.L., Weissert, H., 2005. Timing of Early Cretaceous angiosperm diversification and possible links to major paleoenvironmental change. *Geology* 33, 141–144.

-
- Heimhofer, U., Hochuli, P.A., Burla, S., Oberli, F., Adatte, T., Dinis, J.L., Weissert, H., 2012. Climate and vegetation history of western Portugal inferred from Albian near-shore deposits (Galé Formation, Lusitanian Basin). *Geological Magazine* 149, 1046–1064.
- Herngreen, G.F.W., 1973. Palynology of Albian-Cenomanian strata of borehole 1-QS-1-MA, state of Maranhão, Brazil. *Pollen et Spores* 15, 515-555.
- Hochuli, P.A., Heimhofer, U., Weissert, H., 2006. Timing of early angiosperm radiation: recalibrating the classical succession. *Journal of the Geological Society* 163, 587-594.
- Horikx, M., Heimhofer, U., Dinis, J., Huck, S., 2014. Integrated stratigraphy of shallow marine Albian strata from the southern Lusitanian Basin of Portugal. *Newsletters on Stratigraphy* 47, 85-106.
- Hughes, N.F., 1994. *The Enigma of Angiosperm Origins*. Cambridge, UK: Cambridge University Press.
- Hughes, N.F., McDougall, A.B., 1987. Records of angiospermid pollen entry into the English Early Cretaceous succession. *Review of Palaeobotany and Palynology* 50, 255–272.
- Ibrahim, M.I.A., 1996. Aptian–Turonian palynology of the Ghazalat-1 Well (GTX-1), Qattara Depression, Egypt. *Review of Palaeobotany and Palynology* 94, 137–168.
- Ibrahim, M.I.A., 2002. New angiosperm pollen from the upper Barremian-Aptian of the Western Desert, Egypt. *Palynology* 26, 107-133.
- Jardiné, S., Magloire, L., 1965. Palynologie et stratigraphie du Crétacé du Sénégal et de Côte d'Ivoire. *Mémoires du Bureau de Recherches Géologiques et Minières* 32, 187–245.
- Kemp, E.M., 1968. Probable angiosperm pollen from British Barremian to Albian strata. *Palaeontology* 11, 421-434.
- Krutzsch, W., 1959. Einige neue Formgattungen und -Arten von Sporen und Pollen aus der mitteleuropäischen Oberkreide und dem Tertiär. *Palaeontographica Abteilung B*, 125-157.
- Krutzsch, W., 1970. Atlas der mittel- und jungtertiären dispersen Sporen- und Pollen- sowie der Mikroplanktonformen des nordlichen Mitteleuropas. Lieferung VII. Monoporate, monocolpate, longicolpate, dicolpate und ephedroide (polylicate) Pollenformen. Gustav Fischer Verlag Jena, 1-175.
- Lidgard, S., Crane, P.R., 1988. Quantitative analyses of the early angiosperm radiation. *Nature* 331, 344-346.
- Lidgard, S., Crane, P.R., 1990. Angiosperm diversification and Cretaceous floristic trends: a comparison of palynofloras and leaf macrofloras. *Paleobiology* 16, 77-93.
- May, F., 1975. *Dichastopollenites reticulatus*, gen. et sp. nov. — potential Cenomanian guide fossil from southern Utah and northeastern Arizona. *Journal of Paleontology* 49, 528–533.
- Masse, J-P., Arias, C., Vilas, L., 1998. Lower Cretaceous rudist faunas of Southeast Spain: An overview. *Geobios* 31, 193–210.
- Médus, J., 1982. Palynofloristic correlations of two Albian sections of Portugal. *Cuadernos Geología Ibérica* 8, 781–809.
- Médus, J., Berthou, P-Y., 1980. Palynoflores dans la coupe de l'Albien de Foz do Folcao (Portugal). *Geobios* 13, 263–269.
- Mendes, M.M., Dinis, J., Pais, J., Friis, E.M., 2011. Early Cretaceous flora from Vale Painho (Lusitanian Basin, western Portugal): an integrated palynological and mesofossil study. *Review of Palaeobotany and Palynology* 166, 152-162

-
- Mendes, M.M., Dinis, J., Pais, J., Friis, E.M., 2014a. Vegetational composition of the Early Cretaceous Chicalhão flora (Lusitanian Basin, western Portugal) based on palynological and mesofossil assemblages. *Review of Palaeobotany and Palynology* 200, 65-81.
- Mendes, M.M., Grimm, G.W., Pais, J., Friis, E.M., 2014b. Fossil *Kajanthus lusitanicus* gen. et sp. nov. from Portugal: floral evidence for Early Cretaceous Lardizabalaceae (Ranunculales, basal eudicot). *Grana* 53, 1-19.
- Monteil, E., Foucher, J.C., 1998. Cretaceous biochronostratigraphy. In: De Graciansky, P.-C., Hardenbol, J., Jacquin, T., Vail, P. (Eds.), *Mesozoic and Cenozoic Sequence Stratigraphy of European Basins*. SEPM Special Publication, vol. 60. chart.
- Norris, G., 1967. Spores and pollen from the Lower Colorado Group (Albian–?Cenomanian) of Central Alberta. *Palaeontographica Abteilung B* 120, 72–115.
- Pedersen, K.R., Crane, P.R., Drinnan, A.N., Friis, E.M., 1991. Fruits from the mid-Cretaceous of North America with pollen grains of the *Clavatipollenites* type. *Grana* 30, 577–590.
- Pedersen, K.R., Von Balthazar, M., Crane, P.R., Friis, E.M., 2007. Early Cretaceous floral structures and in situ tricolpate-striate pollen: New early eudicots from Portugal. *Grana* 46, 176-196.
- Penny, J.H.J., 1986. An Early Cretaceous angiosperm pollen assemblage from Egypt. *Special Papers in Palaeontology* 35, 121-134.
- Penny, J.H.J., 1988. Early Cretaceous striate tricolpate pollen from the Borehole Mersa Matruh 1, North West Desert, Egypt. *Journal of Micropalaeontology* 7, 201–215.
- Penny, J., H., 1992. The relevance of the Early Cretaceous angiosperm palynology of Egypt to biostratigraphy and reconstruction of angiosperm palaeolatitudinal migrations. *Cretaceous Research* 13, 369-378.
- Pierce, R.L., 1961. Lower Upper Cretaceous plant microfossils from Minnesota. *Minnesota Geological Survey Bulletin* 42, 1–86.
- Regali, M.S.P., Viana, C.F., 1989. Late Jurassic–Early Cretaceous in Brazilian sedimentary basins: correlation with the international standard stratigraphic scale. *Petrobrás Petroleo Brasileiro S. A, Rio de Janeiro*.
- Rey, J., 1979. Le Crétacé inférieur de la marge atlantique portugaise: biostratigraphie, organisation séquentielle, évolution paléogéographique. *Ciencias Terra* 5, 97–120.
- Rey, J., 1992. Les unités lithostratigraphiques du Crétacé inférieur de la région de Lisbonne. *Comunicações dos Serviços Geológicos de Portugal* 78, 103–124.
- Rey, J., Dinis, J.L., Callapez, P., Cunha, P.P., 2006. Da rotura continental à margem passiva. Composição e evolução do Cretácico de Portugal. *Cadernos de Geologia de Portugal*. INETI, Lisbon, 75 pp.
- Sah, S.C.D., 1967. Palynology of an Upper Neogene profile from Rusizi Valley (Burundi). *Koninklijk Museum voor Midden-Afrika-Tervuren, Belgie Annalen-Reeks in 8° Geologische Wetenschappen* 57, 173pp.
- Sampson, F.B., Endress, P.K., 1984. Pollen morphology in the Trimeniaceae. *Grana* 23, 129-137.
- Saporta, G.D., 1894. Flore fossile du Portugal. Nouvelles contributions à la flore mésozoïque. Accompagnées d'une notice stratigraphique par Paul Choffat. Imprimerie de l'Académie Royale des Sciences, Lisbon.
- Schrank, E., Mahmoud, M.S., 2002. Barremian angiosperm pollen and associated palynomorphs from the Dakhla Oasis area, Egypt. *Palaeontology* 45, 33-56.

Sender, L.M., Villanueva-Amadoz, U., Diez, J.B., Sanchez-Pellicer, R., Bercovici, A., Pons, D., Ferrer, J., 2012. A new uppermost Albian flora from Teruel province, northeastern Spain. *Geodiversitas* 34, 373-397.

Singh, C., 1971. Lower Cretaceous microfloras of the Peace River area, northwestern Alberta. *Research Council of Alberta Bulletin* 28, 1–299.

Singh, C., 1983. Cenomanian microfloras of the Peace River area, northwestern Alberta. *Research Council of Alberta Bulletin* 44, 1–322.

Srivastava, S.K., 1969. Some angiosperm pollen from the Edmonton Formation (Maestrichtian), Alberta, Canada. *J. Sen Memorial Volume* 47-67.

Stampfli, G.M., Borel, G.D., 2002. A plate tectonic model for the Paleozoic and Mesozoic constrained by dynamic plate boundaries and restored synthetic oceanic isochrons. *Earth and Planetary Science Letters* 196, 17–33.

Teixeira, C., 1948. *Flora mesozóica portuguesa Part I*. Serviços Geológicos de Portugal, Lisbon.

Traverse, A., 2007. *Paleopalynology*. Dordrecht: Springer, 813pp.

Villanueva-Amadoz, U., Pons, D., Diez, J.B., Ferrer, J., Sender, L.M., 2010. Angiosperm pollen grains of San Just site (Escucha Formation) from the Albian of the Iberian Range (north-eastern Spain). *Review of Palaeobotany and Palynology* 162, 362-381.

Villanueva-Amadoz, U., Sender, L.M., Diez, J.B., Ferrer, J., Pons, D., 2011. Palynological studies of the boundary marls unit (Albian-Cenomanian) from northeastern Spain. *Paleophytogeographical implications*. *Geodiversitas* 33, 137-176.

Walker, J.W., Walker, A.G., 1984. Ultrastructure of Lower Cretaceous angiosperm pollen and the origin and early evolution of flowering plants. *Annals of the Missouri Botanical Garden* 71, 464–521.

Ward, J.V., 1986. Early Cretaceous angiosperm pollen from the Cheyenne and Kiowa Formations (Albian) of Kansas, U.S.A. *Palaeontographica Abteilung B* 202, 1–81.

Ward, J.V., Doyle, J.A., 1994. Ultrastructure and relationships of mid-Cretaceous polyforates and triporates from Northern Gondwana. *Ultrastructure of Fossil Spores and Pollen*. Royal Botanic Gardens Kew, 161-172.

Williams, G.L., Brinkhuis, H., Pearce, M.A., Fensome, R.A., Weegink, J.W., 2004. Southern ocean and global dinoflagellate cyst events compared: index events for the Late Cretaceous–Neogene. In: Exon, N. F., Kenneth, J. P., Malone, M. J. (Eds.), *Proceedings of the Ocean Drilling Program, Scientific Results* 189, 1–98

Zhang, M., Dai, S., Pan, B., Wang, L., Peng, D., Wang, H., Zhang, X., 2014. The palynoflora of the Lower Cretaceous strata of the Yingen-Ejinaqi Basin in North China and their implications for the evolution of early angiosperms. *Cretaceous Research* 48, 23-38.

Appendix 1

Genus *Ajatipollis* Krutzsch 1970

Species	Author	Size (µm)	Amb/ Shape	Exine (µm)	Sexine (µm)	Nexine (µm)	Reticulum	Columellae (µm)	Aperture Type	Plate
<i>Ajatipollis</i> sp. 1	Informal species	21-25 (tetrad) 10-13 (grain)	permanent tetrad	columellate, semitectate 2.2	1.4-1.7	0.5	perforate	densely spaced head Ø 0.4µ	Triporate pore size 5-6 µm	Plate I, Fig. 1-2

Genus *Asteropollis* Hedlund & Norris 1968

Species	Author	Size (µm)	Amb/ Shape	Exine (µm)	Sexine (µm)	Nexine (µm)	Reticulum	Columellae (µm)	Aperture Type	Plate
<i>A. asteroides</i>	Hedlund & Norris 1968	16-24	(sub)circular	columellate, semitectate 1.3-1.9	0.6-1.0	0.5-0.7	-	densely spaced head Ø 0.4-0.6	tri- to pentachotomocolpate	Plate I, Fig. 3-4
<i>A. aff. asteroides</i>	Hedlund & Norris 1968	~21	circular	columellate, semitectate 1.1	0.5-0.7	0.4-0.6	-	widely spaced head Ø 0.4	hexachotomocolpate	Plate I, Fig. 5-6
<i>A. sp. 3</i>	Heimhofer et al. 2007	~25	circular	columellate, semitectate 1.3	1.0	0.3	perforate	very densely spaced head Ø 0.4	tri- to pentachotomocolpate	Plate I, Fig. 7
<i>A. sp. 2</i>	Heimhofer et al. 2007	19-28	(sub)circular	columellate, semitectate 1.4-1.5	0.8-1.0	0.5-0.7	-	widely spaced head Ø 0.5	trichotomocolpate	Plate I, Fig. 8-9

Genus *Clavatipollenites* Couper 1958

Species	Author	Size (µm)	Amb/ Shape	Exine (µm)	Sexine (µm)	Nexine (µm)	Reticulum	Columellae (µm)	Aperture Type	Plate
<i>C. sp. A</i>	Doyle & Robbins 1977	18-26	(sub)circular - elliptical	columellate, semitectate 1.5-2.0	0.9-1.5	0.6-0.8	-	very widely spaced head Ø 0.6-1.0	monocolpate	Plate I, Fig. 10-11
<i>C. hughesii</i>	Couper 1958	19-30	(sub)circular - elliptical	columellate, semitectate 1.0-1.8	0.6-1.4	0.5-1.0	-	densely spaced head Ø 0.5-1.0	monocolpate	Plate I, Fig. 14-15
<i>C. sp. 1</i>	Brenner 1963	14-16	(sub)circular	columellate, semitectate 1.5-1.9	1.0	0.9	-	widely spaced head Ø 0.5	monocolpate	Plate I, Fig. 12-13
<i>C. sp. 2</i>	Heimhofer et al. 2007	20-30	(sub)circular - elliptical	columellate, semitectate 0.5-1.5	0.4-0.8	0.2-0.6	perforate	densely spaced head Ø 0.2-0.4	monocolpate	Plate I, Fig. 16
<i>C. tenellis</i>	Phillips & Felix 1971	20-30	(sub)circular	columellate, semitectate 1.5-2.5	0.7-1.5	0.5-1.5	-	densely spaced head Ø 0.5-0.7	indistinct	Plate II, Fig. 1-2

Genus *Cretacaeiporites* Hermgreen 1973

Species	Author	Size (µm)	Amb/ Shape	Exine (µm)	Sexine (µm)	Nexine (µm)	Reticulum	Columellae (µm)	Aperture Type	Plate
<i>C. aff. polygonalis</i>	Hermgreen 1973	~20	(sub)circular	reticulate-semitectate 1.2	0.7	0.5	scabrate-granulate	densely spaced barely visible	polyporate	Plate II, Fig. 3
<i>C. aff. scabratus</i>	Hermgreen 1973	~20	(sub)circular	columellate, semitectate 1.0	0.8	0.3	perforate	densely spaced head Ø 0.4	polyporate	Plate II, Fig. 4
<i>C. sp. 1</i>	Informal species	19-23	(sub)circular	reticulate-semitectate 1.7-2.4	1.0-1.2	0.5-1.2	irregular homobrochate lumen size: 0.5-1.0	densely spaced head Ø 0.5	polyporate	Plate II, Fig. 5-6
<i>C. sp. 2</i>	Informal species	~20	(sub)circular	reticulate-semitectate ~1.8	1.0-1.2	0.7	irregular heterobrochate lumen size: 0.5-2.5	widely spaced head Ø 0.8 muri verrucate through overtopping columellae	polyporate	Plate II, Fig. 7-9
<i>C. sp. 3</i>	Informal species	~16	(sub)circular	reticulate-semitectate 0.7	0.3	0.4	very finely striate	striae densely spaced head Ø 0.3	polyporate	Plate II, Fig. 10-11
<i>C. sp. 4</i>	Informal species	15-18	(sub)circular	reticulate-semitectate 0.9	0.4	0.3	perforate-scabrate	densely spaced barely visible	polyporate	Plate II, Fig. 12-13

Genus *Dichastopollenites* May 1975

Species	Author	Size (µm)	Amb/ Shape	Exine (µm)	Sexine (µm)	Nexine (µm)	Reticulum (µm)	Muri width (µm) & supra-tectal ornamentation	Columellae (µm)	Aperture Type	Plate
<i>D. dunveganensis</i>	Singh 1983	30-45	elliptical	reticulate-semitectate	-	-	heterobrochate lumen size: 3.0-12.0	0.8-1.3	widely spaced head Ø 0.9-1.0	zonosulcate	Plate II, Fig. 14
<i>D. reticulatus</i>	May 1975	19-30	(sub)circular - elliptical	reticulate-semitectate 1.7-2.7	1.2-2.0	0.3-0.7	homobrochate lumen size: 1.0-3.5*	0.8-1.4	widely spaced head Ø 0.4-0.8	zonosulcate	Plate II, Fig. 15-16
<i>D. sp. 1</i>	Informal species	22-27	(sub)circular	reticulate-semitectate 1.4-1.7	1.0-1.5	0.3	heterobrochate lumen size: 0.4-3.6*	~0.3	widely spaced head Ø 0.9	zonosulcate	Plate II, Fig. 17-18
<i>D. sp. 4</i>	Heimhofer et al. 2007	30-50	(sub)circular - elliptical	reticulate-semitectate 3.0-3.5	2.0-2.5	0.6-1.0	irregular heterobrochate meandering muri	~1.0	widely spaced head Ø 1.0	zonosulcate	Plate III, Fig. 1-2
<i>D. sp. 5</i>	Heimhofer et al. 2007	~23	elliptical	reticulate-semitectate 2.0	1.0-1.5	0.5	irregular heterobrochate meandering muri	0.5-0.6	widely spaced head Ø 0.7	zonosulcate	Plate III, Fig. 3-4
<i>D. sp. 6</i>	Heimhofer et al. 2007	25-50	(sub)circular - elliptical	reticulate-semitectate 2.8	2.0	0.8	irregular heterobrochate meandering muri	0.5-0.8 muri verrucate through overtopping columellae	widely spaced head Ø 0.5-1.0	zonosulcate	Plate III, Fig. 5-7

*sometimes with small (<1.0 µm) additional luminae adjacent to larger lumen

Genus *Hammenia* Hedlund & Norris 1968

Species	Author	Size (µm)	Amb/Shape	Exine (µm)	Sexine (µm)	Nexine (µm)	Reticulum (µm)	Columellae (µm)	Aperture Type	Plate
<i>H. sp. A</i>	Burger 1993	~23	(sub)circular	columellate, semitectate 1.5	0.4	1.1	perforate lumen size: <0.3	widely spaced head Ø 0.6	hexa-aperturate	Plate III, Fig. 8-9

Genus *Penetetrapites* Hedlund & Norris 1968

Species	Author	Size (µm)	Amb/Shape	Exine	Reticulum	Aperture Type	Plate
<i>P. mollis</i>	Hedlund & Norris 1968	~22	(sub)circular - triangular	reticulate-semitectate	perforate-scabrate	three lentular equatorial apertures with a fourth aperture developed at one pole	Plate III, Fig. 10-11

Genus *Pennipollis* Friis, Pedersen & Crane 2000

Species	Author	Other publications	Size (µm)	Amb/Shape	Exine (µm)	Sexine (µm) detached	Nexine (µm)	Reticulum (µm)	Muri width (µm) & supra-tectal ornamentation	Aperture Type	Plate
<i>P. peroreticulatus</i>	(Brenner 1963) Friis et al. 2000	-	~15	(sub)circular	reticulate-semitectate 1.5 acolumellate	1.0	0.5	heterobrochate lumen size: 1.0-3.7*	0.7 single row verrucae	monocolpate	Plate III, Fig. 12-13
<i>P. reticulatus</i>	(Brenner 1963) Friis et al. 2000	-	15-17	(sub)circular	reticulate-semitectate 1.0-2.0 acolumellate	1.0-1.5	0.5-1.0	homobrochate lumen size: 0.5-2.3	0.5-0.7 single row verrucae	monocolpate	Plate III, Fig. 14-15
<i>P. sp. 1</i>	Informal species	Retimonoknoble (Penny 1992)	~20	(sub)circular	reticulate-semitectate 2.8 acolumellate	1.8-2.2	0.6-1.0	heterobrochate lumen size: 1.5-2.6	0.5 densely verrucated	monocolpate	Plate III, Fig. 16-17
<i>P. sp. 2</i>	Informal species	-	20-27	(sub)circular	reticulate-semitectate 2.0-2.3 acolumellate	1.0-1.5	0.5-0.8	homobrochate lumen size: 1.5-4.0	0.3 no ornamentation	monocolpate	Plate III, Fig. 18-19

* lumen smaller near colpus

Genus *Phimopollenites* Dettmann 1973

Species	Author	Size (µm)	Amb/Shape	Exine (µm)	Sexine (µm)	Nexine (µm)	Reticulum (µm)	Muri width (µm)	Columellae (µm)	Aperture Type	Plate
<i>P. sp. 1</i>	Informal species	~20	prolate to subcircular	reticulate-semitectate 1.1	0.6	0.4	homobrochate lumen size: 0.8-1.2	0.4	widely spaced head Ø 0.4	Tricolpate wide aperture	Plate IV, Fig. 1-2

Genus *Retimonocolpites* Pierce 1961

Species	Author	Size (µm)	Amb/Shape	Exine (µm)	Sexine (µm)	Nexine (µm)	Reticulum (µm)	Muri width (µm) & supra-tectal ornamentation	Columellae (µm)	Aperture Type	Plate
<i>R. dividius</i>	Pierce 1961	25-30	(sub)circular - elliptical	reticulate-semitectate 1.0-1.5	0.5-1.0	0.3-0.5	homobrochate lumen size: 0.5-1.5	0.3	densely spaced head Ø 0.4-0.6	monocolpate elongate colpus	Plate IV, Fig. 3-4
<i>R. aff. dividius</i>	Informal species	12-22	(sub)circular	reticulate-semitectate 1.6-2.3	0.8-1.4	0.6-1.0	homobrochate lumen size: 0.7-1.6	0.2	densely spaced head Ø 0.5-0.7 club shaped	monocolpate elongate colpus	Plate IV, Fig. 5-6
<i>R. sp. 1</i>	Informal species	~15	(sub)circular	reticulate-semitectate 1.6	1.0	0.6	homobrochate loosely attached very fine meshwork <1.0	<0.4	widely spaced head Ø 0.3	monocolpate	Plate IV, Fig. 7-8
<i>R. sp. 2</i>	Informal species	20-27	(sub)circular - elliptical	reticulate-semitectate 1.6-2.0	0.7-1.5	0.5-1.0	heterobrochate lumen size: 0.5-3.5	0.3 muri verrucate through overtopping columellae	widely spaced head Ø 0.7-1.4	monocolpate	Plate IV, Fig. 9-10
<i>R. sp. 3</i>	Informal species	19-23	(sub)circular	reticulate-semitectate 1.6-2.0	1.0-1.2	0.5-0.8	homobrochate lumen size: <1.0	0.2-0.4	densely spaced head Ø 0.4	monocolpate	Plate IV, Fig. 11-12
<i>R. sp. 4</i>	Informal species	~20	(sub)circular	reticulate-semitectate 1.8-2.2	1.4	0.8	irregular heterobrochate meandering muri	~0.5	widely spaced head Ø 1.0-1.3	monocolpate	Plate IV, Fig. 13-14
<i>R. sp. 5</i>	Heimhofer et al. 2007	~30	prolate	reticulate-semitectate 1.6-1.8	0.9	0.8	heterobrochate lumen size: 0.6-1.4	0.5	densely spaced head Ø 0.7 club shaped	monocolpate	Plate IV, Fig. 15
<i>R. sp. 6</i>	Informal species	19-22	(sub)circular - elliptical	reticulate-semitectate 2.8	1.5-2.0 loosely attached	0.8-1.0	heterobrochate lumen size: 0.4-3.2*	0.5-0.6 muri verrucate through overtopping columellae	widely spaced head Ø 0.5-0.8	monocolpate	Plate IV, Fig. 18-20
<i>R. sp. 7</i>	Informal species	27	elliptical	reticulate-semitectate 1.7	1.3	0.4	homobrochate lumen size: 1.4-1.8	0.3 muri verrucate through overtopping columellae	densely spaced head Ø 0.6	monocolpate	Plate IV, Fig. 16-17

* lumen smaller near colpus

Genus *Retitrescolpites* Sah 1967

Species	Author	Size (µm)	Amb/ Shape	Exine (µm)	Sexine (µm)	Nexine (µm)	Reticulum (µm)	Muri width (µm)	Columellae (µm)	Aperture Type	Plate
<i>R. sp. 1</i>	Informal species	19-23	(sub)circular	reticulate-semitectate 2.0-2.9	1.5-1.8	0.5-0.8	homobrochate lumen size: 0.5-3.0	0.4-0.7	widely spaced head Ø 0.7	tricolpate	Plate V, Fig. 1-2
? <i>R. sp. 2</i>	Informal species	18-24	(sub)circular	reticulate-semitectate 2.6	2.0*	0.6	irregular homobrochate lumen size: 0.8-2.0	0.7-1.0	widely spaced head Ø 0.6	tricolpate long colpi, bordered by 2 µm thick margo	Plate V, Fig. 3-4
<i>R. sp. 3</i>	Informal species	~21	(sub)circular	reticulate-semitectate ~1.6	1.0-1.2	0.5	homobrochate lumen size: 1.0-1.3	0.3	widely spaced head Ø 0.6 club shaped	tricolpate short colpi	Plate V, Fig. 5-6
? <i>R. sp. 4</i>	Informal species	~25	(sub)circular	reticulate-semitectate 4.0-5.0	3.1-4.5* loosely attached	0.5-0.9	homobrochate lumen size: 3.7-5.0	0.6	widely spaced head Ø 0.8	tricolpate	Plate V, Fig. 7-8
<i>R. sp. 5</i>	Informal species	~17	(sub)circular	reticulate-semitectate 3.0	2.0	1.0	homobrochate lumen size: 1.2-1.8	0.8-1.0	widely spaced head Ø 1.0	tricolpate	Plate V, Fig. 9-10
<i>R. sp. 6</i>	Informal species	~23	(sub)circular	reticulate-semitectate 1.5	1.0	0.5	homobrochate lumen size: 1.3-2.1	0.4	widely spaced head Ø 0.5	tricolpate	Plate V, Fig. 11

* detached sexine

Genus *Rousea* Srivastava 1969

Species	Author	Size (µm)	Amb/ Shape	Exine (µm)	Sexine (µm)	Nexine (µm)	Reticulum (µm)	Muri width (µm)	Columellae (µm)	Aperture Type	Plate
<i>R. georgensis</i>	Brenner 1963	~25-28	prolate to oblate	reticulate-semitectate 1.5-1.7	1.3	0.4	heterobrochate lumen size: 0.3-2.2°	0.3-0.5	densely spaced head Ø 0.4 club shaped	tricolpate	Plate V, Fig. 12-13
<i>R. aff. prosimilis</i>	Norris 1967	~20	(sub)circular	reticulate-semitectate 2.0-3.0	1.5-2.2*	0.6-0.8	heterobrochate lumen size: 0.5-3.0*	0.4-0.7	widely spaced head Ø 0.7	tricolpate	Plate V, Fig. 14-15
<i>R. prosimilis</i>	Informal species	~18-26	prolate	reticulate-semitectate 1.0	0.7	0.3	irregular heterobrochate lumen size: 0.2-2.1	0.3	densely spaced head Ø 0.4 club shaped	tricolpate	Plate VI, Fig. 9-10
<i>R. sp. 1</i>	Informal species	17-24	prolate	reticulate-semitectate 1.5	1.0	0.5	heterobrochate lumen size: 0.3-1.8*	0.3	widely spaced head Ø 0.7	tricolpate	Plate V, Fig. 16-17
? <i>R. sp. 2</i>	Informal species	20-26	prolate	reticulate-semitectate 2.0-2.6	1.6-2.0*	0.6	heterobrochate lumen size: 0.5-3.8 loosely attached	0.4-0.6 muri verrucate through overtopping columellae	widely spaced head Ø 0.8	tricolpate	Plate V, Fig. 18-19
<i>R. sp. 3</i>	Informal species	20-23	(sub)circular	reticulate-semitectate 1.2	0.6	0.6	irregular heterobrochate small lumen between, larger 0.2-1.7	~0.5	widely spaced head Ø 0.3	tricolpate	Plate V, Fig. 20 Plate VI, Fig. 1
? <i>R. sp. 4</i>	Informal species	~22	(sub)circular	reticulate-semitectate 1.8	1.2*	0.7	irregular heterobrochate lumen size: 0.7-4.0	0.3-0.5	widely spaced head Ø 0.5	tricolpate	Plate VI, Fig. 2-4
? <i>R. sp. 5</i>	Informal species	~22	oblate	reticulate-semitectate 3.0	2.6*	0.4	heterobrochate lumen size: 0.5-2.5°	0.3 muri verrucate through overtopping columellae	widely spaced head Ø 0.5	tricolpate	Plate VI, Fig. 5-6
? <i>R. sp. 6</i>	Informal species	~17	(sub)circular	reticulate-semitectate 1.4	1.0	0.4	irregular heterobrochate lumen size: 0.7-1.8	0.3 muri verrucate through overtopping columellae	widely spaced head Ø 0.5	tricolpate broad colpi	Plate VI, Fig. 7-8
<i>R. sp. 7</i>	Informal species	~27	(sub)circular	reticulate-semitectate 2.2	1.5-1.6	0.6-0.8	heterobrochate lumen size: 0.4-1.6°	0.5 muri verrucate through overtopping columellae	widely spaced head Ø 0.9 club shaped	tricolpate	Plate VI, Fig. 11-12
<i>R. sp. 8</i>	Informal species	16-18	(sub)circular	reticulate-semitectate 2.5-2.7	1.8-2.0	0.7	heterobrochate lumen size: 1.0-3.3	0.8 muri verrucate through overtopping columellae	densely spaced head Ø 0.4-0.6	tricolpate	Plate VI, Fig. 13-14

* detached sexine

* lumen smaller near colpus

* lumen smaller near pole

Genus *Senectotetradites* Dettmann 1973

Species	Author	Size (µm)	Amb/ Shape	Exine (µm)	Sexine (µm)	Nexine (µm)	Reticulum (µm)	Muri width (µm)	Columellae (µm)	Aperture Type	Plate
<i>S. varetriculatus</i>	Dettmann 1973	40-44 (tetrad) 22-32 (grain)	prolate to oblate	columellate, semitectate 1.8-2.8	1.3-2.5	0.5-1.0	heterobrochate Lumen size: 1.3 at pole: 3.0 at equator	0.6	densely spaced head Ø 0.9	tricolpate	Plate VI, Fig. 15-16

Genus *Stellatopollis* Doyle, van Campo & Lugardon 1975

Species	Author	Size (µm)	Amb/ Shape	Exine	Aperture Type	Plate
<i>S. barghoornii</i>	Doyle et al. 1975	~50	elliptical	reticulate-semitectate, supratectal elements with elevated triangular elements, arranged around a circular area	monocolpate	Plate VI, Fig. 17
<i>S. sp. 1</i>	Informal species	~17 (fragment)	unknown (broken)	reticulate-semitectate, supratectal elements irregular shaped, with elevated mostly oval elements, arranged around a circular area (only fragment found)	monocolpate	Plate VI, Fig. 18-19

Genus *Striatopollis* Krutzsch 1959

Species	Author	Size (µm)	Amb/ Shape	Exine (µm)	Sexine (µm)	Nexine (µm)	Reticulum (µm)	Columellae (µm)	Aperture Type	Plate
<i>S. paraneus</i>	Norris 1967	~18-28	prolate	striato-reticulate 1.0	0.8	0.2	striate striae often running oblique to colpus	densely spaced head Ø 0.5	tricolpate	Plate VI, Fig. 20-21
<i>S. trochuensis</i>	Srivastava 1967 Ward 1986	~20	(sub)circular	striato-reticulate 1.1	0.5-0.8	barely visible	striate	widely spaced head Ø 0.4	tricolpate	Plate VI, Fig. 22 Plate VII, Fig. 1-2
<i>S. vermimurus</i>	Srivastava 1977	~17-23	(sub)circular	striato-reticulate 1.7	1.1	0.6	irregular heterobrochate lumen size: 0.3-1.7	widely spaced head Ø 0.5	tricolpate	Plate VII, Fig. 3-5
<i>S. sp. 1</i>	Informal species	19-25	(sub)circular	striato-reticulate 2.5	1.0-2.3	0.5	irregular heterobrochate	widely spaced head Ø 0.6 muri verrucate through overtopping columellae	tricolpate	Plate VII, Fig. 6-7
<i>S. sp. 2</i>	Informal species	25-27	prolate	striato-reticulate 1.3-1.7	1.0-1.4	0.3	irregular heterobrochate lumen circular shaped max 2.5 near equator	irregular spaced head Ø 0.7	tricolpate	Plate VII, Fig. 8-10
<i>S. sp. 3</i>	Informal species	~22	prolate	striato-reticulate 4.0	3.5-3.8	0.5	striate	densely spaced head Ø 0.6	tricolpate	Plate VII, Fig. 11-12
<i>S. sp. 4</i>	Informal species	~20	(sub)circular	striato-reticulate 1.2-1.3	1.2	barely visible	irregular heterobrochate lumen max 1.4 near equator	widely spaced head Ø 0.4	tricolpate	Plate VII, Fig. 13
<i>S. sp. 5</i>	Informal species	~22	(sub)circular	striato-reticulate 1.3-1.5	0.9-1.3	0.3	irregular heterobrochate lumen size < 1.0	densely spaced head Ø 0.6 striae short	tricolpate	Plate VII, Fig. 14-15
<i>S. sp. 6</i>	Informal species	~20	prolate	striato-reticulate 2.0-4.0	2.0-3.5	0.5	striate	densely spaced head Ø 0.3	tricolpate	Plate VII, Fig. 16-18

Tetracolpate form

Species	Author	Size (µm)	Amb/ Shape	Exine (µm)	Sexine (µm)	Nexine (µm)	Reticulum (µm)	Muri width (µm)	Columellae (µm)	Aperture Type	Plate
Tetracolpate form 1	Informal species	~17	circular	reticulate-semitectate 1.0	0.7	0.3	homobrochate lumen size: 0.5-0.8	0.6	densely spaced head Ø 0.5 club shaped	Tetracolpate	Plate VII, Fig. 19-20

Genus *Tricolpites* Cookson ex Couper, 1953

Species	Author	Size (µm)	Amb/ Shape	Exine (µm)	Sexine (µm)	Nexine (µm)	Reticulum (µm)	Muri width (µm)	Columellae (µm)	Aperture Type	Plate
<i>T. aff. albiensis</i>	Kemp 1968	12-15	(sub)circular	reticulate-semitectate 0.7	0.5	0.2	homobrochate lumen size: 0.4-0.9	0.2-0.3	widely spaced head Ø 0.3	tricolpate	Plate VIII, Fig. 1-2
<i>T. blechrus</i>	Ward 1983	~17	(sub)circular	reticulate-semitectate 1.3	0.8	0.5	homobrochate lumen size: < 0.8	0.4	widely spaced head Ø 0.6 club shaped	tricolpate	Plate VIII, Fig. 3-4
<i>T. crassimurus</i>	(Groot & Penny) Singh 1971	~32	prolate	reticulate-semitectate 1.6	1.0	0.5	perforate <0.3	0.6	densely spaced head Ø 0.4	tricolpate	Plate VIII, Fig. 5-7
<i>T. aff. fragosus</i>	(Hedlund & Norris 1968) Ward 1986	18-22	(sub)circular	reticulate-semitectate 0.8-1.3	0.4-0.6	0.4-0.8	heterobrochate lumen size: <0.2 at equator; 0.9 at pole	0.3	densely spaced head Ø 0.2	tricolpate	Plate VIII, Fig. 8-10
<i>T. sagax</i>	Norris 1967	~24	(sub)circular	reticulate-semitectate 1.0	0.7	barely visible < 0.2	perforate-scabrate	barely visible	densely spaced barely visible	tricolpate	Plate VIII, Fig. 11
<i>T. vulgaris</i>	Srivastava 1969	~24	(sub)circular	reticulate-semitectate 1.2	0.8	0.4	homobrochate lumen size: 0.5-0.6	0.3-0.4	densely spaced head Ø 0.4 club shaped	tricolpate	Plate VIII, Fig. 12-14
<i>T. sp. 1</i>	Informal species	~19	(sub)circular	reticulate-semitectate 1.5	1.0	0.5	heterobrochate lumen size: <0.2 at equator; 0.9 at pole	0.4	widely spaced head Ø 0.4	tricolpate	Plate VIII, Fig. 15-16

Tricolporate form

Species	Author	Size (µm)	Amb/ Shape	Exine (µm)	Sexine (µm)	Nexine (µm)	Reticulum (µm)	Muri width (µm)	Columellae (µm)	Aperture Type	Plate
Tricolporate form 1	Informal species	~20	oblate	striato-reticulate 2.3	1.5 (detached)	0.8	striate	0.3	densely spaced head Ø 0.3	Tricolporate	Plate VIII, Fig. 17-18
Tricolporate form 2	Informal species	21	oblate	reticulate-semitectate 1.4 thicker along colpi	1.0 (detached)	0.4	perforate < 0.6	0.4	widely spaced head Ø 0.6	Tricolporate	Plate VIII, Fig. 19-20
Tricolporate form 3	Informal species	19	oblate	reticulate-semitectate 1.4	1.0	0.4	heterobrochate lumen size: 0.2-1.7*	0.4	densely spaced head Ø 0.3	Tricolporate (invaginated)	Plate VIII, Fig. 21-22

*lumen smaller near colpus

Triporate form

Species	Author	Size (µm)	Amb/ Shape	Exine (µm)	Sexine (µm)	Nexine (µm)	Reticulum (µm)	Muri width (µm)	Columellae (µm)	Aperture Type	Plate
Triporate form 1	Informal species	26	(sub)circular	reticulate-semitectate	0.6	0.6 slightly thicker near pores	irregular heterobrochate lumen size: 0.6-1.4	0.3	densely spaced head Ø 0.4	Triporate	Plate VIII, Fig. 23-24

Terrestrial climate and vegetation records from shallow marine deposits: Implications for angiosperm pollen distribution during the Albian

Maurits Horikx¹, Thierry Adatte², Ulrich Heimhofer¹

¹Institute of Geology, Leibniz University Hannover, 30167 Hannover, Germany.

²Institute of Geology and Palaeontology, University of Lausanne, 1015 Lausanne, Switzerland.

1. Abstract

The mid-Cretaceous is characterized by significant evolutionary changes in terrestrial ecosystems. During this period, the typical vegetation consisting of ferns, conifers and other gymnosperms is replaced by angiosperms. At the moment, the lack of high-resolution terrestrial plant fossil records covering mid-Cretaceous strata hampers our understanding to link changes in continental climate evolution and the subsequent impact on angiosperms and other vegetation types. In order to link changes in moisture regime to angiosperm evolution, a stratigraphically well-constrained high-resolution angiosperm and accompanying palynoflora pollen record covering the Albian stage in the Lusitanian Basin, Portugal is presented. Climate indices derived from the spore-pollen association (xerophyte ratio) and the clay mineral composition (weathering index) are used and show an overall aridification trend from the early Albian to early Cenomanian interrupted by an interval of increased moisture availability during the late Albian. The pollen-bearing shallow marine strata document a rich palynoflora that is interpreted to represent an ecosystem dominated by conifer forests with an understory of ferns and angiosperms. The relative angiosperm pollen abundance record shows a distinct increase (from 5% to 15%) but constitutes overall only a minor component in the total pollen assemblage from the early to late Albian. During the latest Albian to early Cenomanian interval, angiosperm pollen shows declining values to average abundances of 6%. In contrast to the abundance trend, poly-aperturate angiosperm pollen of eudicot affinity show a distinct diversification phase relative to monocolpate pollen of magnoliid-monocot affinity as evidenced by the eudicot over magnoliid-monocot E/(M-M) ratio. The rise in E/(M-M) ratio and the total angiosperm pollen diversities coincide with a long term aridity trend and could indicate a preference for early angiosperms towards more arid conditions during the Albian.

Keywords: paleoclimate, vegetation, early angiosperm radiation, Albian

2. Introduction

The profound perturbations in the ocean-atmosphere system during the mid-Cretaceous had a significant impact on the terrestrial realm including fundamental changes in global vegetation patterns and the rise of early angiosperms (Crane et al. 1995). Major tectonic events, climate change and variations in atmospheric CO₂ have been causally linked to the early angiosperm radiation during this interval (Crane et al. 1995, Heimhofer et al. 2005, McElwain et al. 2005, Chaboureau et al. 2014). Unfortunately, most of the above mentioned hypotheses cannot be tested due to the lack of tightly coupled stratigraphic records of mid-Cretaceous climatic and floristic changes. According to compilations of spore-pollen records (Lidgard & Crane 1988, Crane & Lidgard 1989), the Albian interval (113-100 Ma, Gradstein 2012) is marked by the replacement of fern spores, bisaccates and non-saccate gymnosperms by angiosperms at mid-latitudes. However, the exact interaction between angiosperm pollen and the accompanying palynoflora during this important phase in the early radiation of angiosperm is poorly documented. What is missing are detailed and continuous, stratigraphically well-constrained terrestrial records from the mid-Cretaceous coupled with other climatic proxies.

Reconstruction of the mid-Cretaceous climate system is based on high-resolution marine proxy-records and modelling results and shows evidence for higher than present sea surface temperatures (Norris et al. 2002, Bice et al. 2003, Steuber et al. 2005, Hay & Floegel 2012). Following a transient cooling at the Aptian-Albian boundary (Mutterlose et al. 2009, McAnema et al. 2013), a continuous rise in sea surface temperatures culminating in maximum sea surface temperatures of up to 35°C at the Cenomanian-Turonian boundary are recorded (Forster et al. 2007). Despite the wealth of information from the marine record, coeval, continuous, high-resolution and long-lasting terrestrial records remain relatively scarce.

A wealth of information on the systematic relationships of early angiosperm are obtained from angiosperm micro- meso- and macrofossils documented from early Cretaceous continental siliciclastic deposits in the northern part of the Lusitanian Basin (e.g. Saporta, 1894, Teixeira, 1948, Friis et al. 2004, 2011, Mendes et al. 2011, 2014a). Well-preserved fossils of presumably Aptian-Albian age have been described from the Torres Vedras, Juncal, Cercal and Catefica mesofossil sites located near Ericeira (Fig. 1) and the Famalicão, Buarcos and Vale de Agua sites in the northern part of the Lusitanian Basin (Friis et al. 1997, 1999, 2000a, 2000b, 2001, 2009, 2010a, 2010b, Pedersen et al. 2007, Mendes et al. 2014b). According to a conservative estimate, these fossil sites contain over 150 different angiosperm taxa (Friis et al. 2001). Previously, mid-Cretaceous palynofloral and climatic changes have been recorded in the southern part of the Lusitanian Basin (Heimhofer et al. 2008, Heimhofer et al. 2012).

Here we extend this record significantly by presenting a combined spore-pollen and clay mineralogy record from well-dated shallow-marine deposits covering early Albian to early Cenomanian strata from the São Julião section in the Lusitanian Basin, Portugal with a particular emphasis on the role of climatic variations on terrestrial plant communities and the coeval rise of angiosperms.

The aim of the study is therefore:

- (1) Provide a continuous clay mineralogical and palynological record from the southern Lusitanian Basin covering early Albian to early Cenomanian.
- (2) Infer climatic and vegetation changes in the continental hinterland of the basin.
- (3) Investigate the potential relationship between angiosperm radiation and climatic evolution.

3. Geological setting

The Lusitanian Basin is located in the westernmost part of the Iberian Peninsula and filled with Mesozoic strata deposited on a passive margin (Fig. 1). The São Julião section is located near the coastal town of Ericeira and has a total thickness of 192 m (Fig. 2). Here a short description of the section is provided, a detailed description of the lithology and stratigraphic age-assignment of the section is given by Horikx et al. (2014). The lowermost beds are composed of fluvio-deltaic deposits (Rodízio Formation). These sediments are overlain by shallow marine strata of the Galé Formation (16-192 m). The Galé Formation is subdivided into the Água Doce Member and Ponta da Galé Member. The Água Doce Member consists of shallow-marine sandstone and sand-rich limestone beds with changing detrital input.

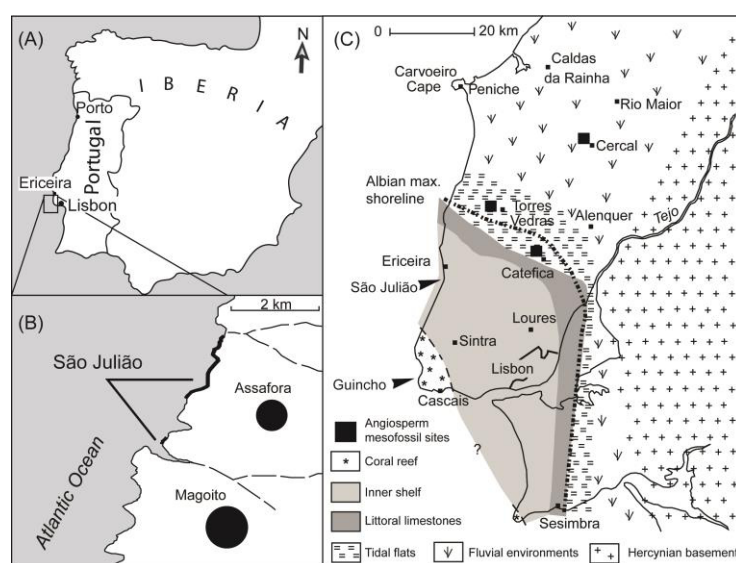


Fig. 1. (A) Map showing the position of the studied section on the Iberian Peninsula near the town of Ericeira, Portugal. (B) Map of the study area showing the location of the coastal São Julião section close to the villages of Assafora and Magoito, ca. 5 km south of Ericeira. (C) Paleocoastline and depositional setting of the southern Lusitanian Basin during the Albian interval, with the position of the shallow marine São Julião and Guincho sections and the location of important terrestrial angiosperm mesofossil sites marked (modified from Dinis et al. 2010).

Thick limestone beds containing the first occurrences of macroscopic rudist remains mark the boundary to the overlying Ponta da Galé Member (Rey 1992). Recently, the São Julião section was dated using dinoflagellate cyst biostratigraphy, carbon-isotope chemostratigraphy and strontium isotope ratios from pristine low-Mg calcite oyster and rudist shells (Horikx et al. 2014). According to the revised age assignment, the lowermost 18 m of the section are of early Albian age, whereas the interval 18-44 m is of middle Albian age. A large part (44-165 m) of the section is composed of strata of late Albian age (Horikx et al. 2014). The Albian-Cenomanian boundary is tentatively placed between 165-175 m in the topmost part of the section (Horikx et al. 2014). The limited thicknesses of the early (113–110.7 Ma) and middle (110.7–107.7 Ma) Albian deposits and the expanded late Albian (107.7–100.5 Ma) in the São Julião section are in line with the estimated duration of the corresponding time intervals, following the geological timescale of Gradstein et al. (2012). Overlying the Galé Formation are brackish-marine to fluvio-lagoonal deposits corresponding to the Caneças Formation (Dinis et al. 2008) of Cenomanian age (Berthou 1984). These sediments have been investigated but produced only barren palynological samples. The São Julião section was positioned close to the paleo-shoreline in Albian times and located at 20-30°N paleolatitude (Stampfli & Borel 2002).

4. Material & methods

4.1 Palynological processing

A total of 82 sediment samples (67 productive samples) have been selected for palynological analyses from various lithologies. All samples were cleaned and dried for 24h at 40°C and 10-30 gram of sample material was sent at the Geological Survey of Nordrhein-Westfalen in Krefeld, Germany for palynological preparation following standard procedures (Traverse 2007). Strew mounts were studied

with an OLYMPUS BX 53 transmitted light microscope using a 100x oil immersion objective and differential interference contrast. Light microphotographs were taken with an OLYMPUS XC 50 digital camera. Both terrestrial (spores, pollen) and marine (e.g. dinoflagellate cysts) palynomorphs were counted in non-overlapping traverses. At least 300 terrestrial palynomorphs were counted per sample, followed by a subsequent qualitative analysis on the remainder of the strew mount to check for rare angiosperm taxa. All slides are stored at the Institute for Geology in Hannover, Germany.

4.2 Statistics

Terrestrial palynomorph assemblage zones were reconstructed using the stratigraphically constrained statistical program CONISS within Tilia (Grimm 1991), which uses constrained cluster analysis using the Ward's method (Ward 1983). This increases the visualization of changes within the palynoflora. A more complete description of the CONISS program is given by Grimm (1987).

4.3 Clay analysis

A total of 64 samples were analyzed for their clay mineralogy content at the University of Lausanne, Switzerland, following the procedure described by Adatte et al. (1996). Grounded samples were treated with de-ionized water and 10% HCl in order to clean the samples and remove excess carbonates. The remaining residue was washed and centrifuged (5–6 times) to obtain a neutral pH (7–8). Separation into two different grain-size fractions (<2 µm and 2–16 µm) was obtained by the timed settling method based on Stokes law. The remaining residue was then pipetted onto a glass plate and air-dried at room temperature. Subsequently, X-ray diffraction (XRD) analysis of oriented clay samples was carried out. The intensities of selected XRD peaks characterizing each clay mineral present in the size fraction (chlorite, mica, kaolinite and illite/smectite mixed-layers) were measured for a semi-quantitative estimate of the proportion of clay minerals present in two size fractions (< 2 µm and 2–16 µm). Determination of the illite/smectite (I/S) mixed-layers and their content in smectitic expandable layers is based on the method of Moore & Reynolds (1997).

4.4 Paleo-environmental indices

The ratio of terrestrial (T; pollen and spores) over marine (M; dinocysts) palynomorphs in the palynological samples is used to infer sea level variations. The $T/(T+M)$ ratio is calculated by dividing the terrestrial palynomorphs (T) by the total (terrestrial and marine; T+M) palynomorph count, following Versteegh (1994) and van Helmond et al. (2014).

The weathering index (WI) and the xerophyte ratio are used to infer changes in humidity. The WI index ($K/(M+Ch)$) is calculated by the ratio of kaolinite (K) over mica (M) and chlorite (Ch) in clay mineral assemblages (Singer 1984, Chamley 1989, Duchamp-Alphonse et al. 2011). Kaolinite minerals are commonly formed under warm and humid (tropical to subtropical) conditions, whereas mica and chlorite reflect formation under cooler and more arid climates (Chamley 1989, Duchamp-Alphonse et al. 2011, Westermann et al. 2013). High values in the WI index therefore represent weathering under humid conditions.

The xerophyte ratio is calculated by dividing the total *Classopollis* (C) pollen by the combined total spores (S) and *Classopollis* count ($C/(C+S)$). *Classopollis* pollen are a common component in Mesozoic palynological assemblages and produced by Cheirolepidiaceae conifers, associated with warm and arid climatic conditions in lowland or shoreline habitats (Vakhrameev 1981, Batten 1984, Abbink et al. 2001), whereas spore-producing plants (pteridophytes, lycopods, bryophytes) are generally considered to flourish under relatively humid conditions (Abbink 1998, Bonis & Kürschner 2012). Low xerophyte ratios are therefore interpreted to represent humid conditions.

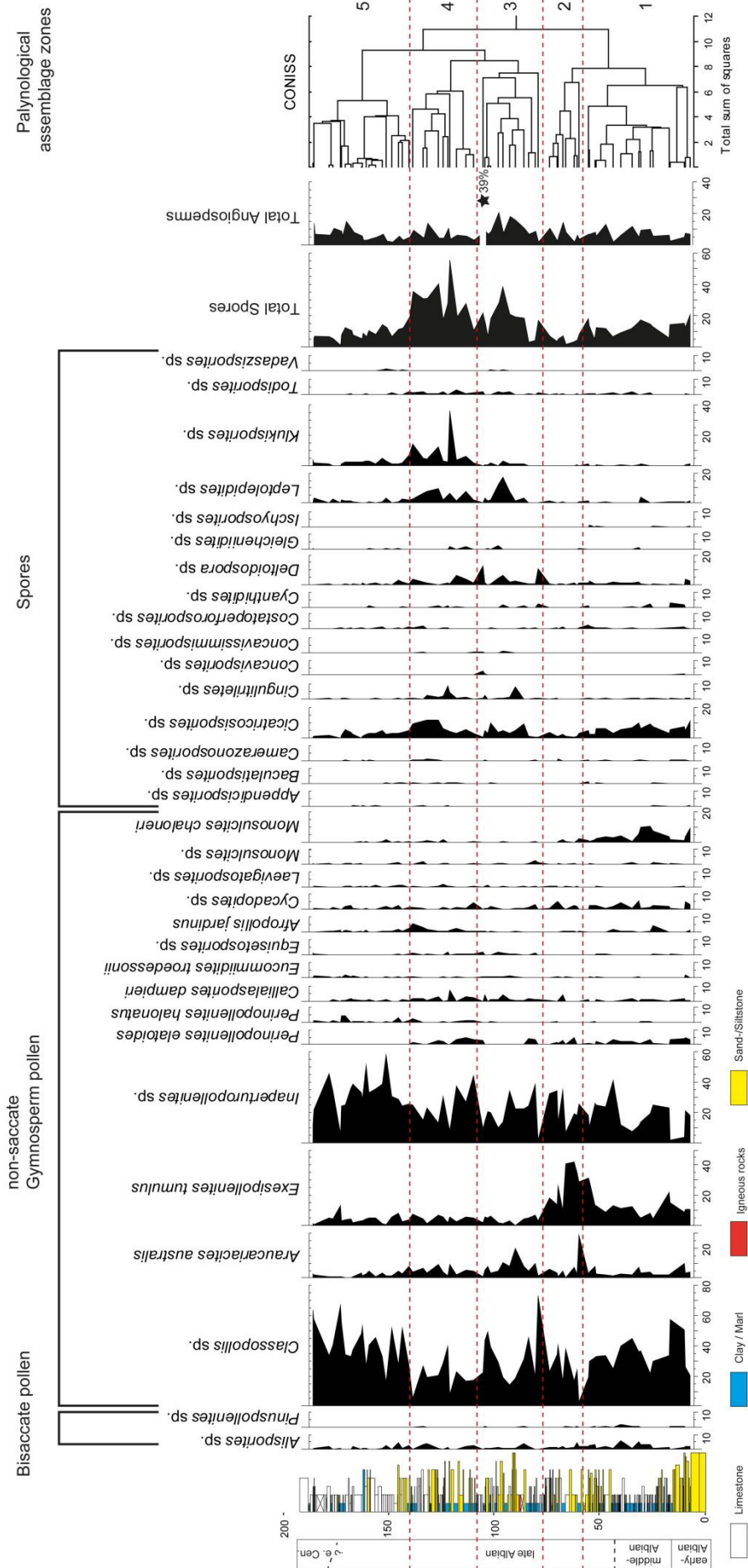


Fig. 2. Relative abundances [%] of the spore-pollen content against stratigraphic age, height and lithological log, during the early Albian-early Cenomanian in the São Julião section, and the palynological zonation scheme based on CONISS cluster analysis.

5. Results

5.1 Palynology & clay mineralogy

The spore-pollen association of the São Julião section is characterized by the dominance of non-saccate gymnosperm pollen (Figs. 2, 3). For most of the section, *Classopollis* (average 32.8%) and *Inaperturopollenites* (average 29.8%) pollen are the most common components in the spore-pollen association. *Araucariacites* (average 4.3%), *Monosulcites chaloneri* (average 1.2%), *Exesipollenites* (average 9.5%) and *Cycadopites* (average 1.7%) occur in relatively low abundances. Bisaccate pollen (average 1.4%) are consistently present but only in low abundance. Spores represent an important component in the palynological assemblage (average 11.1%) and common taxa include *Klukisporites*, *Leptolepidites*, *Cicatricosisporites* and *Deltoidospora*. Angiosperm pollen are present but mostly subordinate throughout the section and relative abundances fluctuate between 1-20% (average 8%). The clay-mineral composition is composed of kaolinite, mica, I/S and chlorite (Fig. 4). Kaolinite and mica dominate the assemblage throughout the section with an average abundance of 62.2% and 26.7% respectively. I/S and chlorite only occur subordinate and have average abundances of 4.3% and 6.8%. In order to better describe changes with stratigraphic height, the section is subdivided into five assemblage zones based on the spore-pollen content in the cluster analysis program CONISS (Fig. 2).

Assemblage zone 1 (0-57 m)

The lowermost assemblage zone 1 (0-57 m) is characterized by high abundances of the pollen *Classopollis* and *Monosulcites chaloneri* (Figs. 2, 3). *M. chaloneri* shows a significant decrease in the overlying assemblage and occurs sporadically (< 1%) throughout the upper part of the section. Consistent occurrences of non-saccate pollen *Inaperturopollenites*, *Cycadopites*, *Perinopollenites elatoides*, *Exesipollenites tumulus*, *Afropollis jardinus*, *Araucariacites* and *Cicatricosisporites* also occur. Angiosperm pollen abundances fluctuate between 3-12% (average 6.7%). The xerophyte ratio ranges between 0.79-0.95 (average 0.86). The T/(T+M) ratio ranges between 0.6-1.0 (average 0.9) (Fig. 4). The clay mineral composition is dominated by kaolinite (average 75.8%), mica (average 14.3%) and chlorite (average 6.9%). The WI index fluctuates between 10.5 and 1.8 (average 4.6) and decreases section-up.

Assemblage zone 2 (57-77 m)

This assemblage is marked by exceptional high abundances of *Exesipollenites* (up to 44 %) (Fig. 2). *Classopollis* pollen are rare in the lower part of the assemblage and becomes increasingly more abundant towards the top of this interval. Angiosperm pollen abundances fluctuate between 1.3-13.6% (average 5.6%), whereas spores show a marked decline. *Cicatricosisporites* and *Deltoidospora* are the most common taxa. The xerophyte ratio ranges fluctuates between 0.83-0.97 (average 0.93), whereas The T/(T+M) ratio shows values ranging between 0.6-1.0 (average 0.9) (Fig. 4). Despite lower values compared to assemblage zone 1, the clay mineral content is dominated by kaolinite (average 60.2%) whereas mica (average 23.3%) and chlorite (average 8.7%) increase. The WI index fluctuates between 5.0 and 0.7 and shows slightly lower values (average 2.7) compared to assemblage zone 1.

Assemblage zone 3 (77-107 m)

A conspicuous decline in *Exesipollenites* pollen to values of <10% and increased abundances of angiosperm pollen (average 13.6%) and *Araucariacites* (maximum 19.6%) mark the spore-pollen record during this interval (Fig. 2). *Classopollis* and *Inaperturopollenites* pollen abundances fluctuate significantly but both types remain a common component in the spore-pollen assemblage. Spore abundances increase in the second half of this zone and are mainly represented by *Cicatricosisporites*, *Deltoidospora*, *Leptolepidites* and to a lesser extent *Todisporites*. The xerophyte ratio shows significant fluctuations between 0.50-0.97 (average 0.78), whereas the T/(T+M) ratio shows values ranging between 0.4-1.0 (average 0.8) (Fig. 4). Kaolinite content in assemblage zone 3 is relatively low (average 57.9%), but remains the dominant component in the clay mineral composition despite significant fluctuations, followed by mica (average 32.0%) and chlorite (average 6.1%). The WI index is slightly lower than assemblage zone 2 (average 2.3) and fluctuates between 6.1 and 0.3.

Assemblage zone 4 (107-139 m)

A distinct increase in spores abundances (average 28.7%) and a decline in angiosperm and *Classopollis* pollen characterize this interval (Fig. 2). The spore taxa *Cicatricosisporites*, *Deltoidospora*, *Gleicheniidites*, *Leptolepidites*, *Klukisporites* and *Cingulatisporites* represent the most abundant forms. *Classopollis* show their lowest abundances in the section (average 20%), whereas angiosperm pollen abundances fluctuating between 2.8-13.5% (average 6.2%). Noteworthy is the relative high abundance of *Afropollis jardinus* (average 1.7%) during this interval. The xerophyte ratio fluctuates between 0.42-0.89 (average 0.68). The T/(T+M) ratio is relatively stable and ranges between 0.6-1.0 (average 0.9). The clay mineral content is marked by a clear decrease in mica (average 16.5%) and an increase in kaolinite (average 74.0%) and chlorite (average 7.4%) content. The WI index (average 3.9) fluctuates between 7.9 and 1.3 (Fig. 4).

Assemblage zone 5 (139-192 m)

The topmost part of the section shows a pronounced change in the assemblage. Assemblage zone 5 is characterized by high abundances of *Classopollis* (average 40.2%) and *Inaperturopollenites* (average 30.4%) and a marked decline in spore abundances (average 8%), as well as the disappearance of *Perinopollenites elatoides*. The most common spores are *Cicatricosisporites*, *Leptolepidites* and *Klukisporites* (Fig. 2). Angiosperm pollen abundances are relatively stable and fluctuate between 1.6-14.7% (average 6.2%). *Afropollis jardinus* occurs regularly but is rare (average 0.6%). The xerophyte ratio shows relative high values ranging between 0.80-0.99 (average 0.90). In contrast, the T/(T+M) ratio is low and fluctuates between 0.2-0.8 (average 0.5) due to a distinct increase in marine-derived dinoflagellates. The clay mineral content is composed of relatively low kaolinite (average 50.4%) and high mica (average 37.7%) content, chlorite content is on average 6.0%. Kaolinite show a clear decreasing trend section-up, whereas mica content increases. The WI index (average 1.3) fluctuates between 3.4 and 0.4 (Fig. 4).

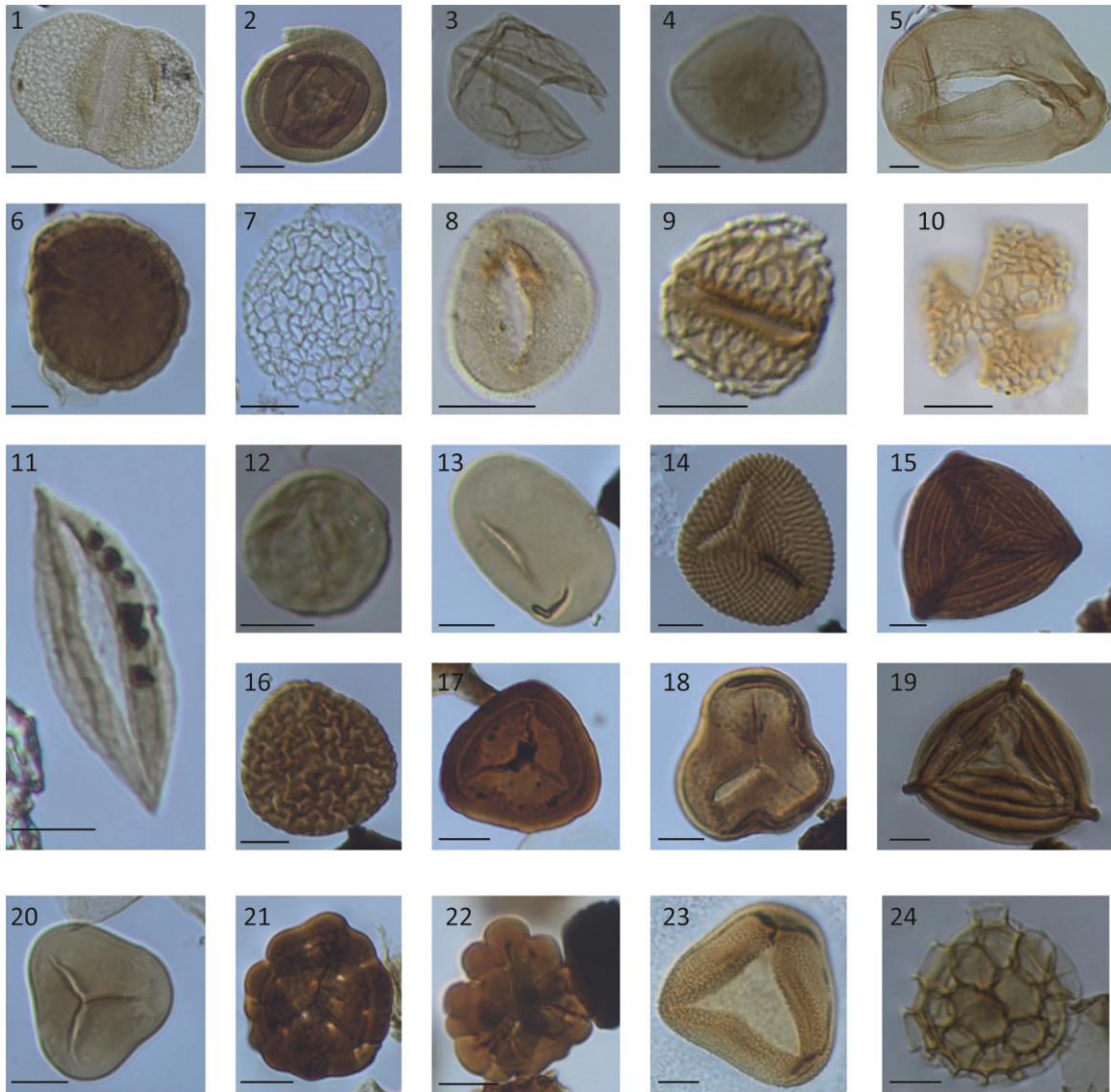


Fig. 3. Photomicrographs of selected pollen and spores from the São Julião section. Scale bar in all photographs is 10 μ m. 1) *Alisporites* sp., SJMH-78, 131.0/6.6, 83.6 m. 2) *Classopollis* sp., SJMH-78, 142.2/21.9, 83.6 m. 3) *Inaperturopollenites* sp., SJMH-4, 128.2/21.4, 10.2 m. 4) *Exesipollenites tumulus* SJMH-4, 148.4/11.7, 10.2 m. 5) *Araucariacites australis* SJMH-4, 135.3/3.5, 10.2 m. 6) *Callialasporites dampieri*, SJMH-32; 148.0/6.7, 43.9 m. 7) *Afropollis jardinus*, SJS-33, 148.5/18.8, 185.1 m. 8) *Clavatipollenites hughesii*, SJMH-177, 146.3/16.1, 158.9 m. 9) *Pennipollis peroreticulatus*, SJMH-101, 132.7/18.7, 105.3 m. 10) *Retitrescolpites* sp. 1 sensu Horikx et al. 2015, SJMH-36, 129.8/17.6, 47.3 m. 11) *Cycadopites* sp., SJMH-32, 141.9/21.9, 43.9 m. 12) *Monosulcites chaloneri*, SJMH-4, 130.0/6.1, 10.2 m. 13) *Laevigatosporites* sp., SJMH-28, 142.5/6.8, 40.2 m. 14) *Cicatricosisporites* sp., SJMH-128, 143.9/19.6, 126.0 m. 15) *Costatoperforosporites* sp., SJMH-43, 125.3/14.0, 51.7 m. 16) *Camerazonosporites* sp., SJMH-2, 125.5/14.0, 7.5 m. 17) *Cingutritetes* sp., SJMH-18, 126.8/16.3, 26.2 m. 18) *Cyathidites* sp., SJMH-83, 148.5/18.8, 89.9 m. 19) *Plicatella* sp., SJMH-2, 127.2/17.7, 7.5 m. 20) *Deltoidospora* sp., SJMH-78, 137.5/3.7, 83.6 m. 21) *Klukisporites* sp., SJMH-156.5 132.5/17.1, 150.5 m. 22) *Leptolepidites* sp., SJMH-106, 132.6/21.2, 109.5 m. 23) *Vadaszisorites* sp., SJMH-156.5, 132.5/6.8, 150.5 m. 24) *Zlivisporis* sp., SJMH-4, 129.0/13.6, 10.2 m.

6. Discussion

6.1 Hydrodynamic sorting effects and burial diagenesis

Before any paleo-climatic interpretations from the clay mineral assemblages and palynofloral record can be made, an assessment of the diagenetic and sorting impact on the composition is needed. The clay mineral composition may be affected by diagenetic alteration during burial (Chamley 1989, Godet et al. 2008, Duchamp-Alphonse et al. 2011, Westermann et al. 2013). According to Chamley (1989) and Deconinck (1993), low abundances of illite/smectite mixed layers and an abundance of kaolinite are indicative of low burial diagenesis. The São Julião section is dominated by kaolinite and mica, with only low illite/smectite mixed layers. Likewise, the excellent quality of the palynomorphs (TAI <2 thermal alteration index of Staplin 1982) in the same deposits suggests that effects of burial diagenesis are limited on both the palynological and clay mineral record. High kaolinite contents up to 90% have been recorded from distinct coarse-grained sandstone-rich intervals (between 7.5-10 m and at 55 m) and these unusual high values are likely an artifact, related to the in-situ formation of kaolinite in siliciclastic deposits kaolinite within the pore space of porous sandstones during early burial (Weaver 1989, Heimhofer et al. 2008).

Sea level fluctuations represent another important process that potentially hampers a direct correlation between the palynological and/or clay mineral assemblage to climatic variations in shallow marine deposits (Chamley 1989, Tyson 1995, Adatte et al. 2002). However, a strong effect of sea level fluctuations on both assemblages can be largely ruled out for most of the section. Despite some scatter, high abundances of terrestrial derived palynomorphs over marine dinoflagellate cysts are evidenced by the continuously high T/(T+M) and point to very proximal and coastal marine conditions (Fig. 4). The decreasing trend in T/(T+M) ratios in assemblage zone 5 is interpreted to represent a sea level rise. However, sea level changes in the uppermost part of the section are most likely in the order of a few meters at most. This is evidenced by the presence of the rudists *Apricardia carentonensis* and *Mathesia darderi* preserved in-situ in the carbonate-rich upper part (Horikx et al. 2014). The sea-level fluctuations from the T/(T+M) ratios are in line with existing sequence-stratigraphic interpretations for the Lusitanian Basin. According to Dinis et al. (2002) and Rey et al. (2003), the Galé Formation in the Lusitanian Basin is characterized by a transgressive phase during the latest Albian (Vraconian). The good to excellent preservation of fine-sculptured and thin-walled (angiosperm) pollen and the low frequency of damage among palynomorphs throughout the record further corroborates a short transportation path and deposition within a proximal marine setting for the São Julião record during the Albian. Therefore, the palynological and clay mineralogy records are interpreted to reflect primary paleo-environmental changes in the adjacent continental hinterland of the Lusitanian Basin.

6.2.1 Paleo-environmental changes and floral response

The spore-pollen record covering the early Albian to earliest late Albian (assemblage zone 1) is characterized by the dominance of *Classopollis* and *Inaperturopollenites* pollen and the presence of *Cicatricosisporites* and *Deltoidospora* spores (Fig. 2). *Inaperturopollenites* pollen are produced by Cupressaceae indicating slightly humid and warm conditions (van Konijnenburg-van Cittert 1971, Abbink 1998). According to Abbink et al. (2001) and Lindström & Erlström (2011), *Cicatricosisporites* is related to the Schizaeaceae and grows in lowland areas associated with marshes, river ecosystems or understory in forests during relatively warm and humid climates. *Deltoidospora* is produced by Dicksoniaceae and has been related to slightly warm and dry conditions (Abbink et al. 2001). Therefore the spore-pollen assemblage of assemblage zone 1 is interpreted to represent a mixed vegetation growing under a climatic regime with intermediate moisture availability. This interpretation is corroborated by the xerophyte ratio and WI index (Fig. 4).

A shift towards high abundances of *Exesipollenites* and a pronounced decrease in spores characterizes assemblage zone 2. According to Watson & Sincock (1992) and Abbink (1998), *Exesipollenites* pollen are produced by Bennettitales and thrive in arid and warm climates. Likewise, increasingly lower values in the WI index and a rise in the xerophyte ratio are recorded and represent a shift towards more arid conditions (Fig. 4).

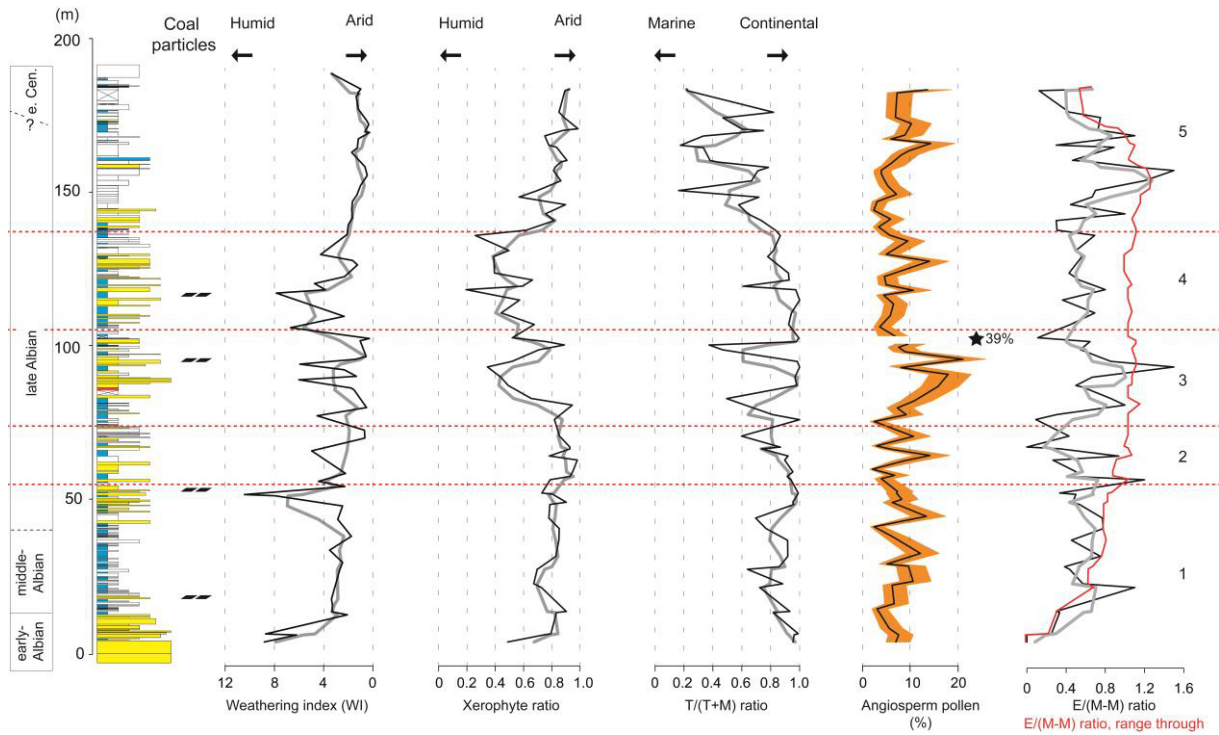


Fig. 4. Lithological log with the occurrence of in-situ coal particles, weathering index, xerophyte ratio, $T/(T+M)$ ratio, relative abundance [%] of angiosperm pollen and $E/(M-M)$ ratio from the São Julião section in the Lusitanian Basin, Portugal. Grey lines indicate 3-point moving average; orange shading indicates the 95% confidence interval. Numbers indicate spore-pollen assemblage zones. Red line indicate $E/(M-M)$ ratio using the range through method and shows increased dominance of eudicots over monocots from bottom to top of the section (see text).

The following spore-pollen assemblage (zone 3) is marked by a rise in the relative abundance of angiosperm and *Araucariacites* pollen and total spores, as well as significant fluctuations in *Classopollis* pollen and a decline of *Exesipollenites*. The increase in spores (*Leptolepidites*, *Cicatricosisporites*) of Schizaeaceae affinity points to more humid conditions (Galloway et al. 2012), whereas higher abundances of *Araucariacites* likely reflect cooler conditions (Abbink et al. 1998). The WI index and xerophyte ratio in the overlying assemblage zone 3 fluctuate significantly, but show a general trend towards more humid conditions (Fig. 4). Therefore assemblage zone 3 represents an interval of increasing humidity and slightly cooler conditions.

The spore-pollen assemblage in assemblage zone 4 is marked by the dominance of spores and low abundance of gymnosperm pollen. The total spores composition is dominated by *Klukisporites*, *Leptolepidites*, *Cicatricosisporites*, *Deltoidospora* and *Cingulatisporites* of mostly Schizaeaceae affinity and have been linked to humid conditions (Abbink 1998, Galloway et al. 2012). This is corroborated by relatively high abundances of *Afropollis jardinus*. According to Doyle et al. (1982), the parent plant of *A. jardinus* is better adapted to humid than dry conditions. Likewise, the xerophyte ratio and WI index show a distinct increase towards more humid conditions.

A clear increase in *Classopollis* pollen and a decline in spores (*Klukisporites*, *Leptolepidites*, *Cicatricosisporites*) in assemblage zone 5 points to a gradual aridification during the latest Albian and early Cenomanian. This is also evident from the decline in the WI index and an increase in the xerophyte ratio. The overall trends in moisture availability obtained from the palynological and clay mineral record are corroborated by sedimentological evidence. For instance, the marked shift in lithology from sandstone-clay alteration, to the build-up of thick limestone beds (~145 m) corresponds to the boundary between assemblage zones 4 and 5. The establishment of a carbonate platform depositional environment is interpreted to represent a reduction of siliciclastics due to reduced fluvial input related to more arid conditions. Likewise, in-situ coal particle formation and deposition is

associated with relative humid conditions in the geological record (Parrish et al. 1982, Hallam 1985). Macroscopic in-situ coal layers several millimeters to centimeters thick have been recorded in strata corresponding to assemblage zones 1, 3 and 4 and provide further evidence for relative humid conditions (Fig. 4). Likewise the lack of coal in assemblage zones 2 and 5 corroborate to relative arid conditions. Overall, the paleo-environmental indices point to an overall shift towards slightly more arid conditions from the lower to the upper part of the São Julião section corresponding to an early Albian to latest Albian-early Cenomanian age, punctuated by a relative wet phase during the late Albian.

6.2.2 Comparison to existing Albian records from Iberia

Information on climatic conditions in the Lusitanian Basin during Albian times can be derived from the Chicalhão section near Juncal, Portugal in the northern part of the Lusitanian Basin and the Guincho section near São Julião (Heimhofer et al. 2012, Mendes et al. 2014a, 2014c). The early Albian plant assemblage from Chicalhão, ~120 km north of São Julião, is composed of a mixed flora of cheirolepidiaceae conifer trees with an understorey dominated by ferns of the Schizaeaceae group. The clay mineralogy record is characterized by a dominance of kaolinite over mica and chlorite. The inferred local climate was humid and warm, with seasonal variations in precipitation but lacking a major drought season (Mendes et al. 2014a, 2014c).

The shallow marine Guincho section is located ~20 km south of São Julião (Fig. 1) and recently the two sections have been correlated stratigraphically (Horikx et al. 2014). The Guincho section covers an extended early Albian and middle Albian. The section is composed of a relatively condensed (~30 m) rudist-rich limestone succession of late Albian strata and this interval is sampled in much lower resolution compared to São Julião. Notwithstanding, the reproducibility of both records is demonstrated by the similarities in clay mineralogy and palynology, despite a different position with regard to the paleo-shoreline (Fig. 1C). The early Albian palynological record at Guincho is composed of pollen with affinities to Cheirolepidaceae (*Classopollis*) and Taxodiaceae (*Inaperturopollenites*, *Perinopollenites*) conifers, with minor influences of ferns and angiosperms. The clay mineral record is dominated by kaolinite, with relative low mica and chlorite contents and indicates a warm and semi-humid climate (Heimhofer et al. 2012). Other evidence for at least episodic humid conditions during the early-middle Albian in Iberia comes from well-preserved macrofossil associations in the Maestrat Basin, Spain (Sender et al. 2014, Villanueva-Amadoz et al. 2014). These fossil-rich beds are interbedded by several coal beds and contain a wealth of fossils from aquatic and/or semiaquatic organisms (e.g. crocodiles, turtles) pointing to humid conditions. Increasingly arid conditions during the late Albian in the Lusitanian Basin is evidenced by the increase of mica over kaolinite and the conspicuous increase of *Exesipollenites* pollen over spores associated with assemblage zone 2. This observation is corroborated by the age-equivalent palynological zone LPZ III from Guincho where a similar increase in *Exesipollenites* is observed (Heimhofer et al. 2012). So far, the late Albian humid phase corresponding to assemblage zone 3 and 4 has not been recorded in other coeval high-resolution studies from the Lusitanian Basin. Regardless, the subsequent aridification phase represented by assemblage zone 5 (Fig. 4) during the late Albian-early Cenomanian and the overall trend towards aridification from the early to late Albian at São Julião is corroborated by previously published palynological records (Hasenboehler 1981, Taugourdeau-Lantz et al. 1982). Likewise, the development of vast erg systems, indicative of desert-like conditions, deposited in eastern Iberia, show evidence of increased aridity during the late Albian (Rodríguez-Lopez et al. 2006, 2008, 2010).

6.3 Angiosperm diversification patterns in the Lusitanian Basin

The diversification of angiosperms growing in the hinterland of the Lusitanian Basin is documented by several palynological studies (Hasenboehler 1981, Chapman 1982, Friis et al. 1999, 2001, 2004, 2011, Heimhofer et al. 2007). The mid-Cretaceous represents an important interval in early angiosperm pollen evolution and diversification and is characterized by the significant rise in pollen morphologies and pollen species. Previously, the eudicot over monocot-magnoliid ratio (E/(M-M) ratio) was used to show the continuous diversification of eudicots and their dominance over monocots during the mid-Cretaceous (Hochuli et al. 2006). From which time onwards eudicots form the most diverse group of angiosperms. The E/(M-M) ratio from the São Julião section shows a continuous rise throughout the section despite significant fluctuations and values mostly varying between 0.5 and 1.0 during the Albian (Fig. 4). This E/(M-M) ratio has also been reconstructed from time-equivalent deposits from the Potomac Group succession in the eastern USA and from the Lusitanian Basin (Doyle & Robbins 1977, Hochuli et al. 2006, Heimhofer et al. 2007). The highest E/(M-M) ratios in age-equivalent sediments are observed in fluvio-deltaic sediments of the Potomac Group succession, whereas the lowest ratios are from the distal marine Guincho section (Hochuli et al. 2006). All three records are from similar paleo-latitudes with broadly similar climate regimes and the observed differences in angiosperm pollen composition are interpreted to represent different pollination-techniques and transportation paths. In contrast to wind-pollinating angiosperms, producing mostly monocolpate pollen of the *Clavatipollenites* and *Asteropolis* groups (Friis et al. 1999), poly-aperturates are mostly insect-pollinated with low pollen production and more difficult to detect in marine sediments (Friis et al. 1994, Crane et al. 1995, Brenner 1996).

The E/(M-M) ratio with a range-through method is used to circumvent this problem (Fig. 4). The range-through method considers angiosperm pollen to be present in all samples between the first and last appearance in the section and eliminates the potential sampling bias of rare angiosperm pollen with reduced pollen production and dispersal (Hammer et al. 2001). On the other hand, this method fails to record the possible absence of pollen-producing plants due to migration or environmental change over shorter time-scales (Boltovskoy 1988). The range-through E/(M-M) ratio shows a continuous increase from values of 0.0 in the lower part of assemblage zone 1 (early Albian to early late Albian) to 1.3 in the lower part of assemblage zone 5 (latest Albian) related to the dominance of poly-aperturate forms over monocolpates (Fig. 4). The decreasing diversity trend at the top of the record is most likely related to the 'edge effect' and is attributed to exaggerated high numbers of last occurrences documented at the end of a palynological record (Boltovskoy 1988, Bonis & Kürschner 2012).

The oldest poly-aperturate (tricolpate) angiosperm pollen have been documented from the low latitudes in Gondwana, associated with semi-arid conditions. The Albian temperature record derived from long-ranging sections or cores from the marine realm shows a generally trend towards warmer ocean water temperatures from the early Albian towards the early Cenomanian (Clarke & Jenkyns 1999, Wilson & Norris 2001, Pucéat et al. 2003, Forster et al. 2007, Tiraboschi et al. 2009, Erbacher et al. 2011, Friedrich et al. 2012). It has been suggested that the rise in global temperatures during the Albian could have triggered the northward spread of angiosperms into new biomes, promoting increased species radiation, especially among eudicots (Stebbins 1974, Coiffard et al. 2007, Coiffard & Gomez 2012, Coiffard et al. 2012). According to Chaboureaux et al. (2014), the break-up of Pangea during the mid-Cretaceous facilitated increased humidity over the continents and triggered the angiosperm diversification. The climatic evolution from the Lusitanian Basin shows increased aridity and a rise of eudicots over magnoliid-monocots is evidenced by the concurrent rise of the E/(M-M) ratio during the Albian. This aridification phase could be related to the expansion of the arid climate belt and triggered the northward migration of poly-aperturate parent-plants from lower latitudes.

Despite the long-term trend towards a dominance of poly-aperturates over monocolpates, significant fluctuations in the total angiosperm diversity record are observed over shorter time scales, corresponding to the different assemblage zones. This is evidenced by the total average angiosperm per sample diversity and shows the highest values in assemblage zone 4 (average 20.2), followed by zone 2 (average 18.7), zone 1 (average 16.3) and zone 3 (average 15.5) (Fig. 5A). The lowest average diversity is recorded in assemblage zone 5 (average 14.6). However, the relative low number of samples in some of the assemblage zones combined with rare occurrences of several angiosperm

pollen species makes undersampling a likely possibility and could underestimate the actual diversity of angiosperm pollen within an assemblage zone (Fig. 5A; Mander et al. 2010, Kürschner et al. 2014). In order to track diversity changes per assemblage zone, the Jackknife2 and Chao2 among-sample

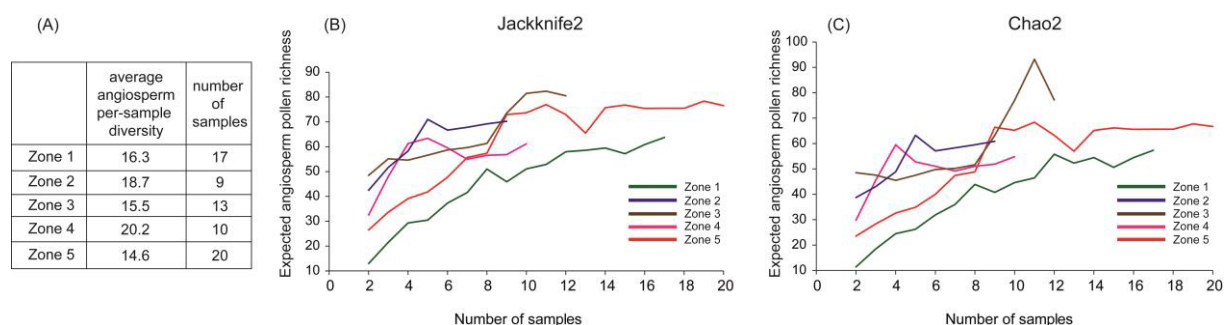


Fig. 5. (A) Average angiosperm pollen diversity and number of samples per assemblage zone. (B) Expected angiosperm pollen richness estimates for assemblage zones 1-5 using the Jackknife2 index (y-axis) plotted against number of pooled samples (x-axis). (C) Expected angiosperm pollen richness estimates for assemblage zones 1-5 using the Chao2 index (y-axis) plotted against number of pooled samples (x-axis). Note the horizontal shape of the curve for zones 1 and 5, indicating a lack of undersampling (see text).

expected richness indices are used. These indices give an estimate on the angiosperm pollen diversity within an assemblage zone based on the counted number of species and samples (Mander et al. 2010). According to Longino et al. (2002) and Mander et al. (2010), the horizontal shape of both indices curves indicate that a particular interval is fully sampled, whereas a continuous rising curve indicates undersampling. Based on this observation both indices show that only assemblage zones 1 and 5 are fully sampled, whereas the other assemblage zones remain under-sampled. Notwithstanding, despite some undersampling in these assemblage zones the Jackknife2 and Chao2 curves show that assemblage zones 1 and 4 are the expected species-poorest assemblages, whereas zones 2, 3 and 5 are the taxonomically richest assemblages (Fig. 5B, 5C). Assemblage zones 2 and 5 correspond to arid conditions, whereas assemblage zones 1, 3 and 4 are associated with more humid conditions (Fig. 4). These per assemblage zones expected richness indices are in clear contrast to the counted per assemblage zone average angiosperm pollen diversity (Fig. 5A). Apart from assemblage zone 3, which shows significant variations in humidity, the other (2 and 5) assemblage zones with the highest expected richness are associated with more arid conditions and might indicate enhanced angiosperm diversity during periods of relative arid conditions.

Currently, most Albian records from the terrestrial realm focus on biostratigraphy rather than continental climate evolution or are composed of siliciclastic-rich sediments with low stratigraphic time control or lack a detailed angiosperm pollen record (e.g. Doyle & Robbins 1977, Villanueva-Amadoz et al. 2010, Wagstaff et al. 2013, Barrón et al, 2015). Therefore, in order to better constrain the links between the early angiosperm diversification to long-term and short-term global climate, more high-resolution angiosperm pollen records are necessary from different low- and high-latitude sites.

7. Conclusions

(1) The importance of shallow-marine strata as a continental climate and ecosystem archive is demonstrated, despite the inferred limitations related to transportation, reworking and particle settling processes of clay minerals and terrestrial palynomorphs.

(2) The São Julião record shows variations in the palynological and clay mineralogy data with stratigraphic height related to changes in regional climate and moisture availability. These trends are expressed in the xerophyte ratio and WI index and show a congruent gradual aridification trend from the early Albian to early Cenomanian, punctuated by an interval of increased moisture availability during the late Albian.

(3) The palynological record is characterized by a rich and diverse palynoflora dominated by gymnosperm pollen (*Classopollis* and *Inaperturopollenites*), with lower abundances of trilete pteridophyte spores and angiosperm pollen. The assemblage is interpreted to represent a mixed-conifer forest with an understory of ferns and angiosperms, growing under dry to semi-humid conditions.

(4) The E/(M-M) ratio and range-through E/(M-M) ratio show a continuous increase of poly-aperturate pollen with eudicot affinity over monocolpate pollen with monocot or magnoliid affinity. This long-term trend coincides with the long-term aridification trend in the Lusitanian Basin during the Albian. Likewise, despite the observed offset between raw counted data and expected species richness indices, the total angiosperm pollen diversity shows a preference for relative more arid conditions during the Albian.

Acknowledgements

Financial support from DFG project HE4467/6-1 is gratefully acknowledged. We thank Peter Hochuli for his help with dinoflagellate cyst and pollen taxonomy, Christoph Hartkopf-Fröder from the Geological Survey of Nordrhein-Westfalen in Krefeld, Germany for preparing the palynological slides and Jorge Dinis for guidance and assistance during the fieldwork campaign.

8. References

- Abbink, O., 1998. Palynological Investigations in the Jurassic of the North Sea region. Ph.D. thesis, Universiteit Utrecht, The Netherlands, 192 pp. Published thesis.
- Abbink, O., Targarona, J., Brinkhuis, H., Visscher, H., 2001. Late Jurassic to earliest Cretaceous palaeoclimatic evolution of the southern North Sea. *Global and Planetary Change* 30, 231-256.
- Adatte, T., Stinnesbeck, W., Keller, G., 1996. Lithostratigraphic and mineralogic correlations of near K/T boundary sediments in northeastern Mexico: implications for origin and nature of deposition. In: Ryder, G., Fastovsky, D., Gartner, S. (Eds.), *The Cretaceous–Tertiary Event and Other Catastrophes in Earth History: Geological Society of America Special Paper 307*, 211–226.
- Adatte, T., Gerta, K., Stinnesbeck, W., 2002. Late Cretaceous to Early Palaeocene climate and sea-level fluctuations: the Tunisian record. *Palaeogeography, Palaeoclimatology, Palaeoecology* 178, 165–196.
- Batten, D.J., 1984. Palynology, climate and the development of Late Cretaceous floral provinces in the Northern Hemisphere; a review. In: Brenchley, P.J. (Ed.), *Fossils and Climate*. Wiley, Chichester, pp. 127–164.
- Barrón, E., Peyrot, D., Rodríguez-López, J.P., Meléndez, N., del Valle, R.L., Najarro, M., Rosales, I., Comas-Rengifo, M.J., 2015. Palynology of Aptian and upper Albian (Lower Cretaceous) amber-

bearing outcrops of the southern margin of the Basque-Cantabrian basin (northern Spain). *Cretaceous Research* 52, 292-312.

Berthou, P.-Y., 1984. Albian-Turonian stage boundaries and subdivisions in the western Portuguese Basin, with special emphasis on the Cenomanian–Turonian boundary in the ammonite facies and rudist fades. *Bulletin of the Geological Society of Denmark* 33, 41–45.

Bice, K.I., Bralower, T.J., Duncan, R.A., Huber, B.T., Leckie, R.M. and Sageman, B.B., 2003. http://www.whoi.edu/ccod/CCOD_report.html.

Boltovskoy, D., 1988. The range-through method and first-last appearance data in paleontological surveys. *Journal of Paleontology* 157-159.

Bonis, N.R., Kürschner, W.M., 2012. Vegetation history, diversity patterns, and climate change across the Triassic/Jurassic boundary. *Paleobiology* 38, 240-264.

Brenner, G.J., 1968. Middle Cretaceous spores and pollen from northeastern Peru. *Pollen & Spores* 10, 341-383.

Brenner, G.J., 1976. Middle Cretaceous floral provinces and early migration of angiosperms. In: Beck, C.B. (Ed.), *Origin and Early Evolution of Angiosperms*. Columbia University Press, New York, 23–44.

Brenner, G.J., 1996. Evidence for the earliest stage of angiosperm pollen evolution: a paleoequatorial section from Israel. In: Taylor, D.W., Hickey, L.J. (Eds.), *Flowering Plant Origin, Evolution and Phylogeny*. Chapman and Hall, London, 91-115.

Chaboureau, A.C., Sepulchre, P., Donnadiou, Y., Franc, A., 2014. Tectonic-driven climate change and the diversification of angiosperms. *Proceedings of the National Academy of Sciences* 111, 14066-14070.

Chamley, H., 1989. *Clay Sedimentology*. Springer-Verlag, Berlin, 623 pp.

Chapman, J.L., 1982. Morphology, classification and interpretation of Aptian and Albian angiosperm pollen from Portugal. Unpublished PhD Thesis, University of Cambridge, 355 pp.

Chumakov, N.M., Zharkov, M.A., Herman, A.B., Doludenko, M.P., Kalandadze, N.M., Lebedev, E.L., Ponomarenko, A.G., Rautian, A.S., 1995. Climatic belts of the mid-Cretaceous time. *Stratigraphy and Geological Correlation* 3, 241-260.

Clarke, L.J., Jenkyns, H.C., 1999. New oxygen isotope evidence for long-term Cretaceous climatic change in the Southern Hemisphere. *Geology* 27, 699-702.

Coiffard, C., Gómez, B., Thévenard, F., 2007. Early Cretaceous Angiosperm Invasion of Western Europe and Major Environmental Changes. *Annals of Botany* 100, 545–553.

Coiffard, C., Gómez, B., 2012. Influence of latitude and climate on spread, radiation and rise to dominance of early angiosperms during the Cretaceous in the Northern Hemisphere. *Geologica acta* 10, 181-188.

Coiffard, C., Gomez, B., Daviero-Gomez, V., Dilcher, D.L., 2012. Rise to dominance of angiosperm pioneers in European Cretaceous environments. *Proceedings of the National Academy of Sciences* 109, 20955-20959.

Crane, P.R., Lidgard, S., 1989. Angiosperm diversification and paleolatitudinal gradients in Cretaceous floristic diversity. *Science* 246, 675-678.

Crane, P.R., Friis, E.M., Pedersen, K.R., 1995. The origin and early diversification of angiosperms. *Nature* 374, 27-33.

Deconinck, J.F., 1993. Clay mineralogy of the Late Tithonian–Berriasian deep-sea carbonates of the Vocontian Trough (SE France): relationships with sequence stratigraphy. *Bulletin des Centres de Recherche Exploration-Production Elf Aquitaine* 17, 223–234.

- Dinis, J.L., Rey, J., De Graciansky, P.C., 2002. The Lusitanian Basin (Portugal) during the late Aptian-Albian: Sequential arrangement, proposal of correlations, evolution. *Comptes Rendus Geoscience* 334, 757–764.
- Dinis, J.L., Rey, J., Cunha, P.P., Callapez, P., Pena dos Reis, R., 2008. Stratigraphy and allogenic controls of the western Portugal Cretaceous: an updated synthesis. *Cretaceous Research* 29, 772–780.
- Dinis, J.L., Oliveira, F.P., Rey, J., Duarte, I.L., 2010. Finding geological heritage: legal issues on private property and fieldwork. The case of outstanding early angiosperms (Barremian to Albian, Portugal). *Geoheritage* 2, 77–90.
- Doyle, J.A., Robbins, E.I., 1977. Angiosperm pollen zonation of the continental Cretaceous of the Atlantic coastal plain and its application to deep wells in the Salisbury Embayment. *Palynology* 1, 43–78.
- Doyle, J.A., Biens, P., Doerekamp, A., Jardiné, S., 1977. Angiosperm pollen from the pre-Albian Lower Cretaceous of equatorial Africa. *Bulletin des Centres de Recherche Exploration–Production Elf Aquitaine* 1, 451–473.
- Doyle, J.A., Jardiné, S., Doerenkamp, A., 1982. *Afropollis*, a new genus of early angiosperm pollen, with notes on the Cretaceous palynostratigraphy and palaeoenvironments of northern Gondwana. *Bulletin des Centres de Recherches Exploration-Production Elf-Aquitaine* 6, 39–117.
- Duchamp-Alphonse, S., Fiet, N., Adatte, T., Pagel, M., 2011. Climate and sea-level variations along the northwestern Tethyan margin during the Valanginian C-isotope excursion: mineralogical evidence from the Vocontian basin (SE France). *Palaeogeography, Palaeoclimatology, Palaeoecology* 302, 243–254.
- Erbacher, J., Friedrich, O., Wilson, P.A., Lehmann, J., Weiss, W., 2011. Short-term warming events during the boreal Albian (mid-Cretaceous). *Geology* 39, 223–226.
- Forster, A., Schouten, S., Baas, M., Damsté, J.S.S., 2007. Mid-Cretaceous (Albian–Santonian) sea surface temperature record of the tropical Atlantic Ocean. *Geology* 35, 919–922.
- Friedrich, O., Norris, R.D., Erbacher, J., 2012. Evolution of middle to Late Cretaceous oceans -A 55 m.y. record of Earth's temperature and carbon cycle. *Geology* 40, 107–110.
- Friis, E.M., Pedersen, K.R., Crane, P.R., 1999. Early angiosperm diversification: the diversity of pollen associated with angiosperm reproductive structures in Early Cretaceous floras from Portugal. *Annals of the Missouri Botanical Garden* 86, 259–296.
- Friis, E.M., Pedersen, K.R., Crane, P.R., 2000a. Reproductive structure and organization of basal angiosperms from the Early Cretaceous (Barremian or Aptian) of Western Portugal. *International Journal of Plant Sciences* 161, S169–S182.
- Friis, E.M., Pedersen, K.R., Crane, P.R., 2000b. Fossil floral structures of a basal angiosperm with monocolpate, reticulate-acolumellate pollen from the Early Cretaceous of Portugal. *Grana* 39, 226–245.
- Friis, E.M., Pedersen, K.R., Crane, P.R., 2001. Fossil evidence of water lilies (Nymphaeales) in the Early Cretaceous. *Nature* 410, 357–360.
- Friis, E.M., Pedersen, K.R., Crane, P.R., 2004. Araceae from the Early Cretaceous of Portugal: evidence on the emergence of monocotyledons. *Proceedings of the National Academy of Sciences of the United States of America* 101, 16565–16570.
- Friis, E.M., Pedersen, K.R., Von Balthazar, M., Grimm, G.W., Crane, P.R., 2009. *Monetianthus mirus* gen. et sp. nov., a nymphaealean flowers from the Early Cretaceous of Portugal. *International Journal of Plant Science* 170, 1086–1101.

Friis, E.M., Pedersen, K.R., Crane, P.R., 2010a. Cretaceous diversification of angiosperms in the western part of the Iberian Peninsula. *Review of Palaeobotany and Palynology* 162, 341-361.

Friis, E.M., Pedersen, K.R., Crane, P.R., 2010b. Diversity in obscurity: fossil flowers and the early history of angiosperms. *Philosophical Transactions of the Royal Society B: Biological Sciences* 365, 369-382.

Friis, E.M., Pedersen, K.R., 2011. *Canrightia resinifera* gen. et sp. nov., a new extinct angiosperm with *Retimonocolpites*-type pollen from the Early Cretaceous of Portugal: missing link in the eumagnoliid tree? *Grana* 50, 3-29.

Galloway, J. M., Sweet, A. R., Pugh, A., Schröder-Adams, C. J., Swindles, G. T., Haggart, J. W., Embry, A. F., 2012. Correlating middle Cretaceous palynological records from the Canadian High Arctic based on a section from the Sverdrup Basin and samples from the Eclipse Trough. *Palynology* 36, 277-302.

Godet, A., Bodin, S., Adatte, T., Föllmi, K.B., 2008. Platform-induced clay-mineral fractionation along a northern Tethyan basin-platform transect: implications for the interpretation of Early Cretaceous climate change (Late Hauterivian–Early Aptian). *Cretaceous Research* 29, 830–847.

Gradstein, F.M., Ogg, J., Schmitz, M.A., Ogg, G., 2012. *A Geologic Time Scale 2012*. Elsevier Publishing Company.

Grimm, E.C., 1987. CONISS: a FORTRAN 77 program for stratigraphically constrained cluster analysis by the method of incremental sum of squares. *Computers & Geosciences* 13, 13-35.

Grimm, E.C., 1991. *Tilia, Tiliagraph and TGView Software*, Illinois State Museum, Springfield, Illinois, USA.

Hallam, A., 1985. A review of Mesozoic climates. *Journal of the Geological Society of London* 142, 433–445.

Hammer, Ø., Harper, D.A.T., P.D. Ryan, 2001. PAST: Paleontological Statistics Software Package for Education and Data Analysis. *Palaeontologia Electronica* 4, 9pp.

Hasenboehler, B., 1981. Étude paleobotanique et palynologie de l'Albien et du Cénomaniens du "Bassin Occidental Portugais" au sud de l'accident de Nazaré (Portugal). Unpublished PhD thesis, Université Pierre et Marie Curie, Paris, Thèse 3ème Cycle, 348pp.

Hay, W.W., Floegel, S., 2012. New thoughts about the Cretaceous climate and oceans. *Earth-Science Reviews*, 115, 262-272.

Heimhofer, U., Hochuli, P.A., Burla, S., Dinis, J.M.L., Weissert, H., 2005. Timing of Early Cretaceous angiosperm diversification and possible links to major paleoenvironmental change. *Geology* 33, 141–4.

Heimhofer, U., Hochuli, P.A., Burla, S., Weissert, H., 2007. New records of Early Cretaceous angiosperm pollen from Portuguese coastal deposits: Implications for the timing of the early angiosperm radiation. *Review of Palaeobotany and Palynology* 144, 39–76.

Heimhofer, U., Adatte, T., Hochuli, P.A., Burla, S., Weissert, H., 2008. Coastal sediments from the Algarve: low-latitude climate archive for the Aptian-Albian. *International Journal of Earth Sciences* 97, 785–797.

Heimhofer, U., Hochuli, P.A., Burla, S., Oberli, F., Adatte, T., Dinis, J.M.L., Weissert, H., 2012. Climate and vegetation history of western Portugal inferred from Albian near-shore deposits (Gale Formation, Lusitanian Basin). *Geological Magazine* 149, 1046–1064.

Horikx, M., Heimhofer, U., Dinis, J., Huck, S., 2014. Integrated stratigraphy of shallow marine Albian strata from the southern Lusitanian Basin of Portugal. *Newsletters on Stratigraphy* 47, 85-106.

- Horikx, M., Hochuli, P.A., Feist-Burkhardt, S., Heimhofer, U., 2015, Albian angiosperm pollen from shallow marine strata in the Lusitanian Basin, Portugal. Review of paleobotany and palynology (in review).
- Kürschner, W.M., Mander, L., McElwain, J.C., 2014. A gymnosperm affinity for *Ricciisporites tuberculatus* Lundblad: implications for vegetation and environmental reconstructions in the Late Triassic. *Palaeobiodiversity and Palaeoenvironments* 94, 295-305.
- Lidgard, S., Crane, P.R., 1988. Quantitative analyses of the early angiosperm radiation. *Nature* 331, 344-346.
- Lindström, S., Erlström, M., 2011. The Jurassic–Cretaceous transition of the Fårarp-1 core, southern Sweden: sedimentological and phytological indications of climate change. *Palaeogeography, Palaeoclimatology, Palaeoecology* 308, 445-475.
- Longino J.T., Coddington J., Colwell R.K., 2002. The ant fauna of a tropical rain forest: Estimating species richness three different ways. *Ecology* 83, 689–702.
- Mander, L., Kürschner, W.M., McElwain, J.C., 2010. An explanation for conflicting records of Triassic–Jurassic plant diversity. *Proceedings of the National Academy of Sciences* 107, 15351-15356.
- McAnena, A., Flögel, S., Hofmann, P., Herrle, J.O., Griesand, A., Pross, J., Talbot, H.M., Rethemeyer, J., Wallmann, K., Wagner, T., 2013. Atlantic cooling associated with a marine biotic crisis during the mid-Cretaceous period. *Nature Geoscience* 6, 558-561.
- McElwain, J.C., Willis, K.J., Lupia, R., 2005. Cretaceous CO₂ decline and the radiation and diversification of angiosperms. In: *A History of Atmospheric CO₂ and Its Effect on Plants, Animals, and Ecosystems* (eds Ehleringer, J.R., Cerling, T.E. & Dearing, M.D.). Springer, N.Y, USA, 133–165.
- Mendes, M.M., Dinis, J., Pais, J., Friis, E.M., 2011. Early Cretaceous flora from Vale Painho (Lusitanian Basin, western Portugal): an integrated palynological and mesofossil study. *Review of Palaeobotany and Palynology* 166, 152-162
- Mendes, M.M., Dinis, J., Pais, J., Friis, E.M., 2014a. Vegetational composition of the Early Cretaceous Chicalhão flora (Lusitanian Basin, western Portugal) based on palynological and mesofossil assemblages. *Review of Palaeobotany and Palynology* 200, 65-81.
- Mendes, M.M., Grimm, G.W., Pais, J., Friis, E.M., 2014b. Fossil *Kajanthus lusitanicus* gen. et sp. nov. from Portugal: floral evidence for Early Cretaceous Lardizabalaceae (Ranunculales, basal eudicot). *Grana*, 1-19.
- Mendes, M.M., Dinis, J., Esteban, L.G., de Palacios, P., Fernández, F.G., Pais, J., 2014c. Early Cretaceous woods of Figueira da Foz Formation in western Portugal: Palaeoenvironmental, palaeoclimatic and palaeobiogeographic insights. *Cretaceous Research* 51, 112-120.
- Moore, D., Reynolds, R., 1997. *X-Ray-Diffraction and the Identification and Analysis of Clay-Minerals*. New York: Oxford University Press, 378pp.
- Mutterlose, J., Bornemann, A., Herrle, J., 2009. The Aptian–Albian cold snap: Evidence for Evidence for “mid” Cretaceous icehouse interludes. *Neues Jahrbuch für Geologie und Paläontologie-Abhandlungen* 252, 217-225.
- Norris, R.D., Bice, K.L., Magno, E.A., Wilson, P. A., 2002. Jiggling the tropical thermostat in the Cretaceous hothouse. *Geology* 30, 299-302.
- Parrish, J.T., Ziegler, A.M., Scotese, C.R., 1982. Rainfall patterns and the distribution of coals and evaporites in the Mesozoic and Cenozoic. *Palaeogeography, Palaeoclimatology, Palaeoecology* 40, 67–101.
- Pedersen, K.R., Von Balthazar, M., Crane, P.R., Friis, E.M., 2007. Early Cretaceous floral structures and in situ tricolpate-striate pollen: New early eudicots from Portugal. *Grana* 46, 176-196.

Pucéat, E., Lécuyer, C., Sheppard, S.M., Dromart, G., Reboulet, S., Grandjean, P., 2003. Thermal evolution of Cretaceous Tethyan marine waters inferred from oxygen isotope composition of fish tooth enamels. *Paleoceanography* 18.

Rey, J., 1992. Les unités lithostratigraphiques du Crétacé inférieur de la région de Lisbonne. *Comunicações dos Serviços Geológicos de Portugal* 78, 103–124.

Rey, J., de Graciansky, P.C., Jacquin, T., 2003. Les séquences de dépôt dans le Crétacé inférieur du Bassin Lusitanien. *Comun. Inst. Geol. Min.* 90, 15–42.

Rodríguez-López, J.P., De Boer, P.L., Meléndez, N., Soria, A.R., Pardo, G., 2006. Windblown desert sands in coeval shallow marine deposits: a key for the recognition of coastal ergs in the mid-Cretaceous Iberian Basin, Spain. *Terra Nova* 18, 314–320.

Rodríguez-López, J.P., Meléndez, N., De Boer, P.L., Soria, A.R., 2008. Aeolian sand sea development along the Mid-Cretaceous Western Tethyan Margin (Spain): erg sedimentology and palaeoclimate implications. *Sedimentology* 55, 1253–1292.

Rodríguez-López, J.P., Meléndez, N., De Boer, P.L., Soria, A.R., 2010. The action of wind and water in a mid-Cretaceous subtropical erg-margin system close to the Variscan Iberian Massif, Spain. *Sedimentology* 57, 1315–1356.

Saporta, G.D., 1894. Flore fossile du Portugal. Nouvelles contributions à la flore Mésozoïque. Accompagnées d'une notice stratigraphique par Paul Choffat. Imprimerie de l'Académie Royale des Sciences, Lisbon.

Sender, L.M., Villanueva-Amadoz, U., Pons, D., Diez, J.B., Ferrer, J., 2014. Singular taphonomic record of a wildfire event from middle Albian deposits of Escucha Formation in northeastern of Spain. *Historical Biology* 27, 1–11.

Singer, A. 1984. The paleoclimatic interpretation of clay minerals in sediments — A review. *Earth-Science Reviews* 21, 251–293.

Stampfli, G.M., Borel, G.D., 2002. A plate tectonic model for the Paleozoic and Mesozoic constrained by dynamic plate boundaries and restored synthetic oceanic isochrons. *Earth and Planetary Science Letters* 196, 17–33.

Staplin, F.L. 1982. Determination of thermal alteration index from color of exinite (pollen, spores). In *How to Assess Maturation and Palaeotemperatures* (ed. F. L. Staplin), pp. 7–11. Society of Economic Paleontologists and Mineralogists.

Stebbins G.L., 1974 *Flowering plants: evolution above the species level*. Cambridge, MA: Harvard University Press.

Steuber, T., Rauch, M., Masse, J.P., Graaf, J., Malkoč, M., 2005. Low-latitude seasonality of Cretaceous temperatures in warm and cold episodes. *Nature* 437, 1341–1344.

Taugourdeau-Lantz, J., Azéma, C., Hasenboehler, B., Masure, E., Moron, J.M., 1982. Evolution des domaines continentaux et marins de la marge portugaise (Leg 47B, site 398D) au cours du Crétacé; Essai d'interprétation par l'analyse palynologique comparée. *Bulletin de la Société Géologique de France* 3, 447–459.

Teixeira, C., 1948. Flora mesozóica portuguesa Part I. *Serviços Geológicos de Portugal*, Lisbon.

Tiraboschi, D., Erba, E., Jenkyns, H.C., 2009. Origin of rhythmic Albian black shales (Piobbico core, central Italy): Calcareous nannofossil quantitative and statistical analyses and paleoceanographic reconstructions. *Paleoceanography* 24.

Traverse, A., 2007. *Paleopalynology* Dordrecht: Springer, 813pp.

Tyson, R.V. 1995. *Sedimentary Organic Matter*. London: Chapman & Hall, 615pp.

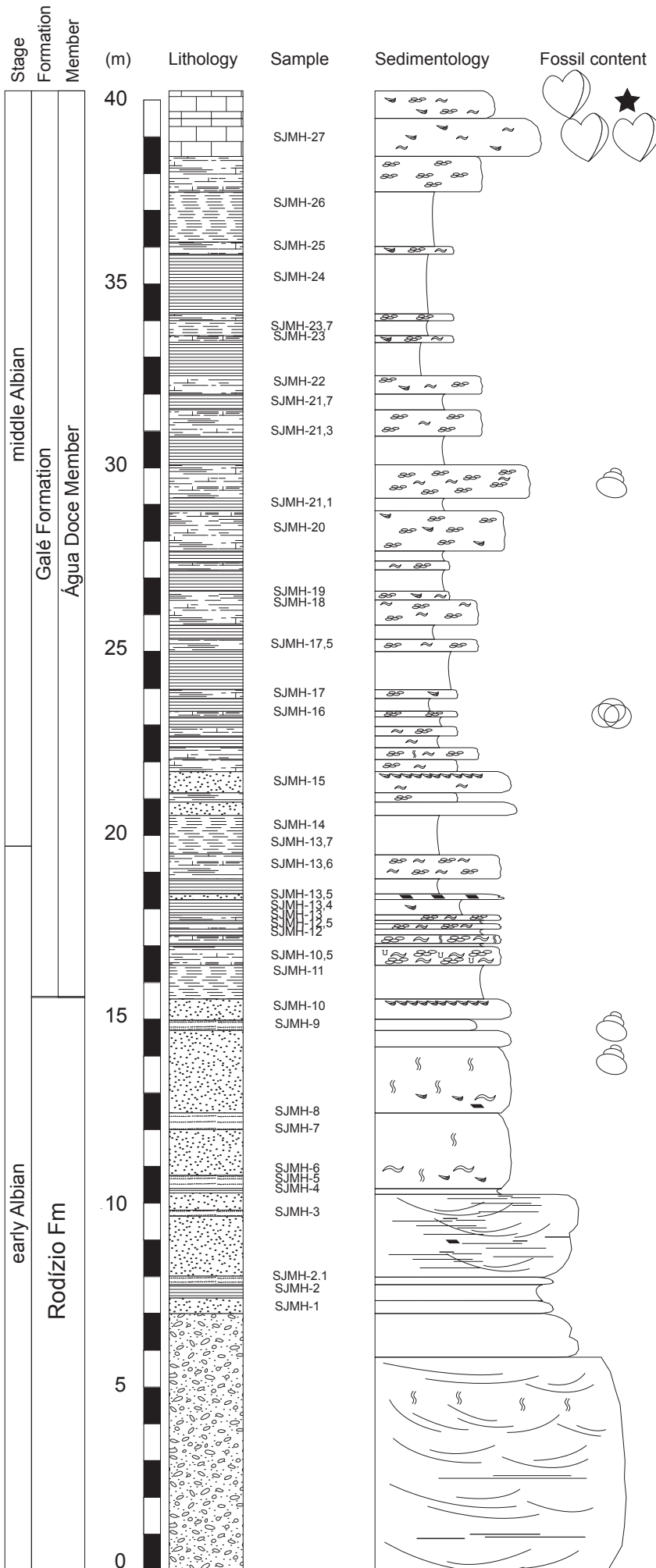
-
- Vakhrameev, V.A., 1981. Pollen Classopollis: indicator of Jurassic and Cretaceous climates. *Palaeobotanist* 28–29, 301–307.
- van Helmond, N.A.G.M, Sluijs, A., Reichart, G.J., Damsté, J.S.S., Slomp, C.P., Brinkhuis, H., 2014. A perturbed hydrological cycle during Oceanic Anoxic Event 2. *Geology* 42, 123-126.
- Van Konijnenburg-Van Cittert, J.H.A., 1971. In situ gymnosperm pollen from the Middle Jurassic of Yorkshire. *Acta Botanica Neerlandica* 20, 1–97.
- Versteegh, G.J.M., 1994. Recognition of cyclic and non-cyclic environmental changes in the Mediterranean Pliocene: a palynological approach. *Marine Micropaleontology* 23, 147-183.
- Villanueva-Amadoz, U., Pons, D., Diez, J.B., Ferrer, J., Sender, L.M., 2010. Angiosperm pollen grains of San Just site (Escucha Formation) from the Albian of the Iberian Range (north-eastern Spain). *Review of Palaeobotany and Palynology*, 162, 362-381.
- Villanueva-Amadoz, U., Sender, L.M., Alcalá, L., Pons, D., Royo-Torres, R., Diez, J.B., 2014. Paleoenvironmental reconstruction of an Albian plant community from the Ariño bonebed layer (Iberian Chain, NE Spain). *Historical Biology* 27, 1-12.
- Wagstaff, B.E., Gallagher, S.J., Norvick, M.S., Cantrill, D.J., Wallace, M.W., 2013. High latitude Albian climate variability: Palynological evidence for long-term drying in a greenhouse world. *Palaeogeography, Palaeoclimatology, Palaeoecology* 386, 501-511.
- Ward Jr., J.H., 1983. Hierarchical grouping to optimize an objective function. *J. Am. Stat. Assoc.* 58, 236-244
- Watson, J., Sincock, C.A., 1992. *Bennettitales of the English Wealden*. London: The Palaeontographical Society, 228 pp.
- Weaver, C.E., 1989. Clays, muds, and shales. *Developments in sedimentology*, vol 44. Elsevier, New York, pp 819.
- Westermann, S., Duchamp-Alphonse, S., Fiet, N., Fleitmann, D., Matera, V., Adatte, T., Föllmi, K.B., 2013. Paleoenvironmental changes during the Valanginian: New insights from variations in phosphorus contents and bulk-and clay mineralogies in the western Tethys. *Palaeogeography, Palaeoclimatology, Palaeoecology* 392, 196-208.
- Wilson, P.A., Norris, R.D., 2001. Warm tropical ocean surface and global anoxia during the mid-Cretaceous period. *Nature* 412, 425-429.

Conclusions

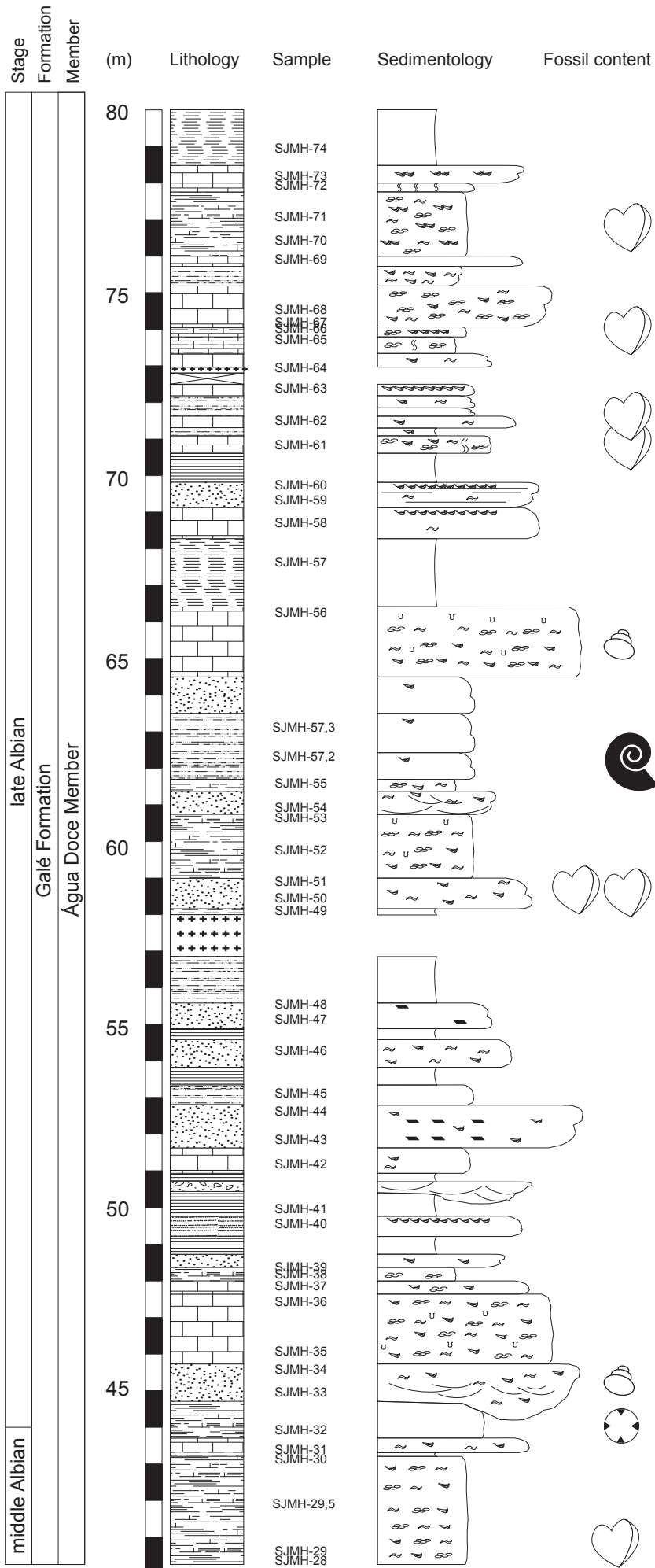
The main aim of this thesis was to document and describe the early angiosperm radiation in detail and in high stratigraphic and temporal resolution from shallow marine deposits in the Lusitanian Basin, Portugal during the Albian-Cenomanian interval. In order to provide such a high-resolution record, major emphasis was placed on the dating of the sedimentary deposits. Using a combined chemostratigraphic and palynological approach, the results of this thesis provide new insights into terrestrial ecosystem dynamics during a critical phase in the early angiosperm pollen diversification. Furthermore, this thesis investigates the external role of climate and its impact on the early angiosperm diversification, as well as on the accompanying terrestrial vegetation. The most important answers to the initial aims and objectives (p. 15) as well as the main results are presented here:

1. Well-constrained stratigraphic age-assignments for several shallow marine sections (Magoito, Praia das Maças, São Julião) in the southern Lusitanian Basin are provided using carbon-isotopes, dinoflagellate biostratigraphy and strontium-isotope stratigraphy from pristine low-Mg calcite shell material. The São Julião section serves as reference record and covers the early Albian to early Cenomanian with an expanded late Albian succession. The new stratigraphic age-assignment significantly improves the temporal framework of the different sections compared to previously published records.
2. The angiosperm pollen record from the São Julião section is characterized by a distinct pattern in the first appearance of important angiosperm pollen morphologies: monocolpates, polyporates and tricolpates are recorded from the early Albian onwards, followed by tricolporates in the late Albian. The pollen record shows a highly diverse assemblage of both monocolpate and poly-aperturate pollen on a so far unmatched temporal resolution and is marked by a significant diversification phase among poly-aperturates during the middle to late Albian. In terms of relative abundance, angiosperm pollen only constitute a minor component of the total palynological record with relative abundances <10%. A detailed analysis of the angiosperm association at São Julião allows a direct comparison with the classical Potomac Group succession (USA). Based on the independently dated age-ranges of several angiosperm pollen, the Portuguese record provides new information in order to recalibrate the age of angiosperm pollen Subzones II-B (middle to late Albian) and II-C (early Cenomanian) in the Potomac Group succession.
3. Clay mineral and palynological analyses from the São Julião section show distinct changes in moisture availability and vegetation composition during the Albian in the Lusitanian Basin. The reconstructed terrestrial vegetation was composed of a mixed conifer forest with an understory of spores and angiosperms, whereas the continental climate record shows an aridification trend from the early Albian to early Cenomanian, punctuated by an interval of increased humidity in the late Albian. In terms of angiosperm pollen composition, the highest pollen diversities are recorded during relative arid conditions. The long-term aridification trend coincides with a dominance of poly-aperturate pollen of eudicot affinity over monocolpate pollen of magnoliid-monocot affinity and is linked to the northward migration of mostly eudicots from the lower latitudes towards the Lusitanian Basin during an interval of rising temperatures.

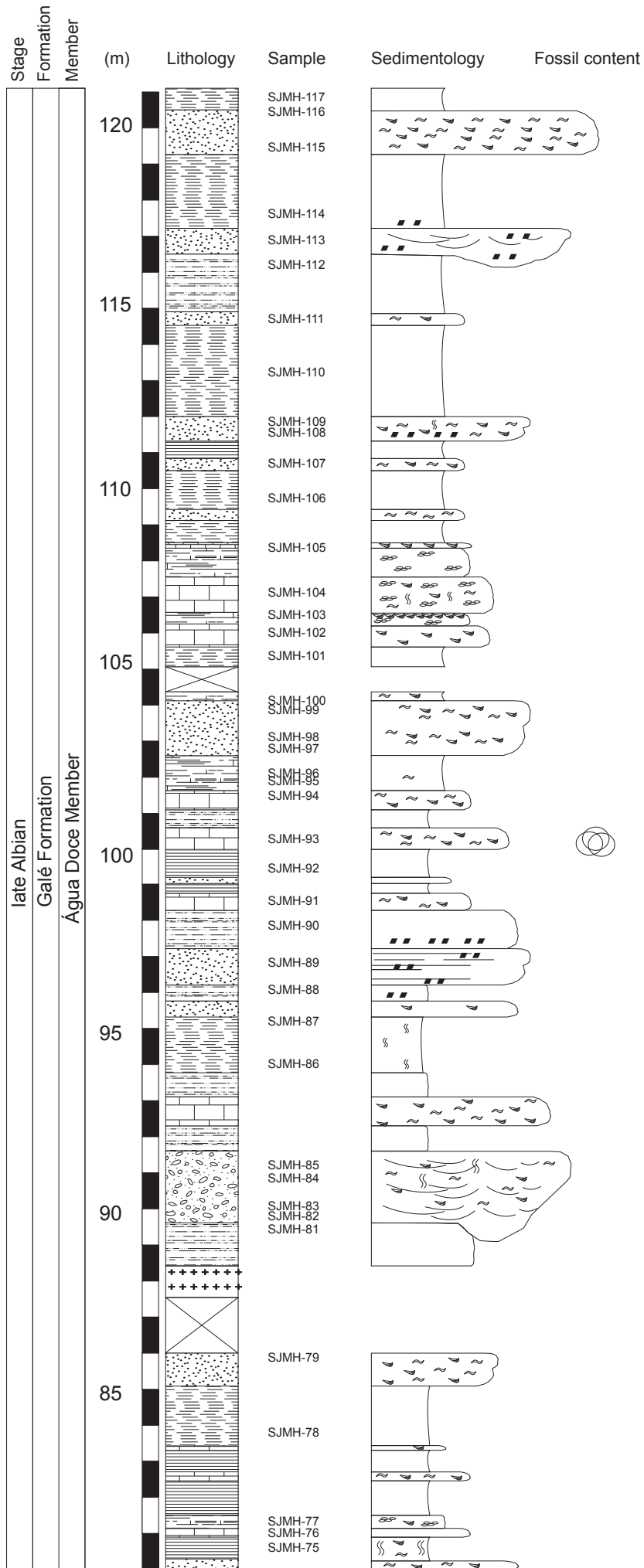
São Julião section (0-40 m)



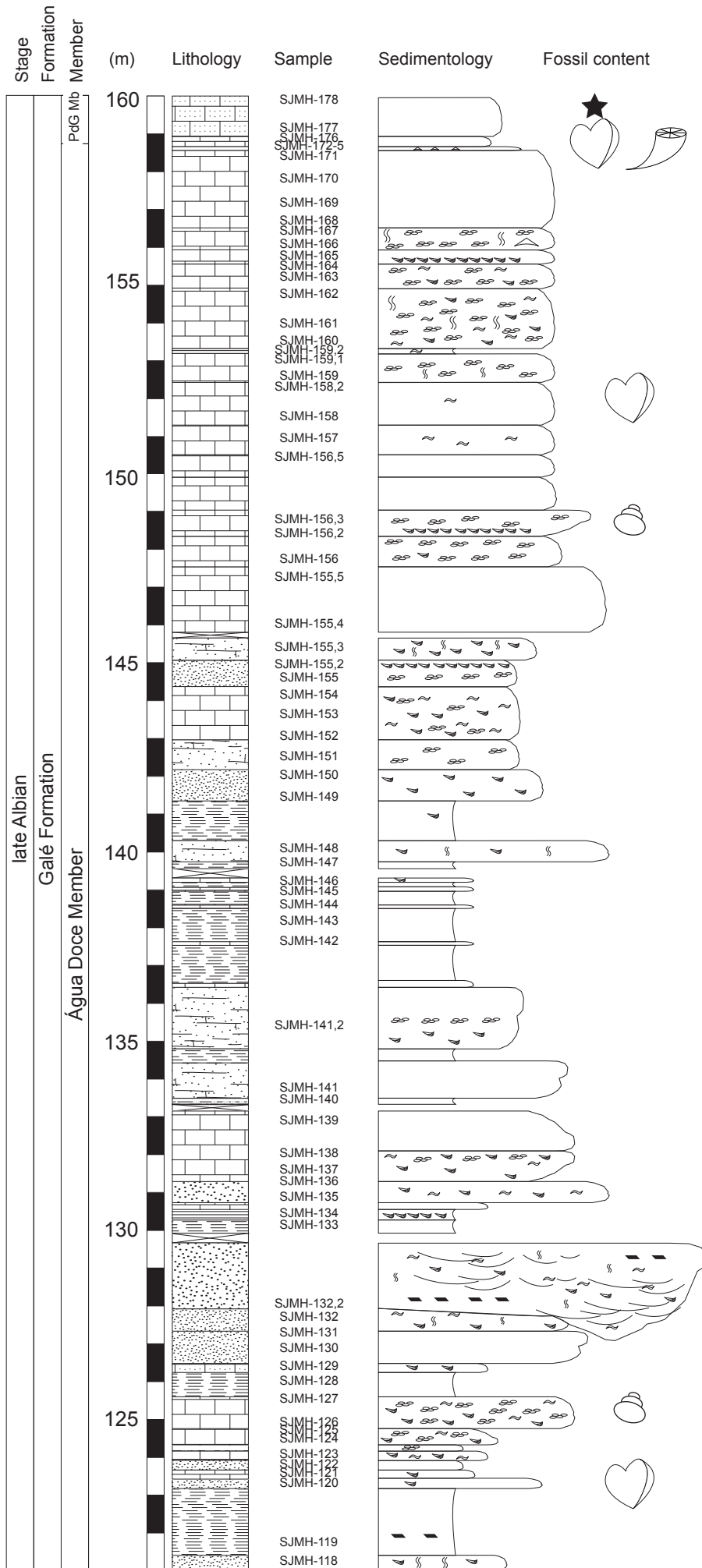
APPENDIX 2
São Julião section (40-80 m)



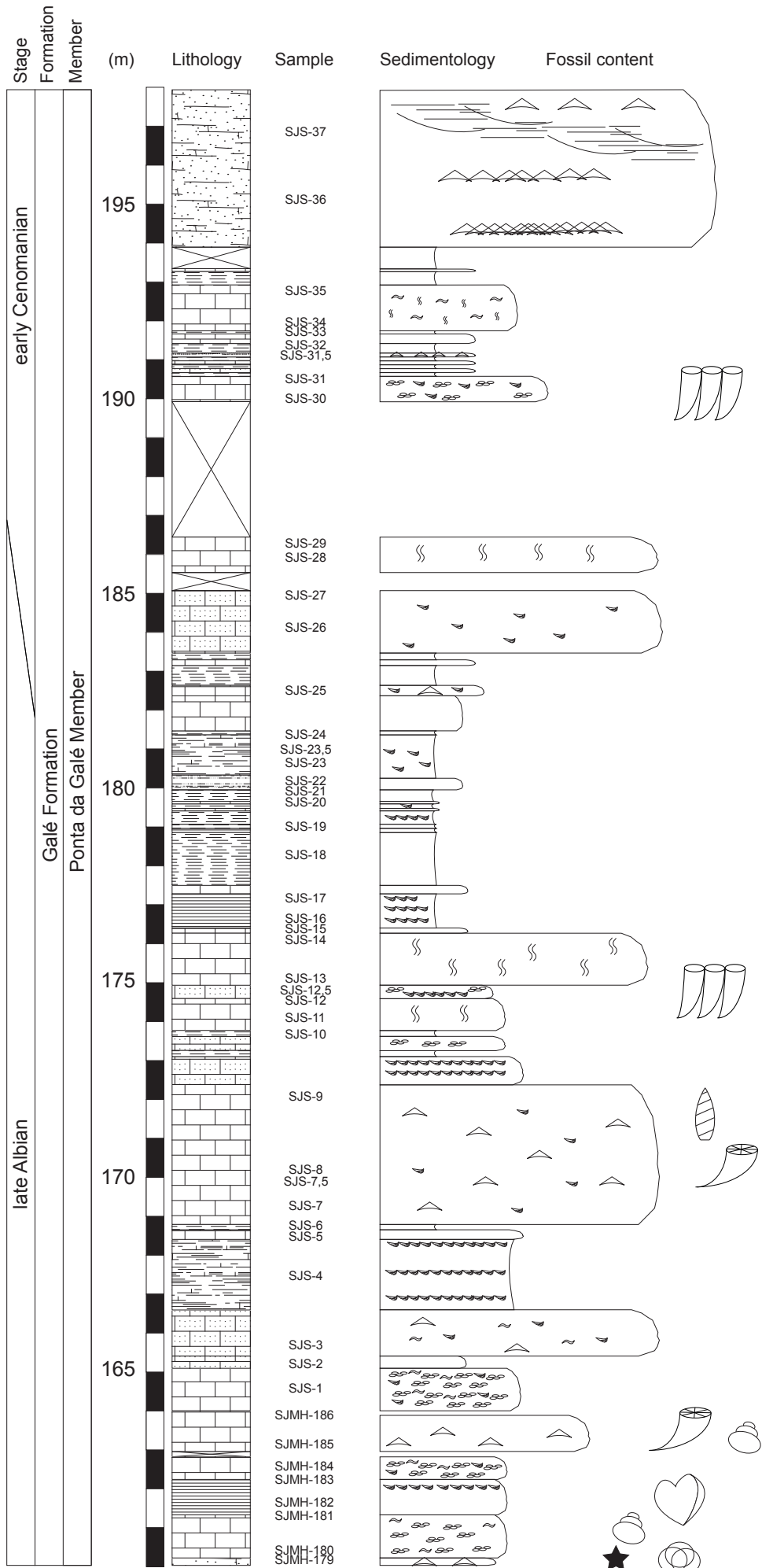
São Julião section (80-120 m)



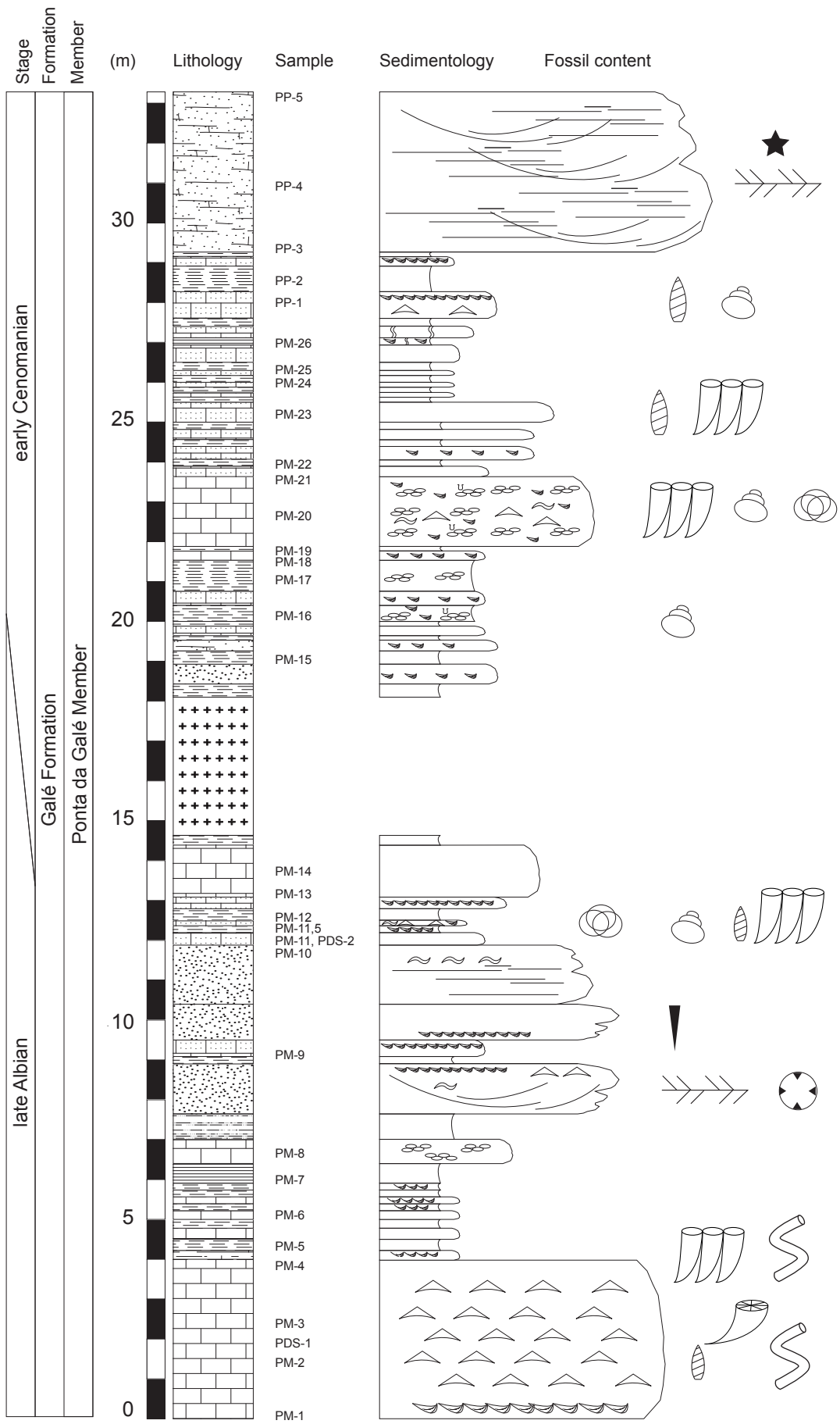
APPENDIX 4
São Julião section (120-160 m)



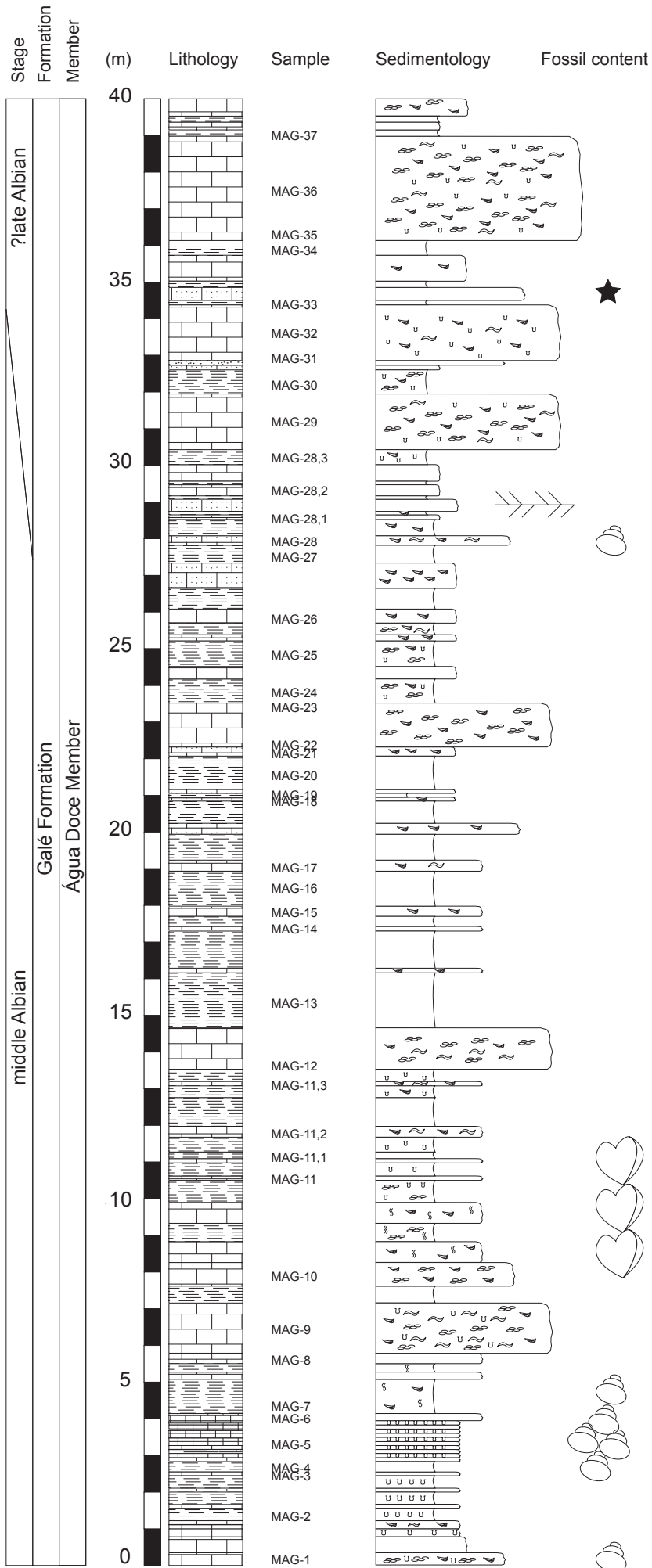
São Julião section (160 m to top)

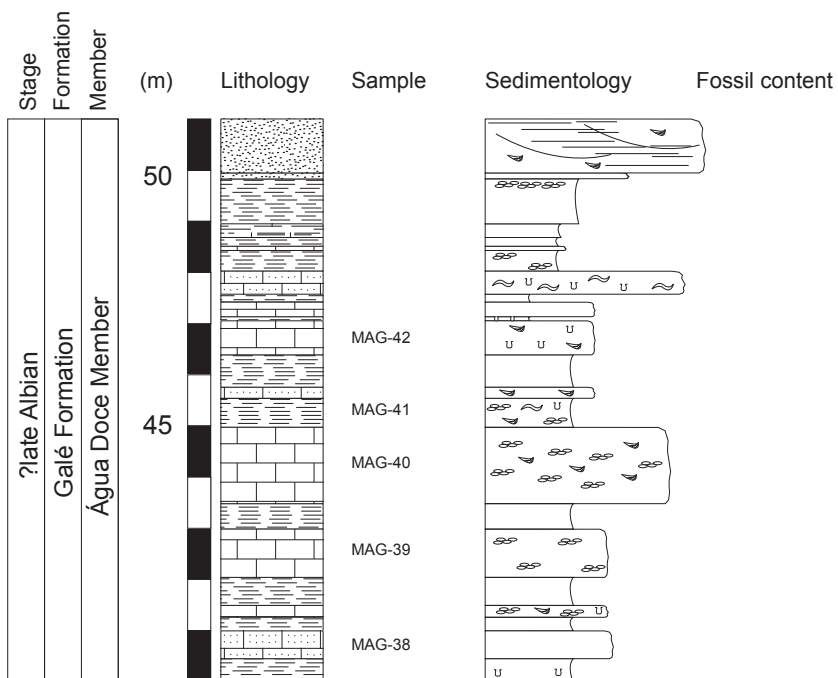
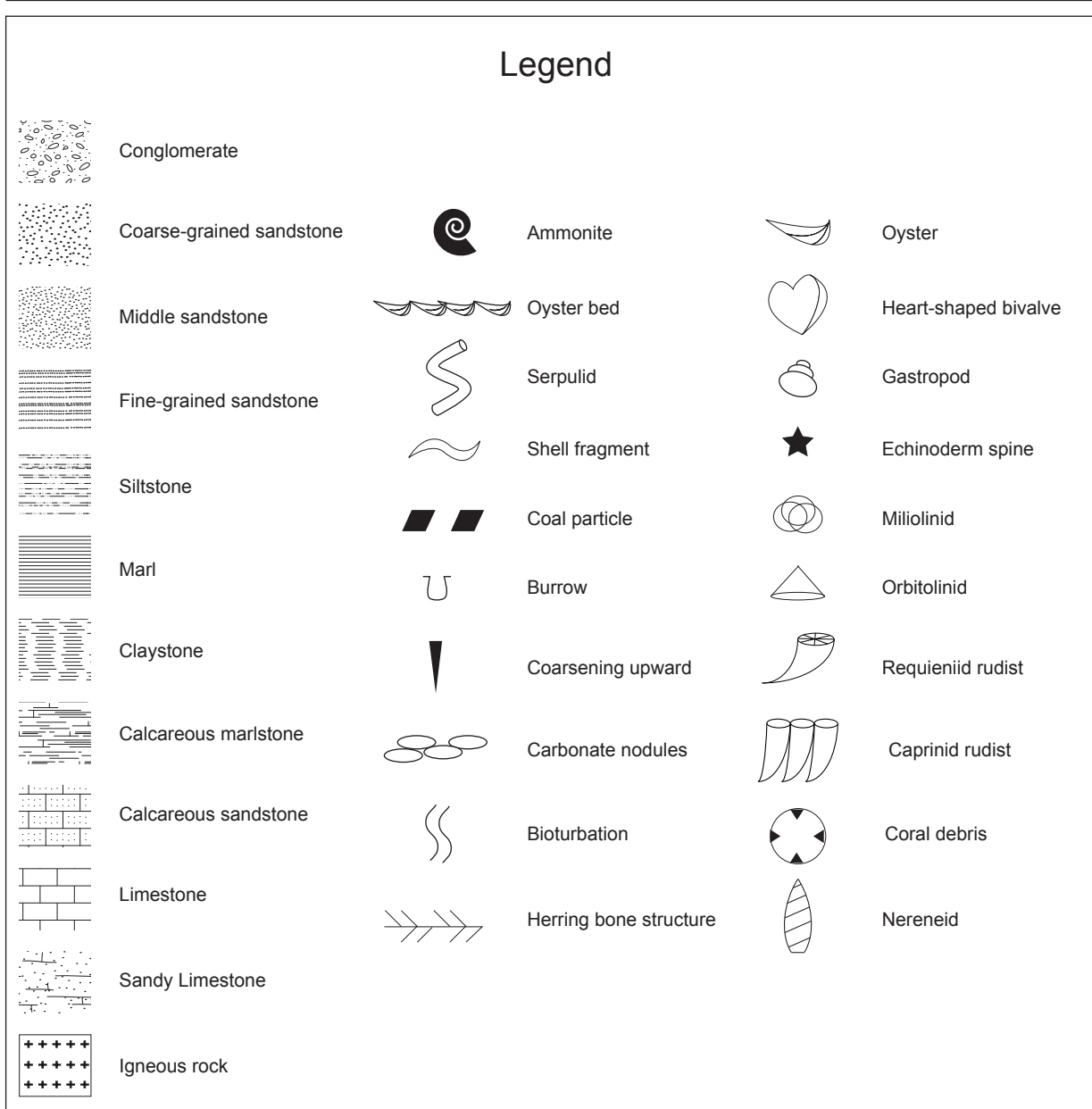


APPENDIX 6
Praia das Maças section



APPENDIX 7
Magoito section (0-40 m)





carbonate content, São Julião section

Sample (SJMh)	Height (m)	CaCO ₃ content (%)	Sample (SJMh)	Height (m)	CaCO ₃ content (%)	Sample (SJMh)	Height (m)	CaCO ₃ content (%)
2	7.5	0.0	71	76.9	71.6	145	138.5	71.5
2,1	7.9	0.0	72	77.8	70.1	146	139.0	79.8
3	9.8	0.0	73	78.0	70.4	147	139.3	4.5
4	10.2	0.0	74	79.0	0.0	148	139.8	41.5
5	10.5	0.0	75	80.6	?	151	142.2	46.6
6	10.9	0.0	76	80.9	72.3	152	142.5	72.4
7	12.1	0.0	77	81.2	63.0	153	142.9	83.2
10,5	16.6	75.7	78	83.6	0.0	154	143.8	80.3
11	17.0	0.0	79	85.7	73.6	155	144.1	7.5
12,5	17.3	64.3	81	89.4	0.0	155,2	144.5	47.5
13,5	18.2	35.1	82	89.7	34.8	155,4	145.1	67.8
13,7	19.7	1.0	83	89.9	0.0	155,5	145.8	90.5
14	20.1	0.0	85	92.6	33.7	156	147.6	44.9
15	21.4	70.5	86	93.7	0.0	156,2	148.0	59.4
16	23.2	51.8	87	95.2	0.0	156,4	148.8	86.5
17	23.8	61.8	91	98.4	54.3	156,5	150.1	88.5
17,5	25.1	80.9	92	99.3	12.5	157	150.5	88.8
18	26.2	70.5	93	100.2	73.6	158	150.9	82.5
20	28.2	74.9	94	101.4	66.1	158,2	152.6	72.2
21,1	29.0	38.7	95	101.7	62.2	159	152.5	73.1
21,3	30.9	70.3	96	102.0	60.2	159,1	152.5	76.9
22	32.2	73.7	97	102.9	74.2	159,2	153.5	60.8
23	33.4	73.5	98	103.2	57.3	160	153.2	80.1
23,7	33.7	0.0	99	103.9	48.5	161	153.3	83.4
24	35.0	48.1	101	105.3	0.0	162	154.9	84.9
25	35.9	75.5	102	106.0	71.5	163	155.2	74.1
26	37.3	1.3	103	106.3	81.8	164	155.5	72.2
27	38.9	70.6	104	107.0	66.0	165	155.7	82.0
28	40.2	49.4	105	108.1	59.8	166	155.8	80.9
29	40.4	78.2	106	109.5	2.8	167	156.6	85.7
29,5	41.8	80.4	108	111.4	52.8	168	156.6	90.6
30	43.1	79.1	110	113.2	0.0	169	157.0	78.8
31	43.2	4.0	112	116.0	0.0	170	157.8	91.3
34	45.6	43.7	114	117.4	0.0	171	158.6	83.7
35	46.0	76.9	115	117.4	57.9	172	158.6	84.8
36	47.3	79.5	117	120.4	0.0	175	158.6	87.5
37	47.7	70.0	118	120.7	7.1	176	158.9	79.1
39	48.3	69.8	119	121.3	0.0	177	158.9	85.3
42	51.0	70.0	121	123.3	60.0	178	160.0	82.9
43	51.7	0.0	122	123.6	18.8	180	160.1	78.4
45	53.2	0.0	123	123.8	49.6	181	161.1	79.0
48	55.4	0.0	124	124.0	83.8	183	162.2	79.4
48,5	57.4	0.0	125	124.3	74.8	185	163.4	91.3
49	58.0	0.0	126	124.5	83.1	186	166.4	88.9
52	59.7	71.2	127	124.6	83.7			
53	60.5	79.3	128	125.7	1.1			
55	61.4	76.1	129	126.0	61.6			
56	62.2	80.6	132	127.2	32.5			
57	66.0	0.0	133	127.9	0.0			
57,2	67.3	0.0	134	129.9	57.3			
58	69.1	73.8	135	130.1	56.9			
61	70.8	67.4	136	130.6	56.7			
62	71.3	75.3	138	131.5	79.4			
65	73.7	81.0	140	132.9	33.2			
66	73.9	70.0	141	133.3	56.1			
68	74.4	80.7	141,2	133.9	47.3			
69	75.8	79.5	142	135.4	77.6			
70	76.3	82.2	144	138.1	71.7			

carbonate content, São Julião, Nazare and Magoito sections

Sample	Height (m)	CaCO ₃ content (%)	Sample	Height (m)	CaCO ₃ content (%)	Sample	Height (m)	CaCO ₃ content (%)
SJS-7	163.4	96.0	NAZ-1	0.7	40.0	MAG-1	0.3	86.4
SJS-7,5	165.5	96.0	NAZ-2	2.5	80.7	MAG-2	1.6	41.4
SJS-8	165.6	96.5	NAZ-3	2.9	55.0	MAG-3	2.6	79.4
SJS-9	166.4	93.1	NAZ-4	3.0	86.7	MAG-4	2.9	47.8
SJS-10	167.1	54.5	NAZ-5	4.3	92.1	MAG-5	3.4	75.4
SJS-11	167.5	95.0	NAZ-6	5.7	86.1	MAG-6	4.1	77.8
SJS-12	168.0	94.0	NAZ-7	5.7	84.5	MAG-7	5.1	44.2
SJS-12,5	168.3	91.1	NAZ-8	6.9	85.6	MAG-8	5.8	88.7
SJS-13	168.3	97.5	NAZ-9	8.7	83.3	MAG-9	7.1	81.4
SJS-14	169.6	97.5	NAZ-10	8.7	80.2	MAG-10	8.2	69.9
SJS-15	169.7	73.5	NAZ-11	9.0	91.2	MAG-11	10.7	72.4
SJS-16	170.1	71.8	NAZ-12	9.7	93.1	MAG-11,1	11.3	59.6
SJS-17	170.6	48.5	NAZ-13	10.3	95.5	MAG-11,2	12.0	68.4
SJS-18	171.8	54.5	NAZ-14	10.7	70.3	MAG-11,3	13.2	90.6
SJS-19	172.4	-	NAZ-15	11.9	98.5	MAG-12	14.7	86.4
SJS-20	173.0	76.2	NAZ-16	12.5	85.1	MAG-13	16.2	28.9
SJS-21	173.2	-	NAZ-17	13.3	38.0	MAG-14	17.4	92.4
SJS-22	173.5	43.6	NAZ-18	14.1	94.1	MAG-15	18.0	86.6
SJS-23	174.2	-	NAZ-19	15.4	95.0	MAG-16	18.9	12.1
SJS-23,5	174.2	59.7	NAZ-20	25.5	93.7	MAG-17	19.3	72.1
SJS-24	174.7	42.0	NAZ-21	25.9	93.0	MAG-18	20.9	68.2
SJS-25	175.9	76.1	NAZ-22	26.4	57.0	MAG-19	21.0	10.5
SJS-26	177.7	89.0	NAZ-23	26.7	92.5	MAG-20	22.1	11.6
SJS-27	178.4	88.6	NAZ-24	27.4	88.8	MAG-21	22.3	64.7
SJS-28	179.4	95.0	NAZ-25	28.9	19.0	MAG-22	23.6	80.8
SJS-29	179.8	94.5	NAZ-26	30.0	88.8	MAG-23	23.6	87.6
SJS-30	183.3	91.5	NAZ-27	30.5	97.0	MAG-24	24.3	16.2
SJS-31	183.9	91.5	NAZ-28	30.9	95.0	MAG-25	25.3	17.9
SJS-31,5	184.5	74.5	NAZ-29	31.9	99.0	MAG-26	25.8	82.8
SJS-32	184.6	-	NAZ-30	32.0	88.7	MAG-27	27.7	29.9
SJS-33	185.1	-	NAZ-31	32.3	19.6	MAG-28	28.1	42.9
SJS-34	185.1	79.6	NAZ-32	32.9	92.5	MAG-28,3	30.4	15.9
SJS-35	186.3	94.0	NAZ-33	33.6	88.2	MAG-29	31.9	79.3
SJS-36	189.3	88.6	NAZ-34	34.5	95.0	MAG-30	32.6	15.4
SJS-37	191.3	86.5	NAZ-35	35.1	93.6	MAG-31	34.4	83.4
			NAZ-36	36.2	94.0	MAG-32	34.4	86.6
			NAZ-37	36.8	71.4	MAG-33	34.5	57.0
			NAZ-38	37.5	89.0	MAG-34	36.2	8.9
			NAZ-39	38.4	91.1	MAG-35	39.0	86.0
			NAZ-40	39.6	99.5	MAG-36	39.0	90.6
			NAZ-41	40.1	52.0	MAG-37	39.2	14.0
			NAZ-42	40.7	96.5	MAG-38	41.0	84.2
			NAZ-43	41.3	73.9	MAG-39	43.0	85.0
			NAZ-44	41.8	93.0	MAG-40	45.0	85.1
			NAZ-45	42.0	29.6	MAG-41	45.6	32.0
			NAZ-46	42.4	96.5	MAG-42	47.1	91.6
			NAZ-47	43.3	95.6			
			NAZ-48	44.3	75.0			
			NAZ-49	45.1	93.6			
			NAZ-50	51.3	83.0			

carbonate content, Praia das Maças and Praia da Pequena sections

Sample	Height (m)	CaCO ₃ content (%)	Sample	Height (m)	CaCO ₃ content (%)	Sample	Height (m)	CaCO ₃ content (%)
PM-1	0.0	95.5	PP-1	27.9	80.4	PP-34	57.3	0.0
PM-2	1.4	94.0	PP-2	28.6	<5	PP-35	58.0	0.0
PM-3	2.5	98.0	PP-3	29.3	95.5	PP-36	59.8	56.5
PM-4	4	92.6	PP-4	31.3	96.0	PP-37	60.0	78.0
PM-5	4.4	14.0	PP-5	33.3	97.5	PP-38	60.8	36.4
PM-6	4.9	73.6	PP-6	33.9	77.6	PP-39	61.4	<5
PM-7	6	33.5	PP-7	35.0	76.4	PP-40	62.8	23.1
PM-8	6.7	28.4	PP-8	35.1	73.1	PP-41	64.0	0.0
PM-9	9.3	80.0	PP-9	36.3	0.0	PP-42	65.0	0.0
PM-10	11.9	26.9	PP-10	37.0	0.0	PP-43	65.6	85.5
PM-11	12.0	84.5	PP-11	37.5	0.0	PP-44	66.7	87.7
PM-11,5	12.3	19.9	PP-12	37.9	<5	PP-45	69.5	86.0
PM-12	12.4	55.0	PP-13	38.3	0.0	PP-46	70.1	12.8
PM-13	13.2	92.0	PP-14	40.2	<5	PP-47	71.3	91.5
PM-14	13.8	97.0	PP-15	40.4	73.4	PP-48	71.6	<5
PM-15	19.1	9.0	PP-16	40.8	<5	PP-49	72.6	70.9
PM-16	20.2	85.0	PP-17	42.0	0.0	PP-50	74.9	95.0
PM-17	21.2	69.1	PP-18	43.0	49.3	PP-51	75.8	78.3
PM-18	21.6	83.0	PP-19	44.2	41.8	PP-52	76.8	0.0
PM-19	21.8	<5	PP-20	44.9	91.5	PP-53	77.1	91.0
PM-20	22.7	80.0	PP-21	45.3	0.0	PP-54	77.5	0.0
PM-21	23.6	94.5	PP-22	45.8	0.0	PP-55	78.1	94.6
PM-22	24.0	<5	PP-23	46.6	0.0	PP-56	79.1	53.0
PM-23	25.3	91.5	PP-24	47.3	0.0	PP-57	81.8	96.5
PM-24	26.0	<5	PP-25	48.6	72.1	PP-58	83.5	85.5
PM-25	26.2	86.1	PP-26	49.8	<5	PP-59	83.9	0.0
PM-26	27.1	49.5	PP-27	50.6	41.3	PP-60	85.1	85.2
			PP-28	51.1	11.1	PP-61	86.1	95.5
			PP-29	52.1	<5	PP-62	87.3	95.1
			PP-30	52.4	65.3			
			PP-31	53.0	0.0			
			PP-32	55.1	70.6			
			PP-33	56.7	92.0			

carbon and oxygen isotope results, São Julião section

Sample (SJM)	Height (m)	$\delta^{13}\text{C}$ VPDB	$\delta^{13}\text{C}$ VPDB sd	$\delta^{18}\text{O}$ VPDB	$\delta^{18}\text{O}$ VPDB sd	Sample (SJM)	Height (m)	$\delta^{13}\text{C}$ VPDB	$\delta^{13}\text{C}$ VPDB sd	$\delta^{18}\text{O}$ VPDB	$\delta^{18}\text{O}$ VPDB sd
10.5	16.6	0.00	0.04	-1.81	0.09	102	106.0	0.83	0.06	-3.29	0.09
12.5	17.3	0.82	0.03	-2.72	0.08	103	106.3	1.07	0.03	-2.87	0.05
13	17.6	1.08	0.03	-2.16	0.05	104	107.0	0.84	0.05	-2.77	0.09
13.5	18.2	0.40	0.02	-4.98	0.03	105	108.1	0.99	0.03	-2.31	0.08
13.7	19.7	-0.40	0.03	-7.69	0.07	106	109.5	2.53	0.06	-2.42	0.05
15	21.4	0.98	0.06	-1.53	0.09	108	111.4	0.55	0.04	-3.65	0.05
16	23.2	1.74	0.02	-3.11	0.04	115	119.4	-1.18	0.03	-3.68	0.06
17	23.8	1.80	0.04	-2.31	0.05	118	121.3	0.41	0.02	-5.97	0.06
17.5	25.1	2.06	0.04	-2.93	0.11	121	123.6	1.50	0.05	-3.04	0.10
18	26.2	2.58	0.03	-2.59	0.06	122	123.8	1.89	0.03	-3.64	0.05
20	28.2	2.30	0.02	-2.17	0.07	123	124.0	1.75	0.03	-3.22	0.05
21.1	29.0	1.71	0.03	-2.15	0.07	124	124.3	1.94	0.04	-3.21	0.06
21.3	30.9	2.09	0.05	-2.71	0.09	125	124.5	2.06	0.03	-3.13	0.08
22	32.2	2.05	0.04	-3.07	0.05	126	124.6	1.70	0.03	-3.01	0.06
23	33.4	1.96	0.02	-2.45	0.05	127	125.7	1.71	0.03	-2.95	0.04
24	35.0	1.85	0.02	-2.93	0.09	128	126.0	1.86	0.05	-3.40	0.08
25	35.9	2.29	0.02	-2.70	0.05	129	126.3	1.69	0.03	-3.25	0.07
26	37.3	1.51	0.04	-2.80	0.04	132	127.6	-1.66	0.03	-5.21	0.09
27	38.9	1.95	0.04	-2.41	0.05	134	130.1	1.45	0.04	-3.56	0.06
28	40.2	1.97	0.03	-2.63	0.04	135	130.6	1.69	0.02	-3.64	0.06
29	40.4	2.35	0.03	-2.65	0.03	136	131.3	1.40	0.02	-3.57	0.06
29.5	41.8	2.31	0.03	-1.91	0.05	138	131.7	2.01	0.09	-2.87	0.12
30	43.1	1.97	0.06	-2.82	0.09	139	132.9	2.38	0.03	-2.95	0.08
31	43.2	1.43	0.04	-2.05	0.06	140	133.3	2.39	0.05	-2.02	0.07
33	44.8	1.94	0.06	-2.97	0.07	141	133.9	2.29	0.04	-2.56	0.09
34	45.6	1.53	0.03	-5.90	0.08	141.2	135.4	2.84	0.03	-2.41	0.09
35	46.0	2.18	0.04	-2.55	0.07	142	137.7	2.45	0.05	-2.72	0.13
36	47.3	1.92	0.04	-2.58	0.04	144	138.5	2.26	0.06	-2.83	0.10
37	47.7	1.37	0.02	-2.91	0.05	145	139.0	1.92	0.03	-3.26	0.09
39	48.3	1.95	0.04	-2.52	0.10	146	139.3	0.76	0.03	-3.78	0.07
42	51.0	1.63	0.03	-2.51	0.06	147	139.8	2.63	0.05	-1.74	0.04
52	59.7	2.59	0.04	-1.73	0.05	148	140.1	2.20	0.04	-3.49	0.07
53	60.5	2.73	0.02	-1.94	0.05	151	142.5	2.26	0.05	-3.59	0.09
55	61.4	2.76	0.04	-2.73	0.08	152	142.9	2.25	0.05	-2.30	0.11
56	66.0	2.23	0.06	-3.25	0.07	153	143.8	2.63	0.07	-2.84	0.11
58	69.1	1.65	0.03	-1.88	0.07	154	144.1	2.95	0.05	-3.02	0.06
61	70.8	1.57	0.03	-2.44	0.05	155	144.5	2.69	0.03	-2.15	0.03
62	71.3	1.71	0.05	-2.78	0.08	155.2	145.1	2.27	0.05	-3.39	0.10
65	73.7	1.76	0.03	-2.73	0.05	155.4	145.8	2.96	0.06	-1.92	0.10
66	73.9	1.85	0.03	-2.39	0.05	155.5	147.6	3.12	0.05	-3.23	0.10
68	74.4	1.76	0.04	-2.76	0.10	156	148.0	2.69	0.03	-1.46	0.11
69	75.8	1.52	0.05	-4.16	0.04	156.2	148.5	2.49	0.06	-2.02	0.08
70	76.3	1.78	0.04	-3.03	0.11	156.4	150.1	3.41	0.06	-3.82	0.11
71	76.9	1.53	0.05	-2.76	0.08	156.5	150.5	2.52	0.05	-3.27	0.07
72	77.8	1.46	0.03	-2.72	0.06	157	150.9	3.33	0.03	-4.02	0.05
73	78.0	0.99	0.04	-3.14	0.06	158	151.3	3.12	0.03	-4.10	0.06
76	80.9	-0.60	0.02	-3.92	0.05	158.2	152.5	2.64	0.04	-2.19	0.09
77	81.2	-1.57	0.02	-3.93	0.04	159	152.5	2.70	0.02	-2.15	0.07
79	85.7	0.99	0.04	-2.88	0.06	159.2	153.2	2.19	0.08	-1.87	0.09
82	89.7	0.66	0.03	-3.69	0.07	160	153.3	2.53	0.03	-3.56	0.10
85	92.6	0.39	0.04	-7.64	0.05	159.1	153.5	2.27	0.03	-2.70	0.12
91	98.4	-0.09	0.02	-6.17	0.06	161	154.0	3.23	0.02	-3.15	0.03
92	99.3	0.44	0.03	-4.25	0.05	162	154.9	2.61	0.02	-3.68	0.05
93	100.2	0.53	0.04	-2.21	0.04	163	155.2	2.79	0.03	-2.99	0.05
94	101.4	1.44	0.06	-2.40	0.06	164	155.5	2.98	0.04	-3.18	0.05
95	101.7	1.60	0.03	-1.71	0.10	165	155.7	3.04	0.03	-3.58	0.13
96	102.0	1.56	0.03	-1.95	0.08	166	155.8	3.41	0.04	-3.83	0.09
97	102.9	1.68	0.04	-2.06	0.09	167	156.6	3.16	0.05	-3.99	0.09
98	103.2	1.29	0.04	-1.63	0.05	168	156.6	3.02	0.04	-4.38	0.07
99	103.9	1.09	0.02	-2.79	0.05	169	157.0	2.91	0.04	-4.95	0.05

carbon and oxygen isotope results, São Julião section

Sample (SJM)	Height (m)	$\delta^{13}\text{C}$ VPDB	$\delta^{13}\text{C}$ VPDB sd	$\delta^{18}\text{O}$ VPDB	$\delta^{18}\text{O}$ VPDB sd
170	157.8	2.76	0.03	-4.67	0.09
171	158.5	2.61	0.03	-4.33	0.09
172	158.6	2.52	0.05	-5.16	0.11
175	158.6	0.55	0.03	-3.22	0.06
176	158.9	2.58	0.04	-2.53	0.06
177	158.9	2.64	0.02	-4.17	0.06
178	160.0	2.41	0.02	-3.65	0.05
180	160.1	2.81	0.05	-3.32	0.08
181	161.1	2.98	0.05	-3.22	0.07
182	161.4	2.78	0.06	-2.40	0.07
183	162.2	2.55	0.02	-2.79	0.04
184	162.4	2.80	0.04	-2.29	0.07
185	163.4	2.10	0.03	-5.55	0.07
186	163.9	2.87	0.05	-4.63	0.11
SJS 7.5	165.5	3.48	0.03	-3.57	0.06
SJS 8	165.6	2.91	0.03	-5.55	0.05
SJS 9	166.4	3.58	0.04	-3.16	0.05
SJS 10	167.1	1.77	0.02	-1.73	0.04
SJS 11	167.5	2.89	0.01	-4.27	0.04
SJS 12	168.0	3.34	0.02	-2.71	0.04
SJS 12.5	168.3	2.52	0.02	-4.15	0.03
SJS 13	168.3	3.05	0.03	-3.81	0.06
SJS 14	169.6	2.32	0.06	-4.96	0.08
SJS 15	169.7	2.11	0.03	-2.31	0.05
SJS 16	170.1	0.75	0.03	-2.95	0.05
SJS 17	170.6	0.98	0.04	-2.29	0.06
SJS 18	171.8	1.55	0.04	-1.31	0.08
SJS 20	173.0	0.87	0.02	-2.26	0.06
SJS 22	173.5	0.97	0.03	-0.95	0.02
SJS 23.5	174.2	1.10	0.03	-2.30	0.03
SJS 24	174.7	-0.23	0.02	-2.11	0.05
SJS 25	175.9	-0.06	0.02	-2.32	0.05
SJS 26	177.7	1.65	0.03	-4.53	0.06
SJS 27	178.4	1.27	0.02	-5.03	0.05
SJS 28	179.4	0.82	0.03	-4.63	0.03
SJS 29	179.8	0.37	0.03	-2.82	0.03
SJS 30	183.3	0.44	0.02	-3.53	0.04
SJS 31	183.9	0.54	0.03	-2.53	0.06
SJS 31.5	184.5	0.02	0.02	-2.47	0.03
SJS 34	185.1	-1.73	0.03	-3.03	0.08
SJS 35	186.3	0.63	0.03	-5.76	0.04
SJS 36	189.3	0.92	0.03	-3.91	0.05
SJS 37	191.3	0.09	0.02	-4.02	0.03

carbon and oxygen isotope results, Magoito and Praia das Maças sections

Sample (SJMh)	Height (m)	$\delta^{13}\text{C}$ VPDB	$\delta^{13}\text{C}$ VPDB sd	$\delta^{18}\text{O}$ VPDB	$\delta^{18}\text{O}$ VPDB sd	Sample (SJMh)	Height (m)	$\delta^{13}\text{C}$ VPDB	$\delta^{13}\text{C}$ VPDB sd	$\delta^{18}\text{O}$ VPDB	$\delta^{18}\text{O}$ VPDB sd
MAG-1	0.2	2.09	0.03	-2.76	0.04	PM 1	0.0	2.44	0.02	-3.80	0.03
MAG-2	1.4	2.49	0.03	-2.51	0.03	PM 2	1.4	1.88	0.02	-4.20	0.04
MAG-3	2.5	2.09	0.03	-2.54	0.05	PM 3	2.5	2.34	0.03	-5.19	0.05
MAG-4	2.7	2.19	0.02	-2.41	0.03	PM 4	4.0	2.00	0.03	-5.27	0.04
MAG-5	3.3	1.98	0.02	-3.20	0.04	PM 5	4.4	0.62	0.03	-3.16	0.03
MAG-6	5.1	2.01	0.02	-3.23	0.04	PM-6	4.9	1.75	0.03	-1.92	0.05
MAG-7	5.4	1.57	0.02	-3.08	0.05	PM-7	6.0	1.74	0.02	-0.63	0.06
MAG-8	6.8	1.99	0.03	-2.41	0.05	PM-8	6.7	1.72	0.02	-0.18	0.05
MAG-9	7.6	2.71	0.04	-3.48	0.03	PM-9	9.3	1.18	0.03	-4.27	0.05
MAG-10	9.0	2.29	0.02	-2.52	0.03	PM-10	11.9	1.44	0.02	-4.06	0.05
MAG-11	11.7	2.28	0.02	-3.35	0.03	PM-11	12.0	1.47	0.03	-4.00	0.05
MAG-11.1	12.3	2.49	0.03	-2.87	0.03	PM-11.5	12.3	1.39	0.06	-4.33	0.05
MAG-11.2	12.9	2.02	0.03	-3.04	0.05	PM-12	12.4	1.88	0.02	-2.63	0.03
MAG-11.3	14.3	2.46	0.02	-3.41	0.04	PM-13	13.2	1.27	0.02	-4.37	0.04
MAG-12	15.2	2.98	0.03	-2.67	0.03	PM-14	13.8	1.44	0.03	-4.91	0.04
MAG-13	16.5	1.95	0.03	-3.53	0.06	PM-15	19.1	0.40	0.04	-2.03	0.02
MAG-14	18.4	3.42	0.03	-4.06	0.08	PM-16	20.2	0.73	0.03	-2.60	0.05
MAG-15	18.8	2.39	0.02	-2.98	0.04	PM-17	21.2	0.55	0.06	-2.60	0.09
MAG-16	19.5	1.83	0.03	-5.56	0.06	PM-18	21.6	0.26	0.02	-3.94	0.04
MAG-17	20.2	2.51	0.03	-3.08	0.03	PM-20	22.7	0.37	0.03	-3.51	0.04
MAG-18	21.9	2.52	0.02	-3.18	0.04	PM-21	23.6	1.13	0.02	-3.87	0.03
MAG-19	22.0	1.06	0.04	-3.45	0.05	PM-23	25.3	-0.08	0.03	-3.63	0.03
MAG-20	22.7	2.30	0.03	-4.46	0.05	PM-25	26.2	0.62	0.03	-3.08	0.02
MAG-21	23.3	3.13	0.02	-3.76	0.07	PM-26	27.1	0.57	0.02	-3.29	0.03
MAG-22	23.4	2.47	0.03	-3.25	0.04						
MAG-23	24.7	2.22	0.03	-3.24	0.05						
MAG-24	25.0	1.71	0.03	-2.36	0.03						
MAG-25	26.0	2.05	0.03	-4.43	0.05						
MAG-26	26.7	2.45	0.02	-3.34	0.03						
MAG-27	28.4	2.33	0.02	-4.73	0.04						
MAG-28	29.0	0.65	0.02	-7.71	0.02						
MAG-28.3	31.3	2.10	0.04	-3.09	0.08						
MAG-29	32.2	3.58	0.02	-3.32	0.04						
MAG-30	33.4	2.53	0.02	-2.63	0.02						
MAG-31	34.0	3.83	0.02	-2.11	0.06						
MAG-32	34.7	3.62	0.02	-2.78	0.06						
MAG-33	35.5	3.00	0.02	-2.06	0.07						
MAG-34	37.0	2.13	0.02	-3.96	0.05						
MAG-35	37.3	3.18	0.03	-2.05	0.07						
MAG-36	38.4	3.46	0.03	-2.58	0.06						
MAG-37	40.2	1.37	0.04	-3.69	0.06						
MAG-38	41.8	2.29	0.02	-2.14	0.04						
MAG-39	43.7	2.41	0.03	-1.95	0.05						
MAG-40	45.4	1.41	0.02	-2.81	0.07						
MAG-41	46.4	1.74	0.03	-2.78	0.02						
MAG-42	47.9	1.97	0.03	-3.32	0.04						

trace element results and strontium isotope values

Sample	Height (m)	Ca (ppm)		Mg (ppm)		Sr (ppm)		Fe (ppm)		Mn (ppm)		Ba (ppm)	
		μ	SD	μ	SD	μ	SD	μ	SD	μ	SD	μ	SD
SJMH-13	17.6	391820	748.6	733	11.1	699	2.9	349.0	1.3	54.9	0.09	1.5	0.03
SJ-27.1	45.0	369050	522.0	816	10.0	784	2.9	345.0	1.6	67.3	0.26	1.7	0.03
SJMH-35	46.0	371750	733.0	3533	14.6	702	3.3	3560.0	12.1	426.0	0.86	4.1	0.04
SJMH-46	54.2	392390	813.0	1330	6.3	819	3.6	701.5	3.1	233.0	0.25	2.2	0.02
SJMH-50	58.2	395290	331.0	989	6.1	841	2.0	145.0	1.5	19.2	0.19	3.4	0.04
SJMH-62	71.3	394130	1192.1	596	2.5	868	1.4	133.9	1.6	28.8	0.16	2.1	0.03
SJMH-66(3)	73.9	353900	643.0	969	6.4	729	2.2	72.0	0.9	22.2	0.16	1.3	0.04
SJMH-66(4)	73.9	391750	672.0	1073	6.0	808	2.8	81.0	0.4	22.4	0.19	1.8	0.02
SJMH-73	78.0	392740	1616.6	987	10.5	786	4.0	668.2	4.1	104.0	0.40	5.7	0.04
SJMH-82(1)	89.7	375950	922.0	1432	4.8	906	2.5	2602.0	27.4	184.0	0.55	7.7	0.05
SJMH-82(2)	89.7	386550	235.0	1489	8.5	964	1.5	1759.0	19.4	207.0	0.19	4.6	0.05
SJ-76.1	127.2	387440	383.0	875	13.0	716	3.8	74.0	0.3	25.8	0.18	1.7	0.03
SJ-78.2	130.6	390010	331.0	1602	14.0	962	1.4	244.0	1.1	84.7	0.14	2.8	0.03
SJMH-137	131.5	391570	1065.4	1009	6.1	820	3.2	503.7	3.2	46.0	0.16	3.1	0.02
SJMH-139	132.9	383260	1104.1	2929	11.0	783	2.0	5286.0	6.1	491.0	0.60	6.6	0.02
SJMH-149	141.8	389950	756.9	816	4.1	855	2.4	259.4	1.2	38.6	0.12	2.4	0.02
SJMH-150	142.2	374540	447.0	1961	9.5	810	2.9	723.0	2.6	92.9	0.21	4.7	0.04
SJMH-175-1	158.6	389300	449.0	1510	7.5	1193	3.9	158.4	1.7	22.2	0.08	4.9	0.04
SJMH-175-2	158.6	385900	789.6	1981	5.2	1312	5.0	649.1	1.6	74.4	0.16	7.1	0.04
SJMH-179-1	160.1	373290	647.0	409	6.6	943	2.0	261.8	1.5	31.5	0.22	3.1	0.03
SJMH-179-2	160.1	392230	940.1	1662	10.5	867	2.0	740.6	11.2	118.0	0.47	4.6	0.04
SJMH-185 (1)	163.4	390810	1486.0	1410	5.2	1384	5.4	96.0	0.7	10.1	0.12	1.4	0.01
SJMH-185 (3)	163.4	392530	946.0	1102	7.7	1182	3.5	138.0	0.3	12.6	0.09	0.9	0.02

	sample name	⁸⁷ Sr/ ⁸⁶ Sr measured	± 2σ mean	⁸⁷ Sr/ ⁸⁶ Sr sample corrected to difference: NBS 987 value McArthur and NBS 987 measured with sample	⁸⁷ Sr/ ⁸⁶ Sr sample corrected to difference: USGS EN-1 values McArthur and USGS EN-1 measured with sample	⁸⁷ Sr/ ⁸⁶ Sr sample corrected to difference: NBS 987 value McArthur and NBS 987 Bochum mean value	⁸⁷ Sr/ ⁸⁶ Sr sample corrected to difference: USGS EN-1 value McArthur and USGS EN-1 Bochum mean value
Date: December 2012	NIST NBS 987 35	0.710242	0.000006	0.710247	0.710251	0.710248	0.710257
	50	0.707423	0.000007	0.707428	0.707432	0.707429	0.707438
	66 (3)	0.707407	0.000007	0.707412	0.707416	0.707413	0.707422
	66 (4)	0.707417	0.000006	0.707422	0.707426	0.707423	0.707432
	82 (1)	0.707416	0.000006	0.707421	0.707425	0.707422	0.707431
	C4C-M	0.707451	0.000006	0.707456	0.707460	0.707457	0.707466
	82 (2)	0.707541	0.000007	0.707546	0.707550	0.707547	0.707556
	150	0.707461	0.000006	0.707466	0.707470	0.707467	0.707476
	185 (1)	0.707435	0.000007	0.707440	0.707444	0.707441	0.707450
	185 (3)	0.707414	0.000007	0.707419	0.707423	0.707420	0.707429
	SJ-27.1	0.707410	0.000006	0.707415	0.707419	0.707416	0.707425
	USGS EN-1	0.707399	0.000007	0.707404	0.707408	0.707405	0.707414
	NIST NBS 987	0.709166	0.000006	0.709171	0.709175	0.709172	0.709181
	SJ-76.1	0.710250	0.000006	0.710247	0.710252	0.710256	0.710265
	SJ-78.2	0.707438	0.000006	0.707435	0.70744	0.707444	0.707453
	USGS EN-1	0.707443	0.000006	0.707440	0.707445	0.707449	0.707458
	0.709173	0.000007	0.709170	0.709175	0.709179	0.709188	
Date: April 2013	NIST NBS 987 13	0.710248	0.000007	0.710247	0.710247	0.710254	0.710263
	46	0.707389	0.000007	0.707388	0.707388	0.707395	0.707404
	62	0.707424	0.000006	0.707423	0.707423	0.707430	0.707439
	73	0.707421	0.000007	0.707420	0.707420	0.707427	0.707436
	137	0.707441	0.000006	0.707440	0.707440	0.707447	0.707456
	139	0.707432	0.000007	0.707431	0.707431	0.707438	0.707447
	149	0.707429	0.000007	0.707428	0.707428	0.707435	0.707444
	175 (1)	0.707425	0.000006	0.707424	0.707424	0.707431	0.707440
	175 (2)	0.707418	0.000006	0.707417	0.707417	0.707424	0.707433
	179 (1)	0.707425	0.000006	0.707424	0.707424	0.707431	0.707440
	179 (2)	0.707415	0.000007	0.707414	0.707414	0.707421	0.707430
	USGS EN-1	0.707432	0.000006	0.707431	0.707431	0.707438	0.707447
		0.709176	0.000007	0.709175	0.709175	0.709182	0.709191

Standards	Value McArthur	Mean Value Bochum	± 2σ standard error	± 2σ standard deviation	repetitions (n)
NIST NBS 987	0.710247	0.710241	0.000002	0.000034	241
USGS EN-1	0.709175	0.709160	0.000002	0.000027	215

palynological results, São Julião section

Sample	Height (m)	Total non-saccate Gymnosperms	Alisporites	Parvisaccus radiates	Pinuspollenites	Podocarpidites	Vitreisporites	Cleissopollis	Araucariacites australis	Exesipollenites tumulus	Inaperturopollenites	Perinopollenites elatoides	Perinopollenites halonatus	Callialasporites trilobatus	Callialasporites dampieri	Cerebropollenites	Ephedripites	Eucommidites	Equisetosporites	Afropollis	Afropollis aff. jardiinus	Cycadopites	Monosulcites	Monosulcites minimus	Sciadopityspollenites	Monosulcites chaloneri	Total Angiosperms	Total Spores	Antulsporites	Appendicisporites	Baculatisporites
SJMH-2	7.5	222	6	0	0	0	0	61	13	32	55	10	0	0	2	0	0	0	4	0	10	0	0	0	0	29	21	64	0	1	0
SJMH-3	9.8	250	6	0	0	1	0	81	11	32	66	14	0	0	2	0	0	5	0	0	17	0	2	1	11	23	39	0	0	0	
SJMH-4	10.2	246	4	0	1	0	0	153	29	27	11	12	0	0	5	0	0	0	0	0	0	0	0	0	4	15	47	0	0	0	
SJMH-11	17.0	257	0	0	1	2	0	173	8	46	5	10	0	0	1	0	0	0	2	0	2	2	0	0	5	7	44	0	0	0	
SJMH-12,5	17.3	281	5	0	0	1	107	6	69	72	0	0	0	0	0	0	0	0	0	1	7	0	1	0	12	19	19	0	0	0	
SJMH-13,7	19.7	13	0	0	0	0	0	6	1	2	2	0	0	0	0	0	0	0	0	0	2	0	0	0	0	1	1	0	0	0	
SJ-21	25.0	252	3	0	0	1	0	92	6	14	76	3	0	0	4	0	0	0	2	13	3	8	3	0	0	24	17	40	0	2	1
SJMH-18	26.2	226	10	2	0	1	0	65	13	25	58	10	1	0	4	0	0	0	1	0	4	0	0	0	32	30	44	0	0	0	
SJMH-21,3	30.9	228	11	0	0	0	1	109	10	15	40	3	1	0	4	0	0	0	0	0	2	0	1	0	31	28	54	0	0	0	
SJMH-21,7	31.7	252	17	1	2	0	1	114	22	20	34	3	0	0	0	0	0	1	0	0	0	19	0	0	18	14	51	0	0	0	
SJMH-24	35.0	231	2	1	2	2	1	136	6	37	22	6	0	0	6	0	0	0	0	1	0	3	4	0	0	2	35	36	0	0	0
SJMH-28	40.2	271	18	0	5	0	0	127	8	36	38	7	0	0	2	0	0	0	0	2	0	13	0	0	14	19	29	0	0	0	
SJMH-32	44.0	281	3	0	0	0	0	75	5	40	127	10	0	0	0	0	0	0	0	5	0	6	0	0	10	5	20	0	0	0	
SJMH-36	47.3	234	7	0	1	1	1	103	7	27	72	0	0	0	0	0	0	1	0	0	3	0	0	0	11	40	37	0	0	0	
SJMH-43	51.7	251	2	0	0	0	0	99	8	40	74	7	0	0	3	0	0	1	1	0	0	9	0	0	0	7	17	38	0	0	1
SJMH-44	52.4	265	10	0	1	0	0	97	23	40	79	0	1	0	0	0	0	0	0	0	8	0	0	0	6	23	15	0	0	0	
SJMH-47	55.0	248	8	1	0	0	0	89	13	89	31	2	0	0	0	0	0	2	0	0	9	1	0	0	2	20	43	0	0	0	
SJMH-48	55.4	226	7	0	0	0	0	56	8	92	53	2	0	0	4	0	0	0	0	0	0	0	0	0	4	20	55	1	0	3	
SJMH-49	58.0	25	0	0	0	0	5	0	14	3	0	0	0	0	0	0	0	0	0	0	0	0	1	0	1	2	5	0	0	0	
SJMH-52	59.7	280	6	0	0	0	0	8	89	89	80	0	0	0	0	0	0	0	1	0	0	0	0	0	7	10	26	0	0	0	
SJMH-54	60.7	294	16	0	2	0	0	79	10	115	59	1	0	0	1	0	0	0	0	1	0	6	0	0	5	20	15	0	0	0	
SJMH-57,2	62.2	290	5	0	0	0	0	50	21	128	59	15	0	0	0	0	0	0	1	0	9	2	0	0	4	10	0	0	0	0	
SJMH-56	66.0	274	3	0	1	0	0	115	1	125	21	0	0	0	1	0	0	1	0	1	1	1	0	0	3	24	5	0	0	0	
SJMH-57	67.3	238	6	1	0	1	0	49	13	30	103	8	0	0	13	0	1	0	0	1	0	5	0	2	0	5	41	22	0	0	0
SJMH-60	69.6	279	3	0	0	0	0	124	3	81	41	3	0	0	2	0	0	1	0	0	0	17	2	0	0	2	15	16	0	0	0
SJ-38	70.2	300	4	0	0	0	0	108	10	43	110	4	2	0	1	0	0	0	0	1	0	17	0	0	0	7	12	0	0	0	
SJMH-65	73.7	270	4	0	0	0	0	75	20	59	106	0	0	0	2	0	0	0	0	0	0	2	0	0	1	33	23	0	0	0	
SJMH-74	79.0	245	1	0	0	0	0	220	4	9	5	0	0	0	3	0	0	0	0	0	0	0	3	0	0	4	51	0	0	0	0
SJMH-75	80.6	264	1	0	0	0	0	60	30	20	117	11	0	0	3	0	0	0	0	0	10	7	0	0	2	26	13	0	0	0	
SJMH-78	83.6	273	7	0	0	1	0	137	15	15	74	12	0	0	6	0	0	0	0	0	4	2	0	0	0	20	9	0	0	0	
SJMH-79	85.7	215	13	0	1	0	0	93	24	13	67	0	0	0	1	0	0	0	0	0	2	0	0	0	1	31	56	0	0	0	
SJMH-81	89.4	165	0	0	0	0	0	77	0	21	49	2	0	0	3	0	0	0	0	1	0	1	0	1	2	33	18	0	0	0	
SJMH-83	90.0	200	2	0	0	0	0	57	60	0	69	0	0	0	2	0	0	2	2	0	3	0	1	0	0	47	59	0	0	0	
SJMH-85	92.6	165	2	0	0	0	0	36	20	8	89	0	0	0	4	0	0	2	1	0	0	1	0	0	0	47	56	0	0	0	
SJMH-86	93.7	87	2	0	0	0	0	36	3	6	23	11	0	0	2	0	0	1	0	0	3	0	0	0	0	19	9	0	0	0	
SJMH-88	95.9	168	3	0	0	3	0	59	31	4	41	0	0	0	13	0	0	0	2	3	0	0	0	0	2	23	120	0	0	0	
SJMH-89	96.7	0	0	0	0	0	0	0	0	0	0	0	0	0	0	0	0	0	0	0	0	0	0	0	0	0	0	0	0	0	
SJMH-90	97.7	156	4	0	0	0	1	87	14	6	30	0	0	0	3	0	0	2	6	0	0	2	1	0	0	62	86	0	0	0	
SJMH-92	99.3	48	2	0	0	0	0	14	3	4	20	3	0	0	0	0	0	0	0	0	0	1	0	0	0	11	8	0	0	0	
SJMH-93	100.2	44	0	0	0	0	0	12	11	5	10	0	0	0	1	0	0	0	0	1	0	2	2	0	0	13	39	0	0	0	
SJMH-94	101.4	231	2	0	0	1	0	120	10	19	62	0	2	0	3	0	0	2	0	2	0	7	0	0	1	26	57	0	0	1	
SJMH-97	102.9	261	2	0	0	0	0	150	23	16	62	0	0	0	1	0	0	2	0	0	1	3	0	0	1	21	21	0	0	0	
SJMH-100	104.0	238	3	0	1	0	0	136	17	18	45	0	0	1	13	0	0	1	0	1	0	2	0	0	0	27	48	0	0	0	
SJMH-101	105.3	129	1	0	0	0	0	72	2	5	30	8	0	0	1	0	0	2	6	1	0	1	0	0	0	126	71	0	0	0	
SJMH-106	109.5	273	8	0	0	0	0	54	14	15	140	10	3	0	8	0	0	0	2	1	0	15	1	0	0	2	9	33	0	0	0
SJMH-110	113.2	209	6	0	0	0	0	51	17	18	84	15	3	0	9	0	0	0	2	2	0	2	0	0	0	16	87	0	0	0	
SJ-65 (112)	116.0	0	0	0	0	0	0	0	0	0	0	0	0	0	0	0	0	0	0	0	0	0	0	0	0	0	0	0	0	0	
Sj66 (113)	116.8	0	0	0	0	0	0	0	0	0	0	0	0	0	0	0	0	0	0	0	0	0	0	0	0	0	0	0	0	0	0
SJMH-114	117.4	244	0	0	0	0	1	75	8	9	123	11	1	0	1	0	0	1	1	8	0	4	0	0	0	19	63	0	0	1	
SJMH-117	120.7	133	1	0	0	0	0	25	30	19	27	0	0	0	25	0	0	0	0	5	1	0	0	0	0	12	183	0	0	2	
SJMH-119	121.8	190	4	0	0	0	0	119	5	6	43	0	0	0	1	0	1	0	5	2	0	2	1	0	0	1	31	86	0	1	2
SJMH-122	123.8	234	1	0	0	0	0	86	12	18	93	6	2	0	0	0	0	1	0	2	0	5	2	0	0	6	13	53	0	0	0
SJMH-128	126.0	173	2	0	0	2	0	61	28	21	39	8	0	0	9	0	0	0	2	0	0	0	1	0	0	12	126	0	0	1	
SJMH-133	129.9	0	0	0	0	0	0	0	0	0	0	0	0	0	0	0	0	0	0	0	0	0	0	0	0	0	0	0	0	0	0
SJMH-136	131.3	176	12	0	0	0	1	60	11	3	73	0	0	0	2	0	0	0	2	6	0	0	0	2	0	4	43	99	0	0	0
SJMH-140	133.3	199	11	0	1	0	0	80	19	13	44	0	0	0	5	1	0	0	0	9	1	2	6	5	0	2	13	94	0	1	0
SJMH-143	138.1	166	1	0	0	0	0	15	12	23	73	5	7	0	5	0	0	1	3	16	0	4	0	1	0	0	27	107	0	0	2

palynological results, São Julião section

Sample	Height (m)	Camerazonesporites	Cicalricosporites	Concavisporites	Concavasisporites	Convverucosporites	Cyanthidites	Deltoidospora	Todisporites	Cingulitrites	Gabonsporites	Gleicheniidites	Leptolepidites	Klukisporites	Notosporites	Plicatella	Laevigatosporites	Vedasporites	Spore indet	Costatoperforosporites	Ischyosporites	Verrucosporites	Tauracosporites	Vinculisporites	Zlivisporis	Dinoflagellate cysts	Foram linings	Algae	Acritarch	Botryococcus	Pterospermella	Sum terrestrial palynomorphs
SJMH-2	7.5	0	34	0	0	0	0	8	0	1	0	4	3	0	0	0	0	5	0	3	2	1	0	1	16	3	1	0	0	0	307	
SJMH-3	9.8	1	15	0	0	0	0	13	1	1	0	0	1	0	1	1	0	3	1	1	0	0	0	0	13	4	0	3	0	0	312	
SJMH-4	10.2	1	24	2	0	0	6	1	0	0	0	3	0	0	0	0	0	6	4	0	0	0	0	0	3	0	0	0	0	4	308	
SJMH-11	17.0	1	17	0	0	0	10	2	0	2	0	0	3	0	0	0	0	6	1	1	1	0	0	0	69	0	0	2	6	0	308	
SJMH-12,5	17.3	0	11	0	0	0	0	0	0	0	0	0	2	0	0	0	0	3	1	0	0	0	0	2	23	1	0	0	0	0	319	
SJMH-13,7	19.7	0	1	0	0	0	0	0	0	0	0	0	0	0	0	0	0	0	0	0	0	0	0	0	0	1	0	0	0	0	15	
SJ-21	25.0	0	23	0	0	0	1	3	0	2	0	1	1	0	0	1	0	3	0	2	0	0	0	0	118	1	0	0	0	0	309	
SJMH-18	26.2	0	28	0	0	0	7	0	3	1	0	0	0	0	0	0	0	2	0	1	2	0	0	0	40	6	0	0	0	0	300	
SJMH-21,3	30.9	2	20	0	0	0	0	2	0	0	0	1	12	4	0	1	0	0	12	0	0	0	0	0	175	8	0	0	0	0	310	
SJMH-21,7	31.7	1	31	1	0	0	0	6	0	1	0	5	0	1	0	0	0	4	0	1	0	0	0	0	52	4	0	3	0	0	317	
SJMH-24	35.0	0	21	0	0	1	2	4	4	1	0	0	0	0	0	1	0	0	0	1	1	0	0	0	27	1	0	1	0	1	302	
SJMH-28	40.2	0	18	0	0	0	0	5	0	0	0	0	0	1	0	1	1	0	3	0	1	0	0	0	29	13	0	0	0	0	319	
SJMH-32	44.0	0	9	0	0	0	0	7	3	0	0	0	0	0	0	0	0	0	0	0	0	1	0	0	93	2	0	2	0	0	306	
SJMH-36	47.3	2	19	0	0	0	0	3	1	1	0	1	3	0	0	0	0	4	2	0	0	0	1	0	136	9	0	0	0	0	311	
SJMH-43	51.7	0	20	0	0	0	0	2	0	0	0	0	1	2	0	2	0	0	7	1	2	0	0	0	13	3	0	1	0	0	306	
SJMH-44	52.4	0	7	0	0	0	1	3	1	0	0	0	0	0	0	0	0	2	1	0	0	0	0	0	15	1	0	0	0	0	303	
SJMH-47	55.0	0	7	0	0	1	0	9	1	1	0	1	1	0	0	0	1	10	5	5	0	1	1	0	4	0	0	0	0	0	311	
SJMH-48	55.4	1	15	0	0	0	4	5	1	2	0	1	4	3	0	0	0	7	8	0	0	1	0	0	3	1	0	0	0	0	301	
SJMH-49	58.0	0	1	1	0	0	0	0	1	0	0	0	0	0	0	0	1	0	1	0	0	1	0	0	5	1	0	0	0	0	32	
SJMH-52	59.7	0	10	0	0	0	0	4	0	0	0	2	2	0	0	0	0	7	1	0	0	0	0	0	20	6	0	0	0	0	316	
SJMH-54	60.7	0	5	0	0	0	1	1	1	0	0	1	0	1	0	0	0	4	1	0	0	0	0	0	31	19	12	0	0	0	329	
SJMH-57,2	62.2	0	3	0	0	0	0	5	0	0	0	0	0	0	0	0	0	1	0	0	1	0	0	0	15	2	0	2	0	0	304	
SJMH-56	66.0	0	4	0	0	0	0	0	0	0	0	0	0	0	0	0	0	1	0	0	0	0	0	0	35	5	0	0	0	0	303	
SJMH-57	67.3	0	7	0	0	0	0	2	1	0	0	0	2	0	0	0	0	7	3	0	0	0	0	0	26	0	0	2	0	0	301	
SJMH-60	69.6	3	4	0	0	0	0	2	0	0	0	1	0	0	0	0	0	3	0	1	2	0	0	0	111	2	0	0	0	0	310	
SJ-38	70.2	0	5	0	0	0	1	0	1	1	0	0	1	0	0	0	0	2	1	0	0	0	0	0	49	4	0	0	0	0	319	
SJMH-65	73.7	0	12	0	0	0	0	3	0	0	0	1	4	0	0	0	1	0	2	1	0	0	0	0	220	32	0	0	0	0	326	
SJMH-74	79.0	0	3	1	0	0	8	33	3	2	0	0	0	0	0	0	0	0	0	0	1	0	0	0	0	3	0	0	1	0	300	
SJMH-75	80.6	1	3	0	0	0	0	2	0	2	0	0	1	0	0	1	0	0	2	1	0	0	0	0	70	7	0	0	0	0	303	
SJMH-78	83.6	0	5	0	0	0	0	2	1	0	0	0	0	0	0	0	0	1	0	0	0	0	0	0	182	5	0	0	0	0	302	
SJMH-79	85.7	0	29	0	0	0	3	5	0	0	0	0	11	3	0	0	0	3	2	0	0	0	0	0	310	19	0	0	0	1	302	
SJMH-81	89.4	0	4	0	0	0	0	5	3	3	0	0	0	1	0	0	8	0	0	0	0	2	0	0	20	0	0	0	0	0	216	
SJMH-83	90.0	0	15	0	0	0	0	9	0	25	0	0	5	3	0	1	0	0	1	0	0	0	0	0	6	0	0	0	0	0	306	
SJMH-85	92.6	0	9	1	1	0	0	6	4	3	0	0	20	3	0	1	2	0	7	0	0	0	1	0	9	0	0	0	0	0	268	
SJMH-86	93.7	0	1	0	0	0	0	1	2	0	0	0	0	2	0	0	0	2	0	0	0	0	0	1	14	0	0	1	0	0	115	
SJMH-88	95.9	0	16	0	3	0	6	20	3	1	0	0	52	9	0	0	5	2	7	0	0	0	0	0	1	0	0	20	0	0	311	
SJMH-89	96.7	0	0	0	0	0	0	0	0	0	0	0	0	0	0	0	0	0	0	0	0	0	0	0	0	0	0	0	0	0	0	
SJMH-90	97.7	0	12	1	0	0	0	14	5	2	0	7	37	0	0	2	0	0	5	0	0	0	1	0	5	0	0	0	0	0	304	
SJMH-92	99.3	0	4	1	0	0	1	1	0	0	0	0	1	0	0	0	1	0	0	0	0	0	0	0	3	12	10	0	0	0	67	
SJMH-93	100.2	0	3	1	1	0	0	12	1	2	0	0	1	0	0	0	0	0	1	0	0	0	0	17	0	195	0	2	0	0	0	96
SJMH-94	101.4	0	32	0	0	0	0	3	0	0	0	1	6	5	0	0	0	1	7	1	0	0	0	0	355	15	0	0	0	1	314	
SJMH-97	102.9	0	10	0	0	0	0	1	0	0	0	2	4	1	0	0	0	0	2	0	0	0	1	0	513	8	0	0	0	0	1	303
SJMH-100	104.0	1	15	2	0	0	0	5	0	7	0	0	10	2	0	1	0	0	4	0	0	1	0	0	7	0	31	1	0	0	313	
SJMH-101	105.3	0	3	10	2	0	0	40	6	1	0	1	0	0	0	0	0	6	0	0	0	0	1	1	2	0	0	0	0	0	326	
SJMH-106	109.5	0	10	0	1	0	1	5	3	0	0	1	7	5	0	0	0	0	0	0	0	0	0	0	26	6	1	0	0	0	315	
SJMH-110	113.2	0	18	0	0	0	0	12	1	3	1	7	24	19	1	1	0	0	0	0	0	0	0	0	19	0	0	1	0	0	312	
SJ-65 (112)	116.0	0	0	0	0	0	0	0	0	0	0	0	0	0	0	0	0	0	0	0	0	0	0	0	0	0	0	0	0	0	0	
Sj66 (113)	116.8	0	0	0	0	0	0	0	0	0	0	0	0	0	0	0	0	0	0	0	0	0	0	0	0	0	0	0	0	0	0	
SJMH-114	117.4	0	10	0	0	0	2	21	10	1	0	0	4	12	0	0	1	0	1	0	0	1	0	0	0	0	0	0	0	0	326	
SJMH-117	120.7	0	15	0	0	0	0	2	1	13	0	7	21	120	0	1	0	0	1	0	0	0	0	0	9	0	0	0	0	0	328	
SJMH-119	121.8	0	16	0	0	0	4	5	0	25	0	0	15	7	0	0	0	10	1	0	0	0	0	0	197	0	0	0	0	0	307	
SJMH-122	123.8	0	20	0	0	0	0	3	5	6	0	7	9	0	0	0	0	2	1	0	0	0	0	0	24	46	0	0	0	0	300	
SJMH-128	126.0	1	37	0	0	0	3	0	1	3	0	0	30	38	0	1	0	0	10	0	0	0	0	1	26	22	0	1	0	0	311	
SJMH-133	129.9	0	0	0	0	0	0	0	0	0	0	0	0	0	0	0	0	0	0	0	0	0	0	0	0	0	0	0	0	0	0	
SJMH-136	131.3	3	38	0	0	0	1	5	1	8	0	0	24	13	0	1	0	0	5	0	0	0	0	0	90	3	0	0	0	0	318	
SJMH-140	133.3	2	34	0	1	0	1	6	4	0	0	0	20	15	0	0	0	0	4	6	0	0	0	0	68	7	0	0	0	0	306	
SJMH-143	138.1	2	28	0	0	0	1	12	2	1	0	0	9	42	0	1	0	0	6	1	0	0	0									

age-diagnostic dinoflagellate cyst presence/absence diagram, São Julião, Magoito and Praia das Maças sections

Sample	Height (m)	<i>Dinopterygium cladooides</i>	<i>Xiphophoridium alatum</i>	<i>Chicaouadinium vestitum</i>	<i>Palaeohystrichophora cf. infusooides</i>	Sample	Height (m)	<i>Dinopterygium cladooides</i>	<i>Xiphophoridium alatum</i>	<i>Chicaouadinium vestitum</i>	<i>Palaeohystrichophora cf. infusooides</i>
SJMH-11	17.0	1	0	0	0	MAG-1	0.3	1	1	1	0
SJMH-12,5	17.3	1	1	1	0	MAG-5	3.4	1	1	1	0
SJMH-13,7	19.7	1	1	1	0	MAG-7	5.1	1	1	1	0
SJ-21	25.0	1	1	0	0	MAG-10	8.2	1	1	0	0
SJMH-18	26.2	1	1	0	0	MAG-11,3	13.2	1	1	1	0
SJMH-21,3	30.9	1	1	1	0	MAG-13	16.2	1	1	1	0
SJMH-21,7	31.7	1	0	0	0	MAG-20	22.1	0	0	1	0
SJMH-24	35.0	1	1	1	0	MAG-25	25.3	1	1	0	0
SJMH-28	40.2	1	0	0	0	MAG-27	27.7	1	1	0	0
SJMH-32	44.0	1	1	0	0	MAG-28,3	30.4	1	1	1	0
SJMH-44	52.4	0	0	1	0	MAG-33	34.5	0	1	0	0
SJMH-52	59.7	1	1	1	0	MAG-34	36.2	1	0	0	0
SJMH-54	60.7	1	1	0	0	MAG-37	39.2	1	1	1	0
SJMH-56	66.0	1	1	0	0	MAG-39	43.0	1	1	1	0
SJMH-57	67.3	1	1	0	0	MAG-40	45.0	1	0	1	0
SJMH-60	69.6	1	1	0	0						
SJ-38	70.2	0	0	1	0						
SJMH-65	73.7	1	1	1	0						
SJMH-78	83.6	1	1	0	0						
SJMH-79	85.7	1	0	1	0						
SJMH-83	89.9	0	0	0	0						
SJMH-94	101.4	1	0	1	0						
SJMH-97	102.9	1	1	1	0						
SJMH-110	113.2	1	0	0	0						
SJMH-119	121.8	1	0	1	0	PM-5	4.4	1	1	1	0
SJMH-122	123.8	1	0	0	0	PM-8	6.7	0	0	1	0
SJMH-128	126.0	1	1	0	0	PM-10	11.9	0	0	1	0
SJMH-136	131.3	1	1	1	0	PM-16	20.2	1	0	0	0
SJMH-140	133.3	1	1	1	0	PM-17	21.2	1	1	0	0
SJMH-143	138.1	1	1	0	0	PM-19	21.8	1	0	0	1
SJMH-147	139.8	1	1	1	0	PM-22	24.0	0	1	0	1
SJMH-152	142.9	1	1	1	0	PM-24/ (PM-1)	26.0	1	1	0	1
SJMH-155,2	145.1	1	1	0	0						
SJMH-156	148.0	1	1	1	0						
SJMH-156,5	150.5	1	1	0	0						
SJMH-158,2	152.6	0	1	1	0						
SJMH-165	155.7	1	1	0	0						
SJMH-177	158.9	0	1	1	0						
SJMH-178	160.0	1	1	0	0						
SJS-4	161.7	1	0	0	0						
SJMH-183	162.2	0	0	1	0						
SJS-9	166.4	1	0	1	0						
SJS-10	167.1	1	1	0	0						
SJS-16	170.1	1	1	1	0						
SJS-18	171.9	1	0	0	0						
SSJ-1 (SJS-19)	172.4	0	0	1	1						
SJS-25	175.9	1	0	1	1						
SJS-26	177.7	0	0	1	1						
SJS-32	184.5	1	1	0	1						
SJS-33	185.1	1	1	0	1						

palynofacies results, São Julião section

Sample	Height (m)	Phytoclasts	Phytoclasts	Phytoclasts	Phytoclasts	Wood tracheid	Membranes	Cuticle	Resin	Terrestrial sporomorphs	Dino-cysts	Foram linings	AOM	Total
		< 25µ Translucent	> 25µ Translucent	< 25µ Opaque	> 25µ Opaque	(structured phytoclast)								
SJMH-2	7.5	69	23	101	41	23	3			49	5			314
SJMH-3	9.8	89	50	50	27	15	23			41	4	1		300
SJMH-4	10.2	107	39	73	37	2	10			53	1			322
SJMH-11	17.0	17	20	145	60	6	12			41	4			305
SJMH-12,5	17.3	54	30	112	35	1	3	1		54	9	1		300
SJ-21	25.0	12	22	128	54	3	24			53	9	1		306
SJMH-18	26.2	51	31	95	55	1	50			56	7	3		349
SJMH-21,3	30.9	23	27	127	35	2	37			43	22			316
SJMH-21,7	31.7	31	28	91	25	7	36	2	1	76	17			314
SJMH-24	35.0	47	37	72	24	1	32			58	35	4		310
SJMH-28	40.2	64	40	91	28	2	23			50	7	1		306
SJMH-32	44.0	30	28	110	78	11	6	1		28	19			311
SJMH-36	47.3	46	38	76	42	1	28			50	27	3		311
SJMH-43	51.7	26	30	138	44	8	13		1	47	3			310
SJMH-44	52.4	14		175	110	3				5				307
SJMH-47	55.0	79	20	153	65	6	1			16				340
SJMH-48	55.4	32	18	167	70	10	1	2		11				311
SJMH-52	59.7	21	23	135	55	3	17			60	11	1		326
SJMH-54	60.7	43	41	113	52	2	6	1		60	2	2		322
SJMH-57,2	62.2	43	25	132	37	8	11	1		44	5	2		308
SJMH-56	66.0	5	5	69	48	1	55			103	22			308
SJMH-57	67.3	22	29	102	58	6	24	2		78	15			336
SJMH-60	69.6	79	40	57	32	7	20	2		46	17	2		302
SJ-38	70.2	107	30	102	21	5	2			33	5	1		306
SJMH-65	73.7	37	22	40	33	1	30			58	86	3		310
SJMH-74	79.0	4	6	250	84	2		2		21				369
SJMH-75	80.6	92	25	70	17	4	24	2		45	21			300
SJMH-78	83.6	30	28	46	25	3	2	2		61	108	2		307
SJMH-79	85.7	46	26	115	29	1	18			35	32	2		304
SJMH-81	89.4	7	2	218	63	4				4	2			300
SJMH-83	89.9	96	34	112	30	6	2	1		33				314
SJMH-85	92.6	57	20	180	43	4								304
SJMH-88	95.9	62	28	170	40	3	1							304
SJMH-90	97.7	110	72	60	60	1								303
SJMH-94	101.4	36	5	105	39		12	1	1	30	71	2		302
SJMH-97	102.9	33	14	34	16	1	30			32	156			316
SJMH-100	104.0	23	12	115	74		11	3		31	53			322
SJMH-101	105.3	26	23	138	62	19	1	2		34				305
SJMH-106	109.5	79	33	81	45	17	4			34	9	3		305
SJMH-110	113.2	46	47	110	54	3	5	1	1	49	4	1		321
SJMH-114	117.4	215	58	13	20	2			1	9				318
SJMH-117	120.7	123	42	66	30	5	2	3	2	55	3			331
SJMH-119	121.8	8	5	220	81				1	5				320
SJMH-122	123.8	97	70	48	50	3	1		1	27	4	6		307
SJMH-128	126.0	75	51	52	57	10	7	2		40	6			300
SJMH-136	131.3	91	33	66	34	2	25	3		39	24	3		320
SJMH-140	133.3	39	32	83	44	9	27	1	2	52	21	1		311
SJMH-143	138.1	77	51	56	23	4	24	2	1	46	20	2		306
SJMH-147	139.8	49	25	86	38	25	15			49	13			300
SJMH-152	142.9	39	39	40	34	1	78	2		42	29	2		306
SJMH-155,2	145.1	90	77	38	28		30	3		30	9	4		309
SJMH-156	148.0	22	19	26	14	7	82			82	45	13		310
SJMH-156,5	150.5	66	50	50	45	2	40			41	10	12		316
SJMH-158,2	152.6	24	11	34	16	2	77			19	130	2		315
SJMH-165	155.7	45	41	76	17	4	55	1		53	16	7		315
SJMH-177	158.9	46	40	54	38	4	22			55	40	10		309
SJMH-178	160.0	67	29	105	33	4	14	6	1	36	13	3		311
SJS-4	161.7	29	31	47	11	2	65	1		61	65	2		314
SJMH-183	162.2	33	29	31	16	1	59	2	1	52	82	2		308
SJS-9	166.4	41	18	39	14		77	1	1	23	100	2		316
SJS-10	167.1	5	6	8	3		123	1		25	126	9		306
SJS-16	170.1	5	8	39	19	2	75	1		24	130	6		309
SJS-18	171.9	26	12	22	13	4	83	2		95	35	15		307
SSJ-1 (SJS-19)	172.4	19	22	60	28	3	23	6		64	77	1		303
SJS-25	175.9	26	20	71	25	5	104		2	20	47	5		325
SJS-26	177.7	45	23	95	67	3	41	1		25	30			330
SJS-32	184.5	2		7	4		62			17	33	15	160	300
SJS-33	185.1	25	12	35	9		195			27	42			345

palynofacies results, Magoito and Praia das Maças sections

Sample	Height (m)	Phytoclasts < 25µ Translucent	Phytoclasts > 25µ Translucent	Phytoclasts < 25µ Opaque	Phytoclasts > 25µ Opaque	Wood tracheid (structured phytoclast)	Membranes	Cuticle	Resin	Terrestrial sporomorphs	Dino-cysts	Foram linings	AOM	Total
MAG-1	0.3	8	16	106	31		24	1	1	49	45	25		306
MAG-5	3.4	27	9	77	33		43		1	51	59	7		307
MAG-7	5.1	11	17	43	19		45			34	170	6		345
MAG-10	8.2	23	19	119	36		23		2	46	38	5		311
MAG-11,3	13.2	52	19	102	25	1	14			79	34	10		336
MAG-13	16.2	37	26	100	21	1	44			47	31	3		310
MAG-17	19.3	46	27	65	35	1	27			77	18	6		302
MAG-20	22.1	118	43	50	30	5	29	1		28	14	2		320
MAG-25	25.3	28	11	135	24	5	23			72	25	1		324
MAG-27	27.7	58	40	86	49	4	20			51	15	4		327
MAG-28,3	30.4	60	45	66	48	4	18		1	43	16	6		307
MAG-33	34.5	69	28	65	29	1	33			63	9	7		304
MAG-34	36.2	38	26	95	40	4	10	2	1	77	13	2		308
MAG-37	39.2	73	45	43	21	1	75	1		36	22	4		321
MAG-39	43.0	25	18	81	52	4	31	1	1	38	36	22		309
MAG-40	45.0	31	21	73	30	8	24	1		51	58	4		301
PM-5	4.4	11	5	15	2	1	78	2		36	157	22		326
PM-10	11.9	105	55	8	6	1	63	2	2	18	34	8		300
PM-16	20.2	10	12	2	3	1	235	6		5	23	5	1	301
PM-17	21.2	7	7	9	4		170	3		12	94	2		312
PM-19	21.8	14	17	6	6		198			19	41			304
PM-22	24.0				5	2	20	8		2		3	270	302
PM-24	26.0	39	42	18	6		77			36	66	8		302

clay mineral data, São Julião section

Sample	Height (m)	Mica	IS	Chlorite	Kaolinite	Sum	Sample	Height (m)	Mica	IS	Chlorite	Kaolinite	Sum
SJMH-2	7.5	900	83	126.1	9100.9	10210	SMJH-101	106.0	363	35	65.2	141.8	605
SJMH-3	9.8	951	90	615.5	9796.5	11453	SJMH-106	109.5	857	93	223.5	7288.5	8462
SJMH-4	10.2	477	103	138.4	5395.6	6114	SJMH-110	113.2	650	205	441.1	2610.9	3907
SJMH-11	16.4	1435	121	645.2	4447.8	6649	SJMH-117	120.7	659	75	70.5	5755.5	6560
SJMH-12.5	17.3	655	338	308.7	3249.3	4551	SJMH-119	121.8	435	35	382.2	3193.8	4046
SJMH-13.7	19.7	1500	293	313.6	6068.4	8175	SJMH-122	123.8	578	38	87.9	3194.1	3898
SJMH-15	21.4	573	141	546.0	3827.0	5087	SJMH-128	126.0	860	234	520.0	3274.0	4888
SJMH-21.3	30.9	495	164	461.0	2632.0	3752	SJMH-133	129.9	887	35	178.8	1393.2	2494
SJMH-23	33.4	1074	138	384.7	3666.3	5263	SJMH-136	131.3	680	77	683.3	2319.7	3760
SJMH-26	37.3	800	169	623.8	5078.2	6671	SJMH-140	133.3	643	67	186.8	3571.2	4468
SJMH-29.5	41.8	1072	334	556.9	2943.1	4906	SJMH-147	139.8	1239	248	296.3	3310.7	5094
SJMH-36	47.3	734	238	669.6	4088.4	5730	SJMH-152	142.9	861	244	197.7	2169.3	3472
SJMH-43	51.7	1649	308	783.4	6116.6	8857	SJMHJ-155.2	145.1	466	73	109.6	996.4	1645
SJMH-47	55.0	617	160	157.7	6205.3	7140	SJMH-156	148.0	1042	217	203.1	2198.9	3661
SJMH-48	55.4	607	56	167.3	8117.7	8948	SJMH-156.5	150.5	843	50	211.7	1814.3	2919
SJMH-49	58.0	574	85	127.5	1636.5	2423	SJMH-158.2	152.5	1154	136	131.4	1760.6	3182
SJMH-52	59.7	410	81	129.4	2412.6	3033	SJMH-165	155.7	825	127	263.8	1159.2	2375
SJMH-57.2	62.2	588	139	844.2	3260.8	4832	SJMH-177	158.9	608	30	96.1	361.9	1096
SJMH-60	69.6	260	181	165.3	2136.7	2743	SJS-4	161.7	876	127	324.0	836.0	2163
SJMH-65	73.7	848	165	180.1	728.9	1922	SJS-9	166.4	773	55	68.0	1502.0	2398
SJMH-70	76.3	484	137	181.3	495.7	1298	SJS-10	167.9	1572	107	159.3	2288.7	4127
SJMH-76	80.9	139	16	96.8	1082.2	1334	SJS-16	170.8	922	322	123.1	1299.9	2667
SJMH-78	83.6	756	90	66.3	474.7	1387	SJS-18	172.9	1062	405	136.9	390.1	1994
SMJH-81	89.4	737	180	151.8	1415.2	2484	SJS-19	173.1	1712	324	110.5	1283.5	3430
SMJH-83	89.9	1392	162	194.2	2902.8	4651	SJS-24	175.5	1123	211	85.8	481.2	1901
SMJH-85	92.6	403	80	92.3	3005.7	3581	SJS-25	176.7	681	153	108.8	437.2	1380
SJMH-86	93.7	1077	190	298.3	1926.7	3492	SJS-28	180.5	427	36	54.8	602.3	1120
SJMH-88	95.9	775	78	21.1	1895.9	2770	SJS-30	184.6	569	37	119.4	970.6	1696
SJMH-90	97.7	448	15	374.1	4920.9	5758	SJS-32	185.4	924	87	71.1	1205.9	2288
SJMH-92	99.3	1492	147	74.3	2293.7	4007	SJS-33	185.7	1235	143	142.1	1766.9	3287
SMJH-93	100.2	967	132	69.9	626.1	1795	SJS-34	186.9	555	36	27.4	604.6	1223
SMJH-100	105.3	333	23	172.0	552.0	1080	SJS-37	191.9	211	24	90.0	1024.0	1349

Acknowledgements

Finally, here it is.....Three years of hard work which resulted in this thesis. Of course I could not have done this work without the help of several other people and I would like to take the opportunity given here to show them all my deepest appreciation.

Firstly, I would like to say a big and sincere *thank you* to the main contributors who helped and guided me in a great way during the three years of my PhD; Ulrich Heimhofer, Peter Hochuli and Stefan Huck.

Dear Uli, I would like to thank you for giving me the opportunity to write this thesis. You were always there to answer any of my questions and provide logistical or other support. I will always remember your sharp, analytical and critical suggestions when we were discussing results or future prospects and I am grateful that you shared your experience with me throughout my period as a PhD student, both in the field in Portugal (during and after working hours) and at the institute.

Dear Peter, I am pleased that you shared your great knowledge on dinoflagellate cysts and angiosperm pollen morphology with me, as we worked on the microscope for several hours. Likewise, I am pleased you acted as co-examiner at my PhD defense. You were always there for assistance and answering any scientific question. I will not forget your valuable comments and suggestions that significantly improved the quality of this thesis, not only here at the Institute, but also at the EPPC conference in Padova, Italy which we both attended.

Dear Stefan, your room was always open to talk about 'hard' science or just the little things in life. Thank you for sharing your knowledge on strontium and carbon isotope stratigraphy with me. It has also been a great pleasure to go to the football stadium with you every two weeks as we shared our frustration or joy at the performance of the local 96 football team.

My co-examiners Prof. Dr. Andrea Hampel from the Institute of Geology and Prof. Dr. Francois Holtz from the Institute of Mineralogy are gratefully acknowledged for their constructive comments, questions and suggestions. I am pleased that you were willing to act as co-examiner without hesitation and on such short notice.

Susanne Feist-Burkhardt, thank you for your help and assistance while we worked with the confocal laser scanning microscopy at the University of Darmstadt. The angiosperm pollen pictures we took look really nice and I am happy we included these results into the manuscript. Leopold Sauheitl, Silke Bokeloh and Pieter Wiese; I really appreciated the collaboration at the Institute of Soil Sciences in Hannover. Furthermore, I would like to mention Jorge Dinis and Pedro Callapez from the University of Coimbra for their help and assistance in the field in Portugal. It was a great pleasure working with you during my field campaign prospecting potential outcrops. At the Ruhr University in Bochum, I would like to thank Rolf Neuser for sharing his knowledge of cathodoluminescence microscopy with me and Dieter Buhl for the trace element and strontium isotope analyses of rudist and oyster shell material. I would like to thank Thierry Adatte from the University of Lausanne Switzerland for the clay mineral analyses, Peter Skelton for assistance in rudist biostratigraphy and Nathalie Lübke for helping with the German translation of the abstract.

Stuart Robinson and Corinne Fay from UCL, London are thanked for their support during my stay in London. I hope that the palynological results of the Albian Greenland samples will provide some interesting results on mid-Cretaceous floral change and CO₂ evolution. Niiden Ichinnorov, I really appreciated the time we spend looking at the angiosperm pollen and I hope our collaboration will lead to new and improved insights in early angiosperm evolution in the Asian interior during the mid-Cretaceous.

Furthermore, I would like to thank everybody of the staff working here at the Institute of Geology for enabling me to complete my thesis in a smooth manner; Doris, Uli, Jeanette, Christiane, Christian, George, Andreas, Stefanie, Christoph and Jutta. Thank you for all your help and assistance!

A special tribute goes to my fellow PhD students here in Hannover. 'Roomies' Lukas, Heidi, Tao, Dominik, Lars and Meike, as well as the 'people from the other room' Axel, Ariana, Jörg, Julia, Conny, Lena, Jean, Philipp and Fanfan. I really enjoyed the numerous and sometimes long coffee breaks, filled with everyday chit-chat and evenings out.

The guys participating in the many Mannenavonden and Mannenweekenden are of course also not forgotten and I would like to thank you all for the great and relaxing moments we all spend over the last 11(!) years. Likewise, the weekend excursions with the Roze Ridders futsal team provided great joy and allowed me to recharge the batteries.

Finally, I would like to thank my parents for their support in times of need and a special thanks to my girlfriend Renske. Your positivism, moral support and helpful encouragements during the many 'highs and lows' during one's PhD life was of great help during these three years. Thank you for proof reading some parts of the manuscript and most of all for keeping my spirits up during times when it was most needed.

Curriculum Vitae

Name: Maurits Horikx
Date & place of birth: 18.03.1986, Amsterdam, the Netherlands
Citizenship: Dutch

Educational background

- 04/2012 – 04/2015 **PhD student, Leibniz Universität Hannover, Germany.**

Project title: *Assessing the temporal patterns of mid-Cretaceous floral change in Portugal – a palynological and chemostratigraphic approach.*
- 12/2010 – 02/2011 **Internship Dutch Geological Survey, TNO (Utrecht).**
(Netherlands Organization for Applied Scientific Research),
Business Unit Petroleum Geosciences.

Project title: *Reservoir Characterization in Carboniferous Coals.*
- 09/2008 – 02/2011 **Master of Science, Biogeology, Utrecht University, the Netherlands.**

Project title: *Late Triassic palynology and carbon isotope stratigraphy from sections in the Germanic Basin and Southern Calcareous Alps.*
- 09/2004 – 08/2007 **Bachelor of Science, Earth Sciences, Utrecht University, the Netherlands.**

Project title: *The neck morphology of Diplodocidae and Dicraeosauridae.*
- 1998 – 2004 **High School, Amsterdam, the Netherlands.**

Employment

- 03/2011 – 03/2012 **Assistant Palynologist (Utrecht, the Netherlands).**
TNO, Business Unit Petroleum Geosciences.

Project titles:
Reservoir Characterization in Carboniferous Coals.

Paleo-environmental change in response to Toarcian Anoxic Event, a palynological and palynofacies study from cored wells in the Dutch onshore and offshore.
- 2008 – 2010 **Data processing assistant (Utrecht, the Netherlands).**
TNO, Department DINO (Data and Information of the Dutch Subsurface).

Publications

Horikx, M., Heimhofer, U., Dinis, J., Huck, S. 2014. Integrated stratigraphy of shallow marine Albian strata from the southern Lusitanian Basin of Portugal. *Newsletters on Stratigraphy*, 47(1), 85-106.

Horikx, M., Hochuli, P. A., Feist-Burkhardt, S., Heimhofer, U., 2015. Albian angiosperm pollen from shallow marine strata in the Lusitanian Basin, Portugal. (*in review at Review of Palaeobotany & Palynology*).

Horikx, M., Adatte, T., Heimhofer, U., Climatic constrains on angiosperm pollen distribution patterns during Albian times: Evidence from the Lusitanian Basin, Portugal. (*in prep.*).

Conference contributions

M. Horikx, P. A. Hochuli, U. Heimhofer, 2014. Climatic constrains on angiosperm pollen distribution patterns during Albian times: Evidence from the Lusitanian Basin, Portugal. *Oral Presentation, Geological Society of America (GSA), Vancouver, Canada.*

M. Horikx, C. Fay, S. Robinson, S. Feist-Burkhardt, U. Heimhofer, 2014. Well-preserved angiosperm pollen from mid-Cretaceous continental strata on the Nuusuaq Peninsula, West Greenland, *Poster Presentation, 9th European Palaeobotany and Palynology Conference (EPPC), Padova, Italy.*

M. Horikx, P. A., Hochuli, U. Heimhofer. 2014. High-resolution angiosperm pollen record from a well-dated Albian section in the Lusitanian Basin, Portugal. *Poster Presentation, 9th European Palaeobotany and Palynology Conference (EPPC), Padova, Italy.*

M. Horikx, J. L., Dinis, U. Heimhofer. 2014. A high-resolution angiosperm pollen record covering Early to Late Albian coastal deposits (Lusitanian Basin, Portugal). *Oral Presentation, Joint Meeting of the Paläontologische Gesellschaft and the Palaeontological Society of China, Göttingen, Germany.*

M. Horikx, J. L., Dinis, U. Heimhofer. 2013. A high-resolution angiosperm pollen reference record covering Albian mid-latitude coastal deposits (Lusitanian Basin, Portugal). *Poster Presentation, EGU (European Geoscience Union), Vienna, Austria.*

